

A compilation of field reports from the 2014 field work in the larger Tasiilaq area, South-East Greenland (SEGMENT-project)

Kisser Thorsøe & Thomas F. Kokfelt (eds)



GEOLOGICAL SURVEY OF DENMARK AND GREENLAND
DANISH MINISTRY OF ENERGY, UTILITIES AND CLIMATE



GEUS

**A compilation of field reports from the 2014 field work in
the larger Tasiilaq area, South-East Greenland
(SEGMENT-project)**

Kisser Thorsøe & Thomas F. Kokfelt (eds)

Contents

Preface	6
Cu mineralization in the Isortoq area (HPA)	7
Introduction	7
Locality descriptions.....	8
Regional geology.....	8
Area 1 and 2: Glacial moraine close to the Inland Ice	9
Area 3: Qiuertalik Island	9
Area 4 and 7: Inigssalik Island	10
Area 5: Unnamed Island.....	12
Area 6: Orsuiatsivaq Island and ‘Camp Island’	14
Area 8: Peninsula to the north of Inigssalik Island.....	16
Area 9: Peninsula to the north of Kitak Island	17
Summary.....	20
Acknowledgement.....	20
Appendix A. Location details (from aFieldwork)	20
Appendix B. Sample details (from aFieldwork)	22
Graphite mineralization in the Auppaluttoq, Kangikajik and Nuuk-Ilinnera areas (NRS)	24
Introduction	24
Fieldwork and observations – Auppaluttoq	25
Fieldwork and observations – Kangikajik	28
Fieldwork and observations – Nuuk-Ilinnera	31
References.....	33
Appendix A. Camp locations	33
Appendix B. Locality list (from aFieldwork)	34
Appendix C. Sample details (from aFieldwork)	37
Mineral potential of the Helheim supracrustal sequence and follow up on significant Ujarassiorit localities within the wider Kuummiut Terrane (DRO)	41
Introduction	41
Results	41
Evaluation of the mineral potential of the Helheim Unit supracrustal sequence (camp 1 through 4).....	41
Follow up on significant Ujarassiorit localities within the wider Kuummiut Terrane (out of basecamp and camp 5 and 6).....	42
Appendix A. Camp locations	43
Appendix B. aFieldwork extraction report.....	44
Supracrustal rocks in the Schweizerland area, the Ivnartivaq dunite body and ultramafic rocks in the Niflheim area (KSZ)	48

Introduction.....	48
Camps and reco stops.....	49
Niflheim West – Camp 1.....	49
Niflheim East – Camp 2.....	50
Western nunatak – Reco 1.....	52
Y-shaped marble – Camp 3.....	53
Northern nunatak – Camp 4.....	53
Northern chain of nunataks – Reco 2.....	55
Antiformal supracrustals – Camp 5.....	56
Glacier Camp – Camp 6.....	57
Ivnartivaq – Reco 3.....	58
Northeastern shear zone – Camp 7.....	59
Y-shaped marble – Camp 8.....	61
Appendix A. List of camps and reco stops.....	63
Appendix B. List of samples.....	63
Appendix C. Profiles through the Y-shaped marble (C3).....	68
Archean basement rocks and Paleoproterozoic intrusions of the larger Tasiilaq area (TOMN)	70
Introduction.....	71
Camp 1 – Team 10.....	71
Camp 2 – Team 10.....	75
Camp 3 – Team 10/9.....	77
Camp 4 – Team 9.....	77
Camp 5 – Team 9.....	80
Camp 6 – Team 9.....	83
References.....	86
Appendix A. Complete sample list	87
Ultramafic rocks of the Niflheim unit, marbles of the Helheim unit, Johan Petersen Intrusion, Suportoq supracrustals and basement gneisses (JOT)	90
Introduction.....	90
Camp 1 and 2 – Ultramafics in the Niflheim Unit.....	92
Camp 3 – Y-shaped marble in the Helheim Unit.....	93
Camp 4 – Nunatak.....	94
Camp 5 – Marble of the Helheim Unit.....	95
Camp 6 – Southern part of the Johan Petersen Intrusion.....	95
Camp 7 – Northern part of Johan Petersen Intrusion.....	95
Camp 8 – Suportoq supracrustals, Niaqernarsik Peninsula.....	97
Camp 9 – Suportoq supracrustals, Tungujortoq Peninsula.....	98
Camp 10 – On Quinarteq Island.....	99
Structural analysis along the SE Greenland margin (PGUA)	101
Introduction.....	101
Summary of the fieldwork and observations.....	102

From Umiivik to Isortoq.....	102
Kap Japetus Steenstrup	128
Kap Gustav Holm	132
Ammassalik Fjord (65°45'N).....	133
16. September Gletscher	136
Proterozoic and Tertiary mafic dykes (MBK, RBO)	142
Introduction	142
Observations.....	142
References.....	143
Appendix A. Camp locations	143
Appendix B. Sample details (from aFieldwork)	144
Acquisition of on-ground spectral reflectance data (AFJ, PRI, BHM)	149
Introduction	149
Measuring Procedures	149
Outline of report	152
The Fieldwork for Hyperspectral data	152
Concluding remarks regarding the spectral measurements	179
References.....	179
Appendix A. Camp location.....	179
Appendix B. List of localities visited	180

Preface

This report is a compilation of the remaining field reports from the 2014 field season in South-East Greenland that was organized under the joint GEUS-MMR 'SEGMENT'-project (2009-2016), and that focused on reassessing the geology and mineral potential of the area between 62°30'N and 66°30'N. The main results of the SEGMENT-project were reported in Kolb et al. 2016 [Kolb, J., Stensgaard, B.M. & Kokfelt, T.F. Danmarks og Grønlands Geologiske Undersøgelse Rapport 2016/38, 157 pp.]. The field participants that contributed to the work presented in this report providing their initials and affiliations can be seen in Table 1. The report was edited by Kisser Thorsøe and Thomas F. Kokfelt, GEUS.

Table 1. Names and initials of field participants (alphabetically listed).

Name	Initials	Affiliation*
Anne Brandt Johannesen	ABJ	University of Oulo, Finland
Annika Dziggel	ADZ	University of Aachen, Germany
Asta Fabricius Jørgensen	AFJ	University of Copenhagen, Denmark
Bo Møller Stensgaard	BMST	GEUS
Diogo Rosa	DRO	GEUS
Holger Paulick	HPA	GEUS
Jochen Kolb	JKOL	GEUS
Jonas Petersen	JPET	Ministry of Mineral Resources, Government of Greenland, Greenland
Jonas Tusch	JOT	University of Köln, Germany
Kisser Thorsøe	KIT	GEUS
Kristine Thrane	KT	GEUS
Kristoffer Szilas	KSZ	Columbia University, New York, USA
Leon Bagas	LBA	School of Earth and Environment, University of Western Australia, Australia
Majken D. Poulsen	MADP	GEUS
Marco Fiorentini	MFI	Centre of Exploration Targeting, University of Western Australia, Australia
Martin Broman Klausen	MBK	University of Stellenbosch, South Africa
Matti Nellemann Petersen	MNP	GEUS
Nanna Rosing-Schow	NRS	University of Copenhagen, Denmark
Nicolas Thebaud	NTH	Centre of Exploration Targeting, University of Western Australia, Australia
Pierpaolo Guarnieri	PGUA	GEUS
Sam Weatherley	SMW	GEUS
Sascha Müller	SMU	University of Aachen, Germany
Tomas Næraa	TOMN	University of Lund, Sweden
Vincent van Hinsberg	VIVH	McGill University, Canada

* As of in 2014

Cu mineralization in the Isortoq area (HPA)

Introduction

This part of the report is follow-up on Cu mineralisation samples submitted to the Ujarassiorit program.

The field work was carried out from July 30th to August 7th 2014 by Team 14, Holger Paulick (HPA), GEUS and Jonas Petersen (JPET), Ministry of Mineral Resources, Government of Greenland. HPA was a member of Team 1 from July 21st to July 29th, these result are reported separately. Team 12 had joined zodiac operations with Team 5, Martin Bromann Klausen (MBK) and Riaann Bothma (RBO), both University of Stellenbosch.

Between 1990 and 2012 a number of Cu mineralised samples have been submitted to the Ujarassiorit program from the Isortoq area (grades between 0.22 and 1.90% Cu; Table 2). The focus of our field work was to follow-up on these findings, describe the geological setting and assess the potential of these occurrences.

Table 2. *Cu-bearing samples from the Isortoq area – Ujarassiorit program.*

Sample no.	Description	Lat. (N)	Long. (W)	Location	Loc.	Cu [wt.%]	Au [ppb]
2007-0234	Gabbro	65.6563	39.0738	Close to Inland Ice	1	0.88	75
90-1007	Pegmatite	65.6500	39.0700	Close to Inland Ice	1	0.21	41
92-541	Pyrite	65.5900	38.9200	Close to Inland Ice	2	0.63	8
94-271	Hydrothermally altered rock	65.5200	39.0350	Qiuertalik Island	3	1.20	23
2011-0410	Gneiss	65.5136	38.8889	Inigssalik Island	4	0.76	25
2002-761	Amphibolite w, magnetite	65.5315	38.9676	Unnamed island	5	0.40	2
2008-0576	Amphibolite/quartz	65.4960	38.9376	Unnamed island	5	0.22	1720
90-800	Pegmatite	65.4900	38.7350	Orsuiatsivaq Island	6	0.32	34
91-808	Pegmatite	65.4800	38.8800	Orsuiatsivaq Island	6	1.90	204
92-535	Quartz	65.4800	38.8800	Orsuiatsivaq Island	6	1.66	24
92-553	Pyrite gravel	65.4800	38.8800	Orsuiatsivaq Island	6	0.76	72
92-554	Pyrite- pyrrhotite gravel	65.5700	38.8800	Orsuiatsivaq Island	6	0.56	28
92-556	Pyrite	65.4800	38.8800	Orsuiatsivaq Island	6	0.54	214
92-558	Pyrite gravel	65.4800	38.8800	Orsuiatsivaq Island	6	1.87	13
94-270	Pyrite	65.4800	38.8790	Orsuiatsivaq Island	6	0.91	-5
94-275	Granodiorite	65.5000	38.6900	Orsuiatsivaq Island	6	0.64	17

The settlement Isortoq (ca. 70 inhabitants) is located on the northern coast of one the islands of the Isortoq Archipelago (Figure 1). This area is characterized by shallow channels which separate islands of generally low level altitude (maximum altitude commonly below 100 m). A field camp was established at the southernmost end of Kitak island for the first part of the field work (marked 'C' on Figure 1), and later the Isortoq service house served as the base. On two occasions, locals from Isortoq helped to locate the positions of Ujarassiorit samples.

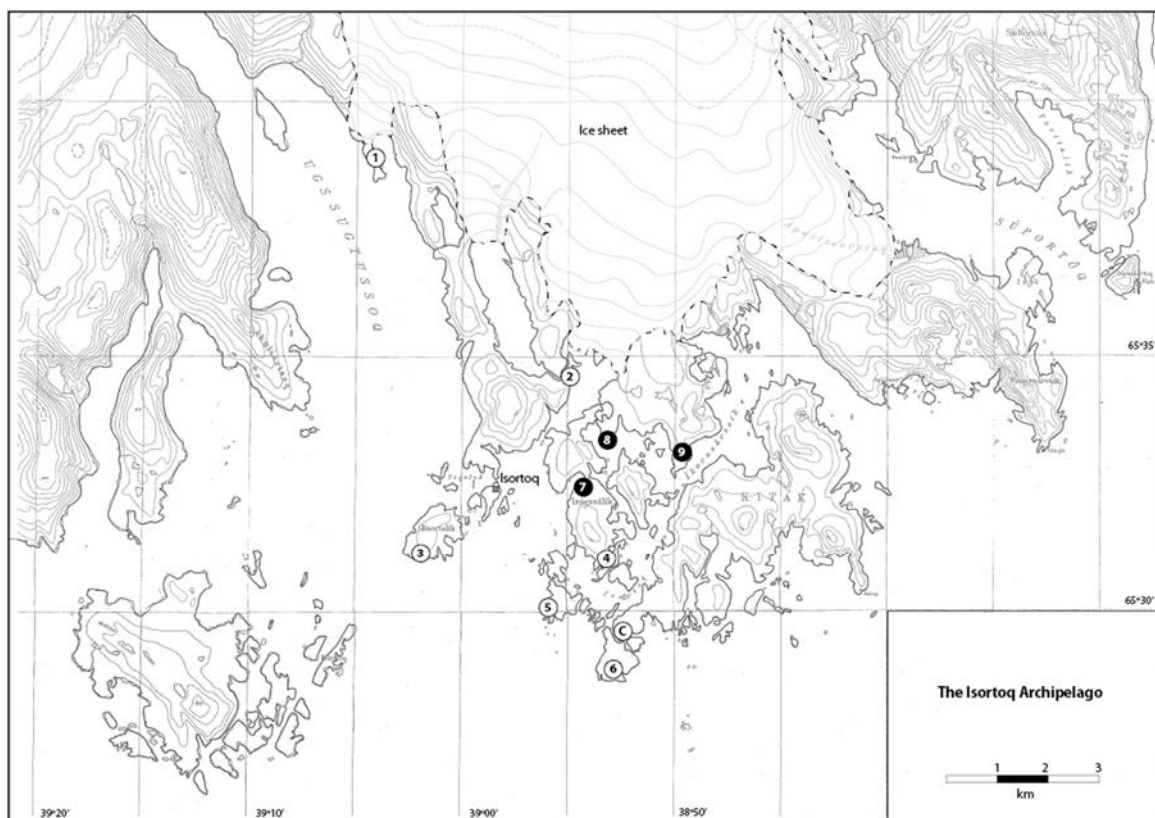


Figure 1. Overview of the areas visited in the Isortoq Archipelago. Area 1 to 6: Known occurrences of Cu mineralisation from Ujarassiorit program. Area 7 to 9: Occurrences of sulfides discovered and sampled during this field work. C: Field camp. Base topography: 1: 50 000 map, Geodætisk Institut (65Ø2); 50 m lines for elevation.

Locality descriptions

In this section, the major geological features of the areas marked on Figure 1 are described with particular reference to any sulfide occurrences.

Regional geology

The Isortoq Archipelago is dominated by banded orthogneiss, amphibolites and granite intrusions which belong to the Archean North Atlantic Craton in South-East Greenland. The general geologic and geodynamic setting is summarized in Kolb (2014), Bridgwater (1990), Kalsbeek (1993) and references therein. In a regional context, the study area is located to the southwest of the Palaeoproterozoic Nagssugtoqidian orogenic zone approx. 50 km from the Ammassalik Intrusive Complex.

Area 1 and 2: Glacial moraine close to the Inland Ice

Area 1 and 2 were visited together with the collectors of the original Ujarassiorit samples (Rosa and Dines Jonathansen; residents of Isortoq). These samples were rounded float boulders of gabbroic composition with up to 5% sulfide minerals (pyrite, chalcopyrite, pyrrhotite) from the polymictic glacial moraine deposits at the outflow area of Inland Ice glaciers. The outcropping rock units on the shore line are barren banded gneiss.

Area 3: Qiuertalik Island

Qiuertalik Island is located ca. 1 km to the SW of Isortoq and on the NE shore there is remnants of previous dwellings/shelters. The eastern portion of the island consists of granite which intruded into a banded gneiss/amphibolite succession. There are wide zones stretching over hundreds of m² of variable textures grading from isolated gneiss/amphibolite xenoliths in granite to volumetrically dominant gneiss/amphibolite zones with granite apophyses separating individual domains. In addition, there are late stage pegmatite dikes which cross cut both gneiss/amphibolite and granite.

An Ujarassiorit sample from the SW shore recorded with 1.2% Cu (sample 94-271), and circumnavigating the island by boat revealed that there was a clearly visible zone of intense rusty alteration at the sample site. However, ground proofing of the area (location 2014HPA076; sample 564553) returned disappointing results: This is a biotite-rich zone in the banded gneiss that was intruded by granite apparently causing the development of an enveloping alteration zone (Figure 2). Sulfides are absent in the area. However, in the adjacent bay to the west (location 2014HPA077) we identified minor sulfide bearing patches and veinlets in a pegmatite dike (sample 564554), which might represent the source of the mineralised Ujarassiorit sample.





Figure 2. *Rusty alteration zone in biotite-rich banded gneiss surrounding a granite intrusive body (A). The alteration is focused in a fracture network and is devoid of sulfides (B).*

Area 4 and 7: Inigssalik Island

Southern and northern areas of Inigssalik Island were visited and field observations show complex contact relationships between granitic intrusive bodies and country rock dominated by banded gneiss and amphibolite. As observed previously, mixing of variable proportions of granite and country rock define contact zones extending for several hundreds of m². In addition, there are numerous pegmatite dikes, gabbro occurrences and dolerite dikes.

In the southern area (area 4 on Figure 1 and Figure 3), the aim was to relocate an Ujarassiorit sample with 0.76% Cu (sample 2011-0410). This rock boulder apparently originated from the floor of a brittle fault zone marking a major topographic linear feature which is clearly recognizable in the satellite image (Figure 3). This sample may represent an exceptional find since we did not localize other sulfide-bearing material in the boulder scree. Visited outcrops in the area show interesting tectonic features such as isoclinal folding (Figure 4; field location 2014HPA038 fold plane at 320/20; dip direction/dip degree) and gabbro and anorthosite boudin within the banded gneiss (Figure 5; field location 2014HPA044).

In the northern area (area 7) we discovered a sulfide-bearing boudin in banded gneiss of approximately 0.4 x 1.3 m dimensions (Figure 6; location 2014HPA047). The boudin rock type is best described as biotite-garnet meta-granite (sample 564545) with ca. 3% sulfide minerals. Overall, this part of the island is dominated by granite and complex, mixed contact zones where variable proportions and dimensions of country rock occur as xenoliths in the granite. Furthermore, there are cross cutting pegmatite dikes which locally contain traces of sulfides (e.g. location 2014HPA052). At one location, isoclinal folding was observed in bedded gneiss (2014HPA054; fold plane at 220/15; dip direction/dip degree).

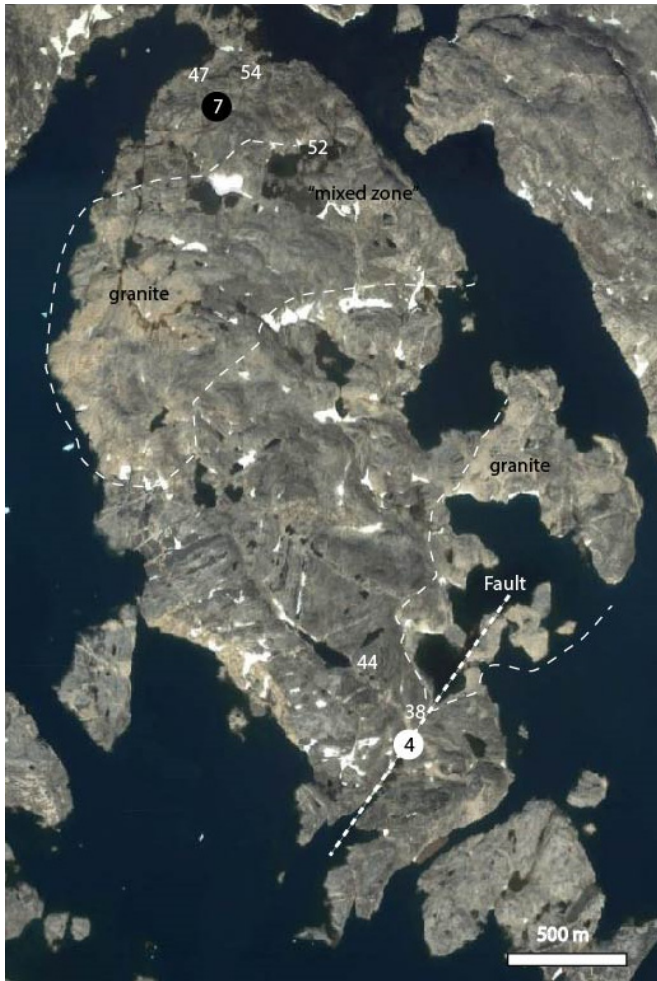


Figure 3. Satellite image of Inigssalik Island (Google Earth). Two areas were visited in 2014 (marked 4 and 7; cf. Figure 1) and major geological features are highlighted. Numbers refer to field locations (i.e., 2014HPA0XX).



Figure 4. Isoclinal folding in bedded gneiss at field location 2014HPA038 (see Figure 3). The fold plane orientation is 320/20 (dip direction/dip degree).



Figure 5. *Gabbro and anorthosite boudins in strongly sheared, banded gneiss at field location 2014HPA044). All three rock types were sampled (564540, 564541, 564542). Dimensions of anorthosite boudin ca. 0.7 m x 0.5 m.*



Figure 6. *Sulfide-bearing boudin (biotite-garnet meta-granite) in banded gneiss in the northern part of Inigssalik Island (location 2014HPA047; sample 564545).*

Area 5: Unnamed Island

A sample of amphibolite with quartz veins from the west coast of an unnamed island in the Isortoq Archipelago was submitted to the Ujarassiorit program in 2008 (2008-0576) and contains 0.22% Cu and 1.7 ppm Au. This island is characterized by banded gneiss with amphibolite bodies that are cross cut by pegmatite dikes. However, field observations show that two prominent pegmatites on the western shore are in fact sills (Figure 7).

Minor sulfide occurrences have been found near the location of the Ujarassiorit sample. At location 2014HPA086 there are malachite staining networks and quartz veins cross cutting amphibolite (sample 564561; Figure 8). However, the malachite is a superficial feature and there are no sulfides in the fracture network. Furthermore, there is a sulfide-bearing quartz vein network just below the basal contact of the adjacent pegmatite sill at location 2014HPA087 (sample 564562). However, concentrations are in the order of 1-2 vol.% and the lateral extend is <5 m.



Figure 7. Satellite image of unnamed island in the Isortoq Archipelago (Google Earth). The area marked '5' was the location of an Ujarassiorit sample with 0.22% Cu and 1.7 ppm Au. Two sites with minor sulfide occurrences have been sampled during field work (2014HPA086: malachite stained fracture network in amphibolite; 2014HPA087: sulfide-bearing quartz veins below basal contact of pegmatite sill).



Figure 8. Fracture network with malachite staining on western shore of unnamed island in the Isortoq Archipelago (location 2014HPA086; sample 564561).



Figure 9. Sulfide-bearing quartz veining below the contact of major pegmatite sill on the west coast of unnamed island (location 2014HPA087; sample 564562).

Area 6: Orsuiatsivaq Island and ‘Camp Island’

The Orsuiatsivaq Island is remarkable for the relicts of a Long Range Navigation (LORAN) radio station that was in operation in the 1960s and 70s. Remnants from that time include houses, engine rooms, water and petrol storage facilities, pipelines and a road connecting the harbor and the station. The radio antenna constructions have been removed.

Geologically, the island consists of banded gneiss with local bodies of amphibolite and cross-cutting pegmatite dikes. The majority of these dikes have an E-W orientation with dips of around 80 degrees and can be traced from Orsuiatsivaq Island to ‘Camp Island’ to the east (Figure 10). Several sulfide-bearing samples have been submitted from this area to the Ujarassiorit program during the early 1990s. Our field work shows that these are related to minor, localized occurrences of sulfides within, or immediately adjacent to, the E-W striking pegmatite dikes. Interestingly, a thick pegmatite dike with a NW-SE orientation in the southern portion of the island (field location 58; Figure 10) shows abundant rusty alteration (related to biotite weathering?) but is devoid of sulfides.

In the following the field locations (on Figure 10) yielding sulfide occurrences are described. At field location 30 there is a minor amphibolite body embedded in banded gneiss. This is cross-cut by an E-W striking pegmatite dike and at the contact there is a rusty alteration zone and associated quartz-pyrite veins (striking N-S) in the amphibolite (samples 564532, 564533, 564534). Interestingly, the amphibolite is garnet-bearing which is unusual in the Isortoq Archipelago.

At field location 33 (Figure 11) there is a similar situation in that a E-W trending pegmatite dike cross-cuts amphibolite and encloses a 20 m long x 1-3 m wide amphibolite body. In this

area, the pegmatite has a rusty zone on its margin (2 m x 1 m) with ca. 5 vol.% pyrite and chalcopyrite (sample 564535).

At field location 55 there are minor sulfide patches on the margin of a pegmatite which are marked by some malachite staining (sample 564549). Here the pegmatite is in contact with banded gneiss. Similar occurrences within the marginal zone of these E-W trending pegmatite dikes were observed at field location 27 and 28 on 'Camp Island' (Figure 10; sample 564531).

At field location 59, in the southernmost part of Orsuiatsivaq Island, there are NW-SE striking rusty quartz veins cross cutting the banded gneiss/amphibolite succession (sample 564551). The amphibolite also contains a brittle fracture network with malachite staining on the surfaces (similar to field location 2014HPA086; Figure 6). Also, amphibolite with sulfide bearing brittle fractures was sampled on 'Camp Island' (field location 98, sample 564570).

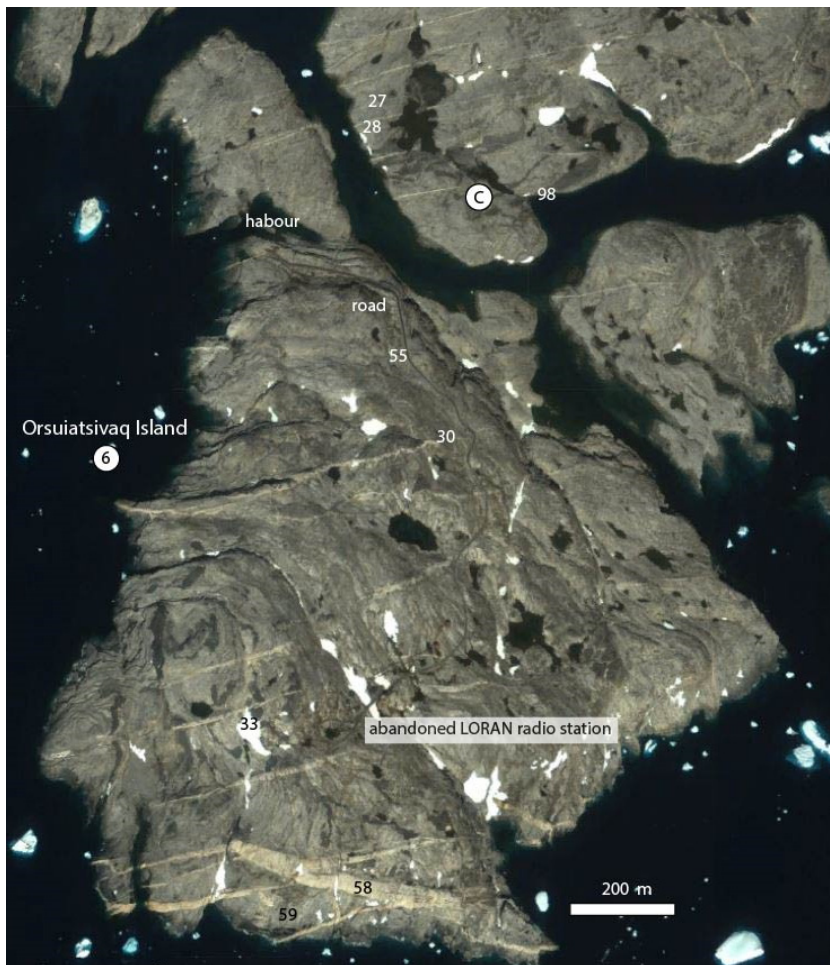


Figure 10. Satellite image of Orsuiatsivaq Island and 'Camp Island' in the Isortoq Archipelago (Google Earth; work area marked 6 on Figure 1). Remnants of infrastructure related to a Long Range Navigation (LORAN) radio station are preserved on the island. Sulfide occurrences are within, or immediately adjacent to, E-W trending pegmatite dikes. A NW-SW oriented pegmatite dike in the southern part of the island is barren (field location 2014HPA058). Also, there are locally sulfide-bearing fracture networks in amphibolite (field locations 2014HPA059 and 2014HPA098).



Figure 11. *Sulfide-bearing pegmatite on Orsuiatsivaq Island (field location 2014HPA033; sample 564535). A: The E-W trending pegmatite dike is locally cross cutting an amphibolite body enclosed in the banded gneisses that make up most of the island. The rusty alteration zone is on the N side of the dike. B: The rusty alteration zone contains pyrite and chalcopyrite.*

Area 8: Peninsula to the north of Inigssalik Island

At the point of this mainland peninsula, facing towards the northern portion of Inigssalik Island, there is a rusty 15 cm wide NW-SE striking pegmatite dike cross cutting banded gneiss. The occurrence was sampled on the shore line by zodiac (field location 2014HPA081; sample 564555).

Area 9: Peninsula to the north of Kitak Island

This mainland peninsula, which faces the middle portion of the northwestern shore of Kitak Island (Figure 1), was visited on two occasions. The western area (field location 2914HPA082) is dominated by banded gneiss with local zones of sulfide concentrations whereas the eastern area (field location 2914HPA097) consists mainly of banded gneiss and anorthosite (Figure 12).

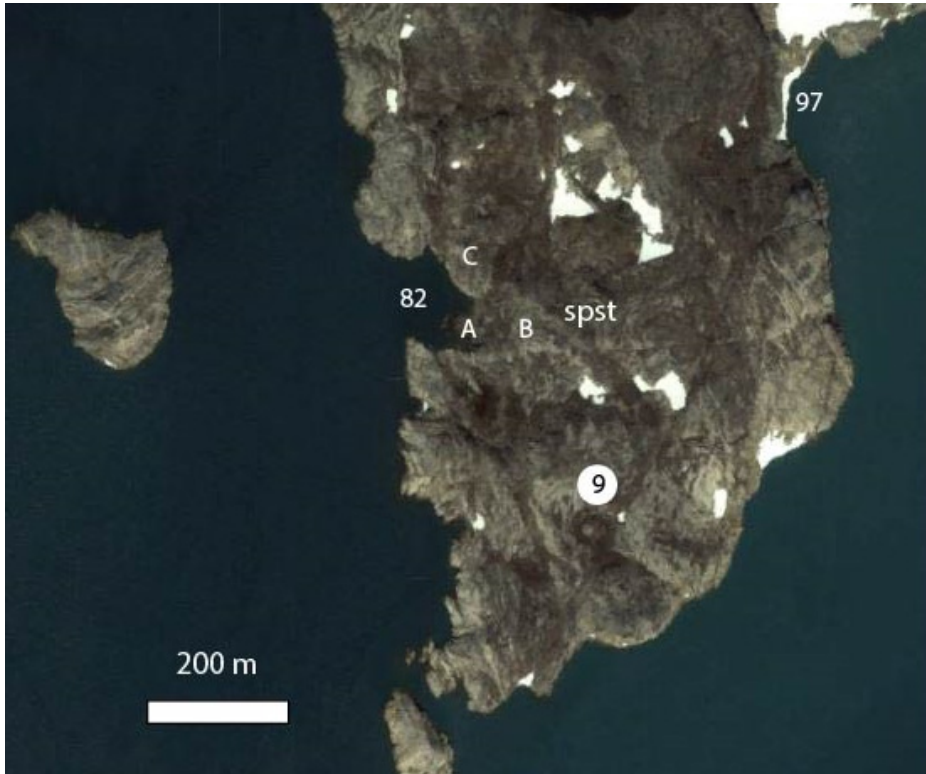


Figure 12. *The mainland peninsula at area 9 was investigated from the western side and from the eastern side. At the western site three occurrences of sulfide-bearing rocks have been sampled (marked A, B, and C). Also an occurrence of soapstone was identified (spst). The eastern site is remarkable for the occurrence of anorthosite, garnet-rich nodular rocks and a sulfide bearing gabbroic boudin in banded gneiss*

At the western bay area (field location 2914HPA082) there are rusty, sulfide-bearing rock bodies (max. 2 x 5 m) within the banded gneiss (Figure 13a and b). Field relationships are ambiguous; however, based on the sharp contacts to sulfide-free banded gneiss it seems likely that these are boudins of different rock types than the banded gneiss. Alternatively, it may be suggested that focused hydrothermal alteration resulted in localized sulfide deposition of the banded gneiss itself. Three occurrences have been sampled (marked A, B, C in Figure 12). The hand specimen can be described as: A) a rusty pyroxene-plagioclase (?) porphyritic rock (samples 564556, 564557), B) is a rusty porphyroblastic banded gneiss with sulfide veining (samples 564558, 564559). The sample is taken from a cliff surface that is a 3 x 4 m area of banded gneiss with abundant sulfide veins. C) is a yellow-stained mica-rich schist with quartz-sulfide veins (sample 564560). In addition, a serpentized ultramafic body is located to the east of site B that is used as a local soapstone supply (Figure 13spst).



Figure 13. Three sulfide-bearing units are present at field location 2014HPA082. A: Site A at field location 82 consists of a rusty, sulfide-bearing pyroxene-plagioclase(?) porphyritic rock. B: Site B is located on a cliff surface and is a banded gneiss with abundant sulfide veins. SPST: Serpentinized ultramafic rock used as soapstone (spst on Figure 12).

At the eastern shore of the peninsula (field location 2914HPA097) there is a complex succession of banded gneiss, anorthosite and a garnet-rich rock type best described as 'black nodular rock' (Figure 14). The anorthosite at the base of the coastal cliff face (sample 564569) is intermixed with banded gneiss at variable proportions. However, there is a sharp contact to the overlying banded gneiss unit which contains a boudin (0.3 x 1.5 m) of a sulfide-bearing gabbroic rock (sample 564568). This in turn is overlain by a ca. 2 m thick and ca. 10 m wide unit of nodular rock with dark garnet-biotite domains in a white quartz-feldspar groundmass (sample 564567).

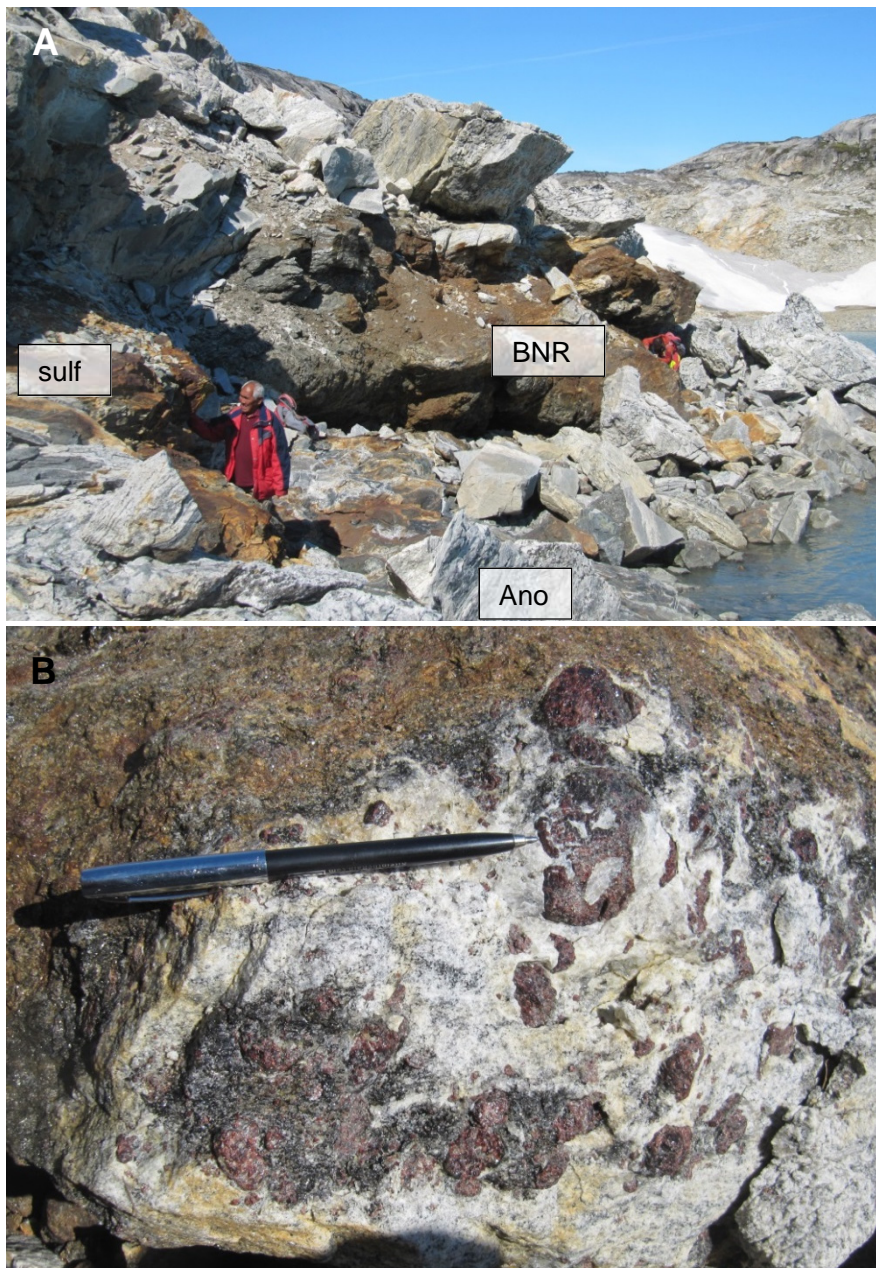


Figure 14. *Field relationships at location 2014HPA097. A: An anorthosite body (Ano; sample 564569) is overlain by banded gneiss which contains a boudin of sulfide-bearing gabbroic (?) rock (sample 564568). This is followed by a unit of 'black nodular rock' (BNR; sample 564567). B: The 'black nodular rock' consists of cm sized garnet-biotite-hornblende nodules in a ground-mass of quartz and feldspar.*

Summary

During field work we investigated 6 areas where Cu-mineralised samples have been reported in the Ujarassiorit program (Figure 1). Furthermore, sulfide-bearing rocks have been identified and sampled in 3 additional areas. The field work showed that all of these occurrences are small and commonly the visual estimates for sulfide abundance are less than 1–2 vol%. These observations, together with the general geology of the area (high grade banded gneisses with amphibolite bodies, granite, pegmatite dikes) point to a low potential of the area for significant sulfide mineral deposits.

A number of different styles of sulfide occurrences have been observed:

- 1) Amphibolite with late stage brittle fractures of quartz, epidote and pyrite and malachite staining on the rock surfaces (area 5, 6 and Camp area marked 'C')
- 2) Pyrite occurrences within quartz veins (area 6 and 7)
- 3) Pyrite-chalcopyrite disseminations/veins within pegmatite dikes (area 3, 6, and 8)
- 4) Sulfide-bearing granitic or gabbroic boudins within banded gneiss (area 7 and 9)
- 5) Sulfide impregnations in banded gneiss (area 9)
- 6) Rounded boulders of sulfide-bearing gabbro (glacial moraine close to Inland Ice, area 1 and 2)

Furthermore, a soapstone occurrence was identified at area 9.

Acknowledgement

We would like to thank our colleagues from Team 5 for their support and 'taxi service' with the zodiac. Also, MBK and RBO discovered the sulfide occurrences on the mainland peninsulas (areas 8 and 9).

Appendix A. Location details (from aFieldwork)

Location	Loc. no.*	Name	Lat. (N)	Long. (W)	Date
Camp Island	C	Camp Island	65.49855	38.87623	30-07-2014
Camp Isortoq	Isortoq	Isortoq	65.64890	38.87740	05-08-2014
2014HPA022	C	Camp Island	65.49855	38.87623	30-07-2014
2014HPA023	C	Camp Island	65.49987	38.88277	30-07-2014
2014HPA024	C	Camp Island	65.50167	38.88492	30-07-2014
2014HPA025	C	Camp Island	65.50145	38.88402	30-07-2014
2014HPA026	C	Camp Island	65.50098	38.88307	30-07-2014
2014HPA027	C	Camp Island	65.50041	38.88284	30-07-2014
2014HPA028	C	Camp Island	65.50014	38.88251	30-07-2014
2014HPA029	C	Camp Island	65.49946	38.88205	30-07-2014
2014HPA030	6	Orsuiatsivaq Island	65.49375	38.87988	31-07-2014
2014HPA031	6	Orsuiatsivaq Island	65.49274	38.87758	31-07-2014
2014HPA032	6	Orsuiatsivaq Island	65.49033	38.87870	31-07-2014
2014HPA033	6	Orsuiatsivaq Island	65.48867	38.88811	31-07-2014
2014HPA034	6	Orsuiatsivaq Island	65.48872	38.89242	31-07-2014
2014HPA036	4	Inigssalik Island	65.52255	38.88790	01-08-2014
2014HPA038	4	Inigssalik Island	65.52625	38.88603	01-08-2014
2014HPA040	4	Inigssalik Island	65.52793	38.88733	01-08-2014

Location	Loc. no.*	Name	Lat. (N)	Long. (W)	Date
2014HPA041	4	Inigssalik Island	65.52640	38.88862	01-08-2014
2014HPA042	4	Inigssalik Island	65.52609	38.89074	01-08-2014
2014HPA043	4	Inigssalik Island	65.52847	38.89360	01-08-2014
2014HPA044	4	Inigssalik Island	65.52788	38.89291	01-08-2014
2014HPA045	4	Inigssalik Island	65.52681	38.89297	01-08-2014
2014HPA046	4	Inigssalik Island	65.52449	38.88564	01-08-2014
2014HPA047	7	Inigssalik Island	65.54646	38.91522	02-08-2014
2014HPA048	7	Inigssalik Island	65.54587	38.91479	02-08-2014
2014HPA051	7	Inigssalik Island	65.54405	38.90644	02-08-2014
2014HPA052	7	Inigssalik Island	65.54694	38.89621	02-08-2014
2014HPA054	7	Inigssalik Island	65.55076	38.90305	02-08-2014
2014HPA055	6	Orsuiatsivaq Island	65.49420	38.87856	03-08-2014
2014HPA056	6	Orsuiatsivaq Island	65.48965	38.87911	03-08-2014
2014HPA057	6	Orsuiatsivaq Island	65.48739	38.88052	03-08-2014
2014HPA058	6	Orsuiatsivaq Island	65.48642	38.88049	03-08-2014
2014HPA059	6	Orsuiatsivaq Island	65.48539	38.87854	03-08-2014
2014HPA061	6	Orsuiatsivaq Island	65.48623	38.88645	03-08-2014
2014HPA062	6	Orsuiatsivaq Island	65.48721	38.88896	03-08-2014
2014HPA063	6	Orsuiatsivaq Island	65.48947	38.89113	03-08-2014
2014HPA064	6	Orsuiatsivaq Island	65.49065	38.88966	03-08-2014
2014HPA065	6	Orsuiatsivaq Island	65.49122	38.88713	03-08-2014
2014HPA066	6	Orsuiatsivaq Island	65.49336	38.87833	03-08-2014
2014HPA067	6	Orsuiatsivaq Island	65.49677	38.88168	03-08-2014
2014HPA073	3	Qiuertalik Island	65.53575	39.01268	05-08-2014
2014HPA075	3	Qiuertalik Island	65.52757	39.02251	05-08-2014
2014HPA076	3	Qiuertalik Island	65.52688	39.02998	05-08-2014
2014HPA077	3	Qiuertalik Island	65.52609	39.03226	05-08-2014
2014HPA078	3	Qiuertalik Island	65.52683	39.03779	05-08-2014
2014HPA079	3	Qiuertalik Island	65.52888	39.03631	05-08-2014
2014HPA081	8	Penninsula north of Inigssalik	65.56285	38.88926	05-08-2014
2014HPA082	9	Penninsula north of Kitak	65.55929	38.83414	06-08-2014
2014HPA085	5	Unnamed island	65.50709	38.93338	06-08-2014
2014HPA086	5	Unnamed island	65.50651	38.93256	06-08-2014
2014HPA087	5	Unnamed island	65.50621	38.93301	06-08-2014
2014HPA088	5	Unnamed island	65.50605	38.93452	06-08-2014
2014HPA091	5	Unnamed island	65.51106	38.91903	06-08-2014
2014HPA092	1	Near Inland Ice NW of Isortoq	65.64930	39.06557	07-08-2014
2014HPA094	3	Qiuertalik Island	65.53431	39.00277	07-08-2014
2014HPA096	2	Near Inland Ice NE of Isortoq	65.58772	38.90938	07-08-2014
2014HPA097	9	Penninsula north of Kitak	65.56051	38.82217	07-08-2014
2014HPA098	C	Camp Island	65.49839	38.87461	07-08-2014

* on Figure 1

Appendix B. Sample details (from aFieldwork)

Location	Sample no.	Loc. no.*	Description	Purpose	Comment
2014HPA027	564531	C	Sulfide-bearing pegmatite	Geochem, mineralisation	off shoot from 1 m thick pegmatite dike; within banded gneiss
2014HPA030	564532	6	Quartz vein with sulfides	Mineralisation	
2014HPA030	564533	6	Rusty vein in amphibolite	Petrography, mineralisation	
2014HPA030	564534	6	Garnet-bearing amphibolite	Metamorphism, petrography	
2014HPA033	564535	6	Sulfide-bearing pegmatite	Geochem, mineralisation	
2014HPA038	564536	4	Banded gneiss	Representative	
2014HPA038	564537	4	Granite	Representative	
2014HPA043	564538	4	Banded gneiss	Mineralisation	rusty alteration
2014HPA044	564540	4	Banded gneiss	Representative	strongly strained with gabbro and anorthosite boudins (sampled)
2014HPA044	564541	4	Gabbro block	Representative	boudin within banded gneiss
2014HPA044	564542	4	Anorthosite	Representative	boudin within banded gneiss
2014HPA045	564543	4	Gabbro	Representative	
2014HPA047	564544	7	Sulfide bearing meta-granite	Geochem, mineralisation	qtz-fsp-bio-gt granite boudin
2014HPA047	564545	7	Strongly foliated biotite schist	Representative	
2014HPA048	564546	7	Rusty alteration biotite schist	Geochem, representative, petrography	rusty altn apperas to follow contact with granite
2014HPA051	564547	7	Granite	Geochem, representative	rusty biogenetic weathering of granite
2014HPA052	564548	7	Quartz vein with sulfides	Geochem, mineralisation	quartz vein in banded gneiss mega-xenolith in granite
2014HPA055	564549	6	Sulfide bearing pegmatite	Mineralisation	same strike orientation as sample 564548
2014HPA059	564550	6	Amphibolite	Mineralisation	malachite staining along rectangular brittle fault network
2014HPA059	564551	7	Quartz vein with sulfides	Mineralisation	
2014HPA075	564552	3	Banded gneiss	Representative	
2014HPA076	564553	3	Banded gneiss	Representative	rusty alteration, No sulfides.
2014HPA077	564554	3	Pegmatite	Geochem, mineralisation	rusty alteration. Sulfides?
2014HPA081	564555	8	Pegmatite	Geochem, mineralisation	
2014HPA082	564556	9	Gneiss with minor sulfides	Geochem, mineralisation	
2014HPA082	564557	9	Gneiss with some sulfides	Geochem, mineralisation	
2014HPA082	564558	9	Sulfide veins in porphyroblastic gneiss	Geochem, mineralisation	
2014HPA082	564559	9	Sulfides and white alteration	Geochem, mineralisation	
2014HPA082	564560	9	Rusty biotite schist	Geochem, mineralisation	

Location	Sample no.	Loc. no.*	Description	Purpose	Comment
2014HPA086	564561	5	Amphibolite	Geochem, mineralisation	malachite staining along rectangular brittle fault network
2014HPA087	564562	5	Banded gneiss	Geochem, representative	rusty weathering
2014HPA087	564563	5	Quartz vein	Geochem, mineralisation	in rusty weathered gneiss
2014HPA092	564564	1	Gabbro	Mineralisation	boulder in glacial moraine. With minor sulfides.
2014HPA094	564565	3	Granite	Representative	
2014HPA096	564566	2	Gabbro	Mineralisation	boulder in glacial moraine. With minor sulfides.
2014HPA097	564567	9	Garnet-rich black nodular rock	Metamorphism, petrography	in banded gneiss
2014HPA097	564568	9	Sulfide-rich gabbro boudin	Mineralisation	in banded gneiss
2014HPA097	564569	9	Anorthosite	Representative	in banded gneiss
2014HPA098	564570	C	Amphibolite	Geochem, mineralisation	

* on Figure 1

Graphite mineralization in the Auppaluttoq, Kangikajik and Nuuk-Ilinnera areas (NRS)

Introduction

The fieldwork lasted from 15th of July to 22nd of August 2014 in the area around Tasillaq, South-East Greenland. The fieldwork was carried out mainly with and under supervision of Leon Bagas (LBA) from University of Western Australia and Jochen Kolb (JKOL) from GEUS, and later with M.Sc. student Anne Brandt Johannesen (JAB).

The purpose was to map and characterize target areas of graphite mineralization. Two main areas (Auppaluttoq and Kangikajik) and one less significant area (Nuuk-Ilinnera) were known beforehand to host graphite mineralization. These were the main areas of interest for targeted field investigations and mapping.

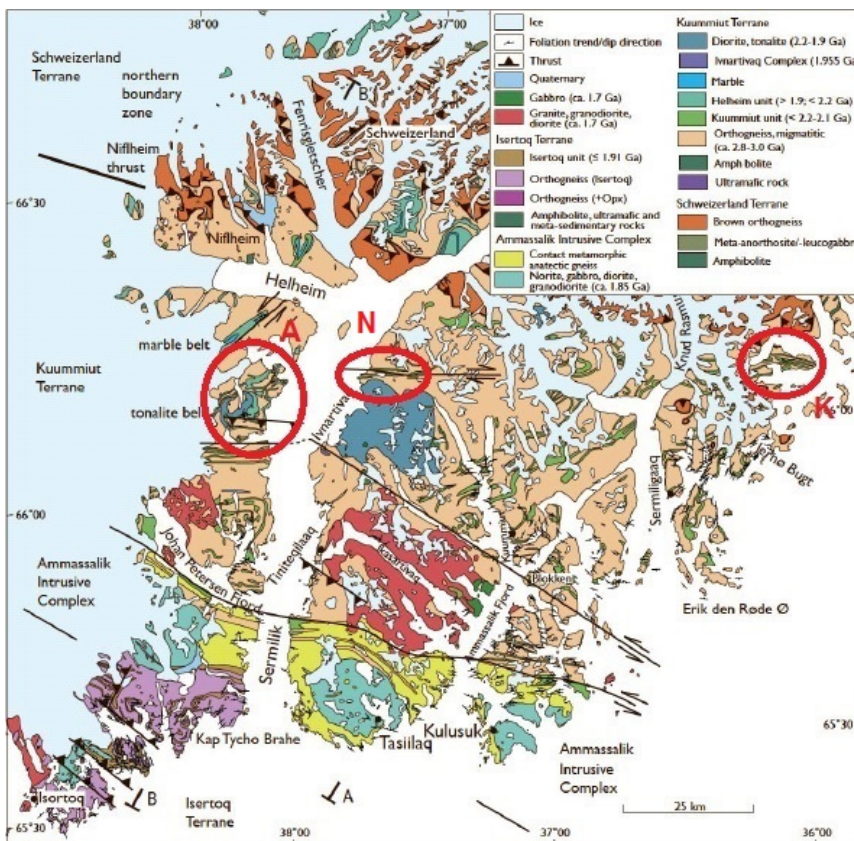


Figure 15. Geological map of the area showing the three focus areas: Auppaluttoq (A), Kangikajik (K) and Nuuk-Ilinnera (N) (modified after Kolb 2014).

One day was spent in the basecamp in Kuummiut before the fieldwork started in Auppaluttoq. Fieldwork was carried out in Auppaluttoq (see Figure 15) from the 16th of July to the 1st of August from camp 1, 2 and 3 with LBA. Thereafter fieldwork was carried out in Kangikajik (Figure 15; camp 4) from 1st of August to 8th of August with LBA and JKOL who joined the team the 4th of August. Fieldwork at Nuuk-Ilinnera (Figure 15; camp 5) was carried out between the 8th of August and the 12th of August with ABJ. The last days of fieldwork except

one day in basecamp were with ABJ in the area of the Johan Petersen Intrusion. The day in the basecamp was spent on a small reconnaissance trip around Kuummiut by zodiac with Trygvi Bech Ártung, Jonas Tusch and Tomas Næraa.

Fieldwork and observations – Auppaluttoq

Observations at Auppaluttoq were mainly done in north-south traverses perpendicular to the main strike of the penetrative foliation in the metamorphic rocks. The main focus was on the rocks of the Kuummiut unit and Helheim unit (Kolb 2014) since they locally contain graphite. The Kuummiut unit is characterized by paragneiss and schist containing quartz, biotite, muscovite, feldspar and minor garnet, kyanite, sillimanite and graphite (Kolb 2014). The Helheim unit consists of meta-diorite, amphibolite, marble, quartzite and garnet-biotite gneiss (Kolb 2014).

The highest estimated grade of graphite (> 20 vol.%) occurs at locality 14NRS022, 14NRS065, 14NRS123 and 14NRS127 (Figure 16). They are all located in the central to southern parts of Auppaluttoq. The northern part of Auppaluttoq was investigated from camp 2 while the central and southern part was investigated from camp 1 and 3 together with helicopter support for reconnaissance, see Figure 16.

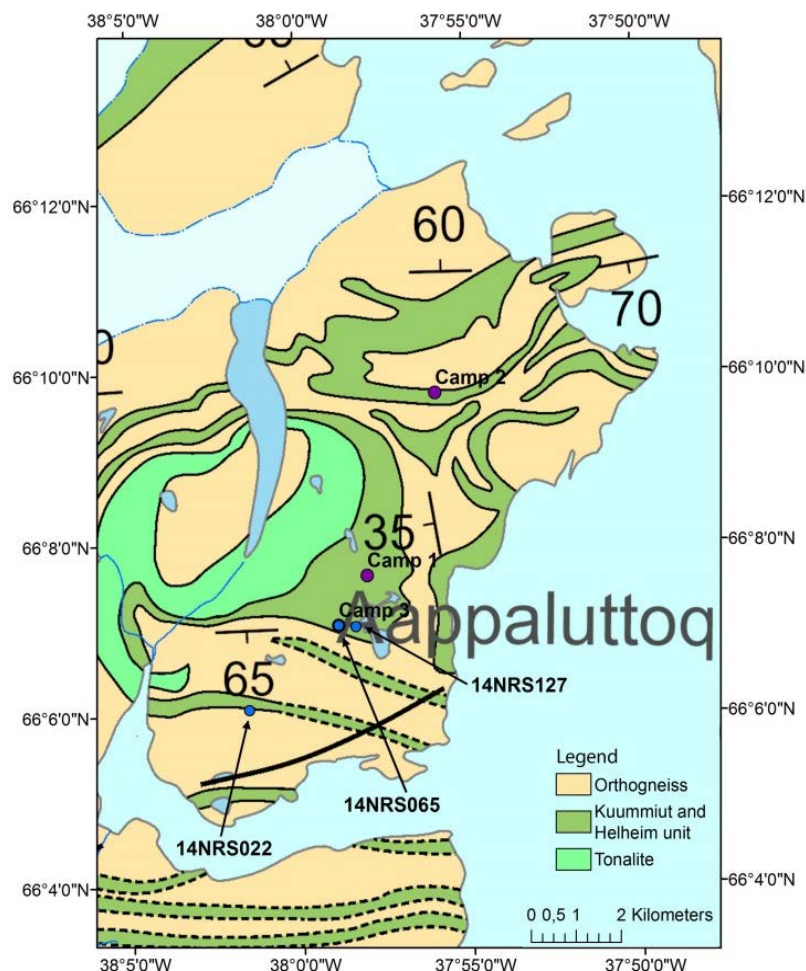


Figure 16. Geological map of Auppaluttoq, north-western corner of Sermilik Isfjord, showing the location of high-grade graphite mineralization (zoom in of A in Figure 15).



Figure 17. Overview of supergene limonite alteration zone in central Auppaluttoq. The zone is approx. 300 m wide and surrounded by orthogneiss.

The rocks of the Kuummiut unit and Helheim unit have undergone strong supergene alteration, altering the rocks to loose limonite gravel on the surface (Figure 17). The areas with limonite gravel often contain graphite flakes which seem to be the second main component of the gravel after limonite. Supergene limonite alteration zones are most prominent in the central and southern part of the area. In the northern part the rocks are dominated by fresh amphibolite, which has undergone less strong supergene alteration. Amphibolite and biotite schist form fragments in the limonite-graphite gravel, which locally contains gossans from sulfide weathering. The rocks have been cut by numerous shear zones of different scale. Graphite is often concentrated in these shear zones. Within the largest supergene alteration zone in the area, high-grade graphite mineralization occurs at locality 14NRS065, 14NRS123 and 14NRS127. Graphite is mainly in flakes of up to 5 mm together with biotite and quartz \pm garnet. The highest grades observed in the area are at 50 vol.% graphite in locality 14NRS065. The host rock for low- (1–10 vol.%) to medium-grade (10–20 vol.%) graphite mineralization is mainly biotite schist and amphibole schist.

The richest graphite ore is found at locality 14NRS065, where it occurs as two 20 cm to 50 cm wide and 2–3 m long, massive graphite seams in amphibolite (Figure 18). The seams crop out as lenses in the schist for about 20 m along strike. The graphite at locality 14NRS123 occurs as bands within biotite schist, while the graphite at locality 14NRS127 occurs in amphibole schist.

Apart from biotite and amphibole schist, graphite occurs in smaller centimeter to meter scale supergene alteration zones within orthogneiss; this can be seen at locality 14NRS022.



Figure 18. 50 cm wide graphite seam within amphibolite at locality 14NRS065.



Figure 19. Approx. 1.5 m wide graphite band between amphibolite (lower part of the picture) and gneiss (upper part of the picture) at locality 14NRS022.

The graphite ore is approx. 20 cm to 1.5 m wide and can be followed for around 20 m along strike (Figure 19). The ore contains mainly biotite and quartz with the graphite. A large amount of up to 30 m x 50 m pegmatite to pegmatitic granite bodies intrude the orthogneiss and rocks of the Kuummiut unit in the central and southern part of Auppaluttoq,

with decreasing abundance in the northern part. In the central part they often occur in the supergene alteration zones with graphite-bearing biotite and amphibole schist, but not necessarily directly adjacent to the ore. Pegmatites do not show signs of deformation, postdating the foliation in the wall rocks. Some pegmatites contain traces of graphite, which is either xenolithic material or graphite mineralization postdating pegmatite emplacement.

There is a coincidence of intense graphite mineralization and pegmatites in the southern and central parts of Auppaluttoq, which may suggest a genetic relationship with the formation of granitic melts, hydrothermal alteration and graphite mineralization.

Fieldwork and observations – Kangikajik

Fieldwork at Kangikajik was carried out from camp 4 (Figure 20). The observations were also done along traverses across graphite mineralization, which were chosen after previous investigations of Kalvig (1992). The rocks of the Kuummiut unit (Kolb 2014) at Kangikajik have been interfolded with amphibolites and gneisses in tight to isoclinal folds. They have undergone strong supergene alteration forming limonite at the surface. The rocks are similar to Auppaluttoq, containing mainly biotite schist but also banded iron formation (BIF) and quartzite. Only few, narrow pegmatite bodies cut the wall rocks, they are undeformed.

Seven areas with high-grade graphite mineralization were observed: 14NRS172, 14NRS173, 14NRS177, 14NRS185, 14NRS202, 14NRS208 and 14NRS212 (Fig. 6). Graphite grades of up to 60 vol.% were observed at locality 14NRS173, 14NRS202 and 14NRS208.

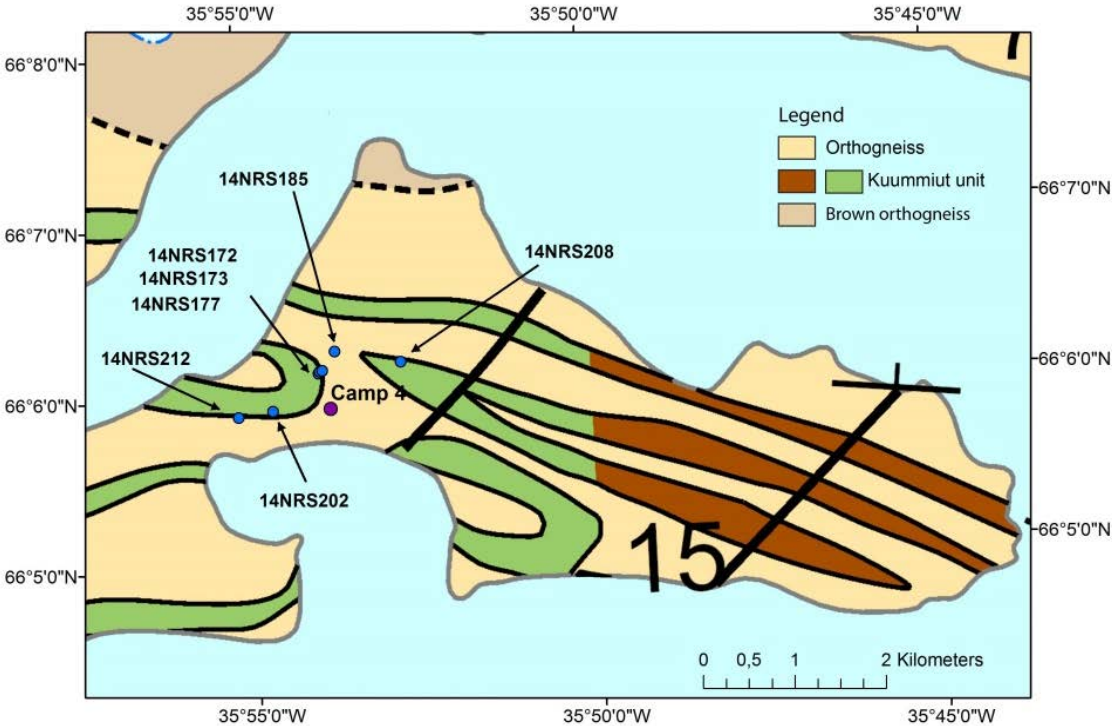


Figure 20. Geological map of Kangikajik, showing the location of high-grade graphite mineralization (zoom in of K in Figure 15).

Graphite mineralization occurs together with mainly biotite and quartz ± garnet. Lower concentrations of graphite occur mainly in biotite schist, where the content varies from 1 vol.%

to 20 vol.%. Graphite is mainly flaky, with sizes up to 5 mm, but also occurs as very fine-grained patches.

Shear zones of different scale cut through the rocks of the Kuummiut unit (Kolb 2014). Graphite is often concentrated within these shear zones forming shear bands around host rock fragments.

This is for example seen at locality 14NRS208 (Figure 21), where graphite occurs in a shear zone. The graphite drapes around boudins of garnet-hornblendite, paragneiss and BIF. The graphite-rich shear zone can be followed for around 200 m.



Figure 21. *Locality 14NRS208. Graphite seams draping around boudins of BIF. The hammer lies on the boundary between BIF boudin and garnet-hornblendite boudin.*

In places graphite occurs as seams in amphibolite without any apparent alteration to the amphibolite. This has especially been observed at locality 14NRS172 and 14NRS173 (Figure 22). At these localities, three 20 cm to 70 cm wide graphite seams occur within the hinge zone of a folded amphibolite. At locality 14NRS177 graphite schist occurs as bands at the contact of amphibolite and paragneiss and within the paragneiss. The bands are 20 cm wide and can be followed for up to 50 m.



Figure 22. *Approximately 50 cm wide graphite band within folded amphibolite at locality 14NRS173. The amphibolite hasn't undergone strong alteration.*

At locality 14NRS185 graphite occurs in graphite-biotite schist which forms an S-fold within amphibolite (Figure 23).



Figure 23. *Graphite-bioite schist occurring as an S-fold within amphibolite.*

Graphite does also occur as almost pure graphite ore as seen at locality 14NRS202 (Figure 24), where two graphite bands occurs between pegmatite and quartz-plagioclase-biotite schist. One of the bands is 40 cm wide and occurs between pegmatite and quartz-plagioclase-biotite schist, the other band is 3-4 m wide and occurs in quartz-plagioclase-biotite schist. The bands can be followed for around 20 m along strike.



Figure 24. *Three to four mete wide graphite band at locality 14NRS202. The band contained a small tight fold.*

Fieldwork and observations – Nuuk-Ilinna

Fieldwork at Nuuk-Ilinna was carried out from camp 5 (see Figure 26). Based on information from Troels F.D. Nielsen, Senior Research Scientist at GEUS, this area was used as graphite source for the local population in the earlier 20st century. The camp was located in a valley and fieldwork was done along the valley towards the west and up the mountain sides towards the north.

The area contains few exposed rocks of the Kuummiut unit (Kolb 2014) surrounded by orthogneiss and amphibolite (Figure 25).



Figure 25. *Supergene altered rocks of the Kuummiut unit cropping out surrounded by orthogneiss at Nuuk-Ilinna.*

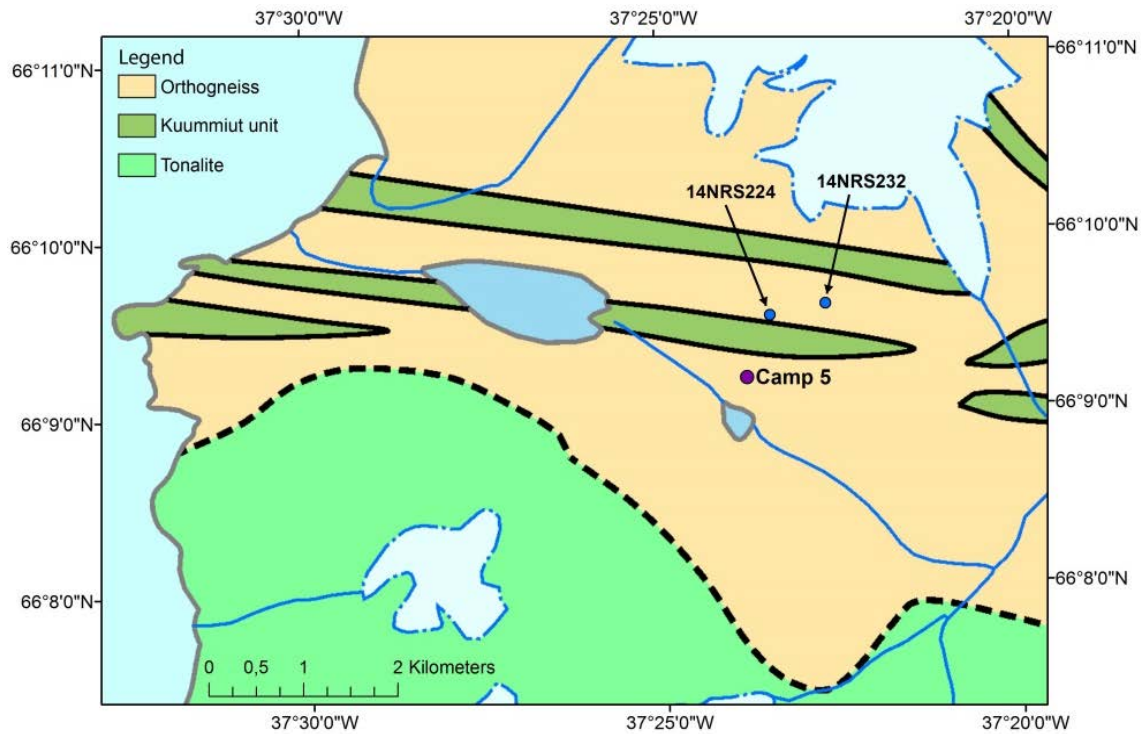


Figure 26. Geological map of Nuuk-Ilinnera showing the location of high-grade graphite mineralization (zoom in of N in Figure 15).

The rocks of the Kuummiut unit underwent intense supergene alteration as at Auppaluttoq and Kangikajik (Figure 27). The rocks are aligned along a general West-East strike with smaller internal S- and Z-folds. A few pegmatite dikes are observed, which show no apparent spatial relation to the graphite mineralization. Graphite was found in supergene alteration zones, mainly hosted by biotite and quartz schist. It occurs mainly as flakes up to 4 mm together with quartz and biotite \pm garnet. Two localities with high-grade graphite mineralization were observed: 14NRS224 and 14NRS232 (Figure 26). The highest graphite content was estimated to around 40 vol.% at locality 14NRS224.

At locality 14NRS224 the graphite is hosted by approximately 20 cm to 70 cm wide quartz-biotite-chlorite schist. The graphite content varies along strike with concentrations down to 2 vol.%. Traces of pyrite and other sulfides are also found in the schist. At locality 14NRS232 graphite ore occurs as 10 cm wide bands in a shear zone. The ore contains quartz, plagioclase, biotite and graphite. It is compositional banded with less graphite in the more quartz-rich bands.



Figure 27. *Strongly supergene altered rocks of the Kuummiut unit at Nuuk-Ilinnera.*

References

- Kalvig, P., Bohse, H., 1992. Geologisk undersøgelse af grafitforekomster Kangikajik, Tasilaq Kommune. Rapport Grønlands Geologiske Undersøgelse 21317.
- Kolb, J., 2014. Structure of the Palaeoproterozoic Nagssugtoqidian Orogen, South-East Greenland: Model for tectonic evolution. *Precambrian Research* 255, 809-822.

Appendix A. Camp locations

Camp	Location	Latitude	Longitude	Team	Dates
Camp 1	Auppaluttoq – center	66.12718	37.9669	NRS, LBA	16.07.14-23.07.14
Camp 2	Auppaluttoq – north	66.16272	37.9322	NRS, LBA	23.07.14-27.07.14
Camp 3	Auppaluttoq – south	66.11750	37.98131	NRS, LBA	27.07.14-01.08.14
Camp 4	Kangikajik	66.09855	35.89673	NRS, LBA, JKOL	01.08.14-08.08.14
Camp 5	Nuuk-Ilinnera	66.15298	37.39674	NRS, JAB	08.08.14-12.08.14

Appendix B. Locality list (from aFieldwork)

Locality	Date	Lat. (N)	Long. (W)
14NRS001	16.07.14	66.12714	37.96503
14NRS002	16.07.14	66.12687	37.96514
14NRS003	17.07.14	66.12704	37.96789
14NRS004	17.07.14	66.12696	37.96858
14NRS005	17.07.14	66.12672	37.96820
14NRS006	17.07.14	66.12706	37.96991
14NRS007	17.07.14	66.12651	37.96931
14NRS008	17.07.14	66.12624	37.96830
14NRS009	17.07.14	66.12560	37.96748
14NRS010	17.07.14	66.12553	37.96728
14NRS011	17.07.14	66.12563	37.96954
14NRS012	17.07.14	66.12534	37.96473
14NRS013	17.07.14	66.12424	37.97113
14NRS014	18.07.14	66.09220	38.04185
14NRS015	18.07.14	66.09223	38.04165
14NRS016	18.07.14	66.09211	38.04116
14NRS017	18.07.14	66.09265	38.03677
14NRS018	18.07.14	66.09463	38.03505
14NRS019	18.07.14	66.09479	38.03342
14NRS020	18.07.14	66.09639	38.03356
14NRS021	18.07.14	66.09854	38.03231
14NRS022	18.07.14 20.07.14	66.10116	38.02574
14NRS023	19.07.14	66.12665	37.36749
14NRS024	19.07.14	66.12621	37.96624
14NRS025	19.07.14	66.12626	37.96667
14NRS026	19.07.14	66.12560	37.96547
14NRS027	19.07.14	66.12525	37.96546
14NRS028	19.07.14	66.12506	37.96593
14NRS029	19.07.14	66.12457	37.96657
14NRS030	19.07.14	66.12285	37.96925
14NRS031	19.07.14	66.11961	37.96975
14NRS032	19.07.14	66.11929	37.96980
14NRS033	19.07.14	66.11910	37.97018
14NRS034	19.07.14	66.11902	37.97055
14NRS035	19.07.14		
14NRS036	19.07.14	66.11813	37.97177
14NRS037	19.07.14	66.10223	38.02382
14NRS038	20.07.14	66.10351	38.02173
14NRS039	20.07.14	66.10387	38.02188
14NRS040	20.07.14	66.10786	38.01700
14NRS041	20.07.14	66.10822	38.01699
14NRS042	20.07.14	66.10848	38.01868
14NRS043		66.12749	37.97047
14NRS044		66.12780	37.97090
14NRS045		66.12813	37.97061
14NRS046		66.12821	37.97095
14NRS047		66.12866	37.97178
14NRS048	21.07.14	66.12871	37.97052
14NRS049	21.07.14	66.12966	37.97211
14NRS050	21.07.14	66.12923	37.97434
14NRS051	21.07.14	66.12975	37.97456
14NRS052	21.07.14	66.12962	37.97501
14NRS053	21.07.14	66.12960	37.97545

Locality	Date	Lat. (N)	Long. (W)
14NRS054		66.11720	37.97264
14NRS055		66.11727	37.97363
14NRS056			
14NRS057		66.11713	37.97507
14NRS058		66.11615	37.97512
14NRS059		66.11587	37.97481
14NRS060	22.07.14	66.11578	37.97472
14NRS061	22.07.14	66.11598	37.97594
14NRS062	22.07.14	66.11691	37.97782
14NRS063	22.07.14	66.11751	37.98540
14NRS064		66.11700	37.98211
14NRS065	28.07.14	66.11750	37.98131
14NRS066		66.12200	37.96801
14NRS067		66.14275	37.99223
14NRS068	23.07.14	66.08807	38.04520
14NRS069		66.16333	37.93245
14NRS070		66.16335	37.93251
14NRS071		66.16354	37.93245
14NRS072		66.16382	37.93383
14NRS073		66.16379	37.93626
14NRS074		66.16417	37.93674
14NRS075		66.16503	37.93869
14NRS076		66.16227	37.93238
14NRS077	24.07.14	66.16189	37.93223
14NRS078	24.07.14	66.16177	37.93165
14NRS079	24.07.14	66.16072	37.93163
14NRS080	24.07.14	66.15965	37.93089
14NRS081	24.07.14	66.15866	37.92938
14NRS082		66.16245	37.93163
14NRS083		66.16240	37.93501
14NRS084	25.07.14	66.16247	37.93709
14NRS085	25.07.14	66.16264	37.93813
14NRS086	25.07.14	66.16235	37.94070
14NRS087	25.07.14	66.16345	37.94528
14NRS088	25.07.14	66.16318	37.94923
14NRS089	25.07.14	66.16335	37.94910
14NRS090	25.07.14	66.16430	37.94927
14NRS091	25.07.14	66.16492	37.95059
14NRS092	25.07.14	66.16488	37.95031
14NRS093	25.07.14	66.16228	37.95346
14NRS094	25.07.14	66.16050	37.95521
14NRS095	25.07.14	66.16058	37.95377
14NRS096	25.07.14	66.16018	37.95064
14NRS097		66.16084	37.94412
14NRS098		66.16095	37.93841
14NRS099		66.16331	37.93155
14NRS100		66.16407	37.92971
14NRS101		66.16411	37.92920
14NRS102		66.16428	37.92938
14NRS103	26.07.14	66.16528	37.92956
14NRS104		66.16070	37.93052
14NRS105			
14NRS106		66.16669	37.93112
14NRS107		66.16690	37.93099

Locality	Date	Lat. (N)	Long. (W)
14NRS108		66.16704	37.93147
14NRS109		66.16715	37.93200
14NRS110		66.16715	37.93118
14NRS111		66.16677	37.93485
14NRS112		66.16858	37.92780
14NRS113		66.16950	37.92276
14NRS114		66.16810	37.92160
14NRS115		66.16650	37.92343
14NRS116		66.16338	37.92737
14NRS117		66.11851	37.97733
14NRS118	28.07.14	66.11885	37.97767
14NRS119	28.07.14	66.11964	37.97596
14NRS120	28.07.14	66.11867	37.97774
14NRS121	28.07.14	66.11802	37.97840
14NRS122	28.07.14	66.11759	37.97959
14NRS123	28.07.14	66.11863	37.98286
14NRS124		66.10619	38.06516
14NRS125	29.07.14	66.11776	37.97511
14NRS126	29.07.14	66.11762	37.97479
14NRS127	29.07.14	66.11722	37.97283
14NRS128	29.07.14	66.11710	37.97240
14NRS129	29.07.14	66.11694	37.97113
14NRS130	30.07.14	66.11886	37.97932
14NRS131	30.07.14	66.12000	37.98009
14NRS132	30.07.14	66.11898	37.98277
14NRS133	30.07.14	66.11873	37.98220
14NRS134	30.07.14	66.11771	37.98313
14NRS135	30.07.14	66.11728	37.98686
14NRS136			
14NRS137			
14NRS138		66.11720	37.98959
14NRS139		66.11643	37.98982
14NRS140		66.11709	37.99228
14NRS141		66.11906	38.00713
14NRS142	31.07.14	66.11679	37.96867
14NRS143	31.07.14	66.11571	37.96811
14NRS144	31.07.14	66.11604	37.96595
14NRS145	31.07.14	66.11675	37.96399
14NRS146	31.07.14	66.11696	37.96075
14NRS147	31.07.14	66.11773	37.95442
14NRS148	31.07.14	66.11814	37.95209
14NRS149	31.07.14	66.11940	37.95248
14NRS150	31.07.14	66.12005	37.95211
14NRS151	31.07.14	66.12005	37.95211
14NRS152	31.07.14	66.12113	37.35338
14NRS153	31.07.14	66.12142	37.94969
14NRS154	31.07.14	66.12308	37.95027
14NRS155	31.07.14	66.12360	37.95126
14NRS156	31.07.14	66.12439	37.95565
14NRS157	31.07.14	66.12487	37.95754
14NRS158	31.07.14	66.12472	37.95877
14NRS159	31.07.14	66.12451	37.95864
14NRS160	02.08.14	66.09855	35.89673
14NRS161	02.08.14	66.09868	35.89691
14NRS162	02.08.14	66.09864	35.89845
14NRS163	02.08.14	66.09878	35.89995

Locality	Date	Lat. (N)	Long. (W)
14NRS164	02.08.14	66.09886	35.90076
14NRS165	02.08.14	66.09987	35.90139
14NRS166	02.08.14	66.09989	35.90001
14NRS167	02.08.14	66.10062	35.89989
14NRS168	02.08.14	66.10100	35.89900
14NRS169	02.08.14	66.10126	35.89878
14NRS170	02.08.14	66.10158	35.89864
14NRS171	02.08.14	66.10202	35.89877
14NRS172	02.08.14	66.10204	35.89924
14NRS173	02.08.14	66.10221	35.89896
14NRS174	02.08.14	66.10251	35.89739
14NRS175	02.08.14	66.10283	35.89732
14NRS176	02.08.14	66.10203	35.89930
14NRS177	03.08.14	66.10231	35.89830
14NRS178	03.08.14	66.10248	35.89747
14NRS179	03.08.14	66.10250	35.89110
14NRS180	03.08.14	66.10283	35.89683
14NRS181	03.08.14	66.10291	35.89678
14NRS182	03.08.14	66.10315	35.89638
14NRS183	03.08.14	66.10335	35.89631
14NRS184	03.08.14	66.10362	35.89561
14NRS185	03.08.14	66.10411	35.89513
14NRS186	03.08.14	66.10419	35.89486
14NRS187	03.08.14	66.10444	35.89422
14NRS188	03.08.14	66.10477	35.89373
14NRS189	03.08.14	66.10506	35.89361
14NRS190	04.08.14	66.08535	36.05211
14NRS191	04.08.14	66.09422	35.81690
14NRS192	04.08.14	66.08763	35.89300
14NRS193	05.08.14	66.09879	35.90194
14NRS194	05.08.14	66.09870	35.90547
14NRS195	05.08.14	66.09910	35.90683
14NRS196	05.08.14	66.09853	35.90754
14NRS197	05.08.14	66.09847	35.90986
14NRS198	05.08.14	66.09858	35.90903
14NRS199	05.08.14	66.09856	35.90953
14NRS200	05.08.14	66.09862	35.91035
14NRS201	05.08.14	66.09856	35.91061
14NRS202	05.08.14	66.09854	35.91069
14NRS203	06.08.14	66.09869	35.89395
14NRS204	06.08.14	66.09886	35.89374
14NRS205	06.08.14	66.09912	35.89289
14NRS206	06.08.14	66.09923	35.88909
14NRS207	06.08.14	66.10263	35.87915
14NRS208	06.08.14	66.10282	35.87923
14NRS209	06.08.14	66.09915	35.91416
14NRS210	07.08.14	66.09895	35.91580
14NRS211	07.08.14	66.09805	35.91867
14NRS212	07.08.14	66.09808	35.91910
14NRS213	07.08.14	66.09799	35.92323
14NRS214	07.08.14	66.09844	35.93020
14NRS215	09.08.14	66.15298	37.39674
14NRS216	09.08.14	66.15368	37.39613
14NRS217	09.08.14		
14NRS218	09.08.14	66.15535	37.39532
14NRS219	09.08.14	66.15595	37.39456

Locality	Date	Lat. (N)	Long. (W)
14NRS220	09.08.14	66.15622	37.39506
14NRS221	09.08.14	66.15707	37.39471
14NRS222	09.08.14	66.15797	37.39269
14NRS223	09.08.14	66.15817	37.39181
14NRS224	09.08.14	66.15878	37.39100
14NRS225	10.08.14	66.15911	37.39206
14NRS226	10.08.14	66.15420	37.39245
14NRS227	10.08.14	66.15440	37.39194
14NRS228	10.08.14	66.15726	37.38256
14NRS229	10.08.14	66.15871	38.37899
14NRS230	10.08.14	66.15904	37.37936
14NRS231	10.08.14	66.15947	37.37873
14NRS232	10.08.14	66.15979	37.37793
14NRS233	10.08.14	66.15517	37.40791
14NRS234	11.08.14	66.16005	37.40139
14NRS235	11.08.14	66.16017	37.40149
14NRS236	11.08.14	66.16099	37.39975
14NRS237	11.08.14	66.16165	37.39611
14NRS238	11.08.14	66.16217	37.39442
14NRS239	11.08.14	66.15594	37.39880
14NRS240	12.08.14	66.04505	38.01377
14NRS241	15.08.14	65.73440	38.44471
14NRS242	22.08.14	65.56026	37.05087

Appendix C. Sample details (from aFieldwork)

Locality no.	GEUS no.	Description	Locality name	Lat. (N)	Long. (W)	Purpose					Comment
						A	B	C	D	E	
14NRS006	563201	Banded gneiss	Auppaluttoq	66.12706	37.96991	x		x			Banded gneiss intruded by granite, strongly grt porphyryblastic
14NRS010	563202	Garnet gneiss	Auppaluttoq	66.12553	37.96728						Garnet porphyryblastic gneiss
14NRS012	563203	Garnet qtz vein	Auppaluttoq	66.12534	37.96473						Garnet quartz vein
14NRS013	563204	Granite	Auppaluttoq	66.12424	37.97113						Fresh unaltered
14NRS013	563205	Garnet qtz vein	Auppaluttoq	66.12425	37.97112	x		x			Garnet rich quartz vein within granite body
14NRS013	563206	Garnet qtz vein	Auppaluttoq	66.12423	37.97116	x			x		Garnet rich vein in the hydrothermal gossan like graphite zone
14NRS013	563207	Gossan	Auppaluttoq	66.12422	37.97117			x	x		Gossan rock from graphite rich zone
14NRS013	563208	Granite	Auppaluttoq	66.12424	37.97115						Garnets assemblage in granite
14NRS013	563209	Grp sample	Auppaluttoq	66.12421	37.97117				x		Grp samples from graphite rich zone
14NRS013	563210	Hematite sand	Auppaluttoq	66.12419	37.97106				x		Hematite rich grp samples from the graphite rich zone
14NRS013	563211	Amphibolite	Auppaluttoq	66.12415	37.97106	x		x	x		Amphibolite
14NRS017	563212	Hematite sand	Auppaluttoq	66.09265	38.03661						Hematite sample rich in graphite flakes
14NRS017	563213	Hematite sand	Auppaluttoq	66.09265	38.03661				x		Graphite rich hematite sand
14NRS017	563214	Granite dike	Auppaluttoq	66.09266	38.03650						Granite dike
14NRS017	563215	Amphibolite	Auppaluttoq	66.09266	38.03671						Amphibolite
14NRS020	563216	Banded gneiss	Auppaluttoq	66.09812	38.03219	x		x			Banded gneiss
14NRS020	563217	Amphibolite	Auppaluttoq	66.09813	38.03223	x		x			Amphibolite interbedded with the banded gneiss
14NRS021	563218	Amphibolite	Auppaluttoq	66.09854	38.03231						Amphibolite with elongated plg aggregates
14NRS022	563219	Amphibolite	Auppaluttoq	66.10116	38.02574						Amphibolite from contact next to granite
14NRS022	563220	Gneiss	Auppaluttoq	66.10116	38.02574						Gneiss next to amphibolite contact
14NRS022	563221	Gneiss	Auppaluttoq	66.10113	38.02569						Gneiss next to contact with graphite mineralization
14NRS022	563222	Graphite mineralization	Auppaluttoq	66.10113	38.02569	x	x		x		Graphite mineralization
14NRS022	563223	Graphite mineralization	Auppaluttoq	66.10113	38.02569				x		Graphite mineralization
14NRS022	563224	Gneiss	Auppaluttoq	66.10109	38.02565	x		x			Gneiss overlying graphite mineralization
14NRS022	563225	Graphite mineralization	Auppaluttoq	66.10113	38.02380				x		Graphite mineralized layer in contact with amphibolite and gneiss
14NRS022	563226	Graphite	Auppaluttoq	66.10106	38.02424				x		Graphite
14NRS022	563227	Graphite mineralization	Auppaluttoq	66.10102	38.02439				x		Graphite mineralization
14NRS023	563228	Schist	Auppaluttoq	66.12666	37.96728				x		Garnet rich biotite schist altered
14NRS023	563229	Schist	Auppaluttoq	66.12665	37.36749				x		Biotite schist with trace graphite
14NRS023	563230	Schist	Auppaluttoq	66.12665	37.36749				x		Graphite rich biotite schist

Locality no.	GEUS no.	Description	Locality name	Lat. (N)	Long. (W)	Purpose					Comment
						A	B	C	D	E	
14NRS023	563231	Pegmatitic granite	Auppaluttoq	66.12665	37.36749			x	x		Pegmatite granite with traces of graphite
14NRS026	563232	Garnet gneiss	Auppaluttoq	66.12560	37.96547	x		x			Garnet-biotite gneiss with maybe two generations of garnet
14NRS032	563233	Schist	Auppaluttoq	66.11929	37.96980	x			x		Hydrothermally altered graphite bearing schist
14NRS032	563234	Granite	Auppaluttoq	66.11929	37.96980						Granite next to graphite schist with garnets
14NRS034	563235	Schist	Auppaluttoq	66.11902	37.97055				x		Graphite bearing hydrothermally altered schist
14NRS036	563236	Gossan	Auppaluttoq	66.11813	37.97177			x			Gossan
14NRS022	563237	Banded gneiss	Auppaluttoq	66.10101	38.02557						Banded gneiss next to graphite mineralization
14NRS038	563238	Qtz vein	Auppaluttoq	66.10351	38.02173						Qtz vein next to granite
14NRS038	563239	Qtz vein	Auppaluttoq	66.10357	38.02005						Qtz vein with green mineral maybe an amphibole
14NRS041	563240	Hematite sand	Auppaluttoq	66.10822	38.01699				x		Hematite sand with graphite
14NRS042	563241	Graphite schist	Auppaluttoq	66.10848	38.01868				x		Graphite schist
14NRS042	563242	Garnet schist	Auppaluttoq	66.12749	37.97047	x			x		Sheared garnet schist
14NRS048	563243	Graphite schist	Auppaluttoq	66.12871	37.97052				x		Graphite schist within hydrothermal zone
14NRS053	563244	Graphite schist	Auppaluttoq	66.12960	37.97545				x		Graphite schist with large graphite flakes
14NRS048	563245	Granite	Auppaluttoq	66.12871	37.97052						Granite block within graphite schist in hydrothermal zone
14NRS053	563246	Pegmatitic granite	Auppaluttoq	66.11710	37.97230						Pegmatite vein within the graphite schist
14NRS053	563247	Graphite schist	Auppaluttoq	66.11710	37.97230				x		Graphite schist
14NRS060	563248	Graphite schist	Auppaluttoq	66.11578	37.97472				x		Graphite schist rich in flakes
14NRS062	563249	Graphite schist	Auppaluttoq	66.11691	37.97782				x		Graphite schist
14NRS063	563250	Hematite sand	Auppaluttoq	66.11751	37.98540						Traverse through graphite rich hematite sand
14NRS068	563251	Graphite schist	Auppaluttoq	66.08807	38.04520				x		Graphite schist layer within amphibolite
14NRS077	563252	Graphite schist	Auppaluttoq	66.16189	37.93223				x		Graphite bearing schist
14NRS081	563253	Graphite schist	Auppaluttoq	66.15866	37.92938				x		Graphite schist
14NRS084	563254	Granitic gneiss	Auppaluttoq	66.16247	37.93709						Granitic gneiss
14NRS084	563255	Pegmatite	Auppaluttoq	66.16247	37.93709						Pegmatite vein with possible beryl
14NRS088	563256	Kyanite-silimanite gneiss	Auppaluttoq	66.16318	37.94923						Kyanite-silimanite gneiss
14NRS096	563257	Graphite schist	Auppaluttoq	66.16018	37.95064				x		Graphite schist within rust zone
14NRS103	563258	Graphite schist	Auppaluttoq	66.16528	37.92956				x		Graphite schist
14NRS103	563259	Garnet vein	Auppaluttoq	66.16528	37.92956						Garnet vein
14NRS103	563260	Mafic banded gneiss	Auppaluttoq	66.16528	37.92956						Mafic banded gneiss
14NRS118	563261	Graphite schist	Auppaluttoq	66.11885	37.97767				x		Altered mafic gneiss with 5% graphite
14NRS122	563262	Garnet gneiss	Auppaluttoq	66.11759	37.97959						Garnet gneiss with kyanite and sillimanite
14NRS065	563263	Graphite layer	Auppaluttoq	66.11750	37.98131	x	x		x		Graphite seem

Locality no.	GEUS no.	Description	Locality name	Lat. (N)	Long. (W)	Purpose					Comment
						A	B	C	D	E	
14NRS065	563264	Amphibolite	Auppaluttoq	66.11750	37.98131	x		x			Amphibolite interlayered with graphite seem
14NRS065	563265	Graphite schist	Auppaluttoq	66.11750	37.98131				x		Graphite schist
14NRS123	563266	Graphite schist	Auppaluttoq	66.11863	37.98286		x		x		Graphite schist
14NRS123	563267	Amphibole schist	Auppaluttoq	66.11863	37.98286				x		Graphite amphibole schist
14NRS125	563268	Gravel	Auppaluttoq	66.11776	37.97511				x		Graphite rich gravel
14NRS127	563269	Graphite schist	Auppaluttoq	66.11722	37.97283		x		x		Graphite schist with 40-50% graphite
14NRS128	563270	Gravel	Auppaluttoq	66.11710	37.97240				x		Graphite rich gravel
14NRS129	563271	Graphite schist	Auppaluttoq	66.11694	37.97113				x		Reference sample of graphite and amphibole schist
14NRS130	563272	Pegmatite	Auppaluttoq	66.11886	37.97932			x	x		Altered pegmatite
14NRS130	563273	Schist	Auppaluttoq	66.11886	37.97932				x		Altered schist
14NRS133	563274	Pegmatite	Auppaluttoq	66.11873	37.98220				x		Altered pegmatite with 10-15% graphite
14NRS134	563275	Pegmatite	Auppaluttoq	66.11771	37.98313						Pegmatite with strange mineral
14NRS135	563276	Biotite schist	Auppaluttoq	66.11728	37.98689				x		Graphite biotite schist. 0-20% graphite. Reference sample
14NRS143	563277	Biotite schist	Auppaluttoq	66.11571	37.96811	x		x	x		Biotite schist with 5-10% graphite. Reference sample
14NRS151	563278	Biotite schist	Auppaluttoq	66.12005	37.95211				x		Biotite schist with 2-5% graphite. Reference sample
14NRS152	563279	Biotite schist	Auppaluttoq	66.12113	37.35338				x		Biotite schist with 10-15% graphite
14NRS153	563280	Biotite schist	Auppaluttoq	66.12142	37.94969				x		Biotite schist with 15-20% graphite
14NRS167	563281	Garnet Qtz vein	Kangikajik	66.10062	35.89989						Garnet-quartz-biotite vein
14NRS168	563282	Graphite schist	Kangikajik	66.10100	35.89900				x		Graphite schist with 5-10% graphite.
14NRS172	563283	Graphite schist	Kangikajik	66.10204	35.89924		x	x	x	x	Graphite schist with grt-graphite vein
14NRS173	563284	Graphite schist	Kangikajik	66.10221	35.89896	x		x	x		Graphite schist
14NRS173	563285	Amphibolite	Kangikajik	66.10221	35.89896	x		x			Amphibolite: Largest samples next to layer 1, smaller samples from hinge zone of the fold
14NRS173	563286	Graphite layer	Kangikajik	66.10221	35.89896				x		Graphite layer 4
14NRS177	563287	Graphite layer	Kangikajik	66.10231	35.89830		x		x		Graphite layer 1
14NRS185	563288	Graphite schist	Kangikajik	66.10411	35.89513		x		x		Graphite schist with Qtz and white material + hem altered schist with grt pseudomorphs
14NRS190	563289	Biotite schist	Kangikajik	66.08535	36.05211			x	x		Biotite schist. Reference sample
14NRS195	563290	Garnet gneiss	Kangikajik	66.09910	35.90683	x		x	x		Garnet-sillimanite-graphite gneiss. Very altered
14NRS197	563291	Marble	Kangikajik	66.09847	35.90986	x		x			Marble looking rock
14NRS198	563292	BIF	Kangikajik	66.09858	35.90903	x		x			BIF + grunerite
14NRS202	563293	Pegmatite	Kangikajik	66.09854	35.91069	x		x			Pegmatite with possible cordierite on the edge of graphite layer
14NRS202	563294	Banded gneiss	Kangikajik	66.09854	35.91069	x		x			Banded gneiss on contact with graphite layer

Locality no.	GEUS no.	Description	Locality name	Lat. (N)	Long. (W)	Purpose					Comment
						A	B	C	D	E	
14NRS202	563295	Graphite layer	Kangikajik	66.09854	35.91069	x	x	x			Graphite sample within the thickest graphite layer close to the felsic bio schist
14NRS202	563296	Graphite layer	Kangikajik	66.09854	35.91069	x			x	x	Graphite sample from middle of the thickest graphite layer
14NRS202	563297	Graphite layer	Kangikajik	66.09854	35.91069				x		Graphite sample from the thinnest graphite layer
14NRS202	563298	Schist	Kangikajik	66.09854	35.91069	x			x		Qtz-plg-bio-schist between the two graphite layers
14NRS160	563299	Pegmatite	Kangikajik	66.09855	35.89673						Pegmatite
14NRS208	570401	Graphite schist	Kangikajik	66.10282	35.87923	x	x		x		Graphite schist from shear zone
14NRS208	570402	Graphite schist	Kangikajik	66.10282	35.87923				x		Graphite schist close to BIF boudin in shear zone
14NRS208	570403	Qtz vein	Kangikajik	66.10282	35.87923				x		Qtz vein between graphite schist and BIF boudin
14NRS208	570404	Graphite schist	Kangikajik	66.10282	35.87923	x	x		x		Graphite schist 200m N up from the other samples
14NRS212	570405	Biotite schist	Kangikajik	66.09808	35.91910		x		x		Qtz-bio-graphite schist. 30% graphite. Reference sample
14NRS213	570406	Biotite schist	Kangikajik	66.09799	35.92323			x	x		Bio-grt-qtz-schist in shear zone within banded amphibolite
14NRS213	570407	BIF	Kangikajik	66.09815	35.92381	x		x			BIF + grt-hematite
14NRS213	570408	Biotite schist	Kangikajik	66.09815	35.92381	x			x		Biotite schist with 5% graphite and possible hematite
14NRS213	570409	Biotite schist	Kangikajik	66.09844	35.92332				x		Bio-graphite schist with 5-10%
14NRS218	570410	Gneiss	Nuuk-Ilinnera	66.15535	37.39532	x			x		Qtz-plg-amp-gneiss. Maybe silicified
14NRS218	570411	Biotite schist	Nuuk-Ilinnera	66.15535	37.39532				x		Graphite-bio-schist with ca. 10% graphite
14NRS218	570412	Amphibolite	Nuuk-Ilinnera	66.15535	37.39532						Amphibolite with retrogressed garnets
14NRS220	570413	Qtz vein	Nuuk-Ilinnera	66.15622	37.39506				x		Qtz-bio-beryl vein with unknown possible plg
14NRS223	570414	qtz-bio-schist	Nuuk-Ilinnera	66.15817	37.39181	x			x		Qtz-bio-chl-mus-schist with 2-5% graphite
14NRS224	570415	Graphite schist	Nuuk-Ilinnera	66.15878	37.39100	x	x		x		Graphite-qtz-schist with 30-40% graphite
14NRS229	570416	Banded gneiss	Nuuk-Ilinnera	66.15871	38.37899						Banded gneiss sample for Leon
14NRS230	570417	Schist	Nuuk-Ilinnera	66.15904	37.37936				x		Rust coloured layer with up to 20% graphite in schist
14NRS232	570418	Qtz-schist	Nuuk-Ilinnera	66.15979	37.37793	x	x		x		Qtz-graphite schist with ca. 20-30% graphite and compositional banding
14NRS232	570419	Qtz-gossan band	Nuuk-Ilinnera	66.15979	37.37793				x		Qtz-gossan-band with 1-2% graphite
14NRS232	570420	Amphibolite	Nuuk-Ilinnera	66.15979	37.37793	x		x			Amphibolite with garnets
14NRS234	570421	Gneiss	Nuuk-Ilinnera	66.16005	37.40139	x					Sheared bio rich gneiss - close to being a schist with 1% graphite
14NRS235	570422	Pegmatite	Nuuk-Ilinnera	66.16017	37.40149						Pegmatite sample for Leon
14NRS238	570423	Gneiss?	Nuuk-Ilinnera	66.16217	37.39442	x		x			Light medium grained rock of mainly plg with some bio and possible tremolite
14NRS240	570424	qtz-bio-schist	Tasilarttik/South of Auppallutq	66.04505	38.01377		x		x		Qtz-bio-graphite schist with 10-15% graphite
14NRS242	570425	Biotite schist		65.56026	37.05087	x	x	x	x		Biotite schist

A – Thin section, B – Isotopes, C – Whole rock geochemistry, D – Graphite geochemistry, E – Liberation and grain size

Mineral potential of the Helheim supracrustal sequence and follow up on significant Ujarassiorit localities within the wider Kuummiut Terrane (DRO)

Introduction

This field report is made by Diogo Rosa, GEUS.

The fieldwork, carried out between July 28th and August 21st, was aimed at the reconnaissance of the mineral potential of specific areas of the Tasiilaq region. This was accomplished through:

- Evaluation of the mineral potential of the Helheim Unit supracrustal sequence (camp 1 through 4)
- Follow up on significant Ujarassiorit localities within the wider Kuummiut Terrane (out of basecamp and camp 5 and 6).

As part of the former objective, the types of mineralisation targeted, considering the reactive nature of marble horizons, included carbonate-hosted Zn-Pb mineralisation (akin to the mineralised Paleoproterozoic marbles of the Karrat Group, in Greenlands' East Coast), and possible skarn deposits (namely Au skarns).

Related to the latter objective, the focus was on possible Au quartz veins and/or Au skarns, whose potential presence is hinted by various Ujarassiorit samples with Au mineralisation.

Results

Evaluation of the mineral potential of the Helheim Unit supracrustal sequence (camp 1 through 4)

Carbonate hosted Zn-Pb

Around camp 1 through 4, while establishing a tectonostratigraphy of the Helheim supracrustal Unit, zinc zap solution was applied to weathered surfaces on calcitic marble out-crops of the Helheim Unit. This was done especially where there was evidence for deformation, brecciation, karstification, etc. Unfortunately no signs of zinc mineralisation were identified. Furthermore, the volume of the recognized marble horizons is relatively small, so that, even if these were mineralised, it is considered extremely unlikely that they would be of economic significance.

Au skarns

Whenever suitable locations were identified, panning was done, with subsequent evaluation of the obtained heavy mineral concentrate for gold. However, none of the pans yielded gold grains. Considering the unpredictable role of the glacial distribution of moraines, which are likely the source for subsequent fluvial reworking, this should not necessarily be taken as evidence for the absence of primary gold mineralisation in the area. Therefore, special attention was paid for other evidence, namely the presence of possible skarn assemblages.

Small garnet + diopside + plagioclase + quartz horizons or boudins were found within amphibolites, namely at Camp 1. These are likely reaction skarns resulting from the reaction of previously carbonatized amphibolites with locally derived silica (no magmatic input), but were sampled nevertheless. At Camp 3, however, along an amphibolite/pegmatite contact, the skarn assemblage also includes pyrite + pyrrhotite. Also at Camp 3, narrow (cm wide) skarn assemblages with garnet + diopside (actinolite) were identified and sampled along marble/pegmatite contacts. Considering the close spatial association between skarn assemblages and pegmatites, it is likely that some magmatic fluids were involved, but the volumes appear to have been small. At Camp 4, wide (m wide) skarn assemblages with garnet + actinolite (proximal) and quartz + actinolite + magnetite (distal) were recognized and sampled along intensely silicified marble/orthogneiss contacts, frequently intruded by pegmatite (including amazonite and magnetite). At this camp, coarse magnetite is also abundant in leucosome domains within the orthogneiss.

While working on the Helheim supracrustal Unit, some quartz veins were identified and sampled. At Camp 1, sheeted quartz veins with rusty selvages (N140, 70), and which have induced graphitization of the hosting marbles, were identified. At Camp 2, the marble graphitization is related to more subtle silicification, lacking well defined quartz veins. Finally, at Camp 3, a prominent N30 trending, 5-10 m wide, structure was identified. It was the focus of intense silicification and epidotization, with development of a chlorite + k-feldspar + pyrite + chalcopyrite assemblage along the contact with the hosting orthogneiss.

Follow up on significant Ujarassiorit localities within the wider Kuummiut Terrane (out of basecamp and camp 5 and 6)

With helicopter support the winner of two Ujarassiorit prizes, William Umerineq, showed the sampling location for his two winning samples. Sample 2008-483 (anomalous in PGE-Co-Cu), is located down from Glacier de France, while sample 11-092 (anomalous in Au, but oddly with little As or Ag! contamination?), is located at Augpalugtoq (Sermilik Fjord).

At the first locality a pegmatite lens was recognized. Within the pegmatite there is coarse calcite of uncertain origin (marble remnants within the hosting gneiss package? hydrothermal?), and along the contact between this calcite and the pegmatite a calc-silicate assemblage with epidote and green actinolite (after diopside?) developed, which locally includes sulfide pods that were submitted to the Ujarassiorit competition.

At the second locality, William showed a garnetite horizon. Considering the extent of garnetite, as well as the presence of possible veins, it was decided to establish Camp 5 at this location for more detailed reconnaissance. This work showed that, within yellow weathering graphitic micaschist, several discontinuous and foliation concordant garnetite bodies are present, probably the result of deformation and formation of boudins due to the garnetite (or its precursor? marble?) more competent behaviour. Several different levels of such boudins can either be tectonic repetitions or original. In some instances, but not always, the garnetite is closely related to subhorizontal pegmatite sheets, also dismembered by tectonism into boudins. While no sulfides were identified, the fact that William sample looks just like these garnetites led us to sample them extensively.

Further sampling was carried out on veins and veinlets that were identified around Camp 5. Two stand out, as they contain sulfides. One of these is located on a beach, right underneath where the Ujarassiorit sample has been collected (could the award-winning sample actually have been from the vein?). It is a pyrite and/or pyrrhotite bearing siliceous vein, ~15 cm thick and trending ~N190, 40, inducing graphitization of the hosting mica-schist (similar to what was documented at Camp 1). Another 10 cm wide quartz-sulfide vein, striking ~N205, 80 and hosted by pegmatite and paragneiss, was collected further south.

The collectors of Ujarassiorit samples 93-354, 00-099 and 07-065 (anomalous in Au) could not be contacted or brought to the field for assistance in finding exact sampling location. The two first samples are float and the latter is in situ but its precise location is unknown. The lack of accurate sampling locations, coupled with the fact that two of these samples are of float, suggested that, as a first approach, panning should be carried out. This was done with boat support, sailing around the island of Qianarteq and around the Ikateq peninsula, towards the Kârale Glacier. However, only two pans yielded a few very small gold grains. Despite the disappointing panning results, considering the uncertainty of its effectiveness in glaciated terrains, Camp 6 was established in the interior of Ikateq. At this location, a ~N170 striking, ~5 m thick quartz-epidote-k feldspar vein was identified and sampled. A couple of sulfide-rich boulders were also collected in the moraine, toward the north of camp.

Appendix A. Camp locations

Location	Name	Lat. (N)	Long. (W)	Dates	Participants
Camp 1	Midgårdgletscher East	66.3500	37.0839	29.-30.7.2014	DRO, KSZ, NTH
Camp 2	Midgårdgletscher West	66.3843	37.2656	31.7.2014	DRO, KSZ, NTH
Camp 3	Helheim Fjord	66.2538	37.9784	1.-3.8.2014	DRO, KSZ, NTH
Camp 4	Fenrisgletscher	66.3865	37.7279	4.-7.8.2014	DRO, KSZ
Basecamp	Kuummiut			8.-11.8.2014	DRO, MADP
Camp 5	Augpalugtoq	66.1164	37.9273	12.-14.8.2014	DRO, JPET, KIT
Camp 6	Ikateq	65.9966	36.6198	15.-19.8.2014	DRO, JPET

Partners

DRO – Diogo Rosa, GEUS

KSZ – Kristoffer Szilas, Columbia University, New York, USA

NTH – Nicolas Thebaud, Centre of Exploration Targeting, University of Western Australia

MADP – Majken D. Poulsen, GEUS

JPET – Jonas Petersen, Ministry of Mineral Resources, Government of Greenland

KIT – Kisser Thorsøe, GEUS

Appendix B. aFieldwork extraction report

GEUS no.	Lat. (N)	Long. (W)	Locality ID	Earth materials	Sample type	Purpose	Notes
566601	66.34901	37.1020	2014DRO003		Rock sample	Ore_Geology	
566602	66.34978	37.1082	2014DRO005		Rock sample	Ore_Geology	Silicified and epidotized amphibolite.
566603	66.36287	37.0968	2014DRO011		Rock sample	Ore_Geology	Diopside, gt, silica, plg boudin.
566604	66.36360	37.0962	2014DRO012		Rock sample	Ore_Geology	Gt, qz, plg, diopside horizon. Assemblage after amphibolite?
566605	66.36219	37.0973	2014DRO009		Rock sample	Ore_Geology	Slightly silicified and graphite enriched country rocks (mica schist/marble).
566606	66.36219	37.0973	2014DRO009		Rock sample	Ore_Geology	Intensively silicified and graphite enriched country rock.
566607	66.36219	37.0973	2014DRO009		Rock sample	Ore_Geology	Rusty vein selvage, with boxworks.
566608	66.36219	37.0973	2014DRO009		Rock sample	Ore_Geology	Channel sample across the sheeted qz vein, with graphite rich bands.
566609	66.38784	37.2712	2014DRO016	metamorphicgneiss (schist>1 cm)	Rock sample	Ore_Geology	Sulfide skarn float.
566618	66.14490	37.9722	2014DRO020		Rock sample	Ore_Geology	Fine garnetite, calcsilicate and graphite enriched layer.
566619	66.14541	37.9724	2014DRO021		Rock sample	Ore_Geology	Coarse garnetite.
566620	66.14541	37.9724	2014DRO021		Rock sample	Ore_Geology	Fine pyroxene garnetite. Px altered, boxworks.
566621	66.14555	37.9717	2014DRO022		Rock sample	Ore_Geology	Garnet pegmatite. Endoskarn?
566622	66.24966	37.9974	2014DRO025		Rock sample	Ore_Geology	Skarn
566623	66.24627	38.0124	2014DRO026		Rock sample	Ore_Geology	Diopside marble and pegmatite.
566624	66.27597	37.9488	2014DRO028		Rock sample	Ore_Geology	Py, cpy, kspar chloritite (after hb or Px?), on contact between N30 trending silica epidote vein and orthogneiss.
566625	66.27597	37.9488	2014DRO028		Rock sample	Ore_Geology	Qz epidote vein; more gray qz from core, brown qz further out and epidoterich green qz from the margin.
566626	66.38670	37.7111	2014DRO030				Silicified and calcsilicate horizons on contact.
566627	66.38697	37.7078	2014DRO031		Rock sample	Ore_Geology	Mt and silica band.
566628	66.38118	37.7196	2014DRO035				Amazonite pegmatite.
566629	66.37183	37.7178	2014DRO040		Stream Sediment		
566630	66.37260	37.7104	2014DRO041		Rock sample	Ore_Geology	Actinolite +epidote+ qz +mt horizon
566631	66.37953	37.7044	2014DRO044		Rock sample	Ore_Geology	Actinolite + epidote + qz+mt horizon
566632	65.89175	36.7244	2014DRO046		Heavy mineral	Ore_Geology	
566633	65.87215	36.6909	2014DRO047		Heavy mineral	Ore_Geology	
566634	65.83322	36.6560	2014DRO048		Heavy mineral	Ore_Geology	
566635	65.80443	36.6339	2014DRO049		Heavy mineral	Ore_Geology	

GEUS no.	Lat. (N)	Long. (W)	Locality ID	Earth materials	Sample type	Purpose	Notes
566636	65.87726	36.6122	2014DRO050		Heavy mineral	Ore_Geology	
566637	65.92103	36.5110	2014DRO051		Heavy mineral	Ore_Geology	Plenty of greenish silt (chlorite or epidote?).
566638	66.04339	36.5013	2014DRO052		Heavy mineral	Ore_Geology	Abundant gt.
566639	66.04350	36.5158	2014DRO053		Heavy mineral	Ore_Geology	Abundant gt
566640	66.05636	36.6095	2014DRO054		Heavy mineral	Ore_Geology	
566641	66.07722	36.5527	2014DRO055		Rock sample	Ore_Geology	Graphite bearing more leucocratic band within graphite mica schist.
566642	66.07694	36.5266	2014DRO056		Heavy mineral	Ore_Geology	
566643	66.07309	36.4478	2014DRO057		Heavy mineral	Ore_Geology	A couple of tiny Au flakes.
566644	66.01685	36.4832	2014DRO058		Heavy mineral	Ore_Geology	
566646	65.99262	36.5011	2014DRO059		float rock sample	Petrography	Float of radial antophyllite? laths. After serpentized dunite?
566645	66.01390	36.5183	2014DRO060	Hydrotherma lvein	Rock sample	Ore_Geology	Rusty qz vein, hosted in epidotized amphibolite. Aprox 10 cm wide.
566647	65.99271	36.4973	2014DRO061		Heavy mineral	Ore_Geology	
566648	65.97101	36.5593	2014DRO062		Heavy mineral	Ore_Geology	
566649	65.93024	36.6467	2014DRO063		Heavy mineral	Ore_Geology	Mt> gt unlike most places
566650	65.94630	36.6589	2014DRO064		Heavy mineral	Ore_Geology	Gt> mt
566651	66.29036	35.4362	2014DRO067	Metamorphic gneiss (schist>1 cm)	Rock sample	Geochemistry	Qzfldbt gneiss, hosting pegmatite. Some epidotization.
566652	66.29036	35.4362	2014DRO067		Rock sample	Geochemistry	Qzfldms pegmatite.
566653	66.29036	35.4362	2014DRO067		Rock sample	Geochemistry	Marble or hydrothermal carbonate?
566654	66.29036	35.4362	2014DRO067		Rock sample	Geochemistry	Epidote and amphibole along pegmatite/carbonate contact.
566655	66.29036	35.4362	2014DRO067		Rock sample	Ore_Geology	Sulfide pod, along pegmatite / carbonate contact.
566683	66.11598	37.9281	2014DRO069		Rock sample		Dolerite from core of dyke.
566656	66.11516	37.9269	2014DRO070		Rock sample	Ore_Geology	Garnetite
566657	66.11518	37.9296	2014DRO072		Rock sample	Ore_Geology	Gossan float (goethite?)
566658	66.11514	37.9299	2014DRO073		Rock sample	Ore_Geology	Coarse gt+qz
566659	66.11514	37.9299	2014DRO073		Rock sample	Ore_Geology	Finer grained garnetite, hosting vein (566658)
566660	66.11498	37.9301	2014DRO074		Rock sample	Ore_Geology	Fine grained, silicified filling of N280 fault.
566661	66.11438	37.9314	2014DRO075		Rock sample	Ore_Geology	Fine grained garnetite, cut by qz.
566662	66.11170	37.9298	2014DRO080	Metamorphic gneiss (schist>1 cm)	Rock sample	Petrography	Coarse gt+ky gneiss
566663	66.11912	37.9336	2014DRO083		Rock sample		Rusty and graphite rich paragneiss. Near contact (1m).
566664	66.11912	37.9336	2014DRO083		Rock sample	Ore_Geology	Paragneiss, with fine gt and green mineral (amphibole after Px?). Collected aprox 5m from contact.

GEUS no.	Lat. (N)	Long. (W)	Locality ID	Earth materials	Sample type	Purpose	Notes
566665	66.12018	37.9330	2014DRO084		Rock sample	Ore_Geology	Gt+bio+graphite garnetite.
566666	66.11932	37.9319	2014DRO085		Rock sample	Ore_Geology	Coarse garnetite, immediate contact with pegmatite.
566667	66.11932	37.9319	2014DRO085		Rock sample	Ore_Geology	Coarse amphibole (after diopside?) and boxworks. Farther, <1m from contact with the pegmatite.
566668	66.11807	37.9272	2014DRO086				Gt+qz+graphite
566669	66.12003	37.9298	2014DRO089		Rock sample	Ore_Geology	Garnetite
566670	66.12461	37.9343	2014DRO091	Metamorphic gneiss (schist>1 cm)	Rock sample	Geochemistry	Bio+fld+qz+gt
566671	66.12533	37.9379	2014DRO092	Metamorphic gneiss (schist>1 cm)	Rock sample	Geochemistry	Qz+fld+bio orthogneiss
566672	66.12619	37.9368	2014DRO093		Rock sample	Ore_Geology	Garnetite
566673	66.12846	37.9359	2014DRO094		Rock sample	Ore_Geology	Green amphibole (after diopside?) in rusty graphitic paragneiss.
566674	66.12846	37.9359	2014DRO094		Rock sample	Ore_Geology	Coarse tp medi grained gt within white qz.
566675	66.12990	37.9347	2014DRO095		Rock sample	Ore_Geology	Hydrothermal or quartzite?
566676	66.13057	37.9311	2014DRO096		Rock sample	Ore_Geology	Yellowbrown gt? crystals from pegmatite.
566677	66.13057	37.9311	2014DRO096	Metamorphic gneiss (schist>1 cm)	Rock sample	Ore_Geology	Amphibolite paragneiss at contact with pegmatite.
566678	66.12558	37.9265	2014DRO098		Rock sample	Ore_Geology	10 cm wide qz+sulfide vein, hosted by pegmatite and paragneiss.
566679	66.12320	37.9267	2014DRO099		Rock sample	Ore_Geology	Garnetite
566680	66.12220	37.9288	2014DRO100		Rock sample	Ore_Geology	Garnetite
566682	66.12022	37.9276	2014DRO102		Rock sample	Ore_Geology	Garnetite
566681	66.12304	37.9299	2014DRO103		Rock sample	Ore_Geology	Garnetite
566684	66.10766	37.9264	2014DRO104		Rock sample	Ore_Geology	Pink garnetite. Gt+qz. Within paragneiss.
566685	66.10797	37.9276	2014DRO105		Rock sample	Ore_Geology	Pink garnetite. Gt+qz. Within pegmatite.
566686	66.10797	37.9276	2014DRO105		Rock sample	Ore_Geology	Rusty qz (from pegmatite?)
566687	66.11615	37.9255	2014DRO106		Rock sample	Ore_Geology	Fine to coarse garnetite. Including biotite mica schist.
566688	66.11615	37.9255	2014DRO106		Rock sample chip	Ore_Geology	15 cm channel at hanging wall margin of fault zone, with graphitic and rusty mica schist.
566689	66.11615	37.9255	2014DRO106		Rock sample chip	Ore_Geology	15 cm channel at hanging wall margin of fault zone, with graphitic and rusty mica schist.
566695	66.11615	37.9255	2014DRO106		Rock sample	Ore_Geology	Hard silicified py or po bearing vein. Foot wall to graphitic and rusty mica schist sampled in 88 and 89.
566696	66.11615	37.9255	2014DRO106		Rock sample	Ore_Geology	Po bearing pyroxenite?
566690	66.11569	37.9259	2014DRO108	Hydrothermal vein	Rock sample	Ore_Geology	Gossanized material
566692	66.11569	37.9259	2014DRO108	Hydrothermal vein	Rock sample	Ore_Geology	Coarse garnetite with white qz.

GEUS no.	Lat. (N)	Long. (W)	Locality ID	Earth materials	Sample type	Purpose	Notes
566691	66.11569	37.9259	2014DRO108	Metamorphic gneiss (schist>1 cm)	Rock sample	Ore_Geology	Hosting gt paragneiss.
566693	66.11613	37.9258	2014DRO109		Rock sample	Ore_Geology	Rusty and clay fault filling.
566694	66.11615	37.9255	2014DRO106	Metamorphic gneiss (schist>1 cm)	Rock sample	Ore_Geology	Gt gneiss.
566697	66.11862	37.9266	2014DRO110		Rock sample	Ore_Geology	Coarse garnetite.
566698	66.11719	37.9254	2014DRO111		Rock sample	Ore_Geology	Coarse garnetite, with white qz.
566699	65.9930	36.6284	2014DRO113		Rock sample	Ore_Geology	Epidote veinlets in gneiss. From N15 set.
566700	65.99315	36.6292	2014DRO114		Rock sample	Ore_Geology	Qz+epidote rich part of vein, western side, approx. 2 m wide.
566701	65.99315	36.6292	2014DRO114		Rock sample	Ore_Geology	Massive qz part of the vein, irregular thickness but up to aprox 0.5 m thick. Central part, but enclosed within the qz+epidote rich part of the vein.
566702	65.99315	36.6292	2014DRO114		Rock sample	Ore_Geology	Qz+kspar rich part of the vein, eastern side, approx. 1 m thick.
566703	65.99563	36.6344	2014DRO117		Rock sample	Ore_Geology	Amphibolite? Ultramafic?
566704	65.99894	36.6334	2014DRO119	Metamorphic gneiss (schist>1 cm)	float rock sample	Ore_Geology	Gt+amph + bio
566705	66.00698	36.6256	2014DRO121		float rock sample	Ore_Geology	Massive sulfide float, mostly po, approx. 20 cm large.
566706	66.00252	36.6263	2014DRO123		float rock sample	Ore_Geology	Coarse po, white qz. Green Cu weathering crust.
566707	66.34489	34.9087	2014DRO128		Rock sample	Petrography	
566708	65.98613	36.6412	2014DRO133		float rock sample	Petrography	Float of radial antophyllite? laths. After serpentinized dunite?

Supracrustal rocks in the Schweizerland area, the Ivnartivaq dunite body and ultramafic rocks in the Niflheim area (KSZ)

Introduction

This report describes the geology and field observations of areas that were visited by Kristoffer Szilas (KSZ), Columbia University, New York, USA, during the 2014 GEUS field campaign in South-East Greenland. The field work was carried out from July 15th to August 6th 2014.

Figure 28 shows the geological map of the region with the localities that were visited by KSZ marked in red. 'C' marks camp sites and 'R' marks reco stops as described in more detail in the following (see Appendix A for a complete list of the GPS-positions). The people involved in the field work are given for each locality in the camp by camp documentation below, and so are the coordinates of camps and reco stops in addition to the GEUS numbers of the samples collected by KSZ. A complete list of the collected samples is given in Appendix B. The following people were participating in the field work: Jonas Tusch (JOT), University of Köln, Germany; Annika Dziggel (ADZ), University of Aachen, Germany; Sascha Müller (SMU), University of Aachen, Germany; Matti Nellemann Petersen (MNP), GEUS; Sam Weatherly (SMW), GEUS; Bo Møller Stensgaard (BMST), GEUS; Vincent van Hinsberg (VIVH), McGill University, Canada; Majken D. Poulsen (MADP), GEUS; Diogo Rosa (DRO), GEUS; Nicolas Thebaud (NTH, Centre of Exploration Targeting, University of Western Australia, Australia.

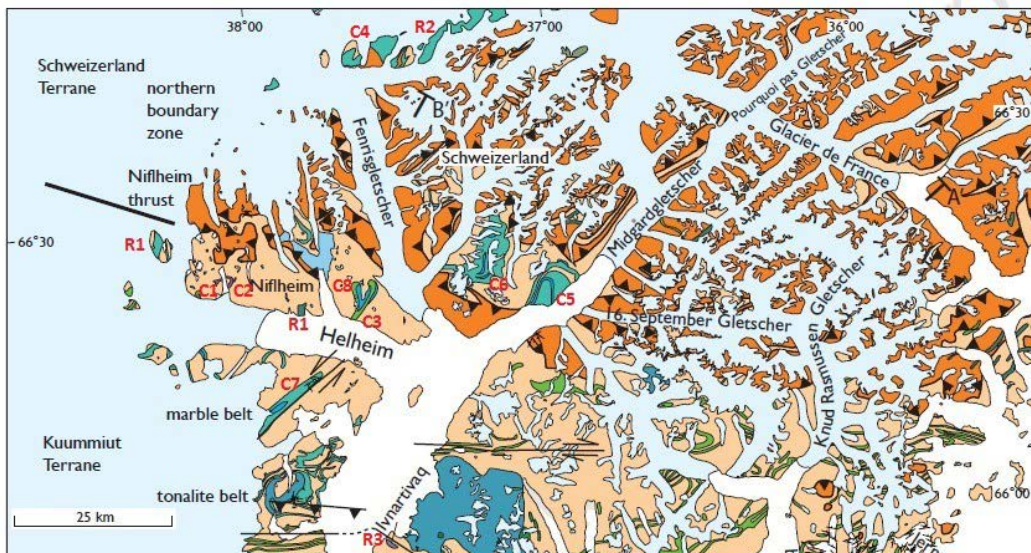


Figure 28. Geological map of the Ammassalik region of SE Greenland showing the approximate locations of KSZ's camps and reco stops during the 2014 field season.

As is evident by the positions of the camp sites, the main purpose with this contribution to the field campaign was to investigate the supracrustal rocks in the Schweizerland area, and

additionally to sample the Ivartivaq dunite body (R3) and the two Niflheim ultramafic outcrops (C1+C2). In the following a detailed description of field observations at each camp and reco stop is given, as well as preliminary interpretations by KSZ.

Camps and reco stops

Niflheim West – Camp 1

The position of this camp was: Lat. 66.41429658N Long. -38.18340012W. This was a joint camp with JOT, ADZ, SMU and MNP. The following samples were collected here in the period July 15th to 17th: 562501-562523.

The aim of this visit was to investigate outcrops of ultramafic rocks marked on the official GEUS map. In the field these rocks were brown with crumbly weathering as seen in Figure 29. The relations between the ultramafic rocks and the surrounding orthogneisses are now tectonic, although we cannot rule out that they may have been originally intrusive and were tectonised later. Granitoid pegmatites cut the ultramafic rocks, and zircon dating of samples such as 562513 would provide a definite minimum age for the ultramafic rocks.



Figure 29. *Ultramafic rocks at Niflheim West.*

The ultramafic rocks are now amphibolites and olivine appears to be present in most of these rocks, but this will have to be confirmed in thin section. Plagioclase veins (a few cm wide) are common in these rocks. It is not clear from the field observations at Niflheim West if the plagioclase veinlets formed by primary cumulate processes or if they represent later intrusive sheets. We found an area consisting of hornblendite, which appeared to be a distinct body

with a size of about 10 x 30 m in the central part of Niflheim West. At the northernmost margin of the Niflheim ultramafic body there is a 5 m wide gabbroic unit at the contact to the surrounding orthogneisses. The gabbro appears to be highly sheared, so it is not possible to say if it represents a tectonic or primary intrusive contact with the orthogneiss. Parts of the ultramafic rocks at Niflheim West contain obvious cumulate textures as seen in Figure 30. Primary igneous layering, evident by modal variation, is also recorded by these ultramafic rocks. The original mineralogy of these rocks appears to have been olivine plus pyroxene. Although it is not apparent if these rocks originally comprised ortho- or clinopyroxene, the former is indicated by the brown to grey colour of the amphiboles.



Figure 30. *Ultramafic rock with coarse cumulative texture.*

Niflheim East – Camp 2

This camp was positioned on the eastern outcrop of the ultramafic rocks at Niflheim. JOT, SMW and I shared this camp. The position was: Lat. 66.42491053N Long. -38.1346834W. Samples 562524-562552 were collected here from July 18th to 19th.

The ultramafic rocks here were identical to those in the western part of the Niflheim body at Camp 1, but two groups of ultramafic rock units appear to be distinguishable: (1) olivine + clinopyroxene (wherlite), and (2) orthopyroxene + clinopyroxene (websterite). These original assemblages are now converted to amphibole-bearing ultramafic rocks. Plagioclase may be present as an interstitial phase, but is only obvious when it forms distinct veinlets. The plagioclase veins seen in Figure 31 contain cavities, which appears to have hosted carbonate before weathering out to form voids. Some of these plagioclase veins are clearly discordant, which may indicate that the plagioclase veins were expelled from a cumulate mush before complete solidification.

The overall impression and interpretation is that the Niflheim body as a whole is part of a mafic to ultramafic intrusion and may represent the lower cumulate portion (see example of cumulate textures in Figure 32). However, it is not clear if these rocks were intrusive into the regional orthogneisses or if they represent a mega-enclave within these. Detailed petrographic work will be carried out on these ultramafic rocks to determine their mineral assemblage and constrain the potential crystallization sequence.



Figure 31. *Plagioclase veins with carbonate cavities in ultramafic rocks.*



Figure 32. *Ultramafic rock at Niflheim East with cumulate textures.*

Western nunatak – Reco 1

This reco was used to sample obvious rusty staining in the valley between Camp 1 and 2 at Niflheim. JOT, SMW and KSZ were part of this sampling (562553+562554) on July 20th. The slope facing east is yellowish-brown and appears to have potential for mineralisation. These rocks turned out to be mainly graphitic schists, but it is unclear if they actually contain any sulphides. Geochemical assay should be done on these samples to test for Au+base metals.

The main aim of this reco was also to investigate the western nunataks at the following coordinates: Lat. 66.47101629N Long. -38.36106454W. Samples 562555-562559 were collected here.

According to the GEUS map there was supposed to be supracrustal rocks (including marble) outcropping on this nunatak. Instead, we found mainly orthogneisses with significant N-S shearing and strong biotite alteration giving them a rusty appearance. At the eastern margin of the nunatak, marble is marked on the map. Here we found extensive epidote alteration of orthogneisses, but no true marbles. Nevertheless, the central to western part of the nunatak consists of fine-grained rusty schists as seen in Figure 33. These may indeed represent metasedimentary rocks. They were cut by granitoid pegmatites, which would provide a minimum age for these biotite schists.



Figure 33. *Rusty schists cut by pegmatite on the western nunatak.*

Finally, we also stopped at a locality on the way to our new camp site, where supracrustal rocks were marked on map: Lat. 66.36767945N Long. -37.91871337W. Samples 562560-562562 were collected here.

Although there were some amphibolites, they do not warrant marking on the map as being a true supracrustal unit. They appeared strongly deformed with layered structures defined by modal variation and contained abundant quartz-veins. They were rather mafic inclusions in the orthogneisses and did not show any evidence of a supracrustal origin. Instead, they could just as well have represented lower crustal intrusions, or more likely random mafic inclusions or melt residues that were trapped during the formation of the regional orthogneisses.

Y-shaped marble – Camp 3

This camp was shared with JOT at position: Lat. 66.35841253N Long. -37.71810127W. Samples 562563-562575+553160-553161 were collected here from July 20th to 23rd.

We measured, described, and sampled two profiles (see Appendix C) through the southern end of the marble sequences at its eastern and western margins, respectively. The marble itself is about 100 m thick stratigraphically at the southern end, and is thus up to 200 m in total thickness because the sequence is repeated structurally by tight folding. The marble has a banded appearance due to silica layering and impurities of mica. Amphibolites and pegmatites are also present as layers along the margins. The marble is clearly cut by an intrusive pegmatite (562566) close to the fold core on the top of the hill above Camp 3. Zircon dating of this sample will yield a minimum age for the marble, and will also date the main deformation as it appears to be syntectonic.

It was not obvious in the field if the biotite schist at the base of the marble represents a metasediment or rather a strongly deformed and altered orthogneiss. Hopefully geochemistry and zircon geochronology will be able to establish which is the case.

There is a large obvious fold in the southern part of the marble immediately west of our camp site (see Figure 34). We took several structural measurements on this feature, which are displayed in Table 3. Lineations on these folds were generally 345/45N and 0/40N. The marble is strongly deformed and we did not observe any features that could have represented primary sedimentary structures. There is some variation in the silica and mica contents of the marble, but it is not apparent if this is due to mobility during deformation or if it represents primary sedimentary variability. There are a few fine grained massive felsic layers that may potentially represent rhyolite beds (e.g. sample 562574). Dating zircon from such horizon could potentially yield direct age-constraint on the marble unit.

Northern nunatak – Camp 4

We had a reco stop on some rusty biotite schists on the way to the camp, which we sampled (562576+562577) in the north-eastern part of the Y-shaped Marble. BMST also took a few samples at this locality. Despite the rusty appearance these rocks did not appear to host any sulphides, but weathering of biotite caused the coloration.

The nunatak camp was shared with JOT at: Lat. 66.70972741N Long. -37.52909959W. The following samples were collected: 562578-562599 + 564901-564906 from July 24th to 26th.



Figure 34. *The folded southern part of the Y-shaped marble seen from a helicopter, looking west.*

Table 3. *Strike-dip measurements around the large fold seen in Figure 34.*

16/52W	28/36W	18/42W	17/45W	174/50W	160/40W	5/50W
170/50W	157/60SW	166/68SW	172/60SW	164/70SW	155/80SW	152/78SW
145/80NE	156/90	145/88NE	160/86NE	130/70NE	58/52NW	12/32NW
176/55W	176/56W	146/88SW	150/90	52/30NW	90/22N	

The highest point on this nunatak consists of a large white granitoid and the surrounding rocks are mostly biotite-sillimanite schists of potentially sedimentary origin. Highly aluminous schists with up to 60% sillimanite and 30% garnet are present in the SW corner of the nunatak (e.g. sample 564906) as seen in Figure 35. Such rocks invariably represent palaeosols as hydrothermal alteration is not capable of producing such extreme leaching as is evident by the extremely aluminous character of these rocks.

In close proximity to the white granitoid there are several outcrops of gabbroic amphibolites and ultramafic rocks. The latter resembles the ultramafic rocks that we sampled at Niflheim and it needs to be tested if they are also geochemically similar. Here the ultramafic rocks were fine grained and commonly displayed garbenschiefer texture.

Pseudo-spinifex textured ultramafic rocks were found at one locality (Lat. 66.6939372N Long. -37.55658033W). These rocks appeared to be similar in composition and mineralogy as those that were found associated with metagabbros further north on the nunatak. Given that komatiites are not normally associated with gabbros, but rather with dunitic cumulates, and form surface lava flows it is proposed that the textures found on the northern nunatak



Figure 35. *Sillimanite-garnet schist at the SW-corner of the northern nunatak (C4).*

represents metamorphic growth of amphibole, which happens to resemble spinifex textures as seen in Figure 36. This will obviously need to be tested in detail by petrographic investigations. Geochemical data should also be used to test if these ultramafic rocks and the gabbros can be related by fractional crystallization.

Northern chain of nunataks – Reco 2

This reco was partly joined by JOT, VIVH and MADP on July 27th. We investigated the northern chain of nunataks with the aim of sampling kyanite schists. The final position was: Lat. 66.3495653N Long. -37.08871697W. The following samples were collected: 564907-564920.

The nunatak west of the one that JOT and I had been working on, gave us a nice perspective from where it became obvious that the former consists of a series of thrust sheets rather than a coherent stratigraphic continuity as seen in Figure 37.

On the northern chain of the nunataks we did find visible kyanite in schists which otherwise had the same appearance as those at Camp 4. The intimate association of these sillimanite-biotite schists and amphibolites, suggest that the schists do in fact represent metasediments. If they had formed by alteration from a orthogneiss precursor the associated amphibolites would certainly also have shown evidence of this. Additionally, the strongly aluminous compositions that were observed for some schists, which essentially consisted of sillimanite, garnet and mica, suggest formation by in situ weathering prior to metamorphism. One robust way of testing the sedimentary vs. alteration origin of these schists is by age dating their zircons. This would show if they contain a single igneous age, as would be expected if they were formed by alteration of granitoids, or if they have a detrital age population derived from a range of sources, as would be expected for metasedimentary rocks.



Figure 36. *Pseudo-spinifex textures in ultramafic rocks (amphibolite) on the northern nunatak.*

Antiformal supracrustals – Camp 5

This camp was shared with DRO, NTH, VIVH and MADP. The position was Lat. 66.35012797N Long. -37.08290134W. Samples 564921-564949 were collected here from July 27th to 30th.

This area was dominated by biotite schists, some of which contained sillimanite, but they were mainly retrogressed chlorite-biotite schists. Marble was also present just north of the camp, see Figure 38. Graphitic schists are also common and a nice example of their formation mechanism was displayed in the steep wall seen in Figure 38. Here a 30 cm wide sheeted quartz-vein cut the marble, which resulted in a 3-5 cm wide graphitic alteration halo surrounding the quartz-vein. An obvious interpretation of this observation would be



Figure 37. *The northern nunatak seen from west showing the white granitoid in the centre of the photo and the layered sequence of gabbroic amphibolites and sillimanite-bearing biotite schists that comprise the main rock types.*

that the introduction of reducing silica-bearing fluids would break down the carbonate to form graphite. This potential mechanism for the formation of graphite in this region should be tested by modelling the carbon-isotope fractionations associated with this type of reaction. The abundances of ultramafic rocks in the area suggests that locally derived fluids would indeed be of reducing character, which in combination with copious marble outcrops, would be able to produce the observed graphite deposits. This further suggests that there would be no need for the involvement of biogenic carbon sources, assuming that the carbonates represent chemical sediments.

Several events of deformation and fluid transport are recorded in the biotite schists in these supracrustal rocks. An example of this was seen at a locality where the foliation of the biotite schists was folded in a ductile fashion towards a steep shear zone, which cut the foliation at about 45 degrees. This shear zone was in turn cut by an epidote-rich breccia and finally quartz-veins were overprinting all of the above structural phases. This observation attests to the complicated evolution that the supracrustal rocks have undergone after their deposition. Thus, one would not expect to find any primary depositional structures in these rocks, despite previous claims of graded bedding etc.

Glacier Camp – Camp 6

DRO, NTH and I spent two days (July 31st and August 1st) at position Lat. 66.38747954N Long. -37.27085659W. The camp was located at a glacial mouth and water was flowing under the ice on melting scree slopes. We attempted to walk along a large cliff on the north-western side of our camp, but were nearly hit by spontaneous rock fall and decided to



Figure 38. *Steep layers of biotite schist, marble and amphibolite above C5.*

relocate the following day as this place was not safe to work in. Samples 564951-564954 were collected here.

The lithological units that we observed included marble, amphibolite, biotite schist, which was all similar to what we had encountered at Camp 5.

Ivnartivaq – Reco 3

On August 1st BMST and I visited the large Ivnartivaq dunite locality at: Lat. 66.03463887N Long. -37.73130388W. The following samples were collected: 564955-564986.

This locality consists of mainly dunite (Figure 39). At the southern margin there is a large (5 x 10 m) magnetite body. The dunite contains minor orthopyroxene (opx) veinlets and magnetite aggregates in the north-western part of the body (Figure 40). The smaller opx veinlets (<2 cm) are oriented in the same plane as the main foliation in the surrounding gneisses, whereas those that are larger than about 2 cm are mostly random in their orientation. The contacts to the orthogneisses are obscured in most places, but at one locality we observed that the orthogneiss was clearly intrusive into the dunite and in turn contained inclusions of dunite that were partly serpentinised. Zircon dating of orthogneiss (e.g. sample 564963) would yield a minimum age of the dunite. Additionally, granitoid pegmatites were commonly intrusive into the dunite, but from experience these are typically later than the regional orthogneisses.



Figure 39. *Ivnartivaq dunite body seen from helicopter.*

Northeastern shear zone – Camp 7

This camp was shared with DRO and NTH at: Lat. 66.25365773N Long. -37.978277W from August 1st to 3rd.

The valley follows the contact between biotite schists and sharp contacts to the surrounding orthogneisses (Figure 41). Large shear zones are present where sulphide mineralisation was found in the SW part of this zone (samples 564988+89). These rocks were all highly strained as seen in Figure 42. We sampled a quartzite, which may potentially represent a true

metasediment (564987). Zircon dating will hopefully yield evidence of the provenance of this rock, which should be compared with similar data from the regional sillimanite schists.



Figure 40. *Dunite with small brown opx crystals and large black magnetite aggregates.*



Figure 41. *NE-shear zone with obvious contact between grey orthogneiss and brown biotite schists. The valley more or less follows the trace of the shear zone.*

Y-shaped marble – Camp 8

This camp was shared with DRO from August 4th to 6th at the north-western part of the Y-shaped marble that was already visited at Camp 3. The position was Lat. 66.38650113N Long. -37.72730395W. Samples 564995-564999 and 565101-565119.

Figure 43 shows the southern end of the Y-shaped marble, where it is obvious that it represents a tightly folded sequence. The structural data in Table 3. may yield the orientation of deformation of the marble. We sampled metasomatic reactions at the NW margin of the marble, which had resulted in quartz-magnetite-amphibole rocks that should be assayed.



Figure 42. *Sheared rocks at the contact between orthogneiss and biotite schists and amphibolite.*



Figure 43. *The Y-shaped Marble seen from the southern margin looking north.*

Appendix A. List of camps and reco stops

Locality name	Latitude (n)	Longitude (W)	Date
Camp 1	66.41429658	-38.18340012	July 15-17 2014
Camp 2	66.42491053	-38.13468340	July 18-19 2014
Camp 3	66.35841253	-37.71810127	July 20-23 2014
Camp 4	66.70972741	-37.52909959	July 24-26 2014
Camp 5	66.35012797	-37.08290134	July 27-30 2014
Camp 6	66.38747954	-37.27085659	July 31 2014
Camp 7	66.25365773	-37.97827700	August 1-3 2014
Camp 8	66.38650113	-37.72730395	August 4-6 2014
Reco 1	66.47101629	-38.36106454	July 20 2014
Reco 2	66.34956530	-37.08871697	July 27 2014
Reco 3	66.03463887	-37.73130388	August 1 2014

Appendix B. List of samples

Sample	Latitude (N)	Longitude (W)	Locality	Lithology	Purpose
562501	66.41604780	-38.18201722	C1	Ultramafic rock	Geochem. + Petro.
562502	66.41774649	-38.17976738	C1	Ultramafic rock	Geochem. + Petro.
562503	66.41910530	-38.17808369	C1	Ultramafic rock	Geochem. + Petro.
562504	66.41973376	-38.17650542	C1	Ultramafic rock	Geochem. + Petro.
562505	66.42078772	-38.17540741	C1	Ultramafic rock	Geochemistry
562506	66.42168919	-38.17780248	C1	Ultramafic rock	Geochemistry
562507	66.42123382	-38.17964365	C1	Ultramafic rock	Geochemistry
562508	66.41665731	-38.18398806	C1	Ultramafic rock	Geochem. + Petro.
562509	66.41704911	-38.18428299	C1	Ultramafic rock	Geochem. + Petro.
562510	66.41750186	-38.18379730	C1	Ultramafic rock	Geochemistry
562511	66.41763230	-38.18377778	C1	Ultramafic rock	Geochem. + Petro.
562512	66.41811174	-38.18337404	C1	Ultramafic rock	Geochem. + Petro.
562513	66.41811424	-38.18336739	C1	Pegmatite	Geochronology
562514	66.41868603	-38.18076112	C1	Hornblendite	Geochemistry
562515	66.42032088	-38.18096576	C1	Ultramafic rock	Geochem. + Petro.
562516	66.42099225	-38.17597166	C1	Ultramafic rock	Geochem. + Petro.
562517	66.42052476	-38.17709558	C1	Hornblendite	Geochemistry
562518	66.41981336	-38.17728524	C1	Ultramafic rock	Geochemistry
562519	66.41984177	-38.17774382	C1	Hornblendite	Geochemistry
562520	66.41871139	-38.17787987	C1	Ultramafic rock	Geochemistry
562521	66.41773817	-38.17859294	C1	Ultramafic rock	Geochem. + Petro.
562522	66.41794993	-38.18097474	C1	Ultramafic rock	Geochemistry
562523	66.41621877	-38.18256701	C1	Amphibolite	Geochemistry
562524	66.42606650	-38.13555020	C2	Ultramafic rock	Geochemistry
562525	66.42631346	-38.1377750	C2	Ultramafic rock	Assay
562526	66.42652684	-38.14090087	C2	Ultramafic rock	Geochemistry
562528	66.42687054	-38.14165834	C2	Ultramafic rock	Geochemistry
562527	66.42725070	-38.14154818	C2	Ultramafic rock	Geochem. + Petro.
562529	66.42742483	-38.14128537	C2	Ultramafic rock	Geochemistry
562530	66.42742483	-38.14128537	C2	Ultramafic rock	Geochemistry

Sample	Latitude (N)	Longitude (W)	Locality	Lithology	Purpose
562531	66.42793022	-38.14152504	C2	Orthogneiss	Geochronology
562532	66.42818775	-38.13553813	C2	Ultramafic rock	Geochem. + Petro.
562533	66.42809930	-38.13535803	C2	Hornblendite	Geochemistry
562534	66.42731435	-38.13361896	C2	Ultramafic rock	Geochemistry
562535	66.42639779	-38.13228207	C2	Ultramafic rock	Geochem. + Petro.
562536	66.42194499	-38.13178033	C2	Ultramafic rock	Geochem. + Petro.
562537	66.42135900	-38.13156396	C2	Ultramafic rock	Geochem. + Petro.
562538	66.42050471	-38.13222947	C2	Ultramafic rock	Geochem. + Petro.
562539	66.41977175	-38.13246119	C2	Ultramafic rock	Geochem. + Petro.
562540	66.41694807	-38.13493193	C2	Ultramafic rock	Geochemistry
562541	66.41597553	-38.13734672	C2	Ultramafic rock	Geochemistry
562542	66.41597553	-38.13734672	C2	Ultramafic rock	Geochemistry
562543	66.41376966	-38.13944164	C2	Ultramafic rock	Geochemistry
562544	66.41457101	-38.13640710	C2	Ultramafic rock	Geochem. + Petro.
562545	66.41600506	-38.13306066	C2	Ultramafic rock	Geochemistry
562546	66.41734020	-38.13340991	C2	Ultramafic rock	Geochem. + Petro.
562547	66.41734020	-38.13340991	C2	Ultramafic rock	Geochem. + Petro.
562548	66.41768320	-38.13283973	C2	Hornblendite	Geochemistry
562549	66.4176520	-38.13280124	C2	Ultramafic rock	Petrography
553151	66.41973091	-38.12951819	C2	Soil	Assay
562550	66.42278617	-38.12625111	C2	Ultramafic rock	Assay
562551	66.42278617	-38.12625111	C2	Ultramafic rock	Assay
562552	66.42475207	-38.13469153	C2	Orthogneiss	Geochronology
562553	66.41924205	-38.17066234	R1	Graphite schist	Assay
562554	66.41928588	-38.17078343	R1	Graphite schist	Assay
562555	66.46294250	-38.37323173	R1	Graphite schist	Assay
562556	66.46243633	-38.37365300	R1	Quartz vein	Assay
562557	66.46210981	-38.37452196	R1	Graphite schist	Assay
562558	66.47134466	-38.36088744	R1	Graphite schist	Assay
562559	66.47200822	-38.32266978	R1	Orthogneiss	Geochronology
562560	66.36780499	-37.91851502	R1	Amphibolite	Geochemistry
562561	66.36767945	-37.91871337	R1	Amphibolite	Geochemistry
562562	66.36765164	-37.91939325	R1	Amphibolite	Geochemistry
562563	66.36007703	-37.71905410	C3	Marble	Geochemistry
562564	66.36007703	-37.71905410	C3	Marble	Geochemistry
562565	66.36019801	-37.71926638	C3	Marble	Geochemistry
563160	66.36019439	-37.71930727	C3	Soil	Geochemistry
562566	66.36026333	-37.71962926	C3	Orthogneiss	Geochronology
562567	66.36245333	-37.71742555	C3	Orthogneiss	Geochronology
562568	66.36425141	-37.71206717	C3	Ultramafic rock	Geochemistry
562569	66.36419704	-37.71202654	C3	Ultramafic rock	Geochemistry
562570	66.36425787	-37.71194718	C3	Orthogneiss	Geochronology
562571	66.36488807	-37.71140582	C3	Biotite schist	Geochemistry
562572	66.36642367	-37.70950232	C3	Marble	Geochemistry
562573	66.36642225	-37.70984303	C3	Marble	Geochemistry
562574	66.36683838	-37.71040534	C3	Biotite schist	Geochemistry
562575	66.36684587	-37.71041636	C3	Marble	Geochemistry
553161	66.36402412	-37.71818480	C3	Soil	Assay
562576	66.38614434	-37.68956088	C3	Biotite schist	Assay

Sample	Latitude (N)	Longitude (W)	Locality	Lithology	Purpose
562577	66.38594837	-37.69004059	C3	Biotite schist	Assay
562578	66.70571163	-37.52466055	C4	Granitoid	Geochronology
562579	66.71221837	-37.54003203	C4	Sillimanite schist	Geochemistry
562580	66.71290888	-37.53744591	C4	Sillimanite schist	Geochemistry
562581	66.71386397	-37.53539102	C4	Sillimanite schist	Geochemistry
562582	66.71449274	-37.53364647	C4	Biotite schist	Geochemistry
562583	66.71417080	-37.52988682	C4	Sillimanite schist	Geochemistry
562584	66.71295930	-37.52655562	C4	Sillimanite schist	Geochemistry
562585	66.71253379	-37.52590879	C4	Sillimanite schist	Geochemistry
562586	66.71226189	-37.51727890	C4	Granitoid	Geochronology
562587	66.70540060	-37.51789487	C4	Amphibolite	Geochemistry
562588	66.70589261	-37.51845726	C4	Amphibolite	Geochemistry
562589	66.70573975	-37.51921618	C4	Amphibolite	Geochemistry
562590	66.70660764	-37.52137744	C4	Amphibolite	Geochemistry
562591	66.70686792	-37.52240579	C4	Amphibolite	Geochemistry
562592	66.70775494	-37.52499287	C4	Ultramafic rock	Geochemistry
562593	66.70657702	-37.53671614	C4	Granitoid	Geochemistry
562594	66.70287745	-37.54397523	C4	Amphibolite	Geochemistry
562595	66.69798214	-37.55043754	C4	Amphibolite	Geochemistry
562596	66.69393720	-37.55658033	C4	Amphibolite	Geochem. + Petro.
562597	66.69393720	-37.55658033	C4	Amphibolite	Geochem. + Petro.
562598	66.69393720	-37.55658033	C4	Amphibolite	Geochem. + Petro.
562599	66.69393720	-37.55658033	C4	Amphibolite	Geochem. + Petro.
564901	66.69393720	-37.55658033	C4	Amphibolite	Geochem. + Petro.
564902	66.69393131	-37.55656397	C4	Amphibolite	Geochem. + Petro.
564903	66.69000545	-37.57027343	C4	Sillimanite schist	Geochem. + Petro.
564904	66.69046710	-37.57502448	C4	Biotite schist	Geochem. + Petro.
564905	66.69074671	-37.57673926	C4	Sillimanite schist	Geochem. + Petro.
564906	66.69143962	-37.57676722	C4	Sillimanite schist	Geochem. + Petro.
564907	66.69918427	-37.63501934	R2	Paragneiss	Geochemistry
564908	66.69945385	-37.63527546	R2	Paragneiss	Geochemistry
564909	66.69945385	-37.63527546	R2	Amphibolite	Geochem. + Petro.
564910	66.70051891	-37.63451898	R2	Paragneiss	Geochem. + Petro.
564911	66.70077270	-37.63400331	R2	Paragneiss	Geochemistry
564912	66.70078518	-37.63391460	R2	Quartz vein	Assay
564913	66.70123825	-37.63369681	R2	Orthogneiss	Geochem. + Petro.
564914	66.70080387	-37.63386929	R2	Biotite schist	Geochemistry
564915	66.70284773	-37.63266277	R2	Biotite schist	Geochemistry
564916	66.69601324	-37.39583395	R2	Kyanite schist	Geochem. + Petro.
564917	66.69694889	-37.39475387	R2	Kyanite schist	Geochem. + Petro.
564918	66.69601324	-37.39583395	R2	Pegmatite	Geochronology
564919	66.71403116	-37.35462379	R2	Biotite schist	Geochem. + Petro.
564920	66.34956530	-37.08871697	R2	Biotite schist	Geochem. + Petro.
564921	66.34956530	-37.08871697	C5	Biotite schist	Geochemistry
564922	66.34803700	-37.09842694	C5	Biotite schist	Geochem. + Petro.
564923	66.34803700	-37.09842694	C5	Amphibolite	Geochemistry
564924	66.34791484	-37.10000713	C5	Amphibolite	Geochem. + Petro.
564925	66.34977037	-37.11280253	C5	Biotite schist	Geochemistry
564926	66.34968430	-37.11391165	C5	Felsic schist	Geochronology

Sample	Latitude (N)	Longitude (W)	Locality	Lithology	Purpose
564927	66.34977436	-37.11596105	C5	Felsic schist	Geochronology
564928	66.34587110	-37.14180805	C5	Orthogneiss	Geochronology
564929	66.34886311	-37.10164302	C5	Amphibolite	Geochemistry
564930	66.34922346	-37.10865128	C5	Quartz vein	Geochem. + Petro.
564931	66.35075310	-37.10754034	C5	Amphibolite	Geochemistry
564932	66.35227573	-37.10515886	C5	Amphibolite	Geochemistry
553185	66.35249591	-37.10495187	C5	Biotite schist	Geochemistry
564933	66.35387331	-37.09810022	C5	Biotite schist	Geochemistry
564934	66.35294870	-37.09448404	C5	Graphite schist	Geochemistry
564935	66.35338919	-37.09346099	C5	Biotite schist	Geochemistry
564936	66.35602225	-37.08883331	C5	Marble	Geochemistry
564938	66.35602225	-37.08883331	C5	Marble	Geochemistry
564940	66.35602225	-37.08883331	C5	Marble	Geochemistry
564937	66.35602225	-37.08883331	C5	Marble	Geochemistry
564939	66.35602225	-37.08883331	C5	Marble	Geochemistry
564941	66.35602225	-37.08883331	C5	Marble	Geochemistry
564942	66.36337892	-37.09618377	C5	Sillimanite schist	Geochem. + Petro.
564950	66.36333502	-37.0962542	C5	Amphibolite	Geochemistry
564943	66.36316432	-37.09813629	C5	Biotite schist	Geochemistry
564944	66.36233616	-37.09700024	C5	Quartzite	Geochronology
564945	66.36236760	-37.09716568	C5	Graphite schist	Geochemistry
564946	66.36238505	-37.0972520	C5	Graphite schist	Geochem. + Petro.
564947	66.36238505	-37.0972520	C5	Graphite schist	Geochemistry
564948	66.36238505	-37.0972520	C5	Graphite schist	Geochemistry
564949	66.36218137	-37.09716635	C5	Quartz vein	Assay
564951	66.37924728	-37.27187949	C6	Orthogneiss	Geochronology
564952	66.37964728	-37.27391911	C6	Schist	Geochemistry
564953	66.37906588	-37.27675113	C6	Amphibolite	Geochem. + Petro.
564954	66.38747954	-37.27085659	C6	Sillimanite schist	Geochem. + Petro.
564955	66.03463887	-37.73130388	R3	Amphibolite	Geochem. + Petro.
564956	66.03468651	-37.73149440	R3	Chromitite	Geochem. + Petro.
564957	66.03473498	-37.73181571	R3	Dunite	Geochem. + Petro.
564958	66.03500962	-37.73305562	R3	Dunite	Geochem. + Petro.
564959	66.03527341	-37.73356848	R3	Dunite	Geochem. + Petro.
564960	66.03529656	-37.73370725	R3	Pyroxenite	Geochem. + Petro.
564961	66.03533921	-37.73501003	R3	Pegmatite	Geochronology
564962	66.03530693	-37.73497298	R3	Dunite	Geochem. + Petro.
564963	66.03500772	-37.73688471	R3	Orthogneiss	Geochronology
564964	66.03421028	-37.73692374	R3	Dunite	Geochem. + Petro.
564965	66.03695559	-37.73433805	R3	Magnetite	Geochem. + Petro.
564966	66.03695559	-37.73433805	R3	Magnetite	Geochem. + Petro.
564967	66.03695559	-37.73433805	R3	Magnetite	Geochem. + Petro.
564968	66.03695559	-37.73433805	R3	Magnetite	Geochem. + Petro.
564969	66.03695559	-37.73433805	R3	Magnetite	Geochem. + Petro.
564971	66.03685964	-37.73405248	R3	Magnetite	Assay
564970	66.03685964	-37.73405248	R3	Magnetite	Assay
564972	66.03685479	-37.73406349	R3	Dunite	Geochem. + Petro.
564973	66.03685479	-37.73406349	R3	Dunite	Geochem. + Petro.
564974	66.03680690	-37.73415330	R3	Dunite	Geochem. + Petro.

Sample	Latitude (N)	Longitude (W)	Locality	Lithology	Purpose
564975	66.03676556	-37.73425230	R3	Magnetite	Geochem. + Petro.
564976	66.03462317	-37.73259981	R3	Dunite	Geochem. + Petro.
564977	66.03204708	-37.72923927	R3	Dunite	Geochem. + Petro.
564978	66.03191971	-37.72918659	R3	Dunite	Geochem. + Petro.
564979	66.03128784	-37.72889092	R3	Dunite	Geochem. + Petro.
564981	66.03194952	-37.73007259	R3	Dunite	Geochem. + Petro.
564982	66.03198057	-37.72986835	R3	Dunite	Geochem. + Petro.
564983	66.03198057	-37.72986835	R3	Dunite	Geochem. + Petro.
564984	66.03198057	-37.72986835	R3	Dunite	Geochem. + Petro.
564985	66.03198057	-37.72986835	R3	Dunite	Geochem. + Petro.
564986	66.03198057	-37.72986835	R3	Dunite	Geochem. + Petro.
564987	66.24388256	-38.02348625	C7	Quartzite	Geochronology
564988	66.24491034	-38.01861350	C7	Schist	Assay
564989	66.24487138	-38.01838296	C7	Schist	Assay
564990	66.24683486	-38.00750083	C7	Sillimanite schist	Geochemistry
564991	66.25229541	-37.99163951	C7	Amphibolite	Geochemistry
564992	66.25376347	-37.98679993	C7	Marble	Geochemistry
564993	66.26343954	-37.95878152	C7	Amphibolite	Geochemistry
564994	66.26343954	-37.95878152	C7	Amphibolite	Geochemistry
564995	66.38722272	-37.70774820	C8	Magnetite	Assay
564996	66.38713544	-37.70772828	C8	Amphibolite	Geochemistry
564997	66.38713544	-37.70772828	C8	Amphibolite	Geochemistry
564998	66.38673533	-37.71114948	C8	Pegmatite	Geochronology
564999	66.38650113	-37.72730395	C8	Schist	Geochemistry
565101	66.38115529	-37.71955418	C8	Pegmatite	Petrography
565102	66.37856943	-37.72127450	C8	Pegmatite	Petrography
565103	66.37952491	-37.71106905	C8	Orthogneiss	Geochronology
565104	66.37796812	-37.71559295	C8	Marble	Petrography
565105	66.37793559	-37.71564301	C8	Marble	Geochemistry
565106	66.37796523	-37.71635967	C8	Marble	Geochemistry
565107	66.37793704	-37.71645538	C8	Marble	Geochemistry
565108	66.37753738	-37.71744398	C8	Marble	Geochemistry
565109	66.37754842	-37.71745988	C8	Marble	Geochemistry
565110	66.37749236	-37.71763551	C8	Marble	Geochemistry
565111	66.37749202	-37.71779877	C8	Marble	Geochemistry
565112	66.36938723	-37.71673954	C8	Marble	Geochemistry
565113	66.36927683	-37.71362662	C8	Marble	Geochemistry
565114	66.36980599	-37.71192230	C8	Biotite schist	Geochemistry
565115	66.37240971	-37.71009538	C8	Quartz vein	Assay
565116	66.37241617	-37.71007530	C8	Quartz vein	Assay
565117	66.37407053	-37.70943260	C8	Quartz vein	Assay
565118	66.38063187	-37.70410567	C8	Quartz vein	Assay
565119	66.38650113	-37.72730395	C8	Orthogneiss	Geochronology

Appendix C. Profiles through the Y-shaped marble (C3)

#1 Eastern margin KSZ Profile 1 part 1

GRAPHIC LOG		Project	SEGMENT	Drill hole no.	
Vibrant Resources Ltd		Location	Y-shaped marble	Location no.	
Co-ords		Scale		Page of	
Azim	Ina	Dtm	Logged by	KSZ	
Date		22nd July 2014			
Sample #	Strike/dip	Log with grain size	Samples	Rock / facies description	Alteration
50	Structure	mud 0.5 2 5 32 mm	TG results		
			Chemistry		
62430	END of sheet 1		Profile 1	Siderite Biotite-veils	Biotite + QZ rock
			Biotite + QZ	Rhyolite patches	Rhyolite vein?
			Boudins of walls	Dissimulated veins	
62424	43/62		Biotite layers	Siderite-veils boudins	
				30cm layers of coarse marble	
				Dirty sheared marble	
62423	42/62			Relatively homogeneous Marble	
				Sparite in places	
				Coarse grained marble	
				10cm contact with spec of graphite	
	40/64		qz-veins	Rusty matrix	Rusty
				Garnet biotite schist	
62421	52		Folded qz-veins	Potentially volcanoclastic due to modal variation.	
	60/55		modal veins	Boudins of 10cm hornblende	
			Black	Largely garnet amphibolite	
62422				contact intruded by pegmatite	
62419	70/25		Darker	Biotite-rich migmatite	
				Leucosome	
				Garnets < 3mm	
62418	60/72		Light	Migmatitic biotite schist	Rusty patches
				Leucosomes	
				Strongly sheared and folded	
				Sheared amphibolite 11544	
62417	66/48		Amphibolite altered?	Sharp contact with no reaction	Biotite/Sulphide?
				Rusty biotite schist	
	80/92			Biotite schist	
	50/62				
62416				Strongly folded biotite schist, folded qz-veins	

0 5m of same rock

#2

Eastern margin

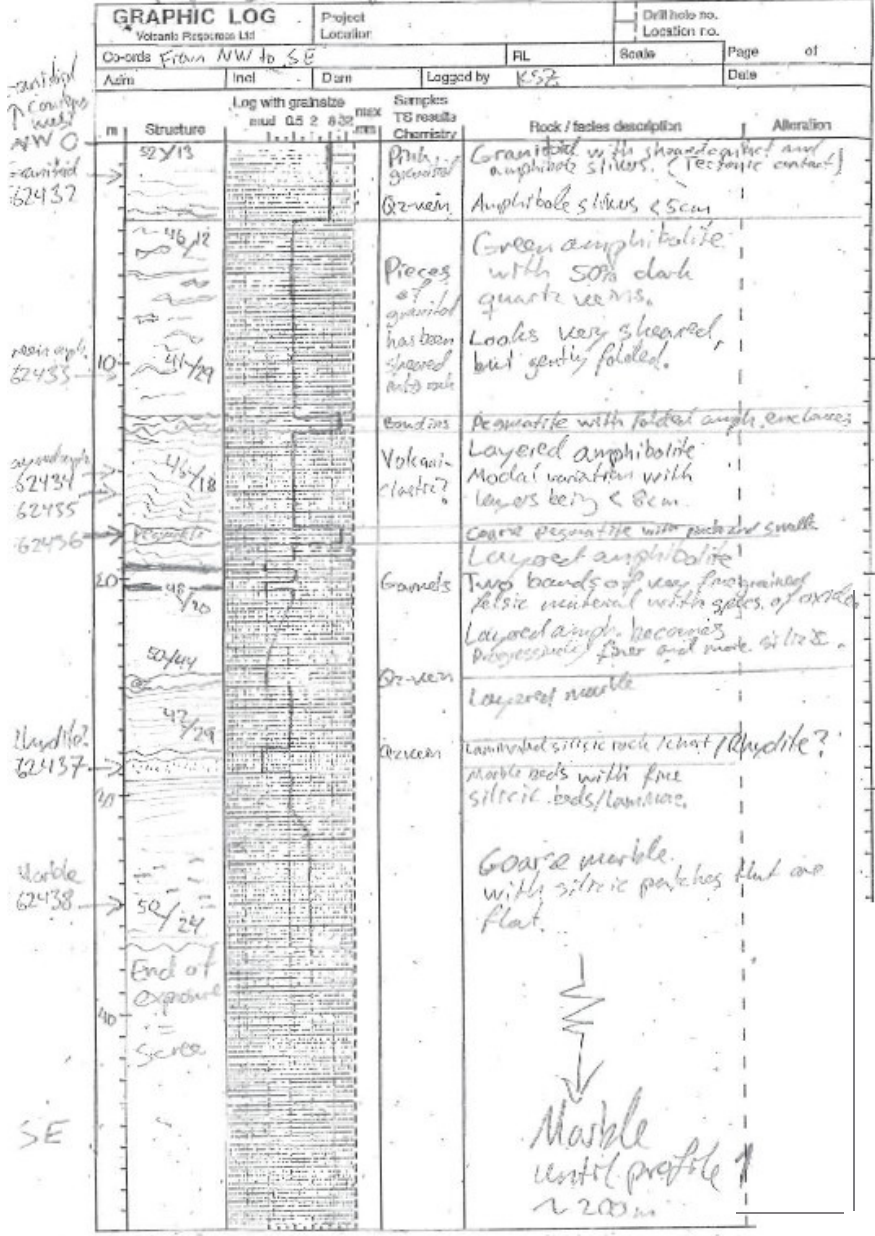
Profile strike 150°

GRAPHIC LOG		Project	Location	Drill hole no.	Location no.	
Vascular Resources Ltd		K-shaped marble	Drift 7 part 2 (upper)			
Co-ords	Incl	Diam	Logged by	Scale	Page of	
			KSZ			
Azimuth	Incl	Diam	Logged by	Scale	Date	
			KSZ		22/1/86	
m	Structure	Log with grainsize		Samples	Reck / facies description	Alteration
		mud	0.5 2 9 32 mm			
100	40/30 *			horizon of well crystals	Coarse marble contains another 150m at least to NW	
90	Pegmatite				TTC-type biotite pegmatite	
80	Pegmatite				Pegmatite stringers with green reaction in marble	
70	Pegmatite				Pegmatite with massive biotite Green reaction rims Pegmatite with inclusions of marble	
60	Pegmatite				Coarse marble Pegmatite. Folded and cuts foliation	
50	Pegmatite				Coarse marble Pegmatite 30cm Coarse marble Pegmatite 40-60 50cm Wollastonite rims between marble and pegmatite	
40	Pegmatite				Coarse marble Pegmatite is subconcordant but outcrops in marble	
30	Pegmatite				92-patches 5x1cm Wollastonite rims Thin chrysolite / Oz-ite bands < 15cm in marble Siderite Layered marble with green mica	
20	Pegmatite				Rhyolite with Boundaries of coarse marble Oz-patches Coarse patches of feldspar Siderite horizons < 10cm	With biotite in rhyolite Rusty patches
10	Pegmatite					

* Coarse Marble
2m wide Peg.
Peg. 562427
Marble 562428
Marl 562429
Rhyolite 562425
siderite 562425
50m

NB 245m rhyolite? (F₉₀ = 0.5 S_{0.015} = 2)

Profile 2 Y-slipodivisbi Profile strikes 110°



Archean basement rocks and Paleoproterozoic intrusions of the larger Tasiilaq area (TOMN)

Introduction

The author of this field report participated in the field work of SEGMENT between July 29 and August 22 2014. Information about the camps (purpose, geographical coordinates, and dates of visit and co-field team participants) can be seen in Table 4, while the names, initials and affiliations of co-field partners can be found in Table 7. A geological map indicating the camp positions can be seen in Figure 44. Appendix A contains information about the individual samples including geographical coordinates, descriptive notes, and the type of analytical procedures applied (if any).

Table 4. Team number, coordinates, dates and participants for the field work.

Location	Purpose	Lat. (N)	Long. (W)	Dates	Participants
Camp 1	Granite and diorite intrusions and the gneissic basement	65.718060	-39.17531	29.7.-2.8.2014	KT, MNP, TOMN
Camp 2	Granite intrusions, anorthosites and the gneissic basement	65.54866	-38.75251	2.-6.8.2014	KT, TOMN
Camp 3	Johan Petersen Intrusion	65.81558	-38.27019	6.-8.8.2014	ABN, JOT, TOMN
Camp 4	Basement gneiss and supracrustal rock units	65.59522	-38.62558	8.-12.8.2014	JOT, TOMN
Camp 5	Basement gneiss and supracrustal rock units	65.61592	-38.39206	12.-18.8.2014	JOT, TOMN
Camp 6	Basement gneiss and supracrustal rock units	65.84414	-36.61569	18.-22.8.2014	JOT, TOMN

Table 5. Initials, names and company/university of the participants.

ABJ	Anne Brandt Johannesen, MSc. student	University of Oulo, Finland
JOT	Jonas Tusch	University of Köln, Germany
KT	Kristine Thrane	GEUS, Denmark
MNP	Matti Nellemann Petersen	GEUS, Denmark
TOMN	Tomas Næraa	University of Lund, Sweden

Camp 1 – Team 10

Isortoq area, diorite and granite intrusion close to ice margin; geological map with camp and locality positions can be seen in Figure 45.

The area consists of three main units, which are also shown on the geological map (Figure 45). The units are: (1) gneiss, (2) diorite and (3) granite (see also Figure 46). However, the actual boundaries and size of these units are somewhat misplaced on the geological map.

The gneiss (1) is isoclinally folded and range in composition from leucocratic to melanocratic gneisses with mafic and ultramafic pods or lenses. One of the marked supracrustal units (marked as amphibolite) on the geological map (the one to the west) were visited and more or less correspond to gneiss with a more mafic character (melanocratic), thicker amphibolite units and a concentration of ultramafic lenses. At this place the gneiss is also intruded by large sheets of granite (20 m or more wide) that can be followed for several kilometres, these granite sheets seem to continue below the surface and constitute a large part of the subsurface geology in the area. Rust weathered (likely with minor amounts sulphate) areas are observed here and there and constitute a minor component of the basement; all rusty outcrops are found in the gneiss and mainly seem to reflect surface weathering.

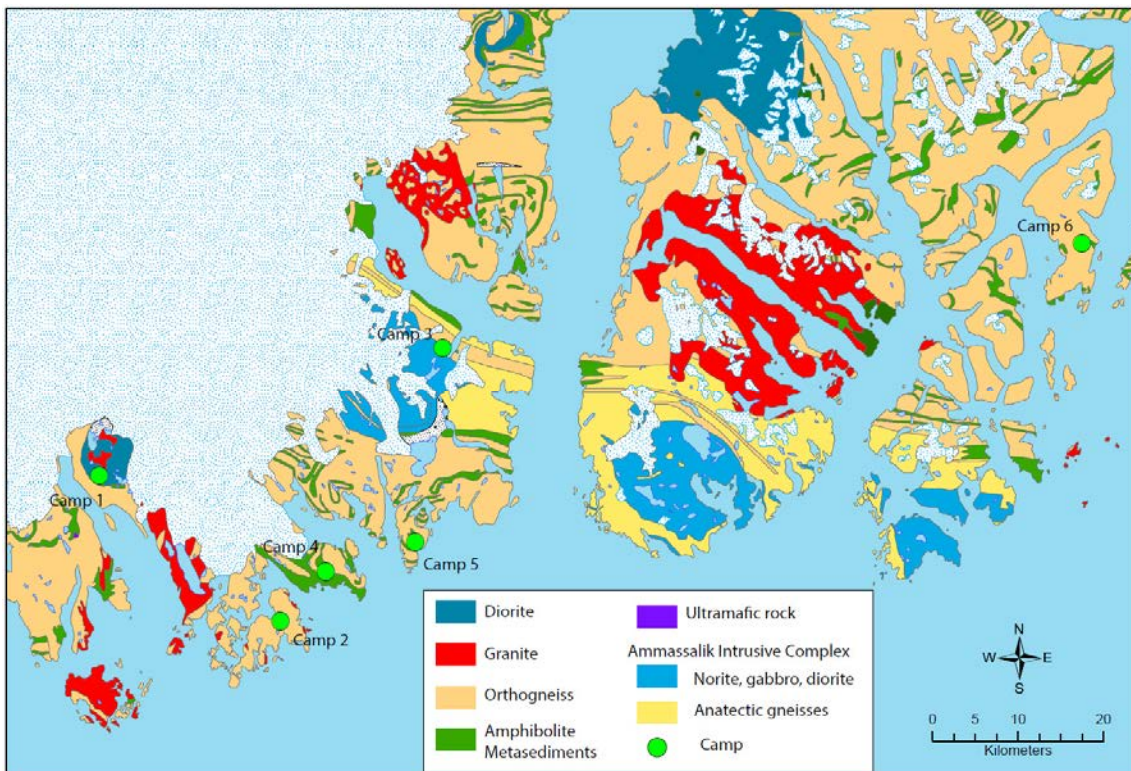


Figure 44. Geological map with the camp positions indicated.

The diorite (2) is undeformed and intrudes into the gneiss basement. Within the area marked as “Diorite” on the map are also large areas of mainly gneiss. Within the diorite several different phases can be distinguished in the field, the main phase is a fine to medium grained grey-black intrusive rock, this rock often display mingling textures with a coarser grained and lighter greyish unit (quartz diorite?) (Figure 46A). In some places the lighter coloured greyish “quartz dioritic” phase dominates over the finer grained dioritic phase. This was observed where the southern granite unit (close to locality 46 on Figure 45) extends toward the south. Diorite with porphyritic textures is observed as a minor phase (Figure 46B). At some places the diorite seems to have reacted with, or partially melted, the contact zones with the gneiss basement.

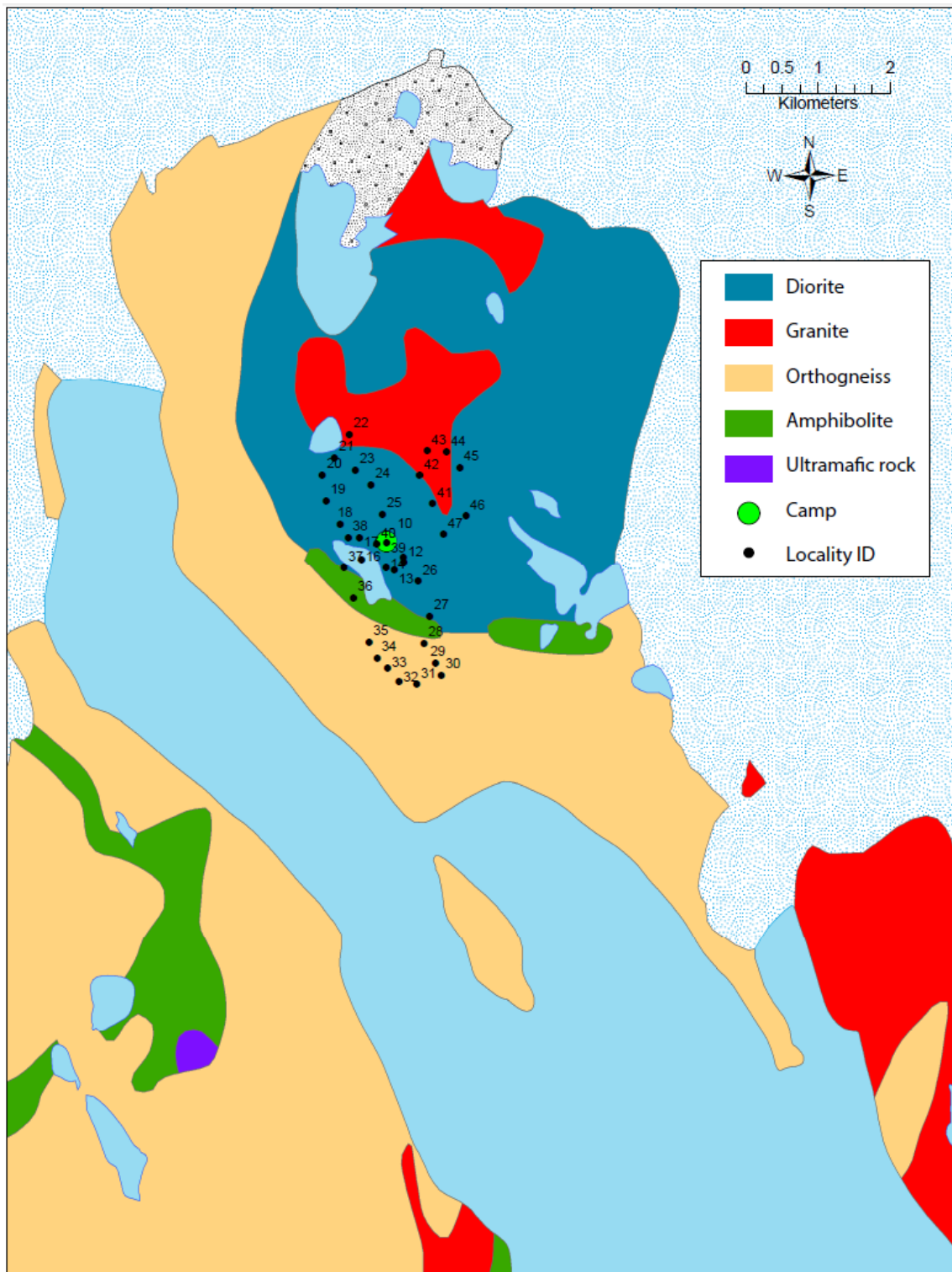


Figure 45. Geological map with Camp 1 and the locality positions indicated.



Figure 46. *Basement gneiss, diorite and granite from the camp 1 area. A) Diorite (black) with clearly irregular boundaries toward a quartz diorite (light grey), maybe the relation by mingling or that the quartz diorite (might be more evolved in composition) is a differentiated liquid from the diorite? B) Diorite (here with porphyritic texture) with irregular boundaries toward the quartz diorite, both units are clearly cut by later granite sheet. C) Granite sample 562918. D) Gneiss sample 562909 (outside the diorite intrusion).*

The granite (3) is undeformed and intrudes the gneiss and the diorite. It mainly occurs as sheets of various sizes and as 2 larger intrusive bodies (as indicated on the geological map). The granite mainly has a granular igneous texture, however, at the border of the larger granite and within some of the larger sheets a foliation is present, likely due to syn- or late magmatic deformation.

Epidote veins crosscut all units, and are observed throughout the area. In some places the epidote veining are observed together with alkali feldspar weathering and might have formed in relation to late pegmatite veining.

At one place (65.70093, -39.16225) we found a loose boulder (sample 562908) with a ruby looking phenoblast, however, no outcrop that matched this were found and no similar boulder in the nearby area.

Our observations from the area suggest that the amount of diorite that is shown on the map is overestimated and that the granite is underestimated. Otherwise we think that the geological map does well in presenting the different lithologies in the area.

Camp 2 – Team 10

Kitak Island, anorthosite rich gneisses and deformed amphibolite dykes; geological map with camp and locality positions can be seen in Figure 47.

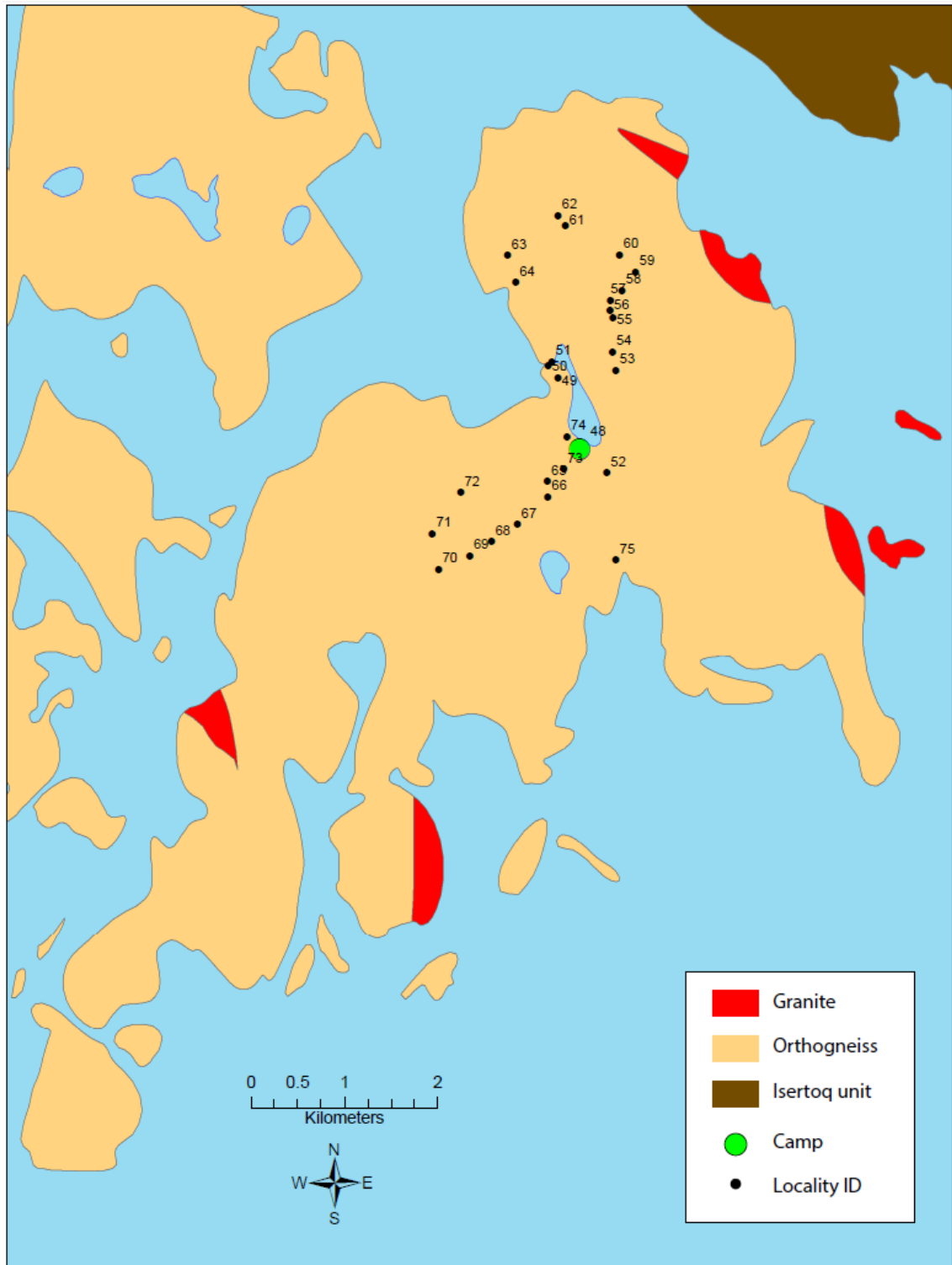


Figure 47. Geological map with Camp 2 and the locality positions indicated.

The main constituent of the area is grey gneiss that contains variously deformed anorthosite lenses (Figure 48A and C). Other gneiss types consist of banded grey gneiss, banded mesocratic (probably tonalitic in composition) gneiss and leucocratic gneiss (Figure 48B). At least some of the leucocratic gneisses have formed where anorthosite lenses have been sheared out into a gneissic fabric (which can be recognized in the field due to observed gradual deformation and shearing of anorthosite lenses into leucocratic gneiss). The grey gneiss with anorthosite lenses have most likely intruded into the anorthosite, and the anorthosite (as also noted in Wright et al. 1973) record an early deformation phase not recorded in the surrounding gneiss; often the anorthosite lenses display an internal foliation oblique to the surrounding gneiss. There is a strong strain variation in the area and strong flattening of the gneiss fabrics occurs mainly in the area north of the camp, in areas where distinct mylonite zones (2–5 m wide) are present. These mylonite zones follow the overall trend of the foliation, and mylonitisation are often pronounced around rocks that envelope ultramafic and mafic bounding's within gneisses. In areas of less strain it is obvious that the gneissic basement is migmatitic and deformed pegmatite lenses are also a common component. From the outcrop strain difference and position of mylonite zones it might be suggested that the central parts of the mapped area (around the camp) are preserved in a low strain fold hinge zone, whereas the strongly sheared and mylonised gneisses toward north and south are hinge zones. Moreover, although not perfectly matching, similar rock types occur north and south of the camp (most strikingly is the band of mafic (mesocratic tonalite) gneisses).

Pegmatites and granite sheets occur throughout the area, the northern most part of the island are marked as late intrusive granite on the geological map. This area was not visited; however, granite sheets become more frequent toward the north whereas pegmatites are more common in the area just south of the camp. Several generations of pegmatite are present, and some are clearly post-tectonic whereas others are pre-tectonic. Both types have been sampled for dating.

The gneisses contain amphibolite layers and lenses that have been described as the Kitak dykes (Wright et al. 1973) and it seems (at least for most examples) that these amphibolite units represent dyke intrusions into the gneissic basement (Figure 48A). All observed amphibolite dykes have tectonic contacts with the surrounding gneiss basement, can often be followed for several hundred meters and are often boudinaged. In one of the dykes garnet was present together with leucocratic veins (sample 562922, locality 49); garnet are present in the amphibolite and within the leucocratic veins that infiltrate the amphibolite. Area surrounding the leucocratic garnet bearing veins were seemingly also clinopyroxene bearing.

A large ultramafic lens are present in the northern most part of the area, this lens is roughly 2 km in length and several 100 meters wide. The ultramafic lens appear as a light brown weathered unit and consist for most part of medium grained orthopyroxene and clinopyroxene (needs to be confirmed by thin-section work), the orthopyroxene seemingly have been more resistant to weathering as often stands out giving the outcrop a strange appearance. More fresh looking units, black (ultramafic or gabbroic) and grey (tonalitic) seem to have intruded the light brownish pyroxenite (Figure 48D).

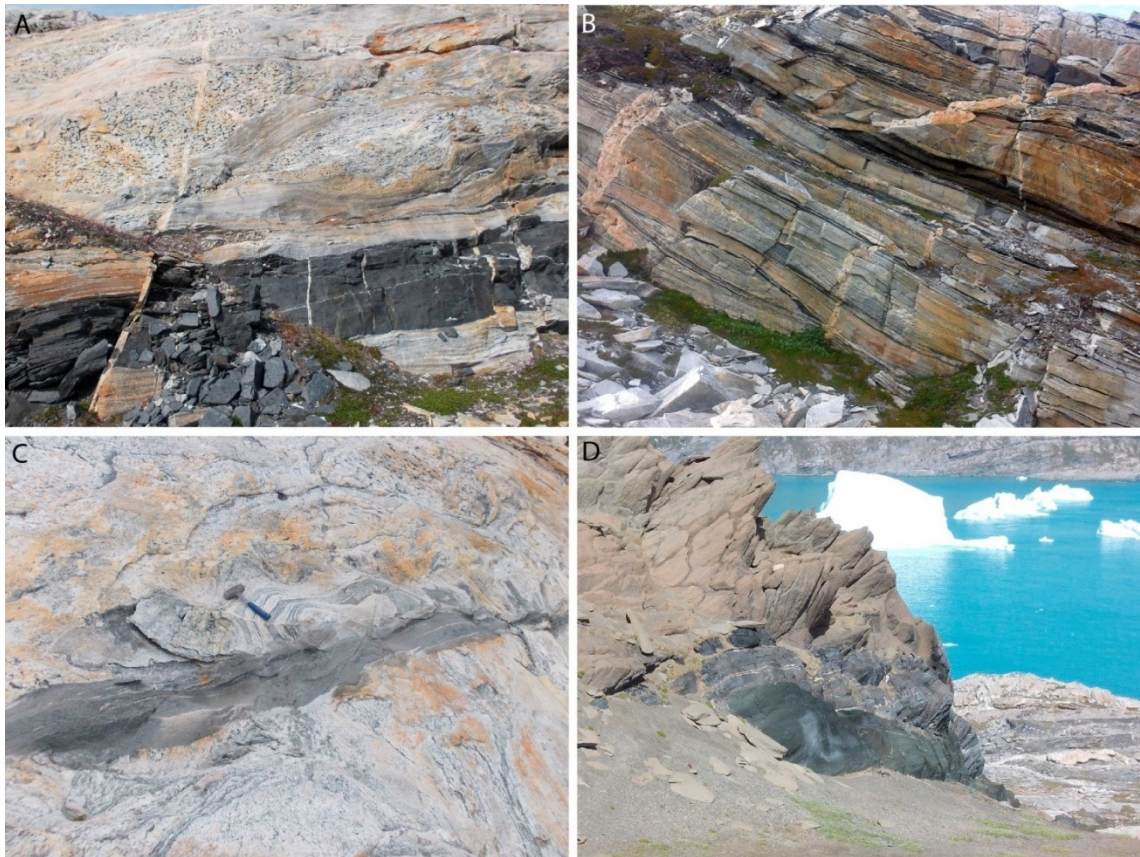


Figure 48. *Gneiss with anorthosite lenses and a tectonised amphibolite dyke (dyke is deformed and is foliation parallel to the surrounding gneiss). B) Banded gneiss (often the gneisses actually have a schistose texture). These gneisses often contain zones (2–5 m wide) with mylonitic textures; sheared dykes and late pegmatites are also common components. C) Late dykes are found in an area north of the camp site, these dykes appear with darker cores and lighter rims, sometimes deformed sometimes undeformed. D) Ultramafic body (light brown weathered) seemingly intruded by fresh looking black (ultramafic) and grey (amphibolite-tonalite) units.*

Camp 3 – Team 10/9

On the Ammassalik Intrusive Complex, together with JTO and ABJ, following up on issues that ABJ was working on. This camp was planned to facilitate a change of team partners and I made no detailed geological observations (no map).

Camp 4 – Team 9

The Suportoq supracrustals on the Niaqernarsik peninsula; geological map with camp and locality positions can be seen in Figure 49.

In this camp rock units are characterised by isoclinal folding and thrusting and are interpreted to reflect part of a thrust and fold nappe. Few late intrusive phases are recognised but the majority of units are tectonites. A large ultramafic unit (locality 94-96) that have been strongly metasomatised occur together with the tectonites.

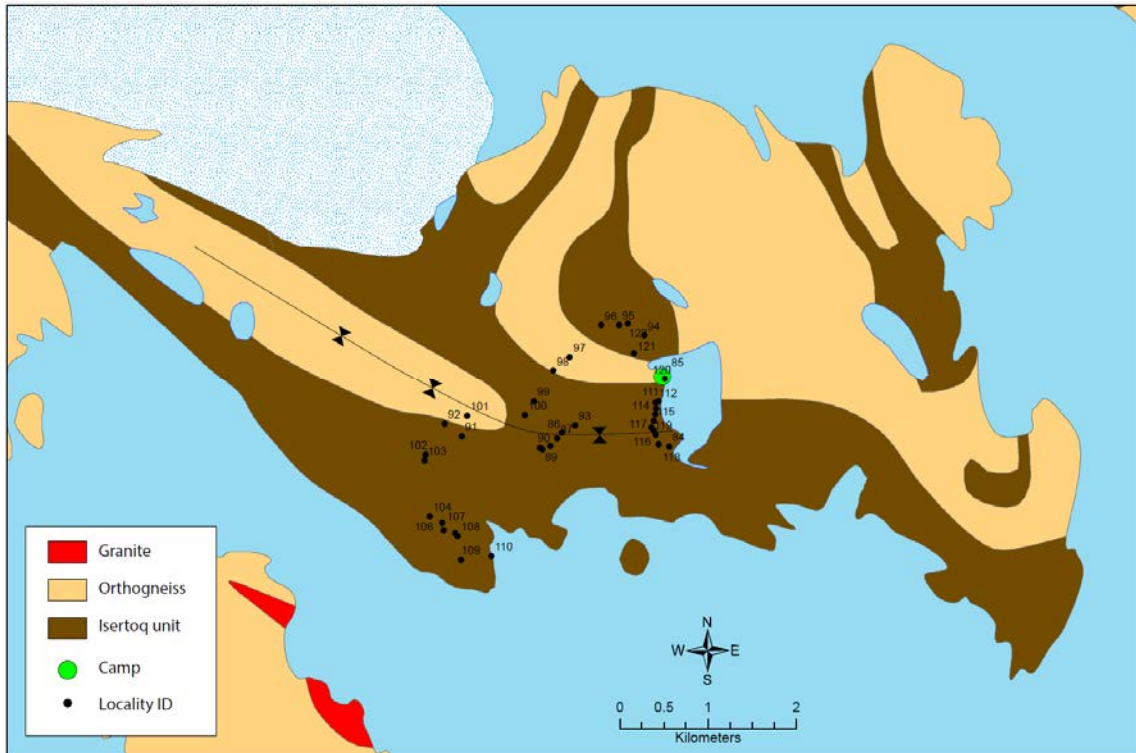


Figure 49. Geological map with Camp 4 and the locality positions indicated.

The main rock types observed in the area are:

1. Mafic units (as amphibolites or with some amount of pyroxene), often with compositional layering (Figure 50A) and often >10 m wide and can be followed locally along strike.
2. Intrusive ultramafic/hornblendites (hornblendite sometimes with plagioclase) (Figure 50B.)
3. Qz-plg-bt schist (\pm garnet) and very often with a feldspar phenoblastic fabric (Figure 50C) and the more strained units have a mylonite fabric.
4. Kya-gt-bt schist often as lenticular units within the qz-plg-bt schists, but occur also as more continuous layers (Figure 50D).
5. Quartzite or greywacke units (qz, plg, \pm bt, \pm hbl) often no more than 20–40 cm wide and often as lenticular unit (often with bt defining a foliation (Figure 50E). Some of these units could in principle be deformed quartz veins; it has not been possibly to distinguish in the field.
6. Deformed intrusive dioritic to tonalitic rocks (often representing more homogeneous units with little porphyroclasts and layering) (Figure 50F).
7. Ultramafic lenses mostly within the mafic units. Two large units are observed and these display strong metasomatic alteration textures, where kyanite is found in some of these zones.
8. Orthogneisses with amphibolite lenses, these units has a strongly banded character and might reflect older Archaean gneiss basement (as also suggested on the geological map).

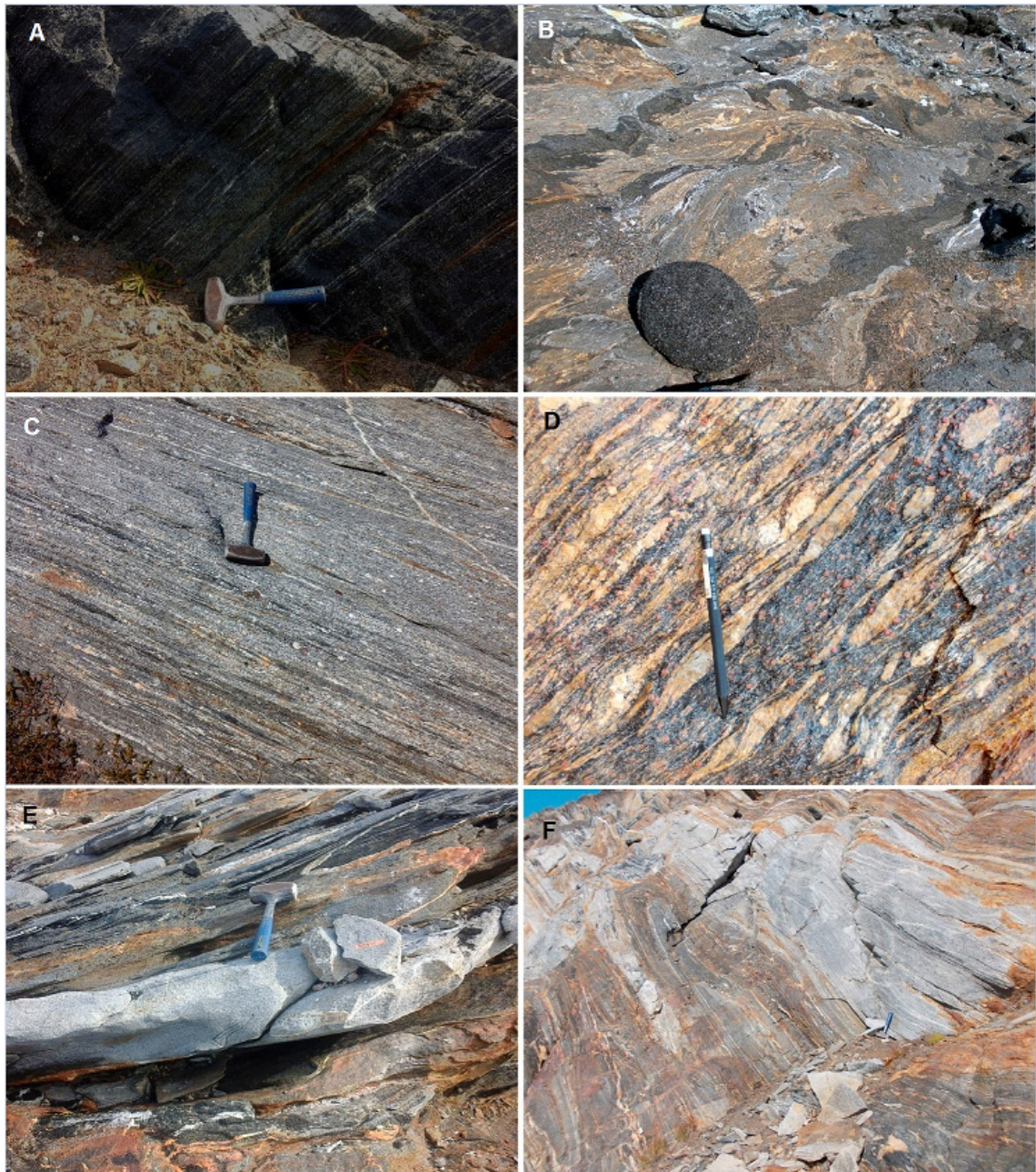


Figure 50. *A) Mafic compositionally layered unit, mainly hbl and plg, but also cpx and qz. B) Mafic unit intruded by ultramafic sheets (hornblendite or gabbroic). C) Phenoblastic qz-plg-bt schist; might appear more or less mylonitic. D) Kya-gt-bt schist. E) Quartzite (qz-plg-bt) layer within mainly mafic unit. F) Inter-folded mafic and felsic (tonalitic?) units.*

We did detailed mapping along a traverse following the lake toward south from the camp position (Figure 49). In this profile repeated sequence of mafic units, rusty garnet bearing zones and felsic units (phenoblastic and mylonitic in texture and \pm garnet) occurred. It thus appears that this area consists of a number of thrust sheets, likely part of a larger fold and thrust system. In the observed outcrops, extremely weathered and rusty zones are interpreted as thrust zones that have been re-used as pathways for fluids.

As marked on the map in Figure 49, the rocks in the area are situated in tight to isoclinal fold structures, and rocks within hinge zones are chaotic folded, and seems to preserve melt.

We made one long hike, in a western direction toward the southern limit of the map unit (toward the fjord). On this traverse, crossing a larger area we encountered more or less the same rock units as described/observed along the lake traverse south of the camp. Rock units are dominated by either mafic, often compositionally banded, units or by quartz, feldspar and biotite rich schists or mylonites. At the southernmost observations on the fjord more homogeneous and likely igneous units were present; these are interpreted as intrusive sheets that are deformed together with the other units.

Besides mainly smaller ultramafic lenses that have been found throughout the area two large ultramafic lenses are found closely together; these units are heavily metasomatised and infiltrated by pegmatites; however, also seems to be intruded by amphibolites. Kyanite seems to have formed during metasomatic reactions in parts of the ultramafics.

Camp 5 – Team 9

Suportoq supracrustals on the Tungujortoq peninsula; geological map with camp and locality positions can be seen in Figure 51.

Rocks in the area are predominantly amphibolites and felsic schists and gneisses (some units are garnet bearing). All these main rock types are isoclinal folded, with the fold-axis dipping roughly 10–20 degrees toward ca. 310 degrees north; the axial plain of these folds defines the local foliation which strikes ca. 90 degree and dip 20–30 degree toward north. As observed in camp 4 the rock units show tectonic contacts and likely constitute a fold and thrust system.

Throughout the region greenish horizons, which we believe could be called diopsidite (however the mineralogy have not been well characterised in the field, could be tremolite), are found within the amphibolite. They are almost always associated with undeformed pegmatites, which intrude rather late in the structural and metamorphic development of the area. When associated with “diopsidite” the pegmatites often have greenish alkali-feldspars. Zones within the amphibolite are garnet bearing, often associated with leucocratic veining and diopsidite horizons. Pegmatites in the area are at least of two ages, one older (isoclinally folded) and a younger type that cuts all other units and is undeformed.

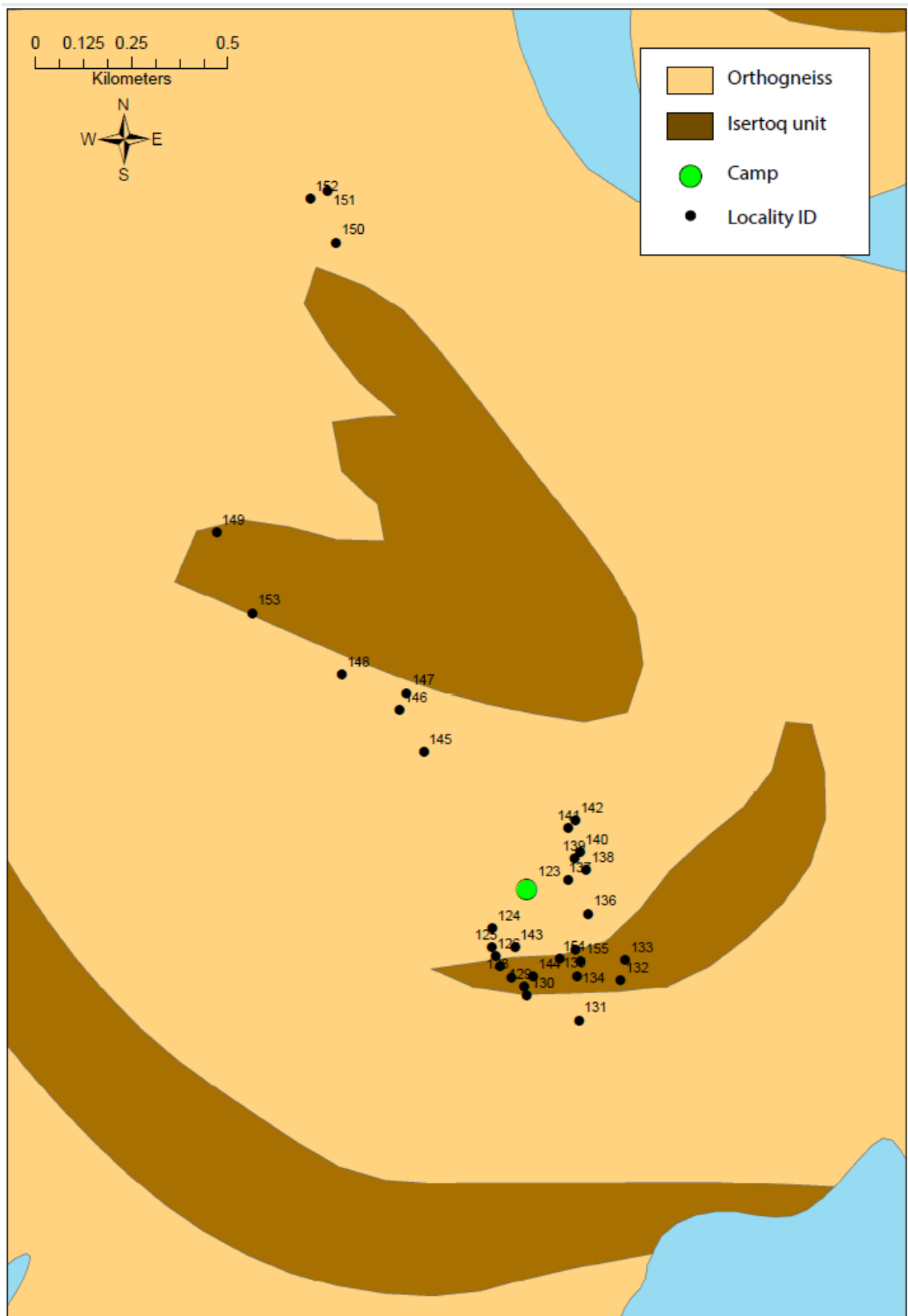


Figure 51. Geological map with Camp 5 and the locality positions indicated.



Figure 52. A) Laminated and isoclinal folded schist, felsic units are garnet bearing. B) Isoclinal folded pegmatite within laminated schist. C, D) Garnet bearing leucocratic veins in amphibolite. E) Part of the profile that was mapped in detail and sampled by saw-cutting. F) Laminated schist with alternating light felsic and greenish horizons (greenish horizons are referred to as diopsidite; the mineralogy of these units were not well characterised in the field).

Field work was mainly done just south of the camp in a profile (a saw-cut profile) covering some 20–40 meters in structural thickness. The rocks in this zone are characterised by large variations in lithology and chemistry, and contain a distinct zone with large ultramafic lenses (Figure 52E top right). The saw-cut profile is bordered at the structurally highest and lowest levels by amphibolites with a high concentration of leucocratic veins, where garnets are often found within the leucocratic veins or within the amphibolites itself bordering the leucocratic veins (Figure 52C,D). These veined and garnet bearing amphibolites occur structurally above a horizon of ultramafic lenses. The ultramafic lenses are up to around 10–15 m wide and 70–

80 m long and are probably pyroxenites (mainly composed of clinopyroxene cpx and opx) and are sometimes weathered into a pebble like unit, where opx is preserved as rounded grains whereas the cpx is weathered out. Below the structurally highest ultramafic lens, a horizon of greenish diopsidetite occurs (Figure 52F). This horizon is associated with pegmatites; below this the amphibolite unit is garnet bearing (throughout) and is highly veined by garnet bearing leucocratic veins that along strike merges/changes into a 1-2m thick kya-gt-ms-bt schist unit that continues throughout the mapped section (at least 200 m along strike). The structurally lowest part of the sequence consists of a layered sequence and a compact sequence (both 2–3 meters wide) and is bordered above by a second horizon of ultramafic rocks, these are minor units compared to the structurally higher horizon and are light brown, finer grained and altered (seemingly consist of cpx and opx (i.e., pyroxenite)). The layered sequence occurs structurally on top and consists of cm thick, intensively interfolded layers of a greenish rock composed of mainly cpx with minor amounts of hbl, qz and quartz rich layers with some amounts of hbl (\pm bt). Below this layered sequence are a compact unit composed of disrupted (boudinaged) cpx (minor amounts of hbl and qz).

Camp 6 – Team 9

On the Qianarteq Island; geological map with camp and locality positions can be seen in Figure 53.

The mapped area mainly consists of felsic grey gneisses with bands or lenses of amphibolites (sometimes garnet and cpx bearing). The grey gneisses and amphibolites are observed as isoclinal interfolded, which is likely a general feature of this early gneiss assemblage in the area. In many places the amphibolites of the early gneiss assemblage contain leucocratic veins; these are sometimes interfolded with the amphibolites or occur as undeformed melt veins. Leucocratic melts are also observed in pressure shadows where amphibolite lenses are boudinaged and in fold hinges (Figure 54A and Figure 54B). In most areas the grey gneisses are strongly banded and seem to be composed of greyish (more mafic minerals) tonalitic bands and leucocratic thinner bands.

Post-gneiss association are intrusive dykes or sills, cross cutting the gneiss basement, these are present in a rather large area west and south of the camp. These intrusive dykes (or sills) are amphibolites or gabbroic to dioritic in composition and seems to retain their magmatic textures in the least strained part (Figure 54C). These units consist of opx, cpx and plg, where opx seems to be overgrown by hbl rims. In more strained areas the dykes/sills appear as amphibolites and are often garnet bearing (and sometimes cpx bearing). In two outcrops (locality 180 and 185) eclogite facies rocks (or more likely retrogressed eclogite) seem to be preserved in late mafic dyke/sill units (Figure 54D). The eclogite assemblage occurs as minor patches within an amphibolite containing varying amounts of hbl, plg, cpx, garnet and qz.

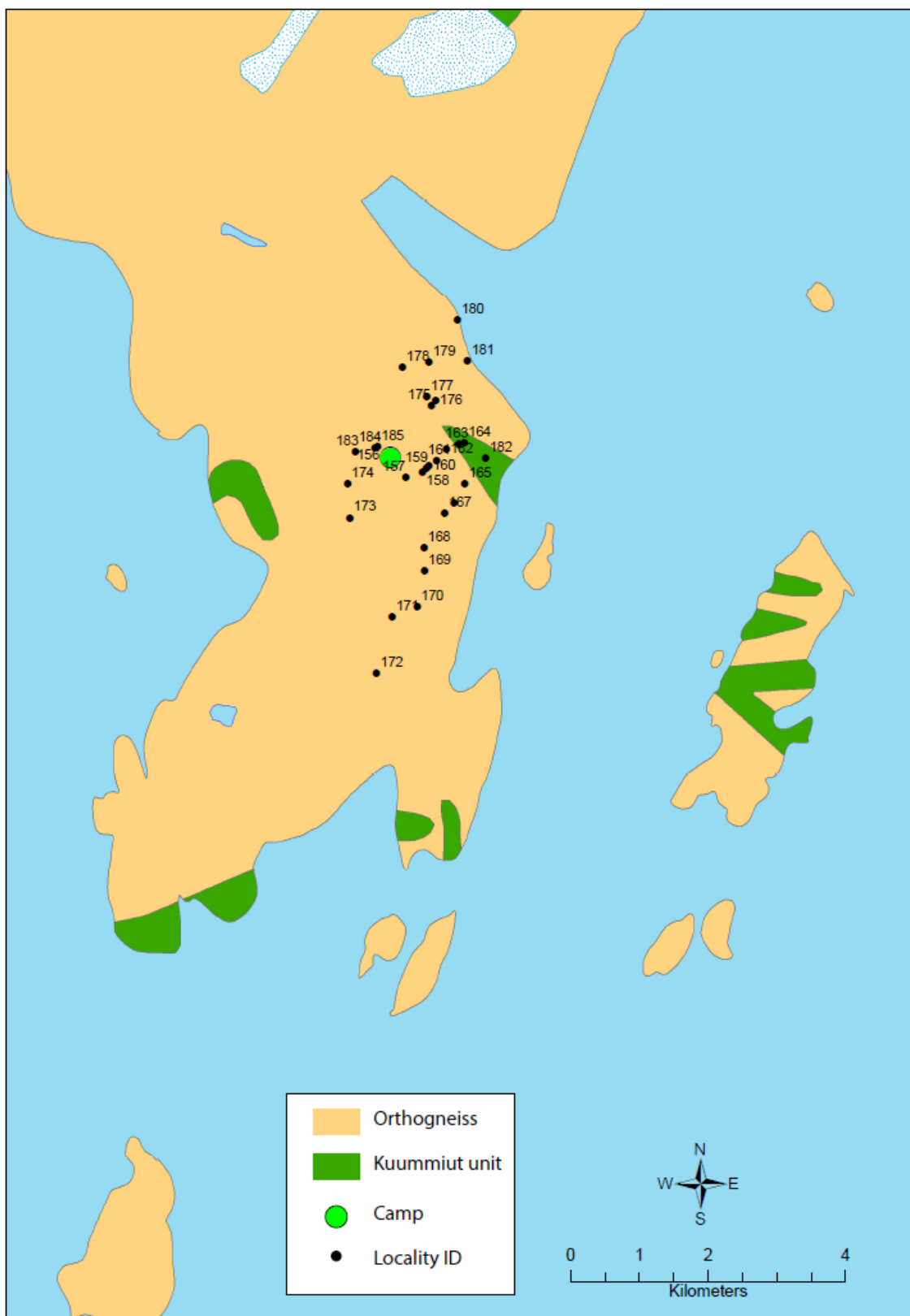


Figure 53. Geological map with Camp 6 and the locality positions.

In an area from the camp and toward east and south and associated with the late dyke intrusions K-spar weathering of the grey gneisses are very prominent and associated with pinkish pegmatites. At some places the rock fabric suggest that late whitish granite are intruding the

area, however, our preferred interpretation is that these features are caused by metasomatic alteration of basement gneisses likely during intrusion of late pegmatites.

A late dyke, only slightly deformed (Cenozoic age?) cross cuts the area. It strikes roughly from 30 to 80 degrees and appears to be steeply dipping or vertical (dip direction could not be established by direct observations).



Figure 54. A) Banded grey gneiss with infiltrated leucocratic late granitic melts. B) Banded gneiss with leucocratic sheets, some clearly situated in pressure shadows of a mafic xenolith (top left). C) Igneous texture in gabbro/diorite. D) Retrogressed eclogite. D, E) Felsic gneisses and granitic to leucocratic pegmatitic veins in the outcrop (loc. 180) seem to preserve retrogressed eclogite.

References

- Wright, A.E., Tarney, J., Palmer, K.F., Moorlock, B.S.P. and Skinner, A.C., 1973. The geology of the Angmagssalik area, East Greenland and possible relationships with the Lewisian of Scotland. In: R.G. Park and J. Tarney (Editors), *The Early Precambrian of Scotland and related rocks of Greenland*. University of Keele, Keele, pp. 157-177.

Appendix A. Complete sample list

Camp	Loc ID	Sample no.	GEUS no.	Purpose	Notes	User	Date and time	Whr. Chemistry	Thin sections
1	21	1	562901	Geochronology/geochemistry	Granite large regional intrusion	Tomn	30-07-2014 14:20	X	
1	23	1	562902	Geochronology/geochemistry	Diorite at the boundary of the regional granite intrusion	Tomn	30-07-2014 16:11	X	
1	24	1	562903	Geochronology/geochemistry	Homogeneous diorite	Tomn	30-07-2014 17:01	X	
1	24	2	562904	Geochronology/geochemistry	Granite sheet	Tomn	30-07-2014 17:01		
1	27	1	562905	Geochronology/geochemistry	Fine grained mafic variant of the diorite	Tomn	31-07-2014 12:52		
1	28	1	562906	Ore_Geology	Rusty outcrop probably representative of the area	Tomn	31-07-2014 13:27		
1	30	1	562907	Geochronology/geochemistry	Foliated granite	Tomn	31-07-2014 14:51		
1	30	2	562908	Geochronology/geochemistry	Boulder sample, ultramafic with corundum/ruby phenocryst	Tomn	31-07-2014 19:05		
1	32	1	562909	Geochronology/geochemistry	Sample of the regional gneiss basement	Tomn	31-07-2014 17:06	X	
1	37	1	562910	Geochronology/geochemistry	Leucocratic, variant of diorite. Mingling with 562911	Tomn	31-07-2014 18:48	X	
1	37	2	562911	Geochronology/geochemistry	Mafic fine grained variety. Mingling with 562910	Tomn	31-07-2014 19:06	X	
1	39	1	562912	Geochronology/geochemistry	Felsic component of the regional gneiss basement	Tomn	01-08-2014 12:49		
1	39	2	562913	Geochronology/geochemistry	Mafic tonalite component of the regional gneiss basement	Tomn	01-08-2014 12:50		
1	39	3	562914	Geochronology/geochemistry	Ultramafic lense within the gneiss basement	Tomn	01-08-2014 13:21		
1	39	4	562915	Geochronology/geochemistry	Isoclinal folded leucocratic granite veins within gneiss basement	Tomn	01-08-2014 13:22		
1	40	1	562916	Geochemistry	Amphibolite	Tomn	01-08-2014 13:51		
1	45	1	562917	Mineralogy	Purple mineral, palegreen mineral. Flurite-epidote	Tomn	01-08-2014 18:04		
1	47	1	562918	Geochronology/geochemistry	Regional medium grained granite	Tomn	01-08-2014 18:54	X	
1	12	1	562919	Geothermometry	Porphyritic diorite	Tomn	01-08-2014 19:34	X	
2	49	1	562920	Geochronology/geochemistry	Undeformed leucocratic granite in pressure shadow	Tomn	02-08-2014 17:29		
2	49	2	562921	Geochronology/geochemistry	Homogeneous grey gneiss, deformed together with anorthosite	Tomn	02-08-2014 18:00	X	
2	49	3	562922	Mineralogy	Garnet bearing amphibolite, with gt bearing melt veins	Tomn	02-08-2014 18:18		
2	59	1	562923	Mineralogy	Ultramafic large unit	Tomn	03-08-2014 16:34		
2	59	2	562924	Geochronology	Felsic sheets within border zone of ultramafic lense	Tomn	03-08-2014 16:34		
2	59	3	562925	Mineralogy	Pyroxenite	Tomn	03-08-2014 16:45		
2	62	1	562926	Geochronology/geochemistry	Granite sheet	Tomn	03-08-2014 18:06	X	
2	62	2	562927	Geochronology/geochemistry	Granite sheet	Tomn	03-08-2014 18:07	X	

2	64	1	562929	Geochronology/geochemistry	Coarse grained hbl bearing melt veins within gneiss unit	Tomn	03-08-2014 19:31		
2	64	2	562930	Geochronology/geochemistry	Gneiss unit	Tomn	03-08-2014 19:32	X	
2	65	1	562931	Geochronology/geochemistry	Late intrusive dyke, leucocratic rim region of dyke	Tomn	04-08-2014 12:45		
2	65	2	562932	Geochronology/geochemistry	Dyke, hbl spotted same as 562931	Tomn	04-08-2014 12:54	X	
2	66	1	562933	Geochronology/geochemistry	Granite sheet mingling with hbl spotted dyke	Tomn	04-08-2014 13:22	X	
2	70	1	562934	Geochronology/geochemistry	Small late pegmatitic veins cross cutting amphibolite	Tomn	04-08-2014 14:39		
2	74	1	562935	Geochronology/geochemistry	Anorthosite boudinaged in gneiss	Tomn	04-08-2014 17:18		
2	74	2	562936	Geochronology/geochemistry	Gneiss with leucocratic veins	Tomn	04-08-2014 17:34	X	
2	74	3	562937	Geochronology/geochemistry	Hbl spotted gneiss	Tomn	04-08-2014 18:05		
2	74	4	562938	Geochronology/geochemistry	Hbl spotted (rimmed by plg?) Gneiss	Tomn	04-08-2014 18:09		
2	74	5	562939	Geochronology/geochemistry	Leucocratic pegmatitic vein within hbl spotted gneiss	Tomn	04-08-2014 18:09		
2	75	1	562940	Geochronology/geochemistry	Felsic vein within amphibolite, gneissic gost texture	Tomn	05-08-2014 16:45		
2	52	1	562941	Geochronology/geochemistry	Surface of malakite	Tomn	05-08-2014 17:40		
4	86	1	562942	Geochronology/geochemistry	Leucocratic unit likely late infiltrating melts	Tomn	09-08-2014 14:30	X	
4	86	2	562943	Geochronology/geochemistry	Garnet, kyanite, biotite schist	Tomn	09-08-2014 14:31	X	
4	86	3	562944	Geochronology/geochemistry	Quartzite	Tomn	09-08-2014 14:31	X	X
4	89	1	562945	Geochronology/geochemistry	Felsic sheet within mafic sequence	Tomn	09-08-2014 16:16	X	
4	89	2	562946	Geochemistry	Quartz, plg, hbl gneiss, gt in some levels	Tomn	09-08-2014 16:24	X	X
4	90	1	562947	Mineralogy	Retrogressed eclogite?	Tomn	09-08-2014 16:58		
4	92	1	562948	Geochemistry	Gt bearing amphibolite	Tomn	09-08-2014 18:18		
4	92	2	562949	Geochronology/geochemistry	Banded grey gneiss	Tomn	09-08-2014 18:30		
4	105	1	562950	Geochronology/geochemistry	Quartzite	Tomn	10-08-2014 16:18		
4	106	1	562951	Geothermometry	Amphibolite	Tomn	10-08-2014 16:35	X	
4	108	1	562952	Geochronology/geochemistry	Greywacke layer within amphibolite unit	Tomn	10-08-2014 16:56	X	
4	109	1	562953	Geochronology/geochemistry	Tonalite grey gneiss	Tomn	10-08-2014 17:10	X	
4	110	1	562954	Geochronology/geochemistry	Tonalite grey gneiss	Tomn	10-08-2014 17:58	X	
4	112	1	562955	Geochronology/geochemistry	Gt, bt, qz schist within tectonised unit	Tomn	11-08-2014 12:28	X	X
4	112	2	562956	Geochronology/geochemistry	Tonalite sheet inter-folded with mafic rocks	Tomn	11-08-2014 13:06	X	
4	113	2	562957	Geochronology/geochemistry	Gt bearing pegmatite	Tomn	11-08-2014 14:00		
4	114	1	562958	Geochronology/geochemistry	Leucocratic granitic sheets infiltrating mafic/ultramafic units	Tomn	11-08-2014 15:54		
4	115	1	562959	Geochronology/geochemistry	Feldspar clastic gneiss	Tomn	11-08-2014 16:43	X	
4	118	1	562960	Geochronology/geochemistry	Felsic gneiss unit	Tomn	11-08-2014 17:34	X	
4	119	1	562961	Geochronology/geochemistry	Pegmatite	Tomn	11-08-2014 17:42		
4	120	1	562962	Geochronology/geochemistry	Leucocratic banded gneiss	Tomn	11-08-2014 19:35	X	

4	120	2	562963	Geochronology/geochemistry	Coarse grained gneiss	Tomn	11-08-2014 19:35	X	
5	140	1	562964	Geochronology/geochemistry	foliated quartz rich lense within gneiss	Tomn	13-08-2014 20:34		
5	140	2	562965	Geochronology/geochemistry	Pegmatite	Tomn	13-08-2014 20:40		
5	145	1	562966	Geochronology/geochemistry	Gt bearing qz-bt-plg schist	Tomn	15-08-2014 11:53	X	X
5	145	2	562967	Geochronology/geochemistry	Pegmatite, isoclinal folded	Tomn	15-08-2014 12:10		
5	145	3	562968	Geothermometry	Amphibolite lense	Tomn	15-08-2014 12:28		
5	147	1	562969	Geochronology/geochemistry	Plg-hbl rich gneiss	Tomn	15-08-2014 13:13	X	X
5	147	2	562970	Geochronology/geochemistry	Bt-qz-gt rich gneiss	Tomn	15-08-2014 13:16	X	X
5	148	1	562971	Geochronology/geochemistry	Pegmatite with greenish fsp	Tomn	15-08-2014 14:47		X
5	148	2	562972	Geochronology/geochemistry	Garnet bearing amphibolite with leucocratic veins	Tomn	15-08-2014 14:48		
5	148	3	562973	Geochemistry	Gt bearing amphibolite	Tomn	15-08-2014 14:48		
5	150	1	562974	Geochronology/geochemistry	Banded gneiss	Tomn	15-08-2014 16:34	X	X
5	153	1	562975	Geochronology/geochemistry	Coarse grained gneiss	Tomn	15-08-2014 17:46	X	
5	132	1	562976	Mineralogy	Layered px, hbl and qz, hbl rock	Tomn	17-08-2014 17:37		
5	132	2	562977	Mineralogy	Pyroxenite or tremolite	Tomn	17-08-2014 17:38		
5	132	3	562978	Geochronology/geochemistry	leucocratic pegmatite with hbl mega crystals	Tomn	17-08-2014 17:39		
6	159	1	562979	Mineralogy	Gt-cpx bearing amphibolite	Tomn	18-08-2014 20:08	X	X
6	161	1	562980	Geochronology/geochemistry	Pinkish white granite	Tomn	18-08-2014 21:03		
6	163	1	562981	Geochronology/geochemistry	Banded gneiss	Tomn	19-08-2014 12:15		
6	168	1	562982	Geochronology/geochemistry	Gabbro-diorite	Tomn	19-08-2014 14:24	X	X
6	172	1	562983	Geochronology/geochemistry	Homogeneous grey gneiss	Tomn	19-08-2014 16:54	X	
6	172	2	562984	Geochronology/geochemistry	Leucocratic vein	Tomn	19-08-2014 16:55		
6	176	1	562985	Geochronology/geochemistry	Agmatitic gneiss	Tomn	20-08-2014 12:38		
6	178	1	562986	Mineralogy	Amphibolite	Tomn	20-08-2014 13:10		
6	179	1	562987	Mineralogy	Gt, cpx bearing amphibolite	Tomn	20-08-2014 13:44		
6	180	1	562988	Geochronology/geochemistry	Eclogite mineralogy	Tomn	20-08-2014 15:31		
6	180	2	562989	Geochronology/geochemistry	Course grained banded gneiss	Tomn	20-08-2014 15:45	X	
6	181	1	562990	Geochronology/geochemistry	Gabbro or tonalite banded gneiss	Tomn	20-08-2014 16:45	X	
6	185	1	562991	Mineralisation	Eclogite or retrogressed eclogite	Tomn	21-08-2014 15:33		X
6	185	2	562992	Geochronology/geochemistry	Eclogite or retrogressed eclogite	Tomn	21-08-2014 15:47		

- All samples are rock samples

Ultramafic rocks of the Niflheim unit, marbles of the Helheim unit, Johan Petersen Intrusion, Suportoq supracrustals and basement gneisses (JOT)

Introduction

I participated in the field work of SEGMENT between the July 15th and August 22nd. I worked together with KSZ in camp 1 to 5. Work was done on ultramafics in the Niflheim unit to investigate its relationship to the basement (camp 1 & 2), on marble horizons in the Helheim unit (camp 3 & 5) and on nunataks to get insight into the lithology of the most northern parts of the mapping area where the project took place (camp 4). I joined ABJ in camp 6 & 7 to work around the Johan Petersen intrusion to examine the emplacement of the intrusion, its internal structure and the reaction with the country rocks. Furthermore work was focused on sulfide mineralisations located in the intrusion. In camp 8 to 10 I investigated the basement gneiss and supracrustal rock units with TOMN. The location of the camps can be seen in Figure 55. Information about the camps (purpose, coordinates, dates and participants) can be seen in Table 6, while initials, names etc. on the participants can be seen in Table 7.

Corresponding parts of the report were done in consultation with TOMN; and the reader is therefore referred to his field report. I am careful to point out that the field reports from KSZ and the coming master thesis by ABJ should also be explicitly taken into account because they are much more involved into the regions geology and are more experienced in doing field work.

Beside the daily work I was anxious for finding garnet bearing rocks, especially metasediments in order to do geochronology and constraints on the metamorphic conditions.

Table 6. *Coordinates, dates and participant for the field work.*

Location	Purpose	Lat. (N)	Long. (W)	Dates	Participants
Camp 1	Niflheim Unit	66.4154	38.1829	15.-18.7.2014	JOT, KSZ, SMW
Camp 2	Niflheim Unit	66.4249	38.1344	19.-20.7.2014	JOT, KSZ, SMW
Camp 3	Helheim Unit	66.3585	37.7179	21.-24.7.2014	JOT, KSZ
Camp 4	Nunataks in the northern part	66.7094	37.5288	25.-27.7.2014	JOT, KSZ
Camp 5	Helheim Unit*	66.3501	37.0829	28.-29.7.2014	JOT, KSZ, MADP, VIVH
Camp 6	Johan Petersen Intrusion	65.7537	38.5007	29.-31.7.2014	ABJ, JOT
Camp 7	Johan Petersen Intrusion	65.8156	38.2705	1.-7.8.2014	ABJ, JKOL, JOT, MFI
Camp 8	Basement gneiss and supracrustal rock units	65.5951	38.6254	8.-12.8.2014	JOT, TOMN
Camp 9	Basement gneiss and supracrustal rock units	65.6160	38.3922	12.-18.8.2014	JOT, TOMN
Camp 10	Basement gneiss and supracrustal rock units	65.8441	36.6155	18.-22.8.2014	JOT, TOMN

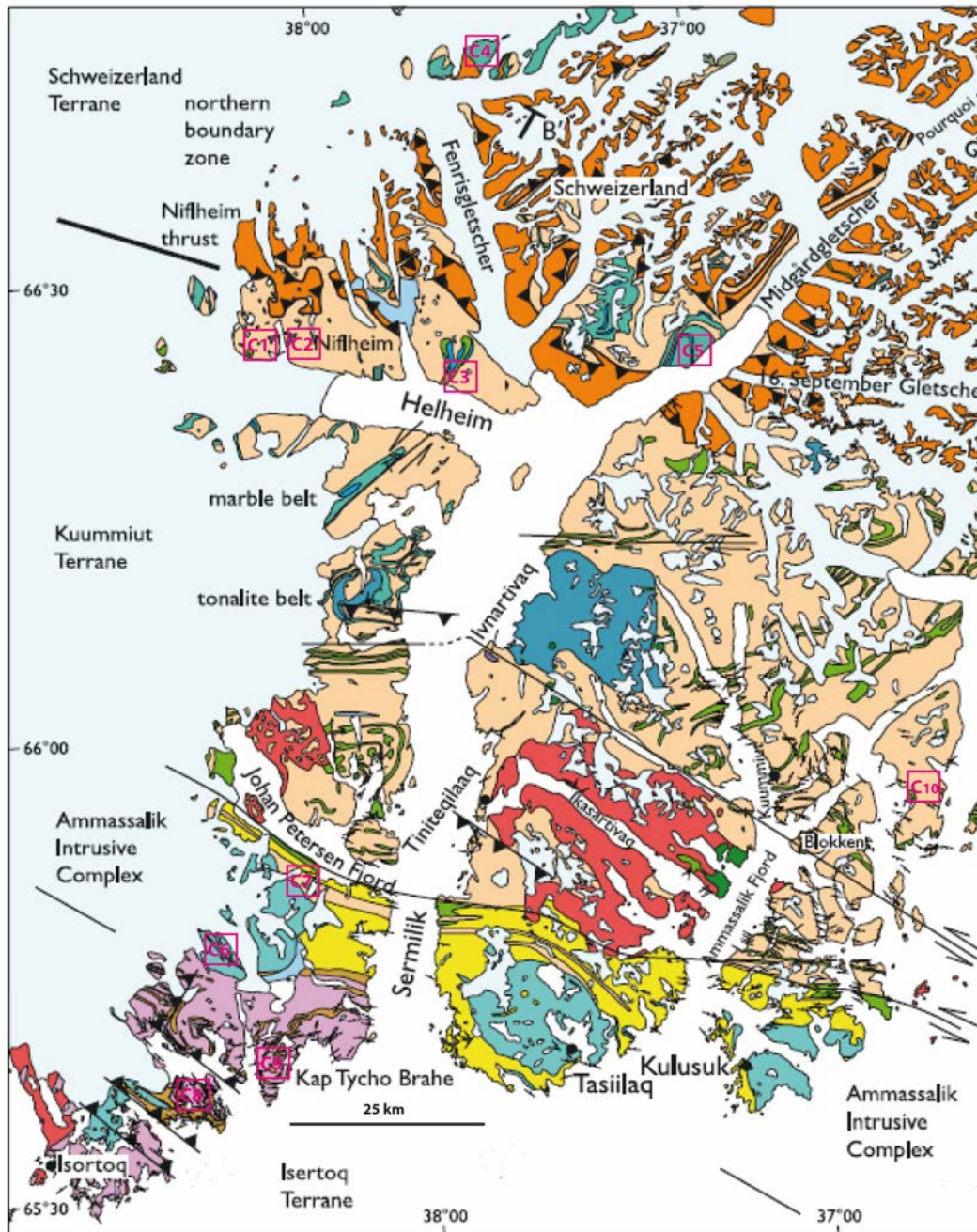


Figure 55. Location of the camps.

Table 7. Initials, names and company/university of the participants.

ABJ	Anne Brandt Johannesen, Stud.Scient.	University of Oulo, Finland
JOT	Jonas Tusch	University of Köln, Germany
KSZ	Kristoffer Szilas	Columbia University, New York, USA
MADP	Majken D. Poulsen	GEUS, Greenland
MFI	Marco Fiorentini	Centre of Exploration Targeting, University of Western Australia
SMW	Sam Weatherley	GEUS, Denmark
TOMN	Tomas Næraa	University of Lund, Sweden
VIVH	Vincent van Hinsberg	McGill University, Canada

Camp 1 and 2 – Ultramafics in the Niflheim Unit

Camp 1 and 2 were localized in the Niflheim Unit near the Inland Ice. The main rock types are mafic to ultramafics, often with cumulative structure, and our purpose was to figure out the relationship of this mafic body to the surrounding tonalitic gneiss basement. The ultramafic unit has a wrapped structure and is separated by a secondary valley (Figure 56A). The gneiss basement has a tonalitic composition, is cross-cut by veins and shows in situ melt features. At some places the gneiss shows an intrusive relationship as dikes intruding into the ultramafics. These dikes are more foliated than the surrounding ultramafics, probably due to strain competition.

A common feature of the ultramafics are plagioclase veins, often with rims of amphibole that developed by the interaction of quartz and olivine, confirmed by remnants of quartz crystals in the veins interior (Figure 56C). Likewise the presence of amphiboles in the ultramafics is probably a secondary hydration feature of pyroxene and olivine. A source might be the gneiss basement. Another proof of interaction between the two rock units is the high amount of garnet in the gneiss that decreases in distance to the ultramafic body before it disappears. The contact seems to be tectonic, indicated by shear zones (Figure 56C), where even in the ultramafics minerals are orientated, whereas they usually show a primary un-orientated layering (compare Figure 56A D and E). Intrusive relationships between the tonalitic basement and the mafic body bear witness to a syntectonic emplacement that brought the two units in juxtaposition with each other.

For further detailed information see field report by KSZ.

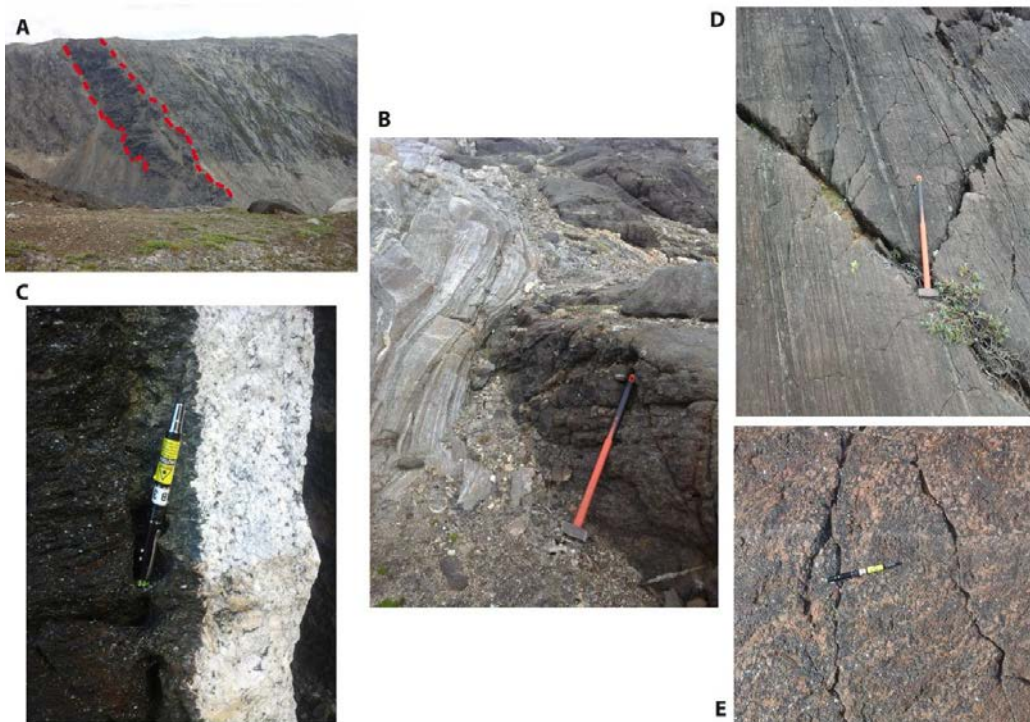


Figure 56. *Ultramafics in the Niflheim Unit. A) View to E on the ultramafics, framed by dashed lines, embedded in the tonalitic gneiss basement; locality 16. B) Contact between basement and ultramafics; loc. 50. C) Plagioclase vein in the ultramafics rimmed by amphiboles; loc. 38. D) Ultramafics with primary un-orientated layering; loc. 40. E) Strongly sheared ultramafics with boudinaged plag veins; loc. 33.*

Camp 3 – Y-shaped marble in the Helheim Unit

Work at Camp 3 (locality 74, Appendix A) was focused on a sequence of marble units, intercalated with other supracrustal rocks (Figure 57C), in a shear zone. A detailed profile was done by sampling along a transect through a fold system (axis dipping with approx. 70°NNW), located just at the NW side of the valley where we camped (Figure 57D, sample 562416 - 562438).

The marble unit is mapped as a homogeneous Y-shaped enclave in the basement. However, this is a simplification that neglects other supracrustal rocks (Figure 57B), often dominating the lithology. These supracrustal rocks are probably metavolcanics, although they could be quartz rich ttgs with underrepresented plagioclase. Using an acid-based indicator reveals that the most common type is smithsonite, which is a carbonate of zinc.

It seems that the marbles and intercalated rocks we mapped on the transect were folded by moving on a shear zone which is characterized by a very deformed quartzite. Deformed pegmatites intruding the system could yield a minimum age of the tectonic event.

For further detailed information see field report from KSZ.

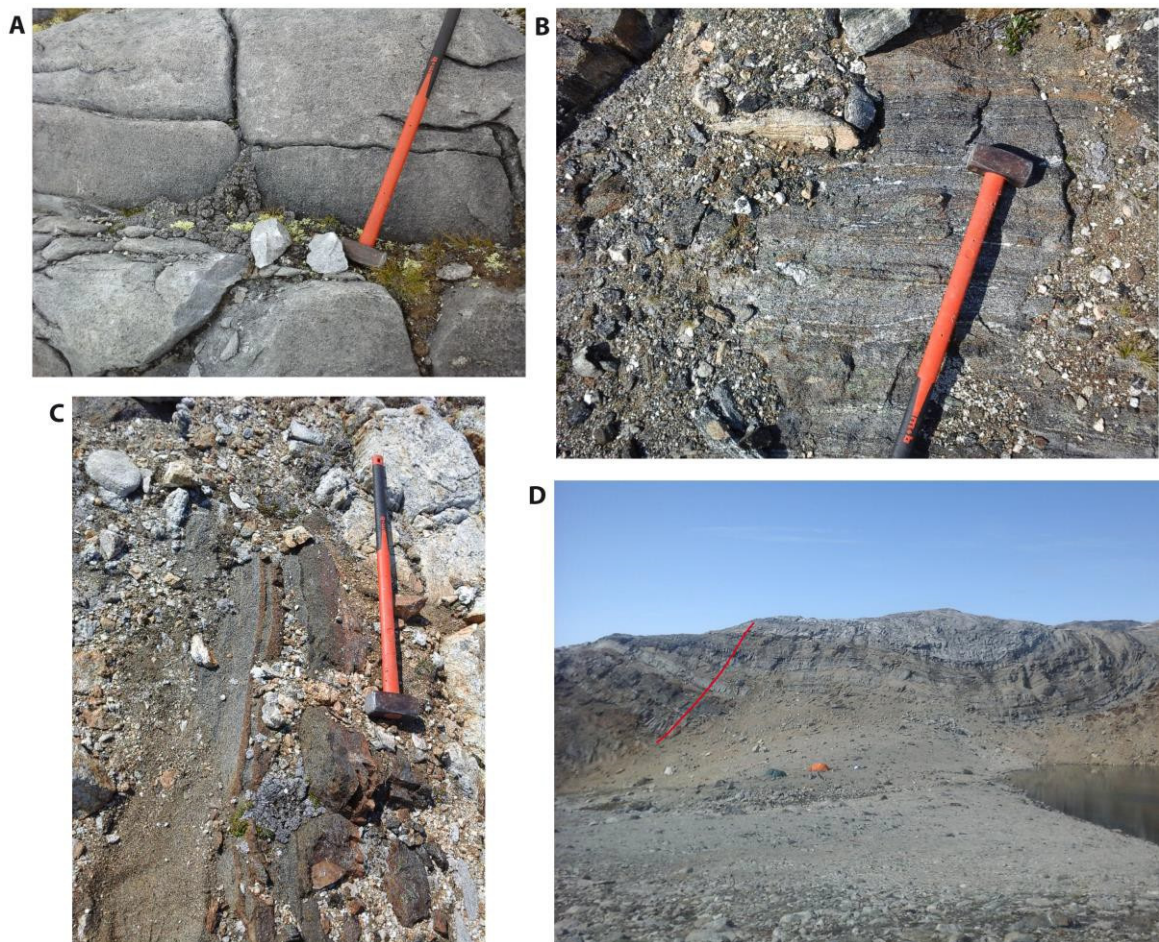


Figure 57. *Y-shaped marble. A) Coarse grained marble, 76 m of profile I; loc. 111. B) Metavolcanic rocks, intercalated with marbles; loc. 87. C) Contact between metasediment and marble; loc. 89. D) Folded sequence of marble units, intercalated with other supracrustal rocks. Red line indicates site of transect.*

Camp 4 – Nunatak

Camp 4 was located on a nunatak in the Inland Ice (locality 142, Appendix A). The nunatak is composed of three different rock units. Mafic to ultramafic rocks (amphibolites and gabbros) can be found SW of camp. As isolated bodies they have a tectonic relationship to Al-rich rocks (sillimanite schist/ gneiss). These Al-rich rocks, probably metasediments, are strongly foliated and dominate N of camp as one complex unit (undisturbed by the ultramafics) but can be found on the whole nunatak. The Al-rich rocks are strongly (sometimes isoclinal) folded, often with pegmatite layers parallel to foliation (Figure 58A). Sillimanite is the most indicative mineral and often concentrated in horizons, probably an orientation phenomenon due to high strain. The third unit is a post kinematic white granitoid, cutting all units and absolutely undeformed. The proposed marble lithology on the nunatak, as marked on the geological map, might be a misinterpretation of this granitoid. It is mainly composed of large crystals of perthitic feldspar, often with lots of muscovite accompanied by garnets. A reco on surrounding nunataks revealed the dominance of the metasediments and the presence of kyanite gave the important proof that metamorphic conditions were higher than previously assumed.

For further detailed information see field report from KSZ.

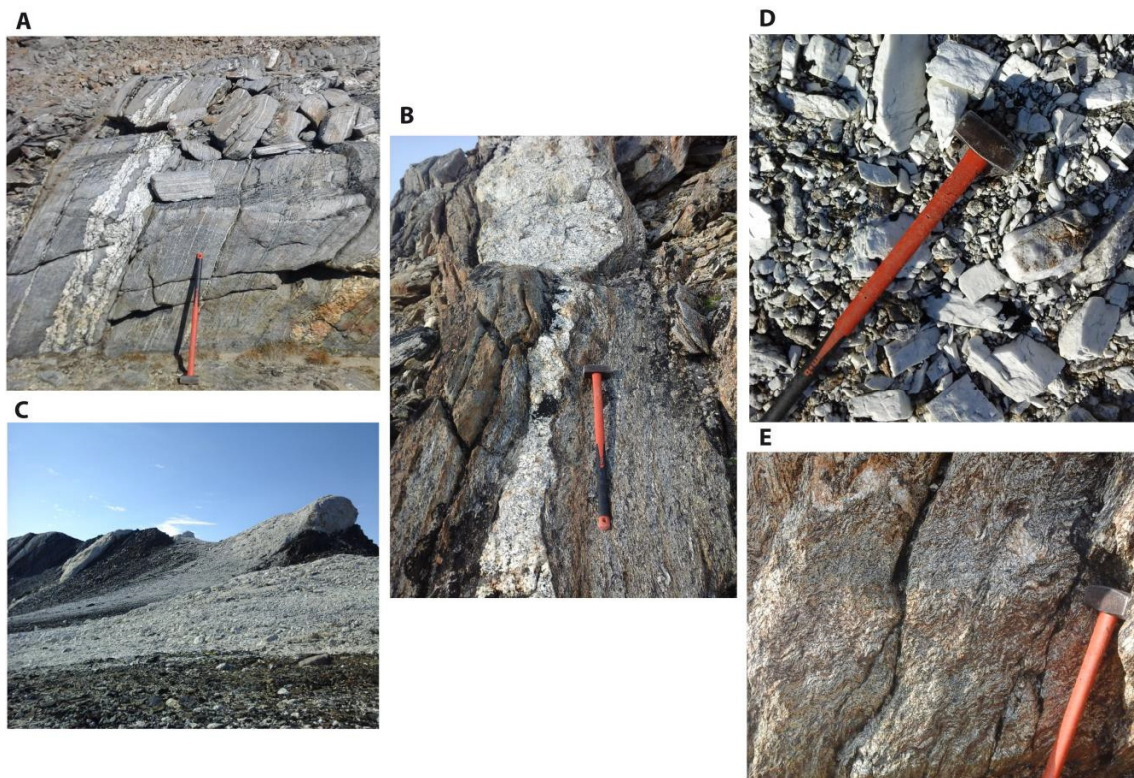


Figure 58. Nunatak. A) Strongly foliated sillimanite schist with pegmatites parallel to foliation; loc. 146. B) White granitoid intruding sillimanite schist; loc. 206. C) White granitoid intruding in ultramafics; loc. 173. D) Boulder field at white granitoid dominated by large feldspar crystals; loc. 169. E) Strongly folded sillimanite gneiss; loc. 196.

Camp 5 – Marble of the Helheim Unit

Camp 5 was located several km E of Camp 3 and is also a region with an occurrence of marble units and other supracrustal rocks embedded in the basement. We joined with team 6 to share our findings in the marble at Camp 3. For me this camp was a transit on my way to Camp 6 and my one day observations are limited and cannot be framed into a bigger picture.

For further detailed information see field report from KSZ.

Camp 6 – Southern part of the Johan Petersen Intrusion

Camp 6 (locality 244, appendix A) was located in the southern part of the Johann Petersen Intrusion. I got an introduction from ABJ about her findings regarding the intrusion, since she worked around Camp 6 several days before I arrived. It turns out that the intrusion is composed of a variety of granitoids with a difference in composition which is indicative for a multiple dynamic setting rather than a single intrusive event. These granitoids are mainly gabbro-norite, diorite and granite. All these orthogneisses show retrograde mineral reaction assemblages like amphibole for pyroxene or plagioclase (+ orthopyroxene) for garnet. The intrusive relationships between the different granitoids, occurring pyroxenites and leuco-cratic veins are complex and indicate a convoluted intrusive setting overprinted by higher metamorphic conditions. The gabbro-norite as the main rock type is intruded by granites (Figure 59D), reveals disrupted pyroxenites which are adjusted to a distinct foliation (Figure 59C) and has also conjugate leucocratic veins (Figure 59A). Diorite is often associated with gabbro-norite (Figure 59E) and shows the same intrusive relationships. Both rock types are cross-cut by amphibolite dikes. Other remarkable units are a metasedimentary, sillimanite bearing sequence (Figure 59B) and a sulfide mineralisation, both occurring in the orthogneiss.

For further detailed information, especially about the sulfide mineralisation, see field report by ABJ.

Camp 7 – Northern part of Johan Petersen Intrusion

Camp 7 (locality 259, Appendix A) was located in the northern part of the Johan Petersen Intrusion. As seen in Camp 6 the main rock type is still gabbro-norite. This gabbro-norite is associated with gabbro that seems to be a younger system as indicated by microgabbroic veins in the gabbro-norite (Figure 60E and confirmed by observations ABJ made from other parts from the intrusion. The emplacement of the gabbro is spatially concentrated along weakness zones parallel to the gabbro-norite's foliation. The transition between these two systems is characterized by intensely brecciated mingling zones (Figure 60A). A slightly foliation corresponding to the gabbro-norite indicates a syntectonic establishment. Cumulate structured pyroxenites (probably iherzolite), found in the gabbro cautiously support a conduit like intrusive system located along faults (Figure 60D). Intense sulfidation of dendroidal swarms of pyroxenites within the mingling zone (Figure 60B) is a very common feature. Gab-

bro and gabbro-norites show (almost always incomplete) retrogression of pyroxene to amphibole. Intrusive relationships with dikes (pyroxenites and pegmatites) are complex and range from pre- to postkinematic.

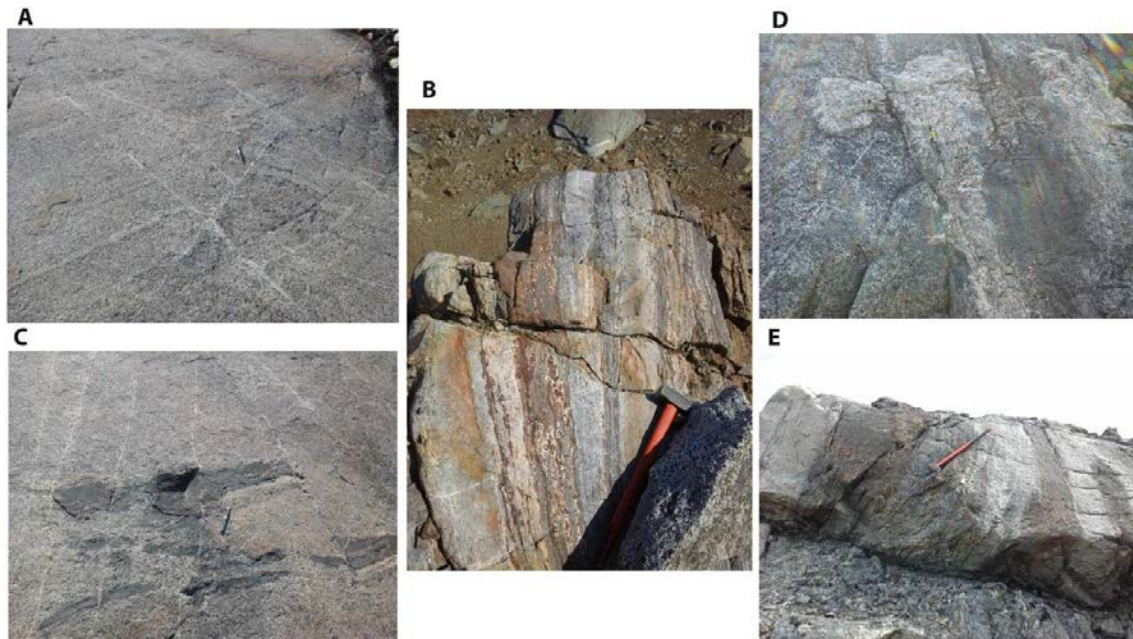


Figure 59. Southern part of the Johan Petersen Intrusion. A) Conjugate veins in gabbro-norite; loc. 245. B) Sillimanite bearing metasediments in the orthogneiss; loc. 258. C) Disrupted pyroxenites in orthogneiss, oriented parallel to foliation; loc. 24 5. D) Granite, intruding orthogneiss; loc. 246. E) Iteration of diorite and gabbro-norite; loc. 256.

The emplacement of the gabbro-norite into the adjacent country rock (amphibolite) seems to be syntectonic, as both rocks are affected by the same foliation (Figure 60F). Further investigations beyond the intrusion revealed metasedimentary rocks from the contact aureole, namely leucocratic garnet biotite schists (Figure 60C), and a unit detached from the emplacement of the Johan Petersen Intrusion whose origin we cautiously attribute to an establishment of a mélangé zone in a subduction setting. This unit (locality 277-281) is characterized by a TTG basement, overprinted by heat metamorphism which is not related to the emplacement of the intrusion, highly complex orthogneisses with multiple folding, blocky parts and partial melting as well as an ophiolite-like sequence.

For further detailed information, especially about the sulfide mineralisation, see the expected master thesis by ABJ.

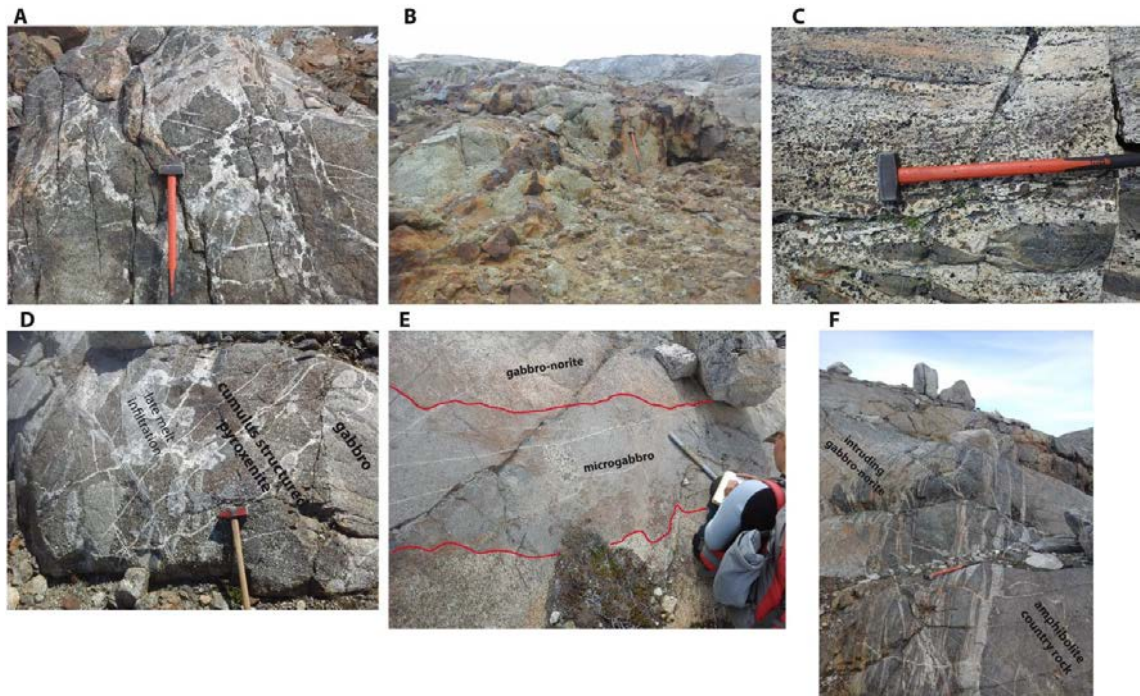


Figure 60. Northern part of Johan Petersen Intrusion. A) Mingling zone of brecciated pyroxenite, microgabbro and leucocratic veins; loc. 302. B) Dendroidal pyroxenite highly sulfide bearing intruding gabbro in mingling zone; loc. 287. C) Leucocratic metasediments from the contact aureole; loc. 270. D) Cumulate structured pyroxenite in gabbro; lo. 285. E) Microgabbro intruding gabbro-norite; loc. 263. F) Contact between intrusive gabbro-norite and the surrounding country rocks (amphibolite); loc. 270.

Camp 8 – Suportoq supracrustals, Niaqernarsik Peninsula

Camp 8 (locality 311, Appendix A) was located in an area where a suture zone was supposed to be. The main lithology was once mapped as orthogneiss with intercalated metasediments.

A detailed mapping along the lake S of our camp showed that a repetition of sequences, consisting of tonalitic gneisses, amphibolites, rusty weathered garnet biotite schists and felsic units (phenoblastic and mylonitic in texture) probably represent a complex thrust system whose effects can be seen in large scale fold structures and chaotic fabrics in hinge zones. The tonalitic gneisses are characterized by heterogeneous appearance (e.g. variations in banding or grain size) and a high amount of mafics and therefore assumed to be metavolcanics. Often they are intruded by amphibolites (Figure 61C). The garnet biotite schists are kyanite bearing and probably of metasedimentary origin (Figure 61A). Competent but boudinaged ultramafic enclaves with leucocratic melts in pressure shadows can be found in all rock units (Figure 61B). Outshearing of quartz veins might be responsible for unexpected high quartz content in some rocks, e.g. amphibolites. Young pegmatites cutting the thrust system and postdate the most formative metamorphic overprint.

Besides the mafic enclaves two massive ultramafic lenses have a unique characteristic in this area. They are intensely metasomatized and infiltrated by pegmatites. Probably due to enrichment in Al as a result of metasomatization in distinct zones, these rocks are highly kyanite bearing (Figure 61D).

For further information see field report from TOMN.



Figure 61. *Suportoq supracrustals, Niaqernarsik Peninsula. A) Kyanite bearing garnet biotite schist; loc. 312. B) Boudinaged ultramafic lense with leucocratic melt in pressure shadow; loc. 312. C) Amphibolite dikes mingled in banded grey gneiss; loc. 324. D) Metasomatised ultra-mafics rich in kyanite; loc. 333.*

Camp 9 – Suportoq supracrustals, Tungujortoq Peninsula

Camp 9 (locality 341, Appendix A) was approx. 10 km from Camp 8. The lithology of the area is dominated by felsic gneisses and amphibolites. Both rock types are isoclinal folded, show tectonic contacts and likely constitute a fold and thrust system as seen in Camp 8. Quartz-rich parts might be due to former pegmatitic veins now sheared in. Younger pegmatites cutting the foliation can be observed. Felsic gneisses and amphibolites are often intercalated (Figure 62A) and the degree of metamorphic overprint can be very high resulting in migmatisation (Figure 62C). Throughout the region greenish horizons can be found in the felsic gneisses and amphibolites. They mainly consist of diopside, maybe actinolite,

are often affected by small scale veining and embedded as boudinaged bodies in a leucocratic matrix (Figure 62C). They also occur as fine disseminated crystals. The presence of massive ultramafic bodies and metasediments give rise to a zone characterised by large variations in chemistry. The main work during the stay in Camp 9 was focused on a saw cut profile in this area. The ultramafic rocks (10-15 m wide and 70-80 long) reveal a cumulate like structure and are mainly composed of pyroxene (Figure 62B). The metasediment is a garnet muscovite schist with a high amount of kyanite, 1-2 m in thickness and continuing along strike along the mapped section (Figure 62D). The succession in the profile involves all rock units on a small scale (~ 30 m).

For further information see field report from TOMN.

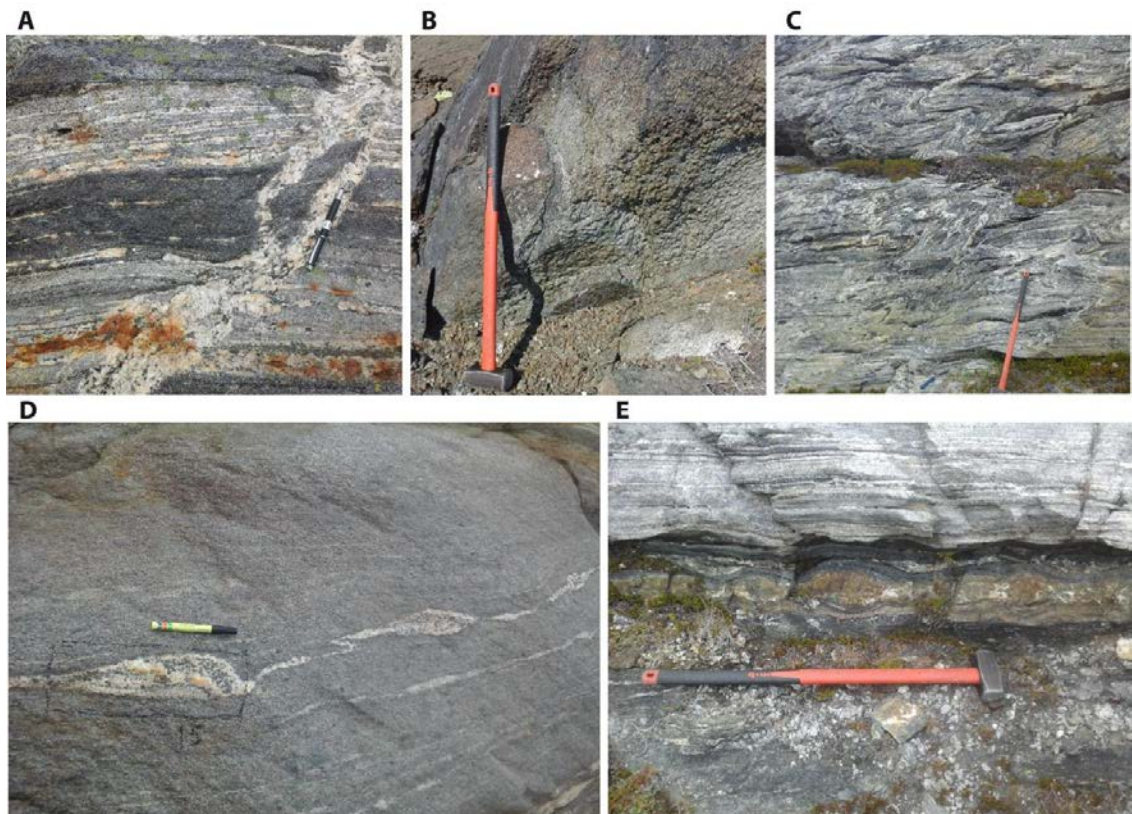


Figure 62. *Suportoq supracrustals, Niaqernarsik Tungujortoq Peninsula. A) Quartz-rich veins and intercalated amphibolite layer in grey gneiss with pegmatite cross-cutting foliation; loc. 348. B) Ultramafics weathered into pebble like unit; loc. 349. C) Migmatized amphibolite gneiss; loc. 352. D) Kyanite bearing garnet muscovite schist with pegmatitic veins, rich in garnet and kyanite; loc. 350. E) Boudinaged 'diopsidetite' in leucocratic matrix between grey gneiss and amphibolite; loc. 345.*

Camp 10 – On Quinarteq Island

Preliminary observations at the coast around the area of Camp 10 (locality 364, Appendix A) promised the presence of granite. It turns out that the amount of k-feldspar is a result of

late alteration that is often accompanied by the presence of epidote. The lithology in question is almost always less affected by foliation and therefore probably different compared to grey gneisses, which are the main rock types. However, these gneisses are also affected by the k-feldspar weathering along intruding veins. As seen in the camps before the gneiss is closely associated with amphibolites, at some places mingling with each other. Both rock types are isoclinal folded and contain abundant leucocratic veins affected by the foliation to a variable extent.

E–NE of camp mafic dikes can be found which are late intrusive but still very sheared. They are amphibolites, gabbroic to dioritic in composition. In less strained parts primary mineral assemblages of eclogite facies conditions are still preserved. In patchy parts of the dikes omphacite is only partly retrogressed to pyroxene/amphibole and plagioclase.

For further information see field report from TOMN.

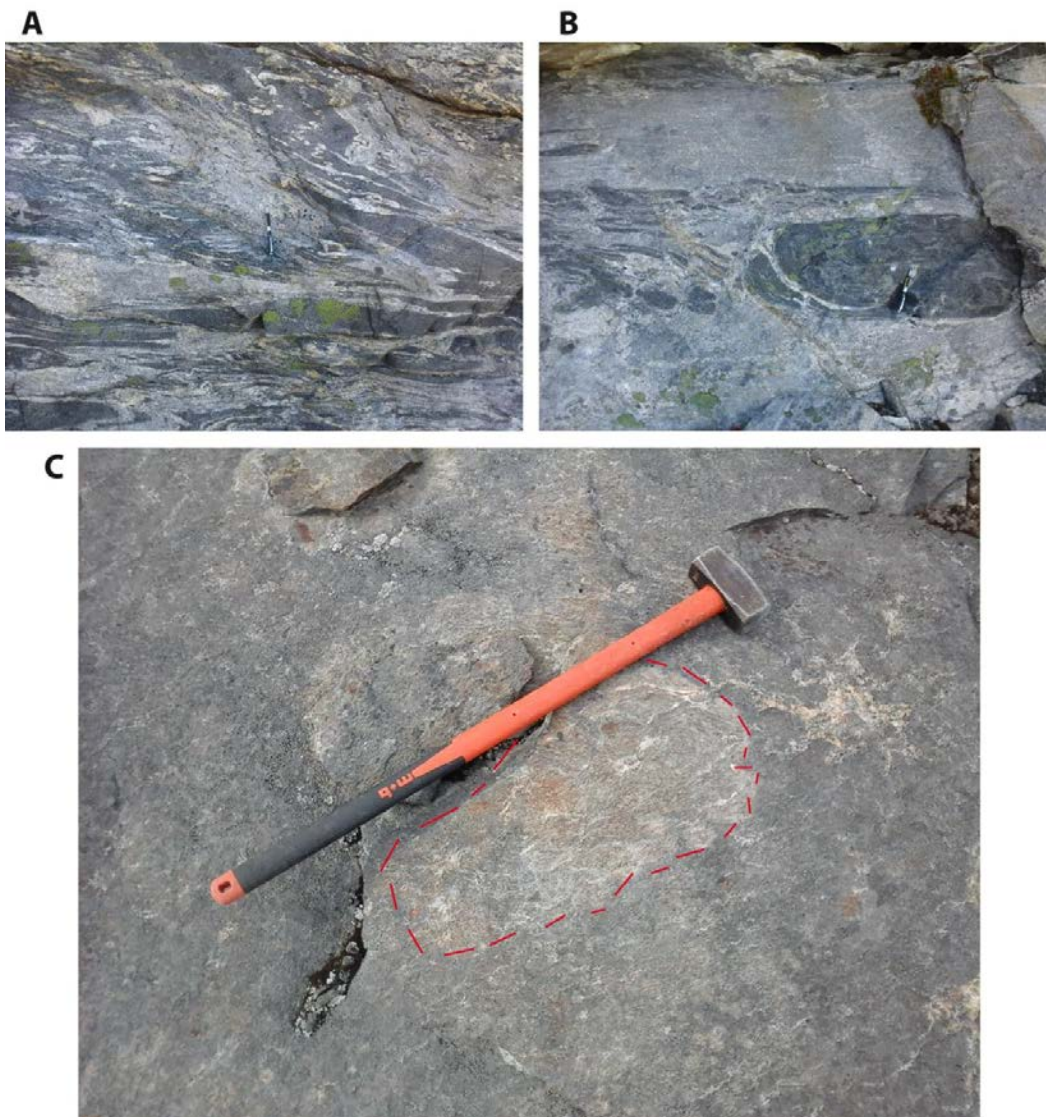


Figure 63. On Qianarteq Island. A) Amphibolite and grey gneiss mingling together; loc. 378. B) Boudinaged amphibolite enclave with leucocratic melt in pressure shadow hosted by grey gneiss; loc. 378. C) Amphibolite dike with patchy parts of relict mineral assemblages reflecting eclogite facies conditions.

Structural analysis along the SE Greenland margin (PGUA)

Introduction

The aim of the fieldwork was to investigate the presence of brittle deformation along the SE Greenland margin and to understand the possible relationship with young deformation in particular related to the NE Atlantic rift and opening. The field season focused on four main areas of interest. The first area was visited in the period August 9th-16th sailing along the coast line from Umiivik to Isortoq. The second target was Kap J. Steenstrup and a long photo flight up to Kap Gustav Holm. The third locality was the Ammassalik Fjord visited August the 18th and the last one was investigated with helicopter support the 19th of August visiting the 16. September Gletscher area. The locations can be seen on Figure 64.

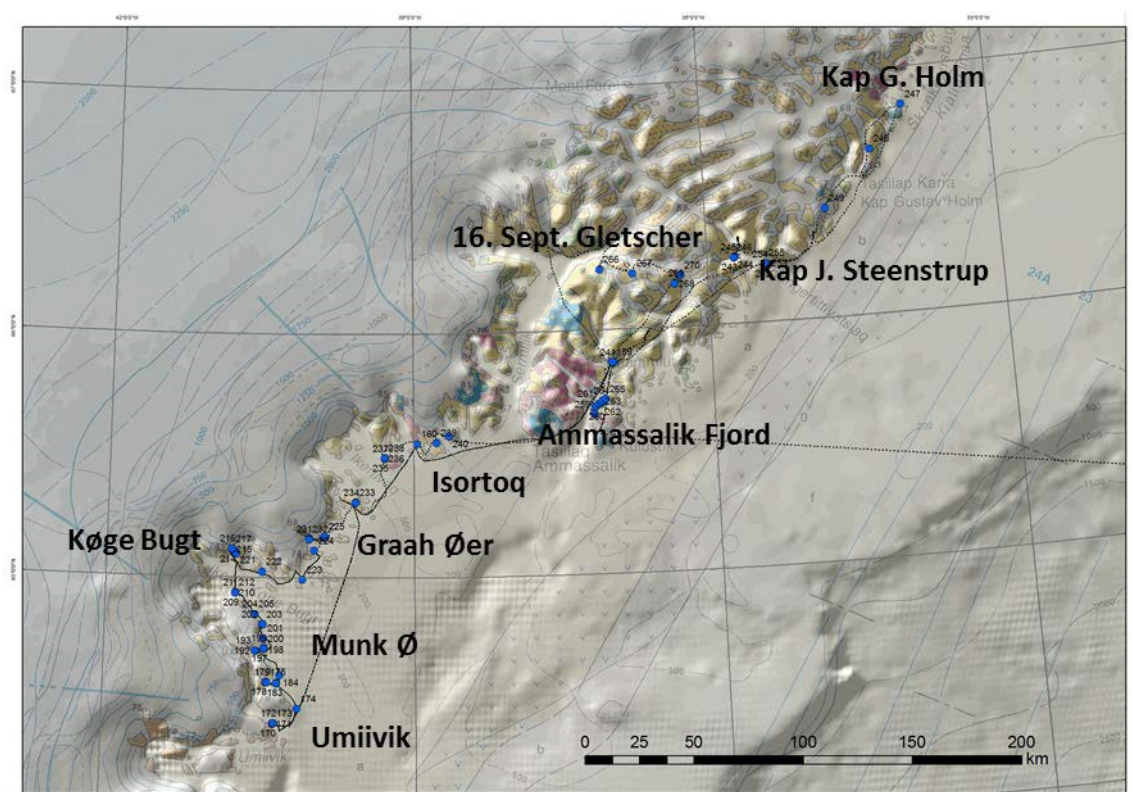


Figure 64. Waypoints and GPS track.

Table 8. Name, dates and participants for the different areas that was visited.

Location	Name	Dates	Participants
Area 1	From Umiivik to Isortoq	9.-16.8.2014	JKOL, LBA, MBK, PGUA, RBO
Area 2	Kap J. Steenstrup and photo flight to Kap Gustav Holm	17.8.2014	MBK, PGUA
Area 3	Ammassalik Fjord	18.8.2014	JKOL, LBA, MBK, PGUA, RBO
Area 4	16. September Gletscher area	19.8.2014	JKOL, MBK, PGUA

Summary of the fieldwork and observations

From Umiivik to Isortoq

The first part of the fieldwork was planned to document the brittle deformation along the coast working along with a boat and sailing from 64° N (Umiivik) up to 66° N (Kuummiut) together with JKOL and LBA. We started sailing to Isortoq August 9th where we had to pick up two participants to the cruise (MBK and RBO). After that we sailed all night long with a short stop on a small bay at Dannebrog Ø. On the way back we had to skip the last part of the cruise because one of the skippers had to reach a doctor and we sailed directly from Isortoq to Kuummiut August 16th.

Umiivik (64°20'N)

Fridtjof Nansen Halvø (August 10th, 2014)

At this locality the ESE-WNW trending dikes of the Umiivik series seems to intrude along the foliation (Figure 65). The almost N-S trending dikes, interpreted as Tertiary, have the same trend as the normal faults and vein systems mapped in the area (Figure 65).

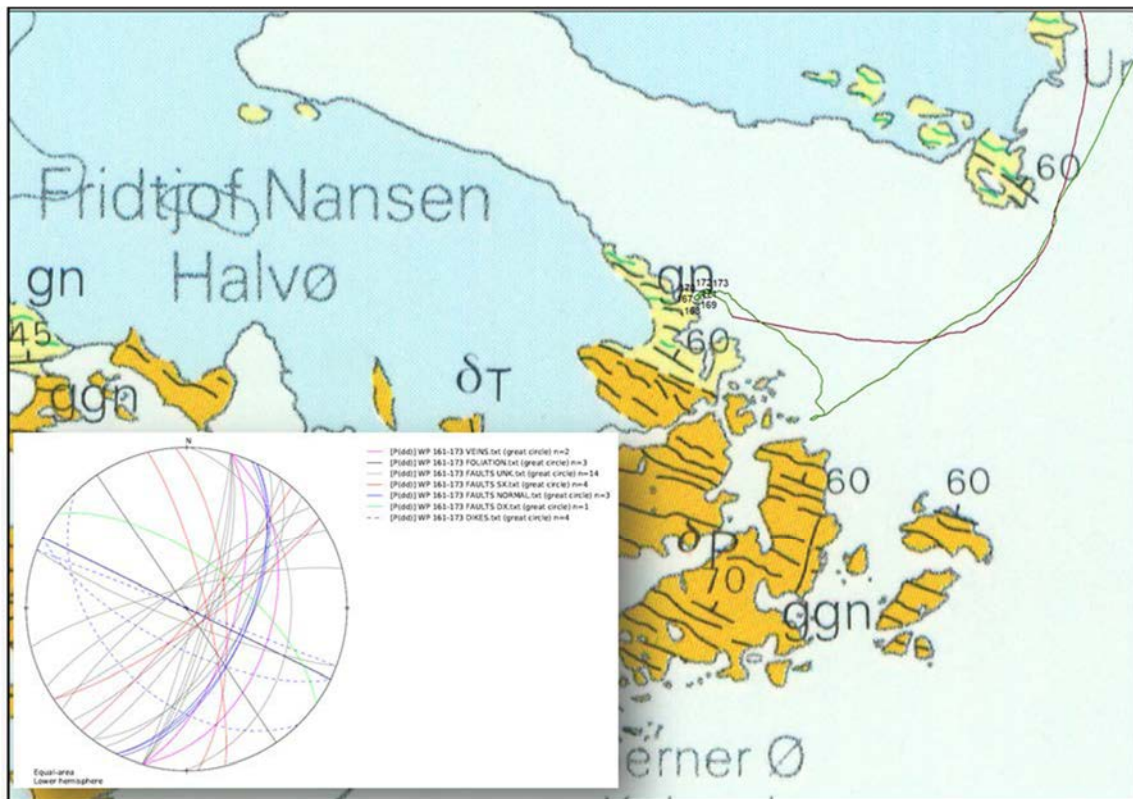


Figure 65. Geological map of Fridtjof Nansen Halvø along with GPS tracks and waypoints. Equal-area Lower Hemisphere stereo plot of structural data collected.



Figure 66. A five m thick ESE-WNW trending dike.



Figure 67. Strike-slip fault plane.

Jens Munk Ø (64°30'-64°50'N)

Sørte Flytter Fjeld-Pros Mund Ø (August 11th, 2014)

In this area (Figure 68) an ESE-WNW trending dextral shear zone with mylonites is documented (Figure 69). The deformation is in greenschists facies in the brittle/ductile transition as shown by the presence of brittle deformation along fault planes with epidote (Figure 70).

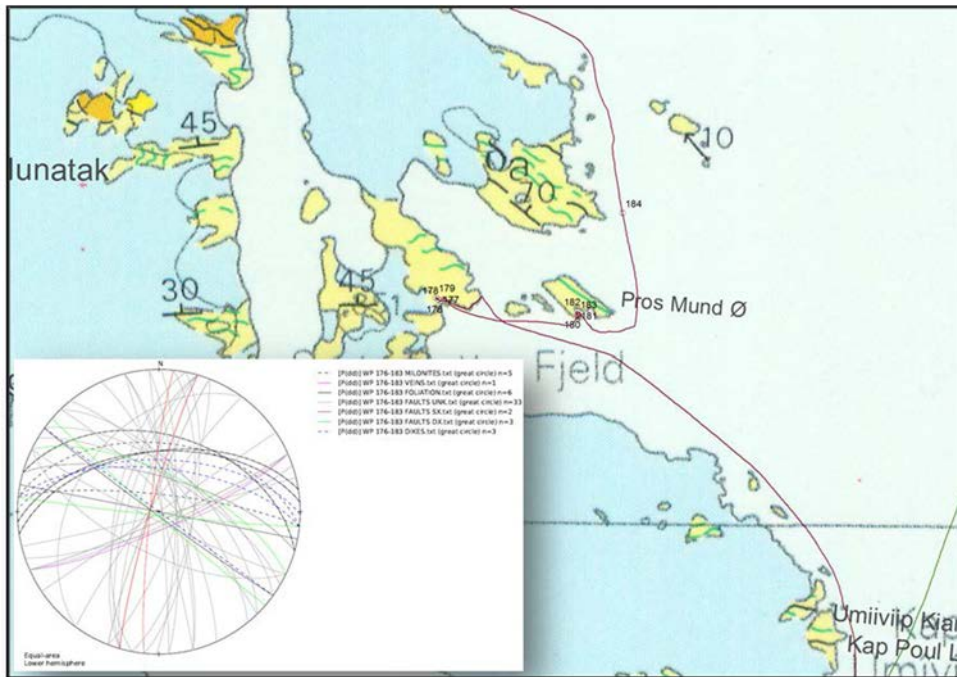


Figure 68. Geological map of Sørte Flytter Fjeld-Pros Mund Ø with GPS tracks and waypoints. Equal-area Lower Hemisphere stereo plot of structural data collected.



Figure 69. The dextral shear zone with mylonites.



Figure 70. Brittle deformation overprinting the shear zone.

Lemons Bugt (August 11th, 2014)

At this locality major NW-SE dextral shear zone with mylonites is documented (Figure 71 and Figure 72). The mylonitic zone is in turn overprinted by brittle deformation (Figure 73 and Figure 74).

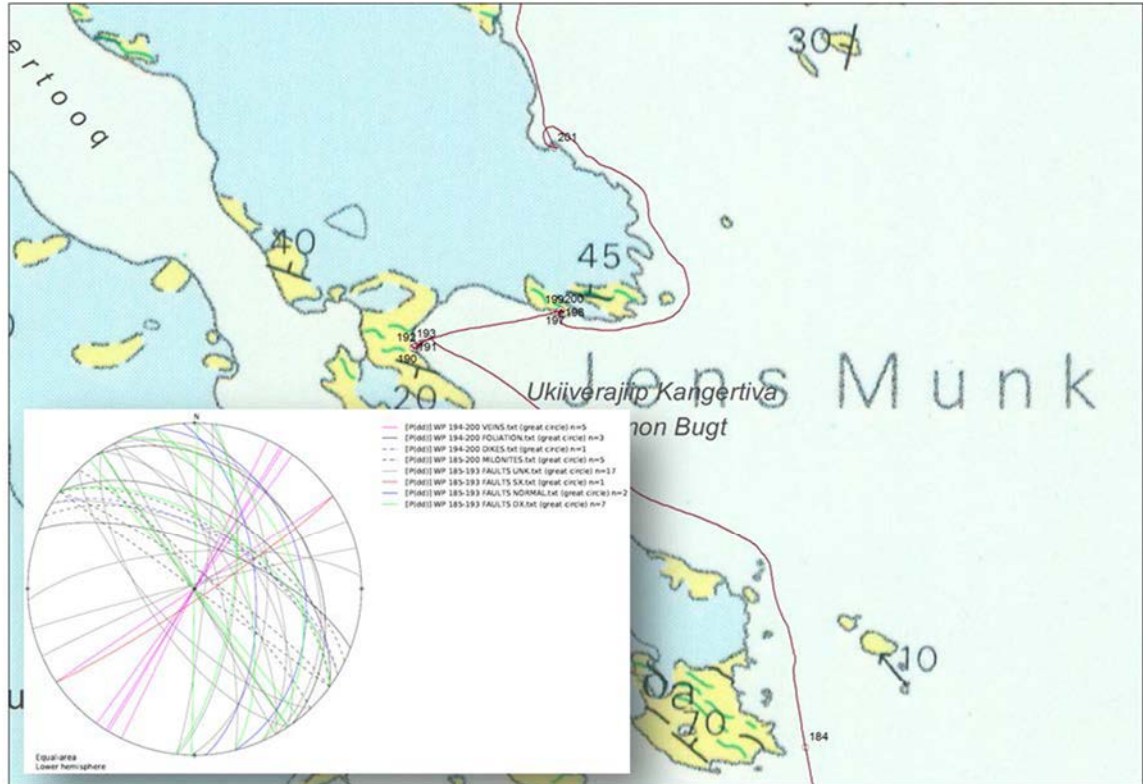


Figure 71. Geological map of Lemon Bugt with GPS tracks and waypoints. Equal-area Lower Hemisphere stereo plot of structural data collected.



Figure 72. *Mylonites developed along the NW-SE trending shear zone.*

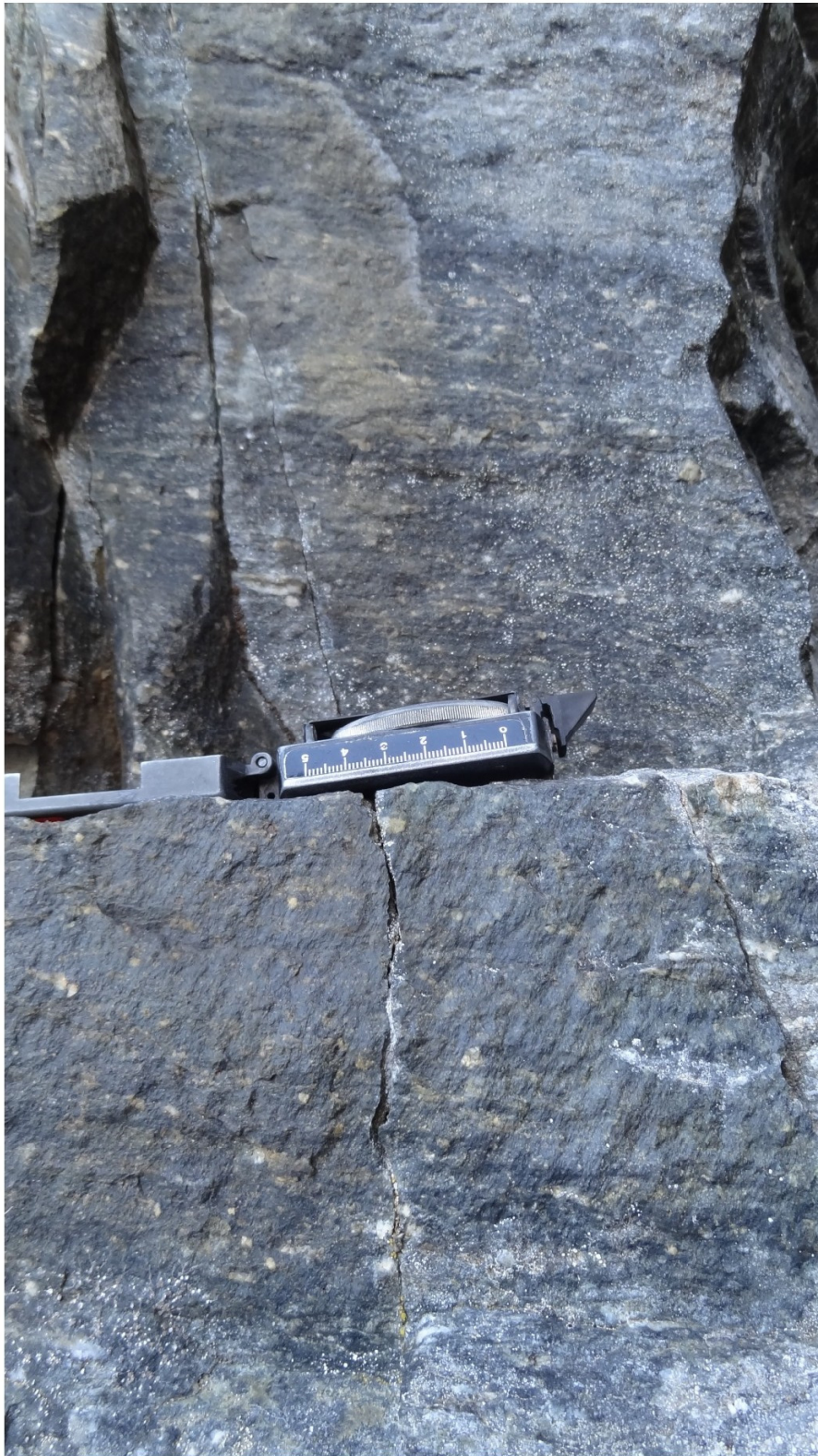


Figure 73. *Dip-oblique brittle stickensides (foreground) overprinting the mylonite (background).*

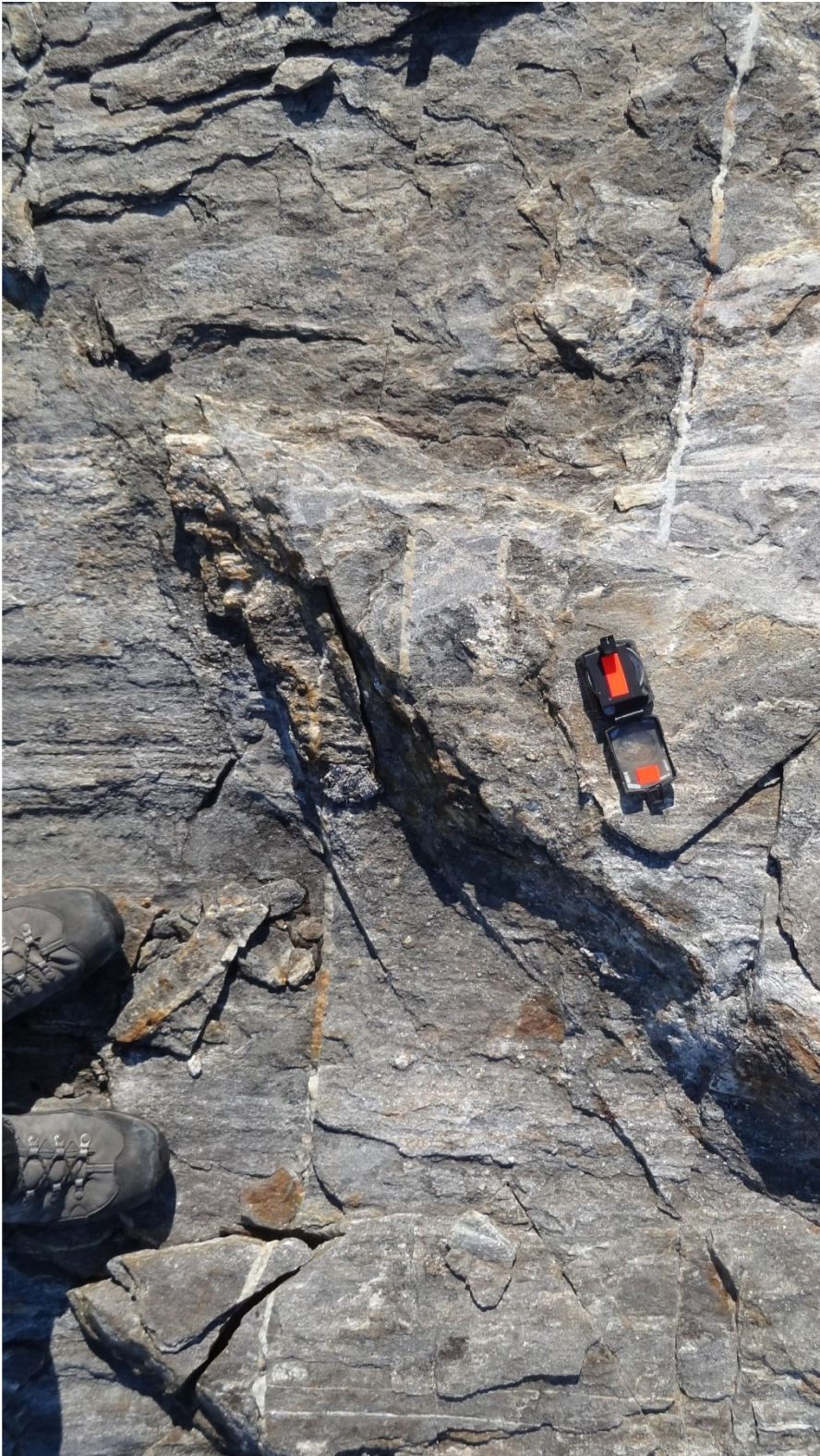


Figure 74. *Dextral movement along brittle faults.*

Jens Munk Ø central (August 11th, 2014)

The area is characterised by the presence of NNE-SSW trending dip-oblique and normal faults and by sub-horizontal mylonites probably related to thrust zones with NW-SE lineations (Figure 75, Figure 76 and Figure 77).

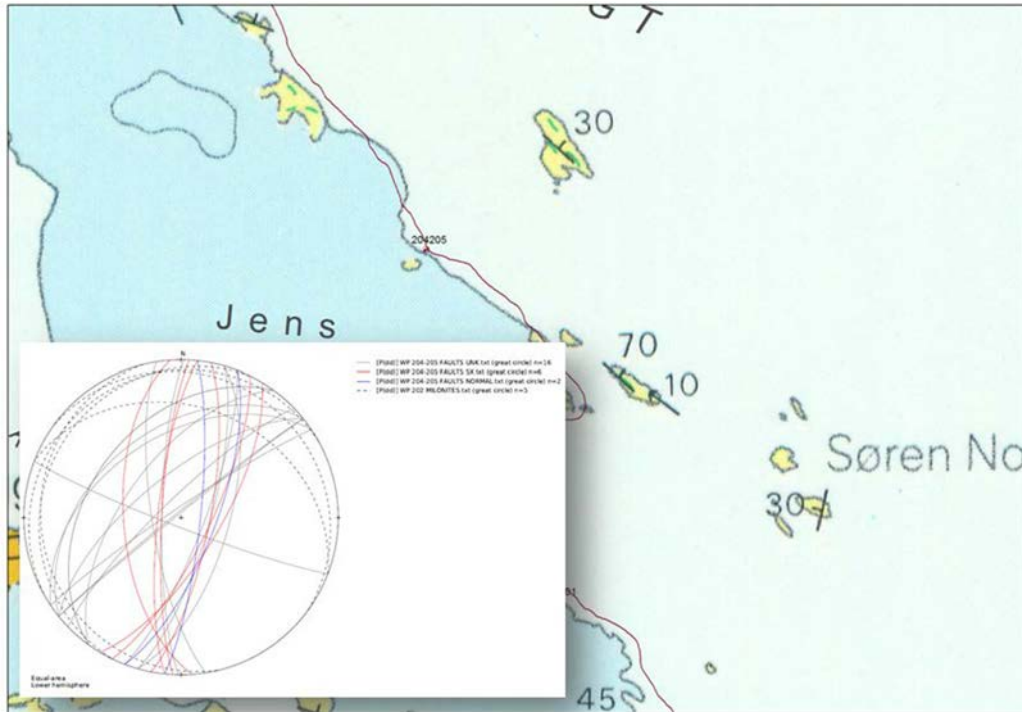


Figure 75. Geological map of Jens Munk Ø (central part) with GPS tracks and waypoints. Equal-area Lower Hemisphere stereo plot of structural data collected.



Figure 76. Slickensides showing the sinistral kinematics of NNE-SSW trending brittle fault with probable epidote along the fault plane.



Figure 77. *NNE-SSW trending brittle fault.*

Jens Munk Ø north (August 12th, 2014)

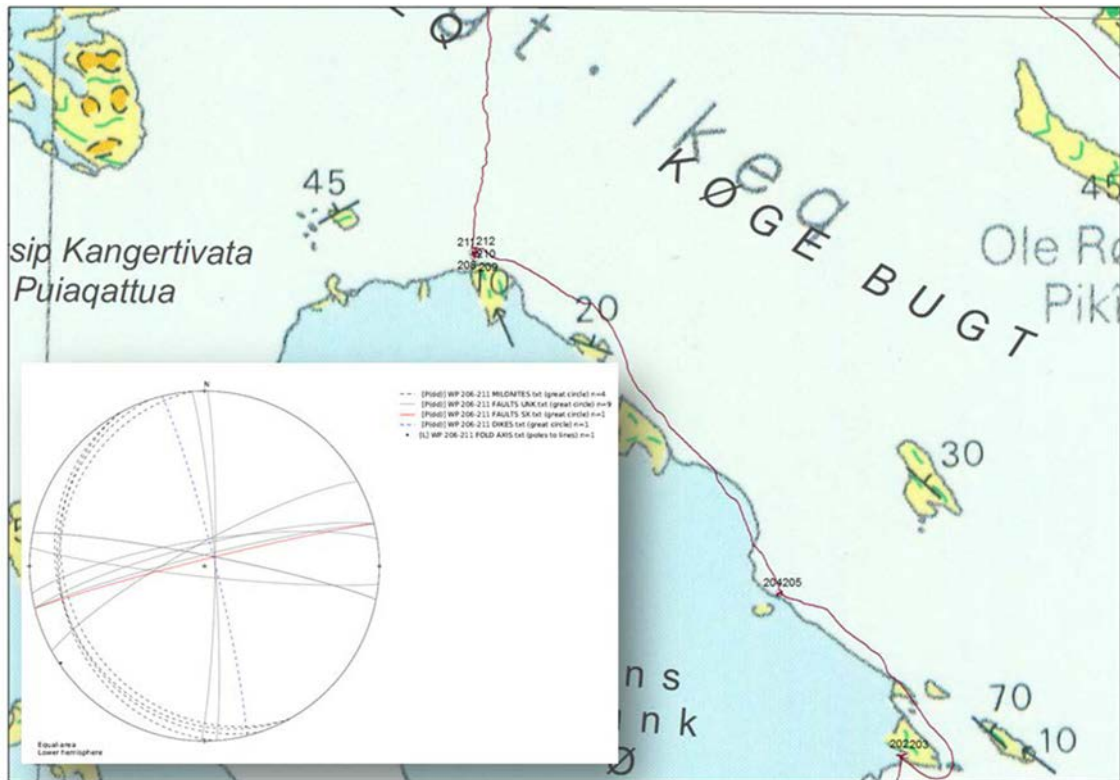


Figure 78. Geological map of Jens Munk Ø (northern part) with GPS tracks and waypoints. Equal-area Lower Hemisphere stereo plot of structural data collected.



Figure 79. Shallow dipping foliation in northern Jens Munk Ø.

Køge Bugt (65°00'N)
Pamiagtik (August 12th-13th, 2014)

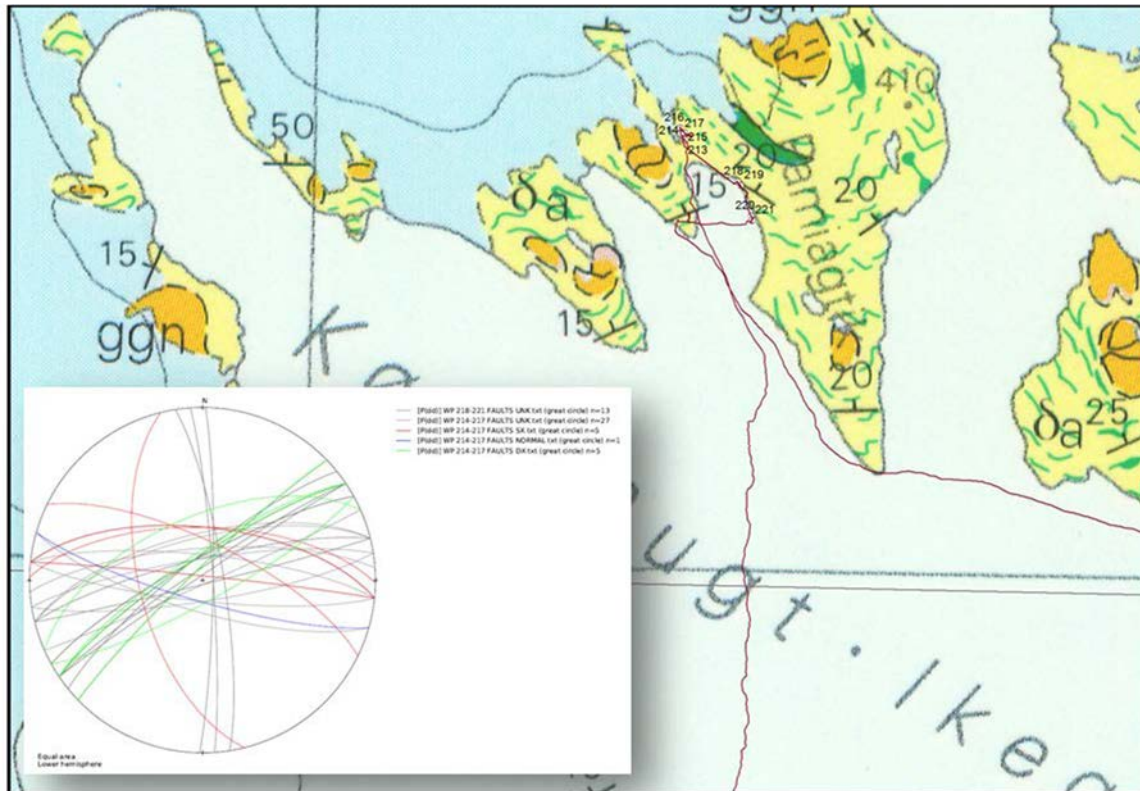


Figure 80. Geological map of Køge Bugt with GPS tracks and waypoints. Equal-area Lower Hemisphere stereo plot of structural data collected.



Figure 81. Parasitic 'Z' folds in a large recumbent fold antiform.



Figure 82. *Brittle fault with strike-slip slickensides with epidote.*



Figure 83. *Right-lateral fault.*

Siarqitseq (August 13th, 2014)

The area is characterized by NE-SW trending faults of unknown kinematics.

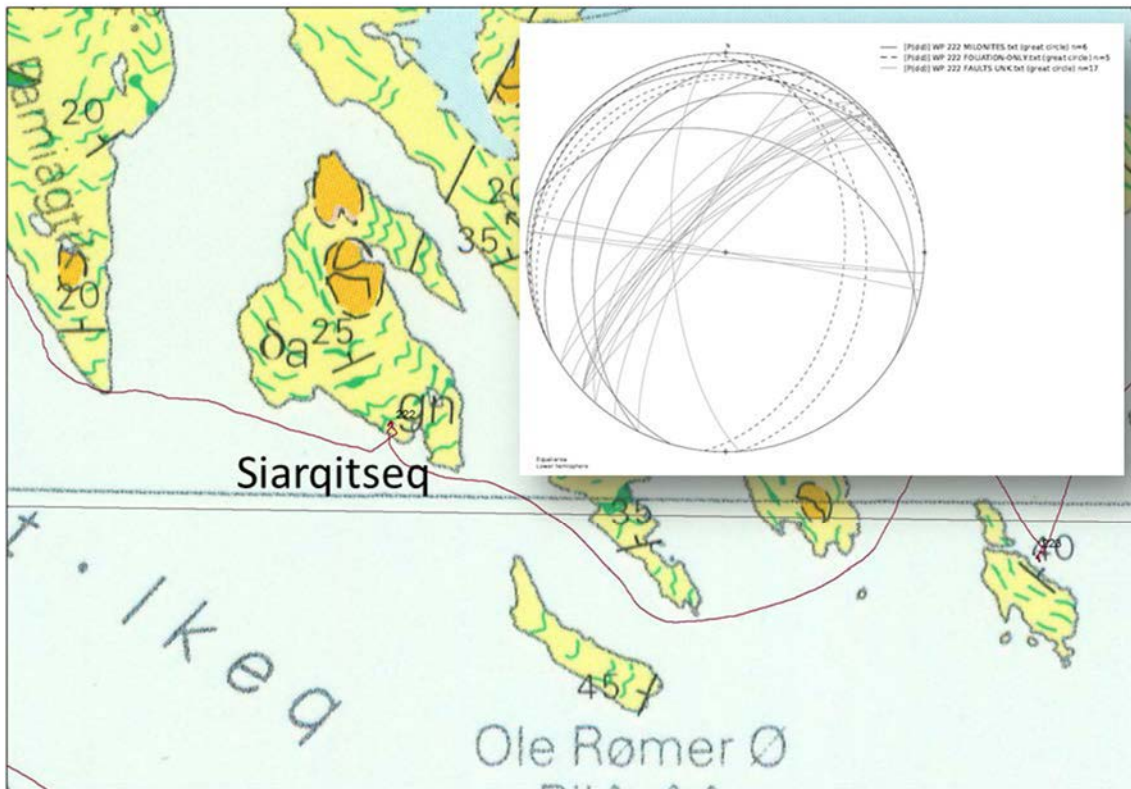


Figure 84. Geological map of Siarqitseq with GPS tracks and waypoints. Equal-area Lower Hemisphere stereo plot of structural data collected.



Figure 85. Lineations.



Figure 86. *Slickensides.*

Aqitseq (August 13th, 2014)

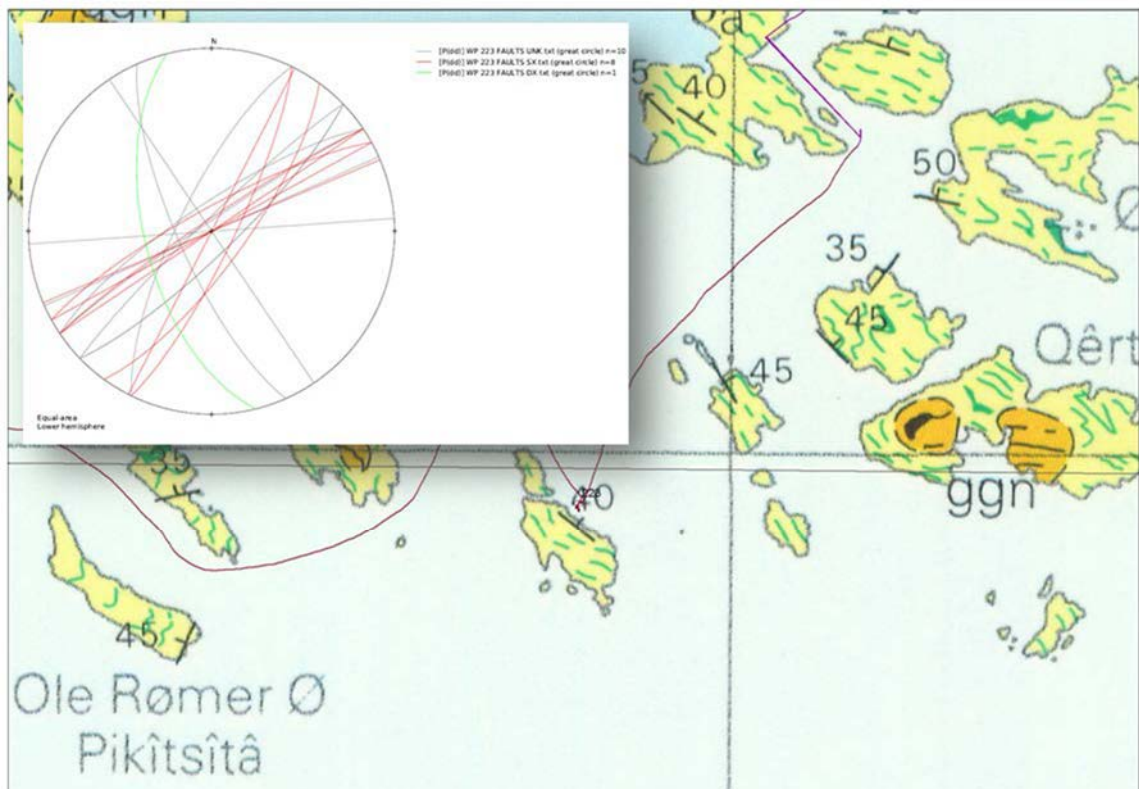


Figure 87. *Geological map of Aqitseq with GPS tracks and waypoints. Equal-area Lower Hemisphere stereo plot of structural data collected.*



Figure 88. Brittle faults.

Graah Øer (65°15'N)
 Ikeq (August 14th, 2014)

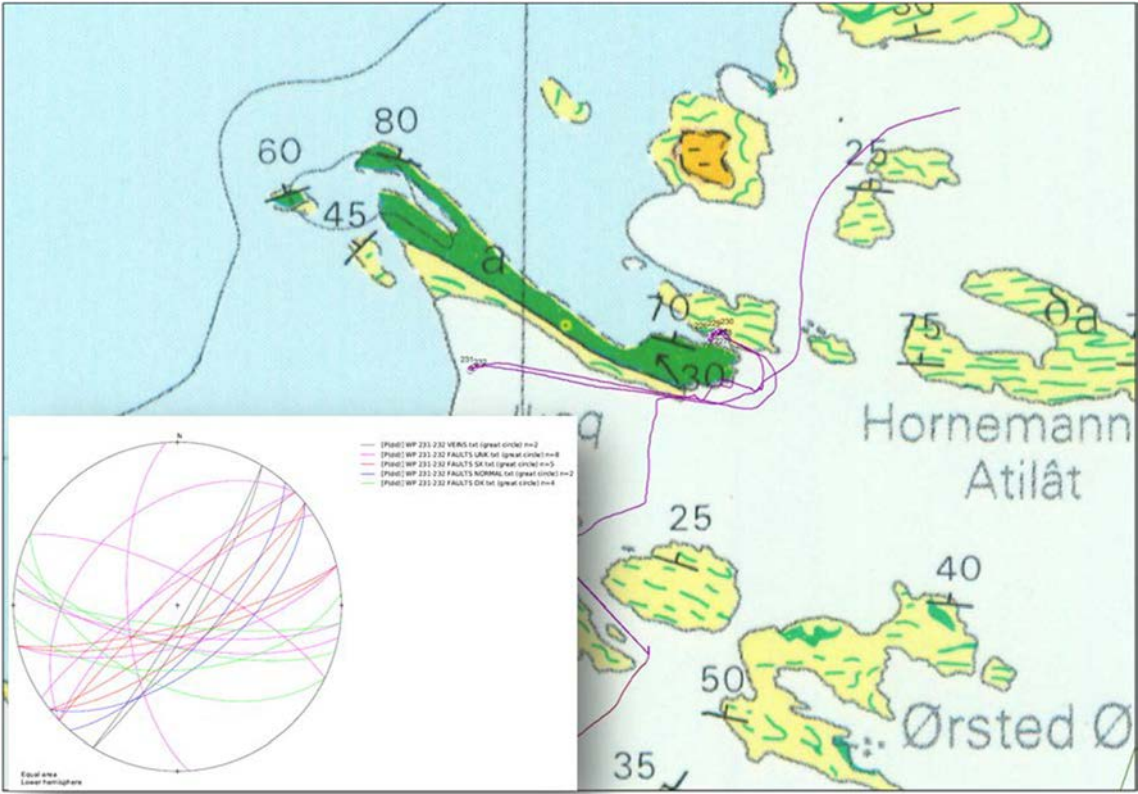


Figure 89. Geological map of Ikeq with GPS tracks and waypoints. Equal-area Lower Hemisphere stereo plot of structural data collected.



Figure 90. *The amphibolites in the Ikeq area.*



Figure 91. *Slickensides with talc steps growing along a fault plane.*

Qernertikajik (August 14th, 2014)

In this area we collected pseudotachylites along normal faults and strike-slip faults.

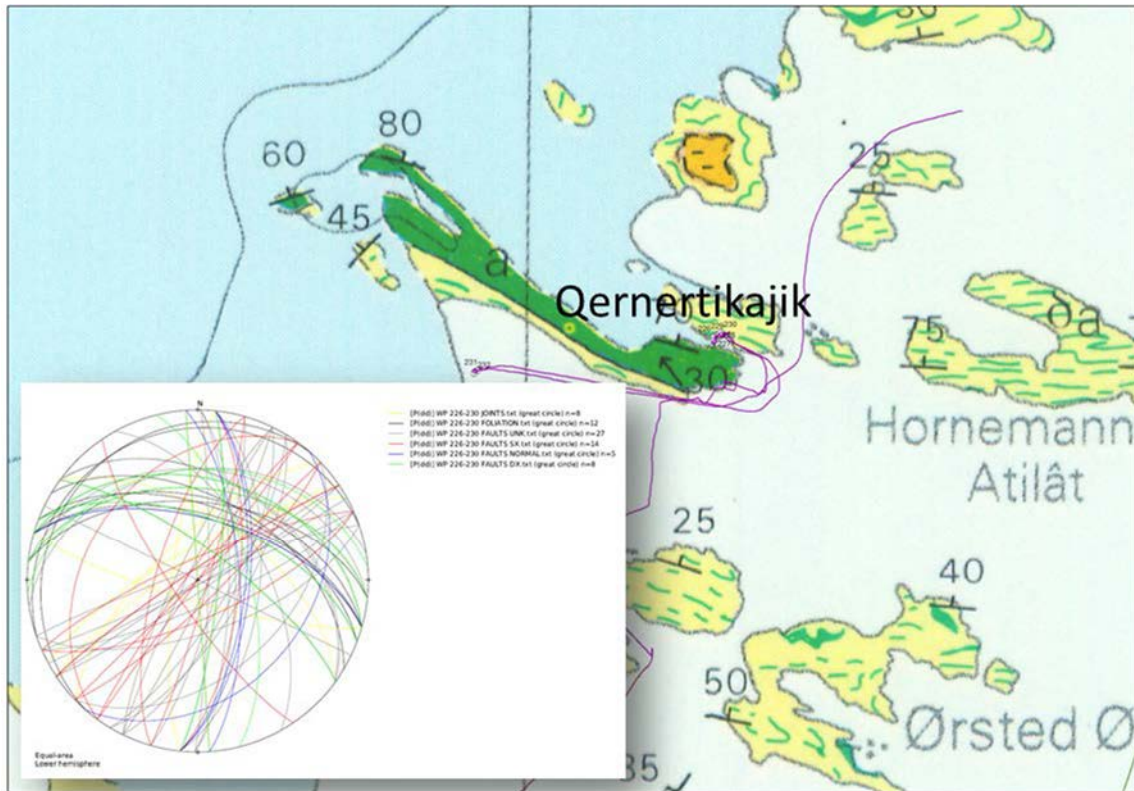


Figure 92. Geological map of Qernertikajik with GPS tracks and waypoints. Equal-area Lower Hemisphere stereo plot of structural data collected.



Figure 93. Pseudotachylites along a fault plane.



Figure 94. *NE-SW trending normal fault.*



Figure 95. *NE-SW trending normal fault.*

Dannebrog Ø (August 15th, 2014)

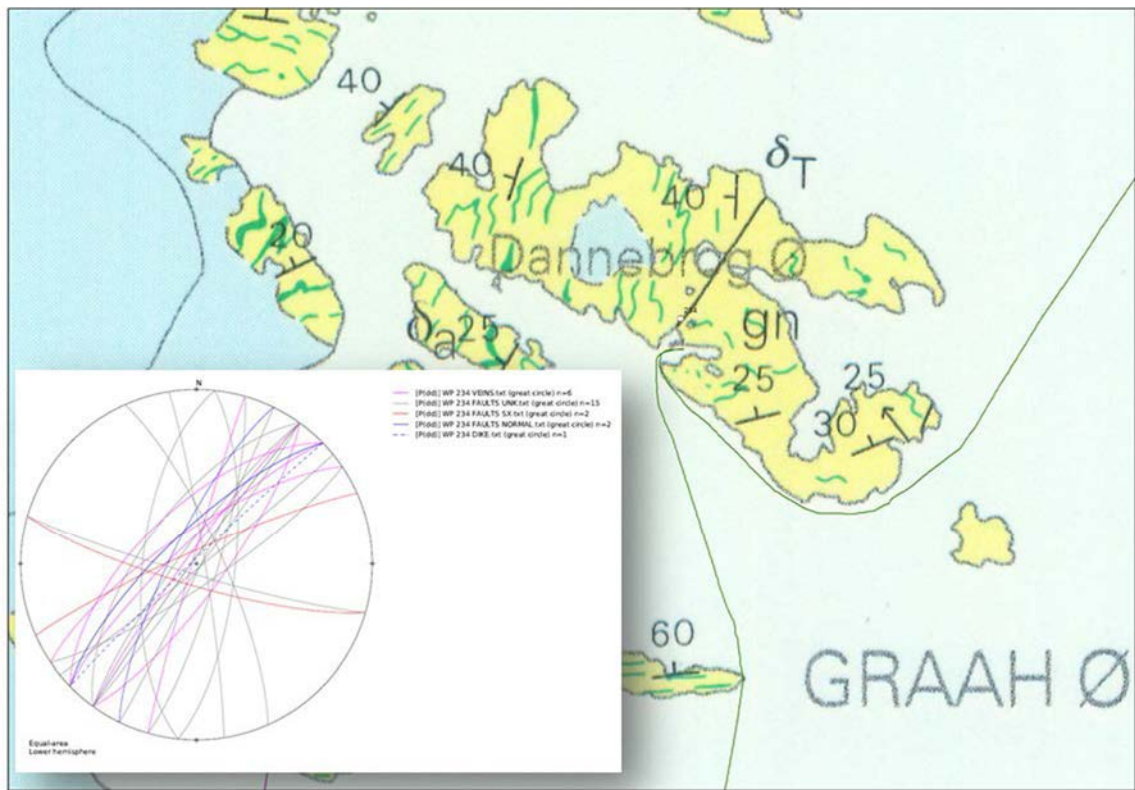


Figure 96. Geological map of Dannebrog Ø with GPS tracks and waypoints. Equal-area Lower Hemisphere stereo plot of structural data collected.



Figure 97. Strike-slip slickensides along the NE-SW trending fault.



Figure 98. *NE-SW trending fault plane.*

Isortoq (65°30'N)
Sunikajik (August 15th, 2014)

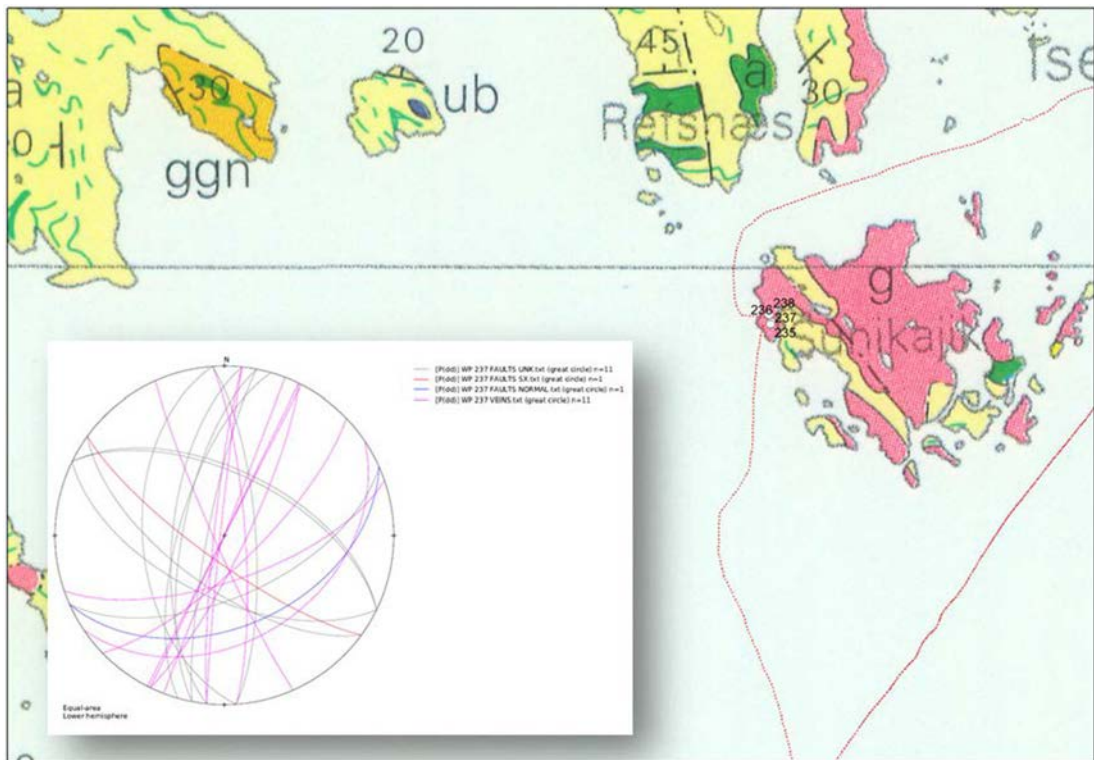


Figure 99. Geological map of Dannebrog Ø with GPS tracks and waypoints. Equal-area Lower Hemisphere stereo plot of structural data collected.

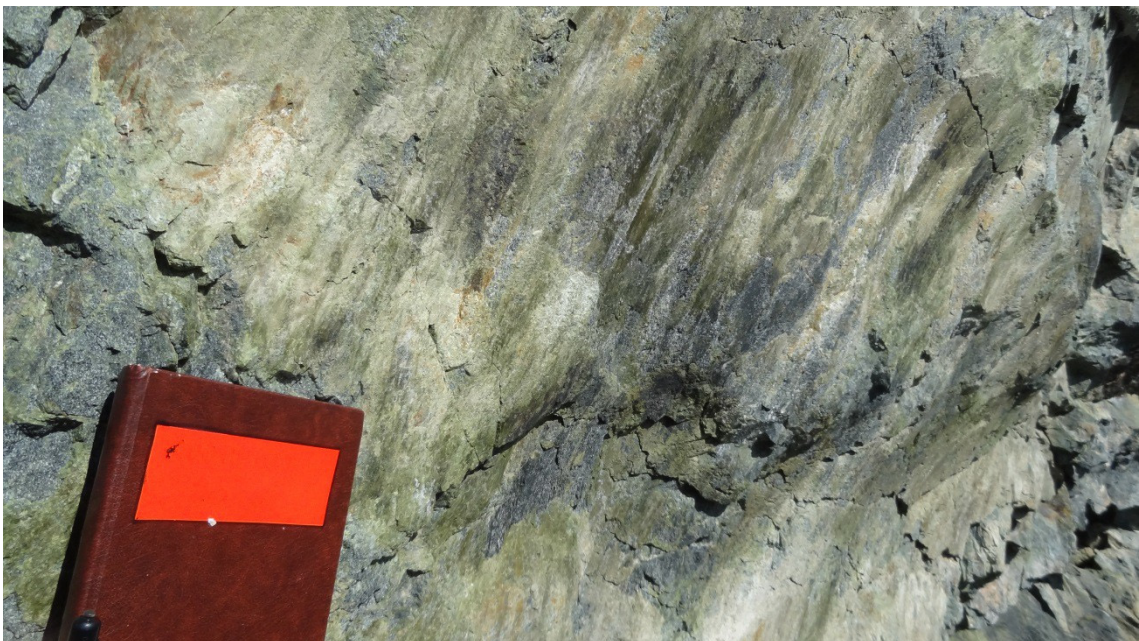


Figure 100. Dip-oblique slickensides along the NE-SW trending fault.



Figure 101. *NE-SW trending fault plane.*

Narssarte (August 16th, 2014)

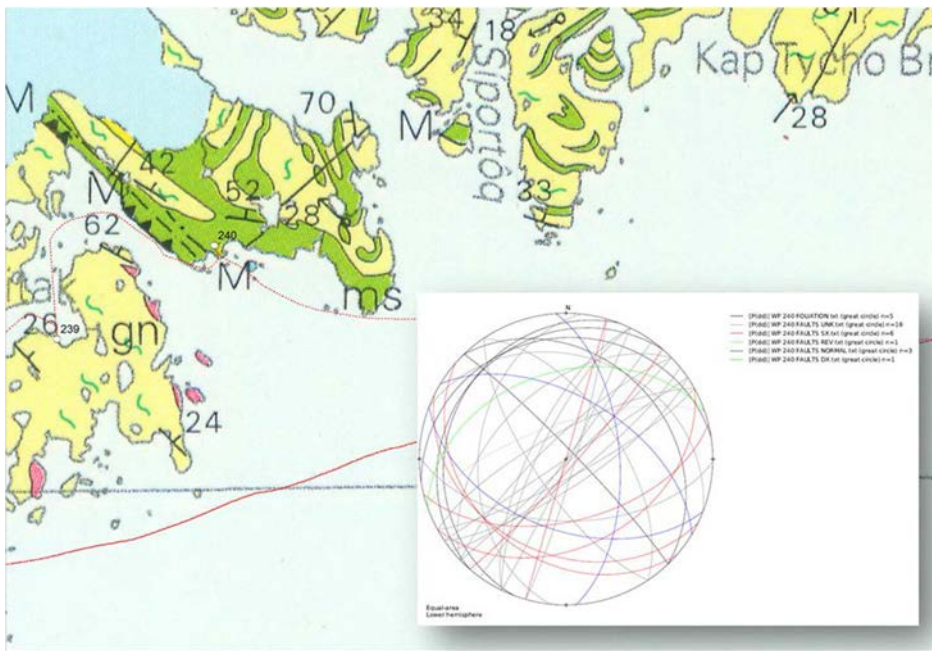


Figure 102. Geological map of Narssarte with GPS tracks and waypoints. Equal-area Lower Hemisphere stereo plot of structural data collected.



Figure 103. NE-SW trending dike.



Figure 104. *Brittle deformation overprinting small dikes.*



Figure 105. *Brittle fault offsetting a quartz vein.*

Kap Japetus Steenstrup

Photo flight and reco together with MBK.

Kangertittivatsiaq (August 17th, 2014)

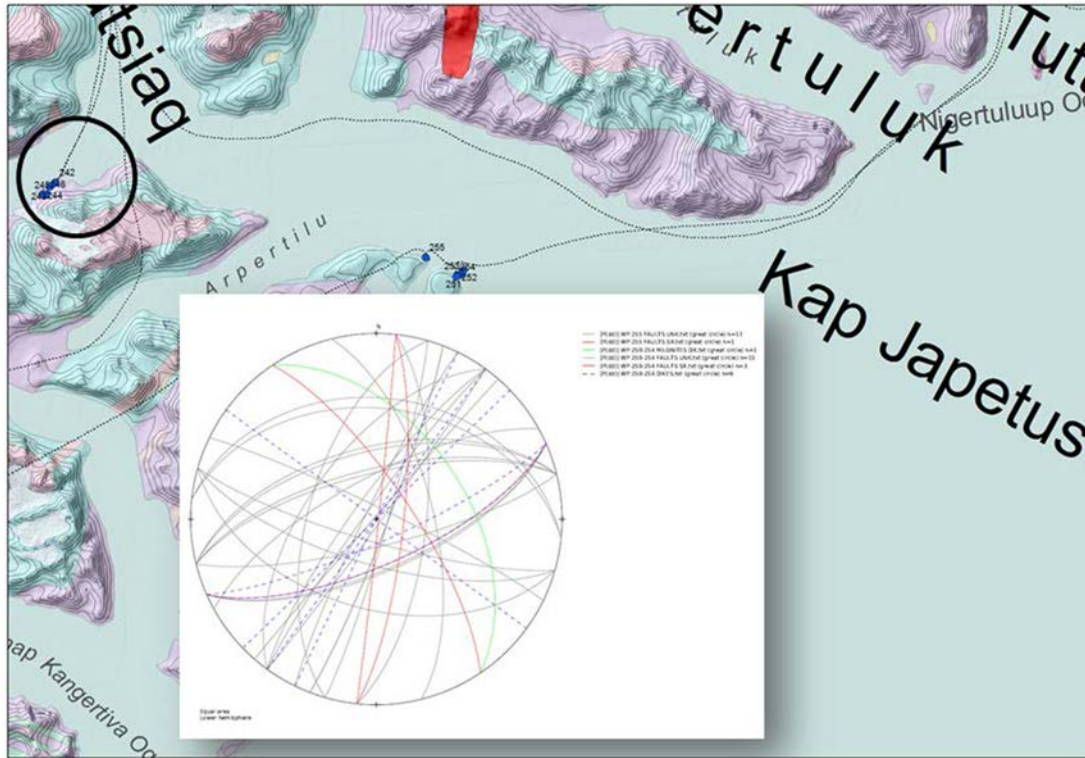


Figure 106. Geological map of Kap Japetus Steenstrup with GPS tracks and Waypoints. Equal-area Lower Hemisphere stereo plot of structural data collected.



Figure 107. Brittle fault with strike-slip slickensides.



Figure 108. *A probable Tertiary dike intruding through an E-W trending fault plane.*

Arpertilu (August 17th, 2014)

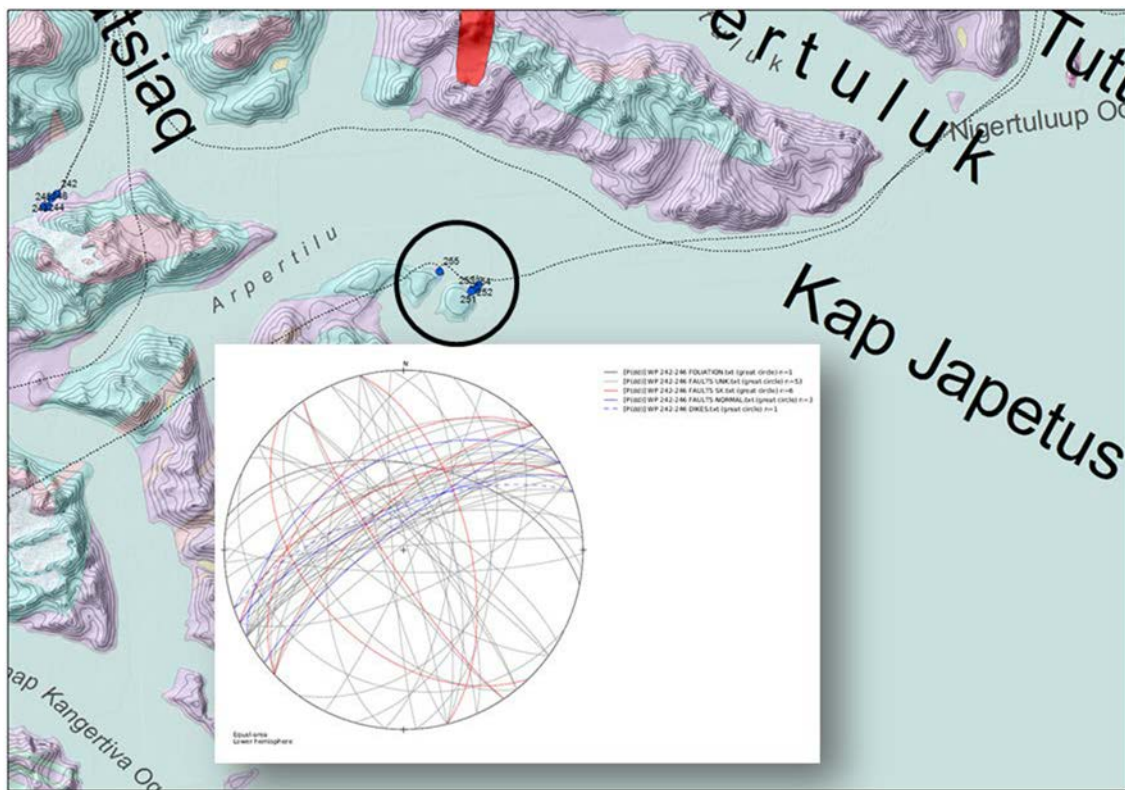


Figure 109. Geological map of Kap Japetus Steenstrup area with GPS tracks and Waypoints; Equal-area Lower Hemisphere stereo plot of structural data collected.



Figure 110. Cross-cutting relationships between dikes and faults.



Figure 111. *Brittle fault with strike-slip slickensides.*

Kap Gustav Holm

Foto flight and reco with MBK (August 17th, 2014).

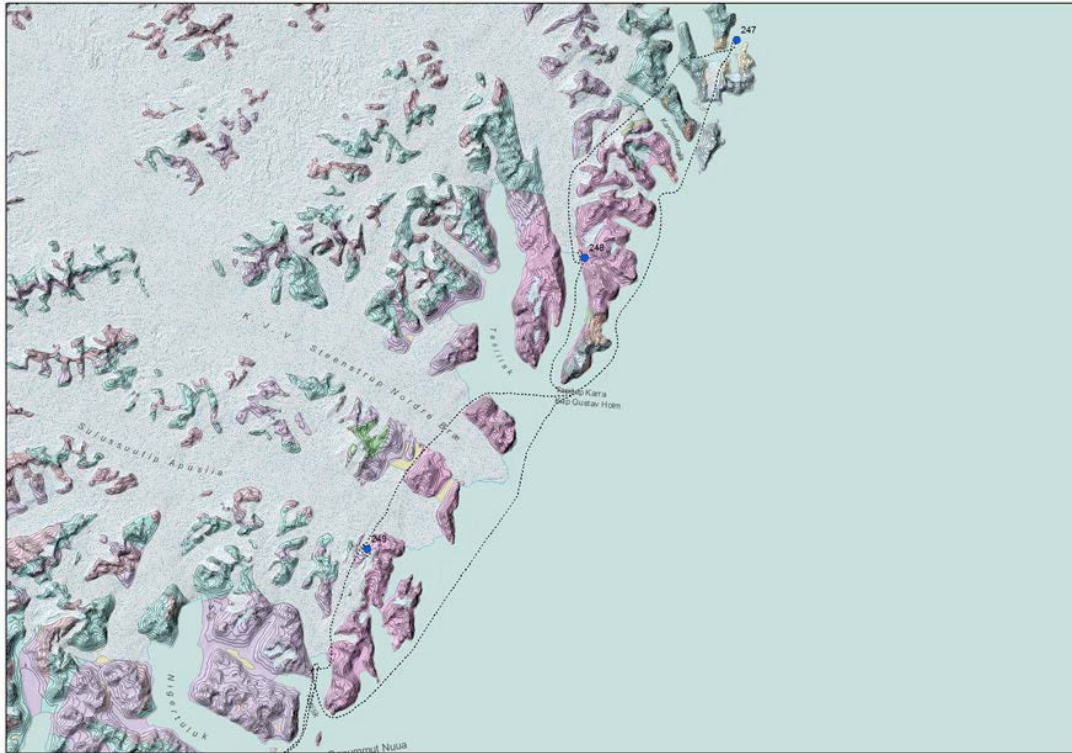


Figure 112. Geological map of the coastal area near Kap Gustav Holm with GPS tracks of the oblique photos collected.

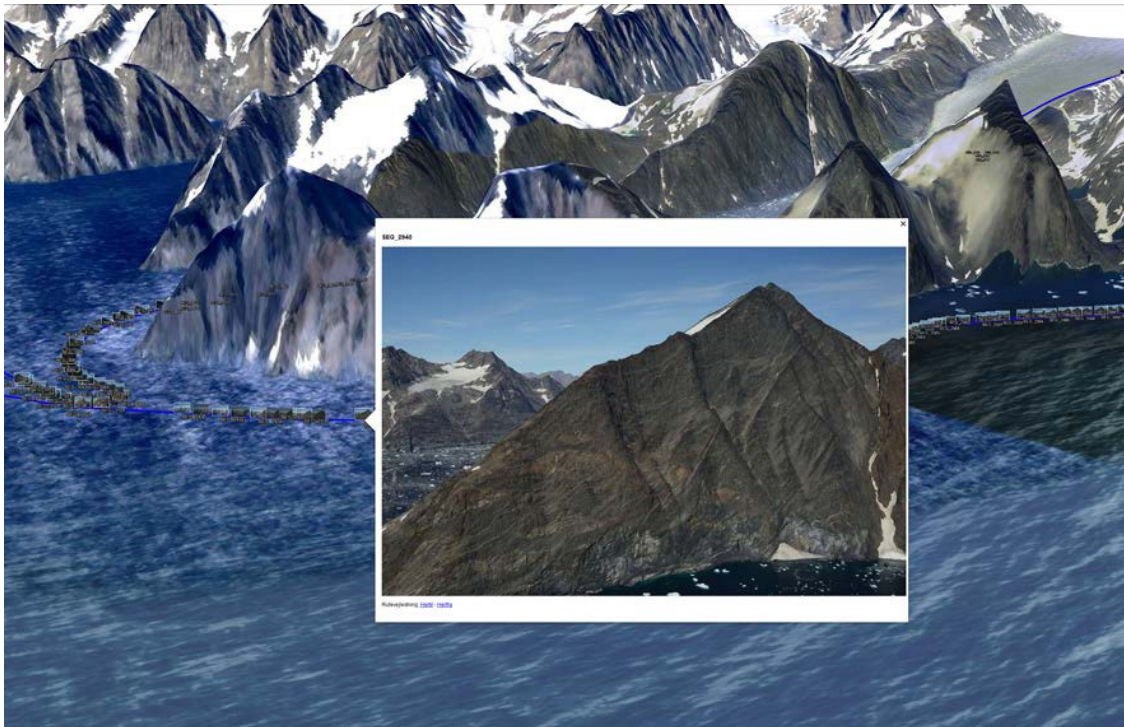


Figure 113. One of the oblique photos of Kap Gustav Holm taken from the helicopter.

Ammassalik Fjord (65°45'N)

We sailed with a fast boat to visit one of the largest E-W trending shear zones with JKOL, LBA, MKB and RBO (August 18th, 2014).

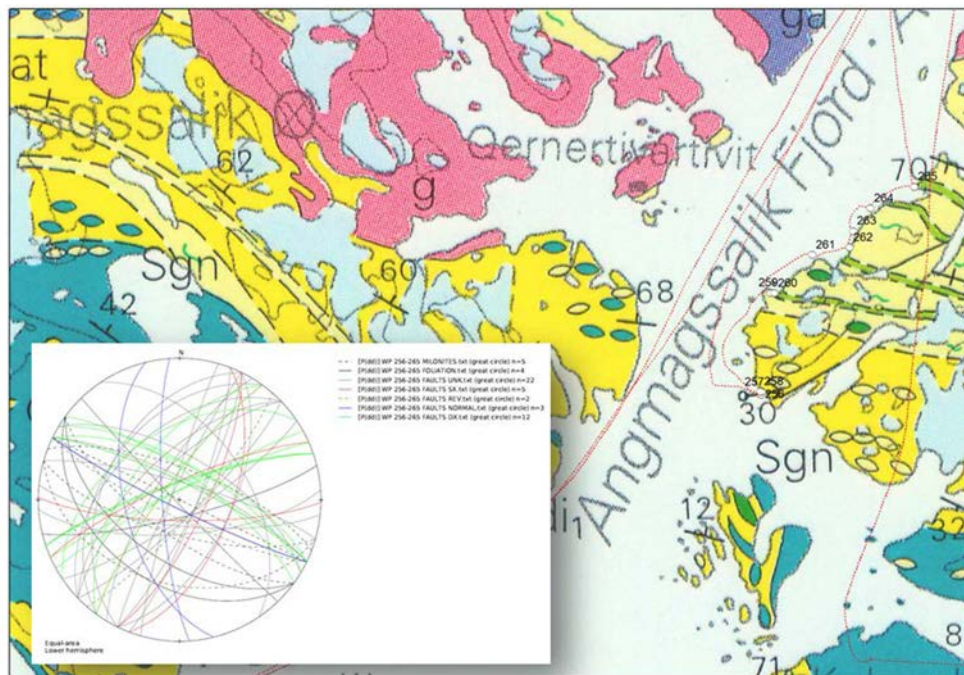


Figure 114. Geological map of Ammassalik Fjord with GPS tracks and waypoints. Equal-area Lower Hemisphere stereo plot of structural data collected.

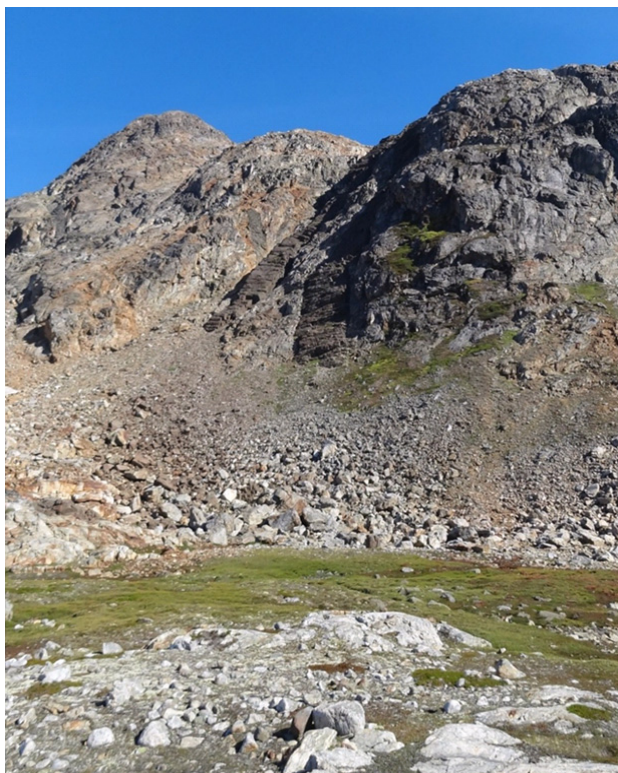


Figure 115. NE-SW trending dikes.



Figure 116. *Foliation along the ESE-WNW trending mylonitic shear zone.*



Figure 117. *Brittle re-activation of the mylonitic zone.*



Figure 118. *Strike-slip slickensides along the shear zone.*

16. September Gletscher

Photo flight and reco together with JKOL and MBK (August 19th, 2014).

Ningerti

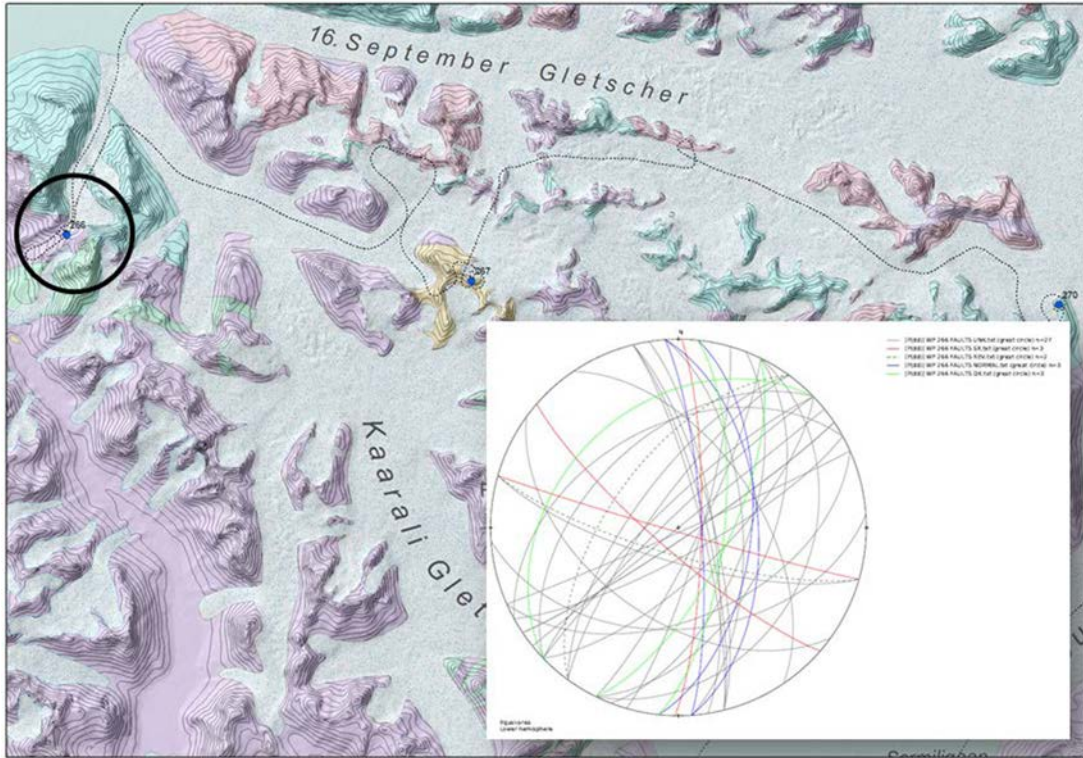


Figure 119. Geological map of 16. September Gletscher area with GPS tracks and way-points. Equal-area Lower Hemisphere stereo plot of structural data collected.

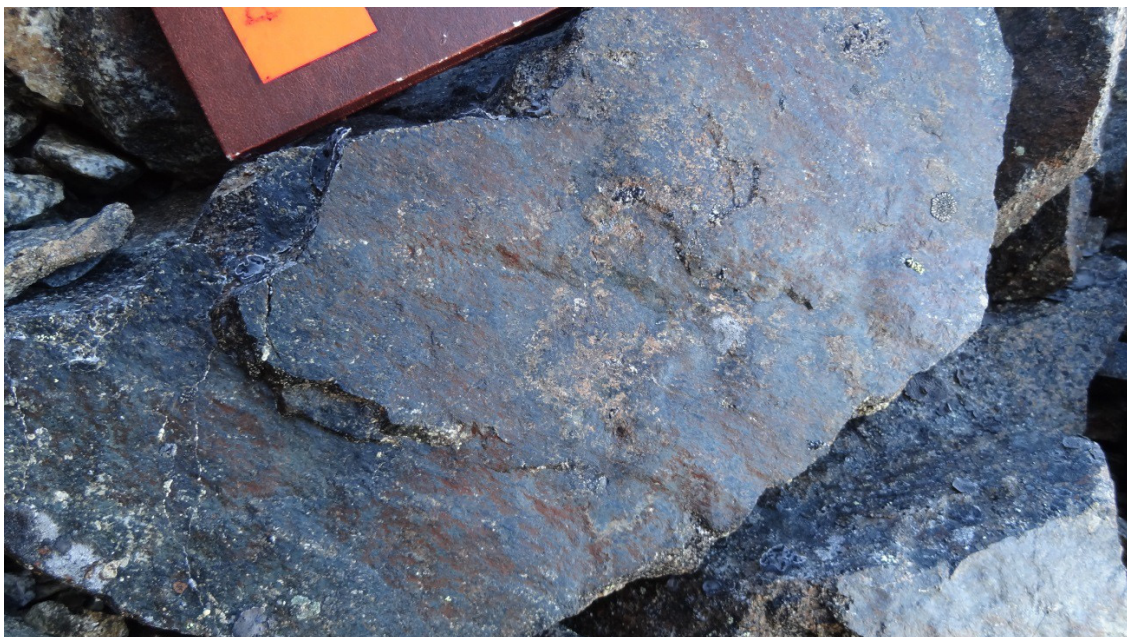


Figure 120. Dip-oblique slickensides along a fault plane.



Figure 121. *E-W trending fault zone.*

Rytterknægten



Figure 122. Geological map of 16. September Gletscher area with GPS tracks and waypoints. Equal-area Lower Hemisphere stereo plot of structural data collected.



Figure 123. Dip-oblique slickensides along a fault plane.

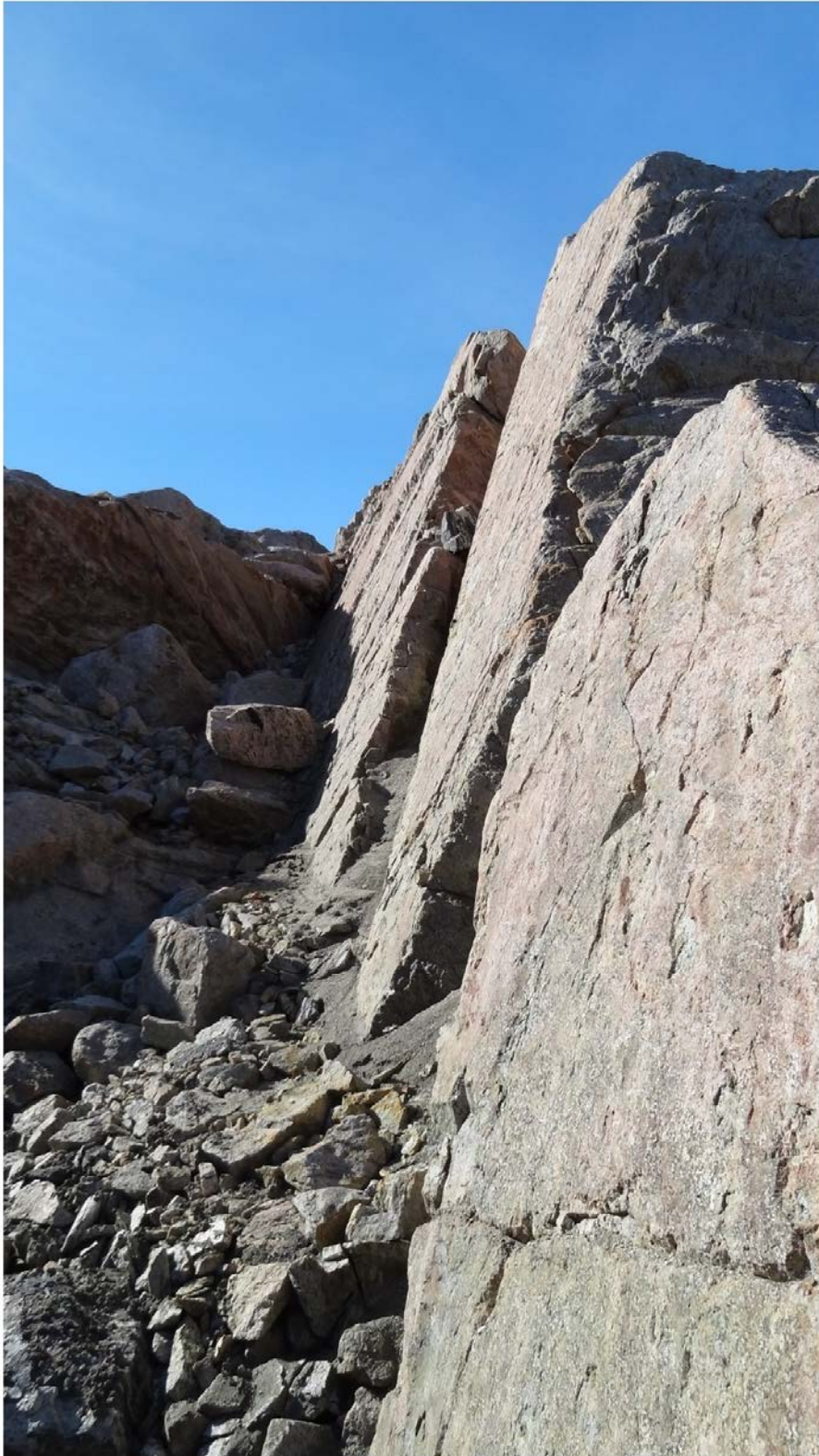


Figure 124. *E-W trending fault plane.*

Apuseeq

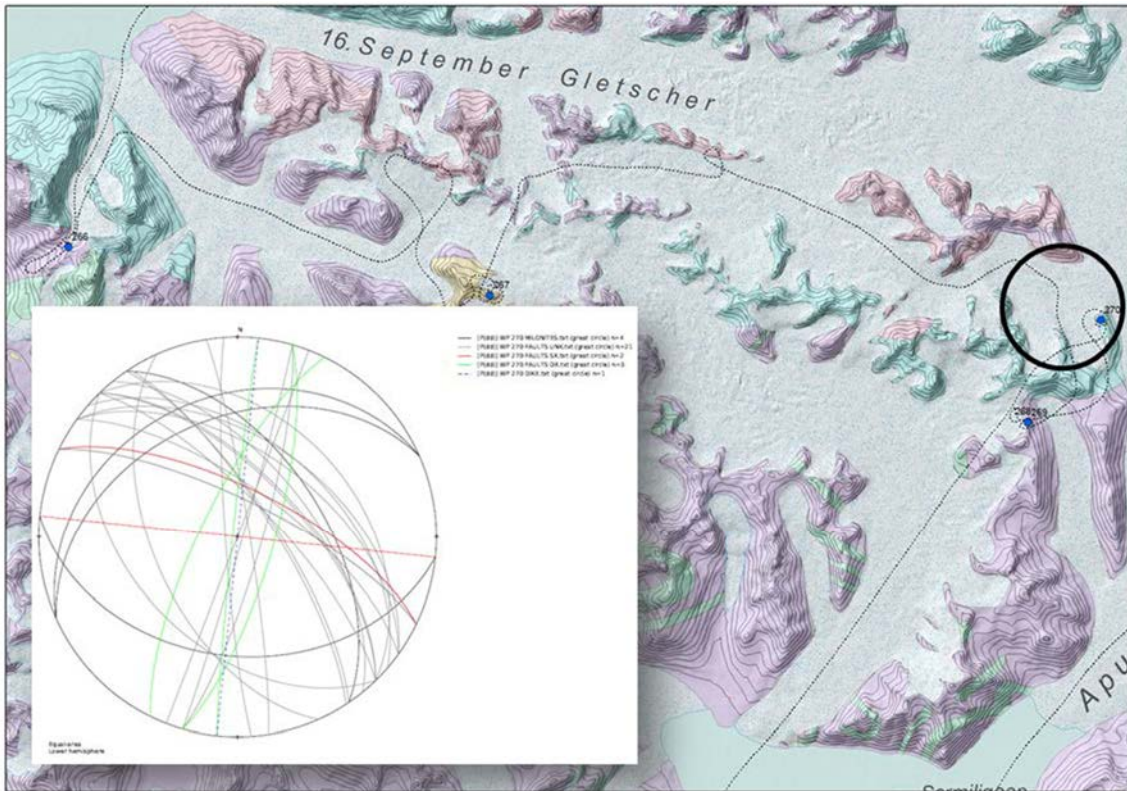


Figure 125. Geological map of 16. September Gletscher area with GPS tracks and waypoints. Equal-area Lower Hemisphere stereo plot of structural data collected.



Figure 126. Dip-oblique slickensides along a fault plane.



Figure 127. *E-W trending fault cutting through amphibolite dikes.*

Proterozoic and Tertiary mafic dykes (MBK, RBO)

Introduction

The fieldwork, done between July 15th and August 23rd, was aimed at collecting samples of dykes for geochemical analysis on a 270 km stretch of coast north of Umiivik. We sampled brown weathered roughly N-S trending dykes and E-W trending Proterozoic amphibolite dykes. Structural data, like dyke thickness and dip and strike were collected for a possible structural study of these dykes.

We travelled by boat to all our camps and conducted case studies around each camp. When we selected the camps we tried to space ourselves so that we had an even sample spread along the coast.

Observations

The first camp was at Hornemann Ø between 15/07/14 and 22/07/14. Samples were collected from dykes on Hornemann Ø, the Qernertikajik peninsula, Ørsted Ø, Tortêrnatit Island, and Dannebrog Ø. A sample was taken, on the Qernertikajik peninsula, of what appeared to be a wide Archaean supracrustal-type amphibolite, already noted on old field maps. Other samples consisted of amphibolite dykes, brown weathered dolerites and amphibolites with garnets concentrated around quartz veins. There is a brown-weathered garnet rich rock presumed to be an Archaean supracrustal on Dannebrog Ø. A 2 km section of 28 tightly folded dykes were sampled on Hornemann Ø.

The second camp was near Køge Bugt where the Pamiagtît peninsula is transected by the narrow Tasilajik strait, between 23/07/14 and 30/07/14. At this camp samples were collected from around camp, Sipulik Island, and Sarpap Island. The samples near camps were of brown-weathered meta-gabbroic boudins. Sarpap Island has foliation parallel amphibolite dykes, plagioclase-phyric amphibolites and a well preserved meta-gabbroic complex. The meta-gabbroic consists of several thick subvertical coarse grained mafic dykes that trend either WNW-ESE or NNW-SSE and a variably dipping sill-like intrusion.

The third camp was on Kitak, SE of Isortoq. A local sighted a polar bear near our camp and we relocated to Isortoq. The surrounding islands and a fjord to the west of Isortoq were sampled. There are less foliation parallel amphibolites in this area and they are not as densely spaced. The amphibolites are locally cut by pervasive granite sheets and pegmatites. The youngest sampled dykes cut the amphibolites. These younger dykes are thick brown weathered doleritic dykes that can be correlated with regular anomalies on the aFieldwork magnetic survey. The amphibolites in this area often had malachite staining, indicating a higher Cu content.

From 09/08/14 to 16/08/14 amphibolites and brown weathered dolerites were sampled on a boat trip from the northern part of Umiivik back to basecamp. The northern part of Umiivik and the southern point of Jens Munks Ø were not sampled due to extreme ice conditions.

On this trip we observed that amphibolite dykes were denser and steeper in the south, becoming shallower dipping around Køge Bugt, and become less dense and steeper again close to basecamp.

The last week of fieldwork was spent at basecamp in Kuumiut from 17/08/14 to 23/08/14. Boat and helicopter excursions in the surrounding islands, up the Ammassalik Fjord and down toward Kulusuk. In this area, the amphibolite dykes tend to be thicker, often contain garnet and are spaced further apart than at our southern camps. There are also more brown-weathered dolerite dykes than in the south. There are two distinct generations of these dolerites. One is plagioclase phyric and has a strike similar to the Melville Bugt swarm. The other is thicker and has a more doleritic texture. These are interpreted as Tertiary dykes related to the North Atlantic breakup.

References

- Bridgwater, D., Austrheim, H., Hansen, B.T., Mengel, F., Pedersen, S. and Winter, J., 1990. The Proterozoic Nagssugtoqidian mobile belt of southeast Greenland: a link between the eastern Canadian and Baltic shields. *Geoscience Canada* 17 (4), 305–310.
- Kalsbeek, F., Austrheim, H., Bridgwater, D., Hansen, B.T., Pedersen, S. and Taylor, P., 1993. Geochronology of Archaean and Proterozoic events in the Ammassalik area, South-East Greenland, and comparisons with the Lewisian of Scotland and the Nagssugtoqidian of West Greenland. *Precambrian Research* 62, 239–270.
- Kolb, J., 2014. Structure of the Palaeoproterozoic Nagssugtoqidian Orogen, South-East Greenland: Model for tectonic evolution. *Precambrian Research* 255, 809-822.

Appendix A. Camp locations

Table 9. *Camp names and locations.*

Location	Name	Lat. (N)	Long. (W)
Camp 1	Hornemann Ø	65.16672	39.67308
Camp 2	Køge Bugt	65.03265	40.34639
Camp 3a	Kitak, 7 km south of Isortoq	65.49856	38.87528
Camp 3b	Isortoq	65.54860	38.97500
Boat trip	Umiivik to basecamp in Kuummiut	-	-
Basecamp	Kuummiut	-	-

Table 10. *Camps, dates and participants.*

Location	Name	Dates	Participants
Camp 1	Hornemann Ø	15.-22.7.2014	MBK, RBO
Camp 2	Køge Bugt	23.-30.7.2014	MBK, RBO
Camp 3a	Kitak, 7 km south of Isortoq	31.7.-3.8.2014	HPA, JPET, MBK, RBO
Camp 3b	Isortoq	4.-8.8.2014	HPA, JPET, MBK, RBO
Boat trip	Umiivik to basecamp in Kuummiut	9.-16.8.2014	JKOL, LBA, MBK, PGUA, RBO
Basecamp	Kuummiut	17.-23.8.2014	JKOL, LBA, MBK, PGUA, RBO, TBA

Appendix B. Sample details (from aFieldwork)

Sample no.	Lat. (N)	Long. (W)	Purpose	Rockname
563301	65.16327	39.95947	wholerock geochem	amphibolite
563302	65.16325	39.95958	wholerock geochem	dolerite
563303	65.16224	39.95974	wholerock geochem	amphibolite
563304	65.16154	39.96049	wholerock geochem	amphibolite
563305	65.16125	39.96149	wholerock geochem	lamprophyre
563306	65.16118	39.96154	wholerock geochem	amphibolite
563307	65.15739	39.90737	wholerock geochem	amphibolite
563308	65.15565	39.88377	wholerock geochem	n/a
563309	65.15659	39.87890	wholerock geochem	amphibolite
563310	65.09335	39.87352	wholerock geochem	amphibolite
563311	65.09350	39.87416	wholerock geochem	amphibolite
563312	65.08294	39.86545	wholerock geochem	amphibolite
563313	65.08280	39.86497	wholerock geochem	amphibolite
563314	65.08301	39.86513	wholerock geochem	amphibolite
563315	65.08245	39.63540	wholerock geochem	n/a
563316	65.08363	39.86428	wholerock geochem	amphibolite
563317	65.08337	39.86394	wholerock geochem	amphibolite
563318	65.21225	39.74159	wholerock geochem	amphibolite
563319	65.21242	39.74095	wholerock geochem	amphibolite
563320	65.21285	39.74075	wholerock geochem	amphibolite
563321	65.21300	39.74034	wholerock geochem	amphibolite
563322	65.21317	39.74054	wholerock geochem	amphibolite
563323	65.21344	39.73998	wholerock geochem	amphibolite
563324	65.32472	39.67941	wholerock geochem	amphibolite
563325	65.32478	39.67845	wholerock geochem	amphibolite
563326	65.32478	39.67836	wholerock geochem	amphibolite
563327	65.32494	39.67814	wholerock geochem	amphibolite
563328	65.32504	39.67895	wholerock geochem	amphibolite
563329	65.32437	39.67985	wholerock geochem	amphibolite
563330	65.32464	39.67976	wholerock geochem	amphibolite
563331	65.32475	39.68097	wholerock geochem	amphibolite
563332	65.32101	39.66589	wholerock geochem	amphibolite
563333	65.31975	39.66384	wholerock geochem	n/a
563334	65.31864	39.66152	wholerock geochem	amphibolite
563335	65.31904	39.66060	wholerock geochem	amphibolite
563336	65.31914	39.65972	wholerock geochem	amphibolite
563337	65.31935	39.66019	wholerock geochem	n/a
563338	65.31039	39.62246	wholerock geochem	n/a
563339	65.31032	39.62265	wholerock geochem	n/a
563340	65.31018	39.62226	wholerock geochem	amphibolite
563341	65.15300	39.63202	wholerock geochem	amphibolite
563342	65.15303	39.63166	wholerock geochem	dolerite
563343	65.15458	39.62632	wholerock geochem	amphibolite
563344	65.15449	39.62578	wholerock geochem	amphibolite
563345	65.15490	39.62562	wholerock geochem	amphibolite
563346	65.15657	39.62784	wholerock geochem	amphibolite
563347	65.15654	39.62770	wholerock geochem	amphibolite
563348	65.15745	39.62718	wholerock geochem	amphibolite
563349	65.15676	39.62854	wholerock geochem	amphibolite
563350	65.16025	39.63598	wholerock geochem	amphibolite
563351	65.16035	39.63570	wholerock geochem	amphibolite
563352	65.16105	39.63540	wholerock geochem	amphibolite
563353	65.16112	39.63536	wholerock geochem	amphibolite
563354	65.15560	39.62658	wholerock geochem	n/a

Sample no.	Lat. (N)	Long. (W)	Purpose	Rockname
563355	65.15861	39.67009	wholerock geochem	amphibolite
563356	65.16009	39.67278	wholerock geochem	amphibolite
563357	65.16050	39.67167	wholerock geochem	amphibolite
563358	65.16107	39.67353	wholerock geochem	amphibolite
563359	65.16115	39.67268	wholerock geochem	amphibolite
563360	65.16126	39.67318	wholerock geochem	amphibolite
563361	65.16174	39.67335	wholerock geochem	dolerite
563362	65.16213	39.67371	wholerock geochem	n/a
563363	65.16276	39.67280	wholerock geochem	amphibolite
563364	65.16424	39.67457	wholerock geochem	amphibolite
563365	65.16467	39.67511	wholerock geochem	amphibolite
563366	65.16952	39.67471	wholerock geochem	amphibolite
563367	65.16847	39.67129	wholerock geochem	amphibolite
563368	65.16802	39.67153	wholerock geochem	amphibolite
563369	65.16804	39.67155	wholerock geochem	amphibolite
563370	65.16754	39.67141	wholerock geochem	amphibolite
563371	65.16732	39.67191	wholerock geochem	amphibolite
563372	65.16707	39.67233	wholerock geochem	amphibolite
563373	65.16666	39.67317	wholerock geochem	amphibolite
563374	65.01949	40.12860	wholerock geochem	amphibolite
563375	65.01728	40.10766	wholerock geochem	amphibolite
563376	65.01673	40.11064	wholerock geochem	amphibolite
563377	65.01603	40.11405	wholerock geochem	amphibolite
563378	65.01608	40.11380	wholerock geochem	amphibolite
563379	64.99462	40.20490	wholerock geochem	amphibolite
563380	64.99190	40.22471	wholerock geochem	n/a
563381	65.05769	40.50970	wholerock geochem	dolerite
563382	65.05867	40.50962	wholerock geochem	amphibolite
563383	65.05964	40.51111	wholerock geochem	amphibolite
563384	65.06016	40.51152	wholerock geochem	amphibolite
563385	65.06043	40.51282	wholerock geochem	amphibolite
563386	65.06141	40.51231	wholerock geochem	amphibolite
563387	65.05849	40.51141	wholerock geochem	dolerite
563388	65.05776	40.51241	wholerock geochem	amphibolite
563389	65.05741	40.51331	wholerock geochem	amphibolite
563390	65.05777	40.51475	wholerock geochem	amphibolite
563391	65.05769	40.51494	wholerock geochem	amphibolite
563392	65.05664	40.52234	wholerock geochem	dolerite
563393	65.05768	40.52466	wholerock geochem	dolerite
563394	65.05858	40.52612	wholerock geochem	dolerite
563395	65.06094	40.52408	wholerock geochem	dolerite
563396	65.06026	40.51921	wholerock geochem	
563397	65.04976	40.49222	wholerock geochem	dolerite
563398	65.05621	40.52008	wholerock geochem	dolerite
563399	65.06621	40.51802	wholerock geochem	dolerite
563400	65.03265	40.34639	wholerock geochem	amphibolite
563401	65.06630	40.52069	wholerock geochem	amphibolite
563402	65.06303	40.50861	wholerock geochem	amphibolite
563403	65.06423	40.51513	wholerock geochem	Qtz diorite 5-20 Qtz; <10 Kfs; An<50
563404	65.07085	40.52381	wholerock geochem	Qtz diorite 5-20 Qtz; <10 Kfs; An<50
563405	65.07023	40.52171	wholerock geochem	dolerite
563406	65.06913	40.52298	wholerock geochem	n/a
563407	65.02637	40.26555	wholerock geochem	amphibolite
563408	65.06297	40.50881	wholerock geochem	amphibolite
563409	65.06297	40.50881	wholerock geochem	dolerite
563410	65.06981	40.52118	wholerock geochem	dolerite

Sample no.	Lat. (N)	Long. (W)	Purpose	Rockname
563411	65.07009	40.52137	wholerock geochem	amphibolite
563412	65.07093	40.52188	wholerock geochem	Qtz diorite 5-20 Qtz;<10 Kfs;An<50
563413	65.07027	40.52146	wholerock geochem	amphibolite
563414	65.03253	40.37167	wholerock geochem	dolerite
563415	65.03326	40.37024	wholerock geochem	dolerite
563416	65.09435	40.53020	wholerock geochem	amphibolite
563417	65.09439	40.53018	wholerock geochem	granite >20 Qtz;65-90 Kfs
563418			wholerock geochem	dolerite
563419	65.53547	38.83982	wholerock geochem	amphibolite
563420	65.54266	38.83152	wholerock geochem	amphibolite
563421	65.56254	38.76476	wholerock geochem	amphibolite
563422	65.58144	38.72936	wholerock geochem	amphibolite
563423	65.57934	38.76229	wholerock geochem	amphibolite
563424	65.57741	38.76786	wholerock geochem	dolerite
563425	65.49938	38.88230	wholerock geochem	amphibolite
563426	65.55761	38.93690	wholerock geochem	amphibolite
563427	65.55728	38.93749	wholerock geochem	n/a
563428	65.54679	38.92722	wholerock geochem	amphibolite
563429	65.54646	38.91500	wholerock geochem	amphibolite
563430	65.54352	38.91857	wholerock geochem	amphibolite
563431	65.54317	38.91868	wholerock geochem	amphibolite
563432	65.53241	38.91351	wholerock geochem	dolerite
563433	65.53238	38.91430	wholerock geochem	amphibolite
563434	65.53233	38.91221	wholerock geochem	dolerite
563435	65.52568	38.91768	wholerock geochem	amphibolite
563436	65.52556	38.91746	wholerock geochem	amphibolite
563437	65.52511	38.91597	wholerock geochem	amphibolite
563438	65.52506	38.91639	wholerock geochem	dolerite
563439	65.53230	38.91241	wholerock geochem	amphibolite
563440	65.52847	38.89360	wholerock geochem	amphibolite
563441	65.58902	38.89762	wholerock geochem	amphibolite
563442	65.08344	39.86401	wholerock geochem	dolerite
563443	65.59962	38.91308	wholerock geochem	dolerite
563444	65.52452	38.80915	wholerock geochem	amphibolite
563445	65.51952	38.77359	wholerock geochem	dolerite
563446	65.21078	39.73986	wholerock geochem	dolerite
563447	65.53589	38.73590	wholerock geochem	amphibolite
563448	65.53539	38.73577	wholerock geochem	amphibolite
563449	65.53685	38.74611	wholerock geochem	amphibolite
563450	65.53184	38.75072	wholerock geochem	amphibolite
563451	65.52473	38.76317	wholerock geochem	amphibolite
563452	65.52484	38.76352	wholerock geochem	amphibolite
563453	65.21156	39.74008	wholerock geochem	amphibolite
563454	65.21156	39.74008	wholerock geochem	amphibolite
563455	65.52402	38.76458	wholerock geochem	amphibolite
563456	65.52446	38.76403	wholerock geochem	amphibolite
563457	65.52244	38.76618	wholerock geochem	n/a
563458	65.52231	38.76588	wholerock geochem	n/a
563459	65.52223	38.76580	wholerock geochem	dolerite
563460	65.52255	38.76605	wholerock geochem	rhyolite >20 Qtz;65-90 Kfs
563461	65.57022	38.98537	wholerock geochem	dolerite
563462	65.57021	38.98533	wholerock geochem	dolerite
563463	65.59168	38.99424	wholerock geochem	dolerite
563464	65.59576	39.00030	wholerock geochem	amphibolite
563465	65.59561	38.99982	wholerock geochem	n/a
563466	65.56285	38.88915	wholerock geochem	dolerite

Sample no.	Lat. (N)	Long. (W)	Purpose	Rockname
563467	65.56071	38.82853	wholerock geochem	amphibolite
563468	65.54490	38.84222	wholerock geochem	dolerite
563469	65.52501	38.87866	wholerock geochem	amphibolite
563470	65.52224	38.88076	wholerock geochem	amphibolite
563471	65.51954	38.87029	wholerock geochem	granite >20 Qtz;65-90 Kfs
563472	65.52181	38.89163	wholerock geochem	dolerite
563473	65.51694	38.87284	wholerock geochem	amphibolite
563474	65.51637	38.87509	wholerock geochem	amphibolite
563475	65.72779	39.25046	wholerock geochem	amphibolite
563476	65.62820	39.24927	wholerock geochem	amphibolite
563477	65.62762	39.24847	wholerock geochem	amphibolite
563478	54.60779	39.25568	wholerock geochem	granite
563479	65.58823	39.28555	wholerock geochem	amphibolite
563480	65.55366	39.29386	wholerock geochem	amphibolite
563481	65.55373	39.29392	wholerock geochem	amphibolite
563482	65.55377	39.29359	wholerock geochem	amphibolite
563483	65.55376	39.29358	wholerock geochem	serpentinite
563484	65.55446	39.29368	wholerock geochem	amphibolite
563485	65.55409	39.29472	wholerock geochem	tonalite >20 Qtz;<10 Kfs
563486	65.55315	39.29715	wholerock geochem	amphibolite
563487			wholerock geochem	n/a
563488	65.55340	39.29622	wholerock geochem	amphibolite
563489	65.55405	39.29339	wholerock geochem	granite >20 Qtz;65-90 Kfs
563490	65.64307	39.18683	wholerock geochem	granite >20 Qtz;65-90 Kfs
563491	65.63721	39.17860	wholerock geochem	amphibolite
563492	65.63697	39.17878	wholerock geochem	amphibolite
563493	65.63277	39.16725	wholerock geochem	n/a
563494	65.60209	39.21181	wholerock geochem	amphibolite
563495	65.60155	39.21036	wholerock geochem	dolerite
563496	65.57477	39.13261	wholerock geochem	amphibolite
563497	64.54828	40.45017	wholerock geochem	amphibolite
563498	64.54927	40.44952	wholerock geochem	amphibolite
563499	64.54913	40.44942	wholerock geochem	amphibolite
565301	65.54961	40.44890	wholerock geochem	amphibolite
565302	64.55902	40.45327	wholerock geochem	dolerite
565303	64.55970	40.45131	wholerock geochem	amphibolite
565304	64.56288	40.44088	wholerock geochem	amphibolite
565305	64.56741	40.33525	wholerock geochem	amphibolite
565306	64.56713	40.33610	wholerock geochem	amphibolite
565307	64.56773	40.33954	wholerock geochem	amphibolite
565308	64.56764	40.31287	wholerock geochem	amphibolite
565309	64.67222	40.47333	wholerock geochem	dolerite
565310	64.67224	40.47455	wholerock geochem	amphibolite
565311	64.67261	40.47556	wholerock geochem	amphibolite
565312	64.70656	40.46113	wholerock geochem	amphibolite
565313	64.70670	40.44518	wholerock geochem	amphibolite
565314	64.70714	40.46251	wholerock geochem	amphibolite
565315	64.80797	40.48058	wholerock geochem	dolerite
565316	64.84937	40.55812	wholerock geochem	amphibolite
565317	64.84962	40.55944	wholerock geochem	amphibolite
565318	64.93496	40.74715	wholerock geochem	amphibolite
565319	64.93509	40.74610	wholerock geochem	metagabbro
565320	64.93547	40.74920	wholerock geochem	amphibolite
565321	64.93666	40.74987	wholerock geochem	dolerite
565322	65.10179	40.78369	wholerock geochem	ultramafic
565323	65.10186	40.78377	wholerock geochem	pegmatite vein

Sample no.	Lat. (N)	Long. (W)	Purpose	Rockname
565324	65.10170	40.78373	wholerock geochem	amphibolite
565327	65.10269	40.78451	wholerock geochem	amphibolite
565328	65.10312	40.78437	wholerock geochem	intermediate amphibolite
565329	65.10313	40.78439	wholerock geochem	mafic amphibolite
565330	65.10357	40.78486	wholerock geochem	amphibolite
565331	65.09674	40.78390	wholerock geochem	amphibolite
565332	65.09644	40.78398	wholerock geochem	intermediate
565333	65.09644	40.78399	wholerock geochem	dolerite
565334	65.10768	40.83200	wholerock geochem	dolerite
565335	65.02383	40.49273	wholerock geochem	intermediate amphibolite
565336	65.02284	40.49326	wholerock geochem	garnet amphibolite
565337	65.02228	40.49426	wholerock geochem	amphibolite
565338	65.16800	39.89117	wholerock geochem	amphibolite
565339	65.16780	39.89079	wholerock geochem	amphibolite
565340	65.16639	39.89288	wholerock geochem	amphibolite
565341	65.16621	39.89365	wholerock geochem	amphibolite
565342	65.16888	39.88832	wholerock geochem	pseudotachylite
565347	65.31010	39.58136	wholerock geochem	dolerite
565348	65.31022	39.58069	wholerock geochem	chilled margin
565349	65.31068	39.58074	wholerock geochem	garnet amphibolite
565350	65.48927	39.29427	wholerock geochem	garnet amphibolite
565351	65.49234	39.29578	wholerock geochem	amphibolite
565353	65.58060	38.65901	wholerock geochem	brown weathered dolerite
565354	65.58062	38.65930	wholerock geochem	brown weathered dolerite
565355	65.91296	37.04817	wholerock geochem	garnet amphibolite
565356	65.92469	37.07128	wholerock geochem	amphibolite
565357	65.93294	37.08357	wholerock geochem	amphibolite
565358	65.93381	37.08230	wholerock geochem	garnet amphibolite
565359	65.91386	37.11898	wholerock geochem	brown weathered dolerite
565360	65.91352	37.11930	wholerock geochem	garnet amphibolite
565361	65.91377	37.11864	wholerock geochem	brown weathered dolerite
565362	65.88250	37.12395	wholerock geochem	garnet amphibolite
565363	65.88323	37.14074	wholerock geochem	brown weathered dolerite
565371	65.65558	37.20755	wholerock geochem	brown weathered dolerite
565372	65.65569	37.20871	wholerock geochem	brown weathered dolerite
565373	65.65459	37.20232	wholerock geochem	amphibolite
565374	65.70976	37.12322	wholerock geochem	amphibolite
565380	65.89240	36.96118	wholerock geochem	garnet amphibolite
565381	65.88972	36.96509	wholerock geochem	brown weathered dolerite
565398	65.84151	36.32405	wholerock geochem	amphibolite
565399	65.83980	36.32423	wholerock geochem	brown weathered dolerite
565701	65.87561	36.26975	wholerock geochem	garnet amphibolite
565702	66.04500	36.26936	wholerock geochem	tertiary brown weathered
565703	66.02241	36.52828	wholerock geochem	amphibolite
565704	65.89323	36.75267	wholerock geochem	brown weathered dolerite
565705	65.88455	36.75853	wholerock geochem	garnet amphibolite

Acquisition of on-ground spectral reflectance data (AFJ, PRI, BHM)

Introduction

The Geological Survey of Denmark and Greenland (GEUS) have successfully operated several airborne remote sensing surveys aimed to map geology and mineral resources onshore Greenland (Tukiainen 2001, Bedini 2012). GEUS have also acquired and processed satellite multispectral data for the same purposes (Bedini 2011). One of the prerequisites for the successful interpretation of these remote sensing datasets is “ground-truth” data.

The present field report documents the land-based and on-ground spectral reflectance measurements carried out in the period 6-22 August 2014, during the SEGMENT 2014 field campaign to South East Greenland. The main aim of the spectral measurements is to create a database of spectral reflectance data for various lithologies in the area. This new database will assist the processing of both the ASTER satellite multispectral data covering the region, and the hyperspectral airborne remote sensing survey scheduled to be flown during the summer of 2015. In simple terms, the new spectral reflectance data will provide the fore mentioned “ground-truth” data that better will allow for the correct interpretation of satellite or airborne remote sensing data in terms of geology and mineral resources. In the following we will also attempt to characterise the measured rocks, comparing our spectral reflectance data and geological observations with already existing spectral libraries.

The spectroscopy measurements were carried out using an ASD FieldSpec 3 spectrometer. Altogether 16 locations were measured, and reported in the following (Figure 128). The field work was carried out in parallel with the magnetotelluric geophysical campaign.

Measuring Procedures

The spectroscopy measurements were carried out in a manner similar to that suggested by Goetz (2012): Before commencing the measurements, the FieldSpec 3 instrument was turned on, and allowed to warm-up for about 10 minutes. The instrument is controlled by a laptop PC using the RS3 software. Before the actual measurement, a white reference measurement is carried out on a spectralon (Figure 129), which is a material with approximately 100 percent reflectance across the entire measured spectrum. The white reference data is used as a calibration-of-sorts, to transfer all the following radiance measurement data into relative reflectance. The crucial assumption is that the sun light reaching the measured sample area is exactly the same as the light reaching the spectralon during the white reference calibration. However, this assumption is only valid while the sun remains in the same position relative to the measuring site, or, in other words, for a short time after the white reference measurement. More importantly, the atmospheric conditions have to remain absolutely stable, as solar light is absorbed in the atmosphere, and changing atmospheric conditions results in largely changed incoming solar light. For these reasons, all measurements were carried out within a period of ca. 3 minutes after the white reference measurement, which is a sufficiently short period of time to make the assumption of stable solar input. Moreover, all measurements were carried out between 10:00 and 14:00 on days with clear sunshine, and

little or no winds. In order to avoid effects caused by terrain, the measurements were taken on relatively flat areas.



Figure 128. Map showing the visited locations.



Figure 129. White reference calibration of the ASD FieldSpec 3.

In theory a single spectral reflectance measurement is enough to characterise a homogeneous and well-exposed lithology. In practice, varying degrees of alteration and lichen and moss coverage necessitate several spectral measurements in order to characterise the average spectral reflectance for a given lithology. We followed the suggestion of Goetz (2012), and, for each site, made 120 spectral reflectance measurements walking randomly around the exposed surface, and holding the sensor away from the body of the operator at an angle perpendicular to the azimuth of the sun, so to minimize reflectance and shadow from the person performing the measurements (Figure 130). In this report we will, for each measuring site, give the minimum, maximum, mean and median spectral reflectance from the 120 spectral reflectance measurements.

Attempts were made to acquire spectroscopy data for larger areas (>50 x 50 m) with homogeneous geology, that are suitable for the calibration of ASTER satellite remote sensing data, where each pixel has a size from 30 x 30 m and up to 120 x 120 m, depending on the wavelength of the electromagnetic solar radiation. Spectral reflectance data from inhomogeneous geological terrains are, however also of use, both as a tool of characterisation, and for building a spectral library that can be used to find similar rocks at other locations. For all measuring sites the extent and homogeneity of the exposed geology is given. Also information of the extent of moss and lichen cover, which can significantly alter the measured spectra, are given.



Figure 130. *The ASD FieldSpec operator walking towards the sun holding the sensor at an arm's length away from the body to minimise the influence on the measurements.*

In general, weather conditions remained favourable throughout the field campaign. A limiting factor was our transportation by boat, allowing us to reach only geological sites exposed along the coast. Another limitation is that our operation was carried out alongside the magnetotelluric measurements (Heincke, 2016), which put a strong restriction on the time available for spectral reflectance measurements.

Outline of report

At each measuring site a hand sample was collected and a photo taken. The GEUS sample number of the collected sample and a short geological site description are given for each measuring site. Other relevant information, such as weather condition and size of the measured area is also given. All measurements are taken in the time frame of 10AM to 3PM.

The Fieldwork for Hyperspectral data

7/8-2014

Weather: Nice and sunny no clouds.

Locality 1: Behind the school in Kuummuit

Geology Grey gneiss

GPS position N65.86674, W37.00832

Description of site A relative small area of 4 x 5m with a slight tilt of approx. 10° inclination, slight overgrow of lichen

Notes This was a test run of the equipment, where we were familiarising ourselves with the equipment, and how to avoid measuring the shadow when turning. No sample was taken here.



Figure 131. *Making sure that everything is ready for the measurements, the white plate is the spectralon for reference measurements.*

9/8-2014

Weather: Light cloud cover, the sky seems blue with white streaks. No shadows from the clouds observed.

Locality 2: Granite, valley in front of a bog

Geology Light grey granite, medium-grained, quartz and feldspar are the main minerals, slight content of amphibole and biotite. The rock surface is very uniform with occasional tygmatic pegmatites that mainly consist of quartz.

GPS position N65.57597, W38.81036

Description of site Flat area of 10 x 10 m just above the tidal mark, will be occasionally flooded during storms, so plagioclase might be destroyed. Little to no lichen. No measurable inclinations of the area.

Sample no. GGU 565501

Notes Three measurements were taken of the granite. The sample was not easy to take as there are only few weaknesses in the rock to be found in a relative flat area.

Photos from locality 2 can be seen in Figure 132 and Figure 133. The sample during extraction can be seen in Figure 133a and xenoliths in the country rock (not measured) can be seen in Figure 133b.

Three measurements were made as locality 2. The measurements can be seen in Figure 134 to 11. When looking at the spectra all data are very uniform what is to be expected

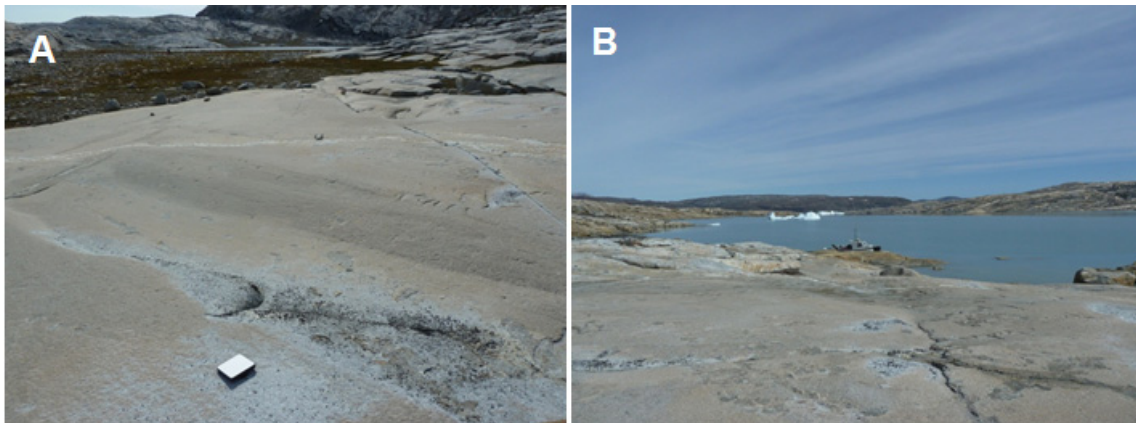


Figure 132. *The area at locality 2 that was measured with the FieldSpec, seen from two different angles.*



Figure 133. *Locality 2. A) The sample during extraction. B) Xenoliths of the country rock with angular sides (not measured).*

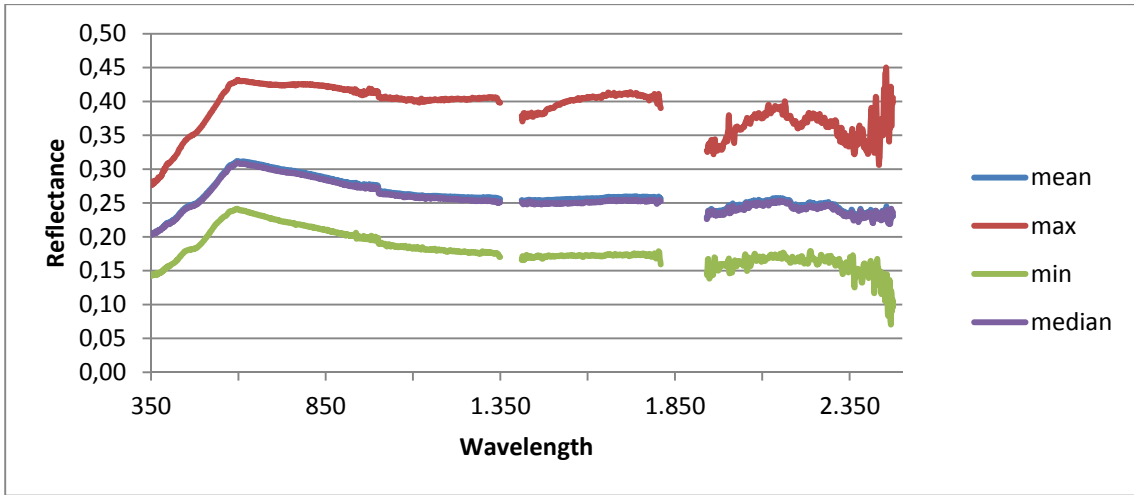


Figure 134. Results of the first measurement at locality 2

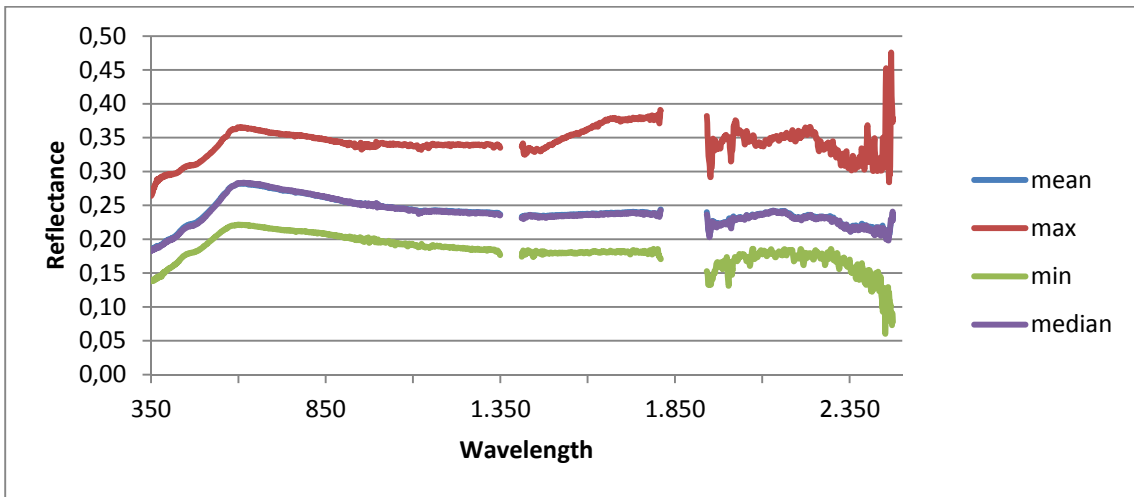


Figure 135. Results of the second measurement at locality 2.

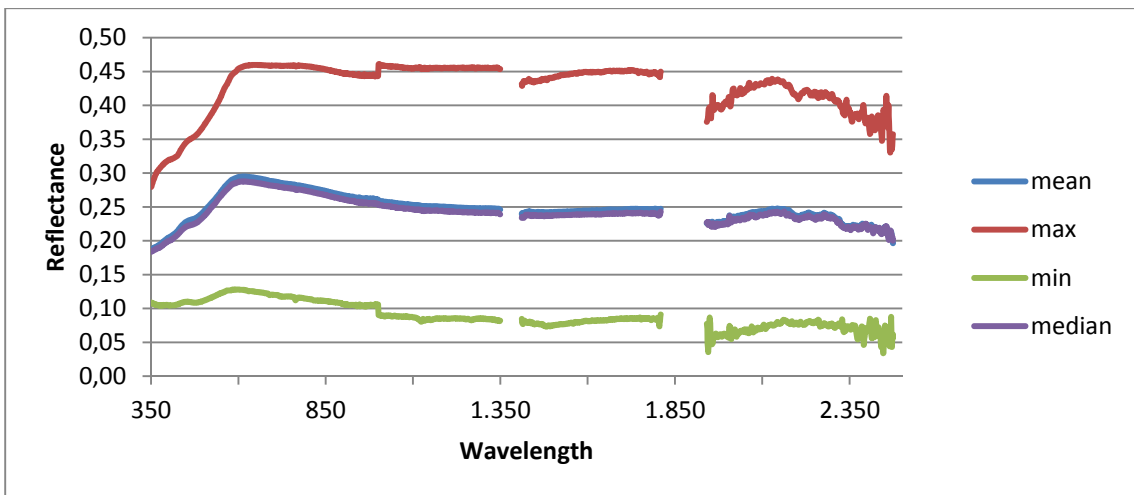


Figure 136. Results of the third measurement at locality 2.

10/8-2014

No measurements with the FieldSpec as we were travelling in the zodiac with MT stations and there were no space for more equipment.

Weather: Nice and clear.

Locality 3: Sulfur rich horizon

Geology Biotite schist with Greisen alteration, pure sulfur, small quartz veinlets

GPS position N65.6611, W38.41373

Description of site Grey gneiss with amphibolite bands is surrounding

Sample no. GGU 565502

Notes This sample was taken as the geology looked interesting for exploration.



Figure 137. *The alteration zone, approx. 2 m thick, with iron at the sides, becomes more sulfur-rich towards the centre.*

11/8-2014

Weather: In the morning there were fog coming in from the sea, it were moving around, but leaving areas free from fog so around noon we decided it would be safe to take some measurements.

Locality 4: Gneiss above camp 1

Geology Heterogenic grey gneiss/migmatite, black and grey bands the shape and foliation indicates that the rock has been partly melted during metamorphism.

GPS position N65.61704, W38.54898

Time of measurements 12:15 PM

Description of site Grey banded gneiss, several areas on top of the hill next to camp several areas were covered and different amounts of lichen

Sample no. GGU 565503



Figure 138. Measuring the gneiss at locality 4.



Figure 139. Getting ready to measure the gneiss at locality 4.

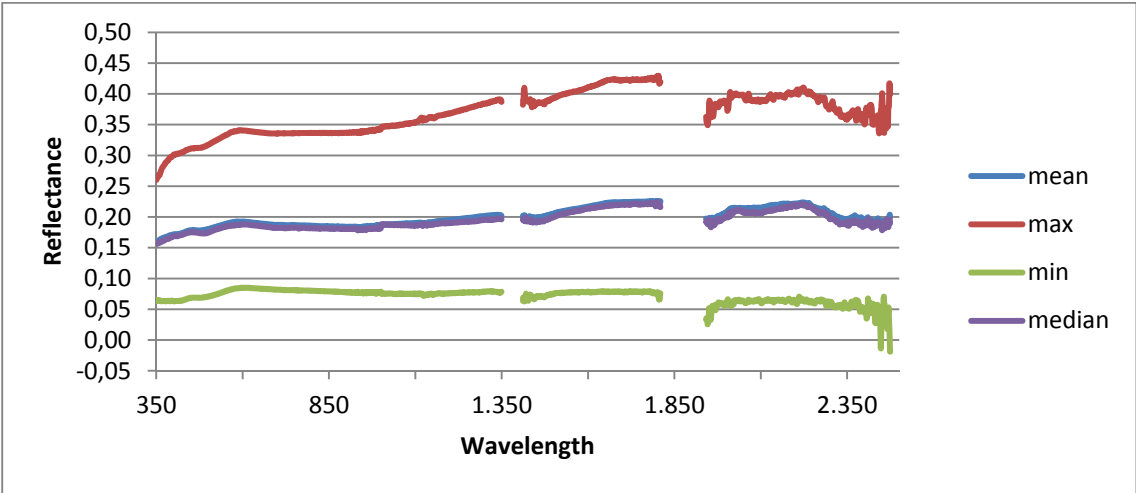


Figure 140. Results of the measurement at locality 4.

Locality 5: Dyke close to camp 1

Geology Mafic dyke that cuts the gneiss close to camp.

GPS position N65.61774, W38.54878

Time of measurements 1:00 PM

Description of site 20 m wide dyke, the surface has goethite, hematite and limonite staining indicating that it has a high iron content.

Sample no. GGU 565504

Notes No to little lichen

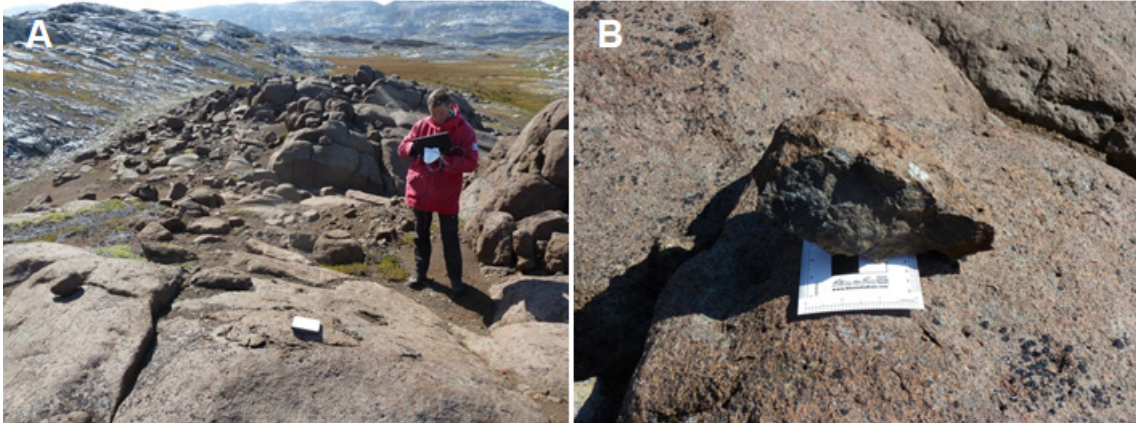


Figure 141. Localities 5. A) The measured dyke. B) The sample from locality 5.

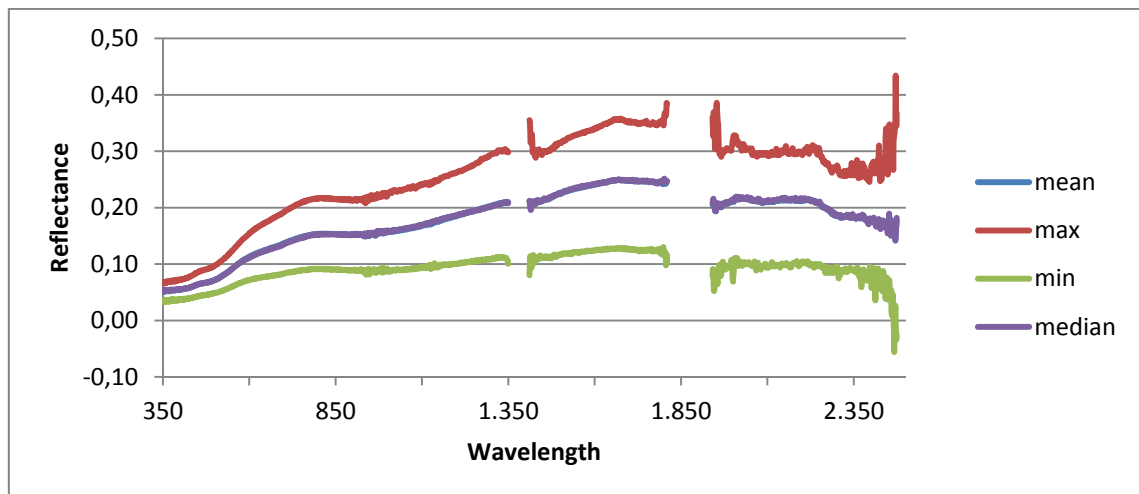


Figure 142. Results of the measurement at locality 5.

12/8-2014

Weather: Fog on the sea, clear sky on land.

Locality 6: Ultra-mafic dyke

Geology Ultra-mafic dyke that has been metamorphosed into lens shapes, and folded in the landscape so that there are two parallel lines of lenses in an anticline. The lens, that were measured, is approx. 20 x 50 m. It has a light brown colour due to weathering. The rock is rich in pyroxenes.

GPS position N65.61876, W38.47968

Description of site The rock does not weather with a smooth surface as the pyroxenes are harder than the rest of the rock, giving it a nubby look.

Sample no. GGU 565506

Notes 1 measurement taken

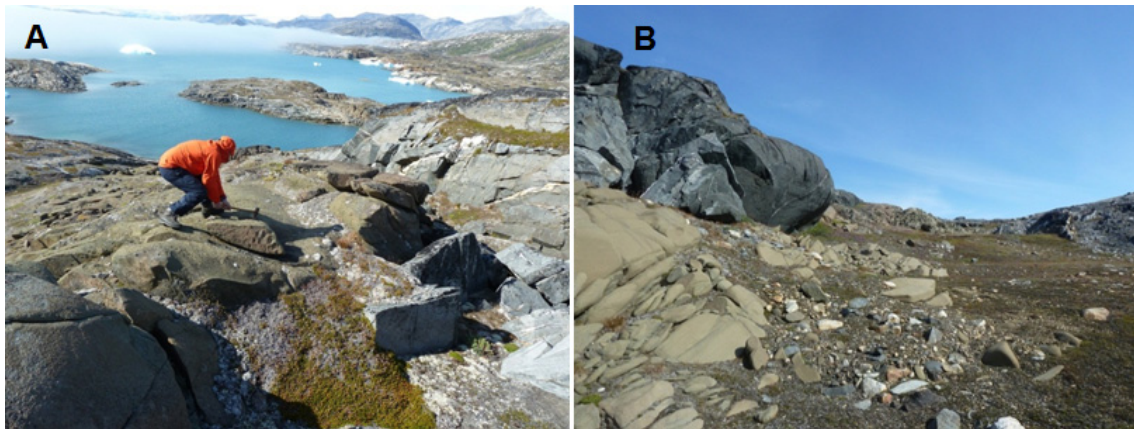


Figure 143. *Locality 6. A) Sample taking next to the area that were measured. B) The relation to the side rock. It is apparent that the area close to the contact zone to the gneiss weathers differently than the contact to the amphibolite.*

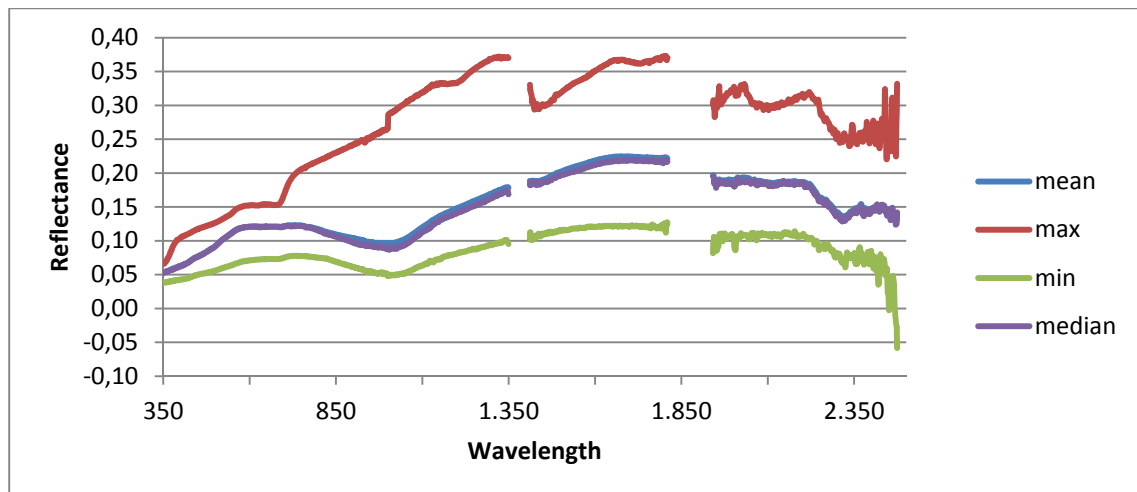


Figure 144. *Results of the measurement of the ultramafic rock at locality 6.*

Locality 7: Dark banded amphibolite

Geology Quartz amphibolite, between the two parallel ultramafic dykes in the center of the anticline. On the contact between this rock type and the ultramafic this rock contains large red minerals that are harder than the rock causing them to stick out, they are redder than the corundum found in the area making me suspect that they are garnets. There are reported to be rubies at a location not far from this on the same boundary.

GPS position N65.61847, W38.47655

Description of site 3 x 5 m flat area, with a few quartz veins of up to 5 cm.

Sample no. GGU 565507 + GGU 565522

Notes 1 measurement taken



Figure 145. *Locality 7. A) Close-up of the measured rock. B) Measurement of the banded amphibolite.*

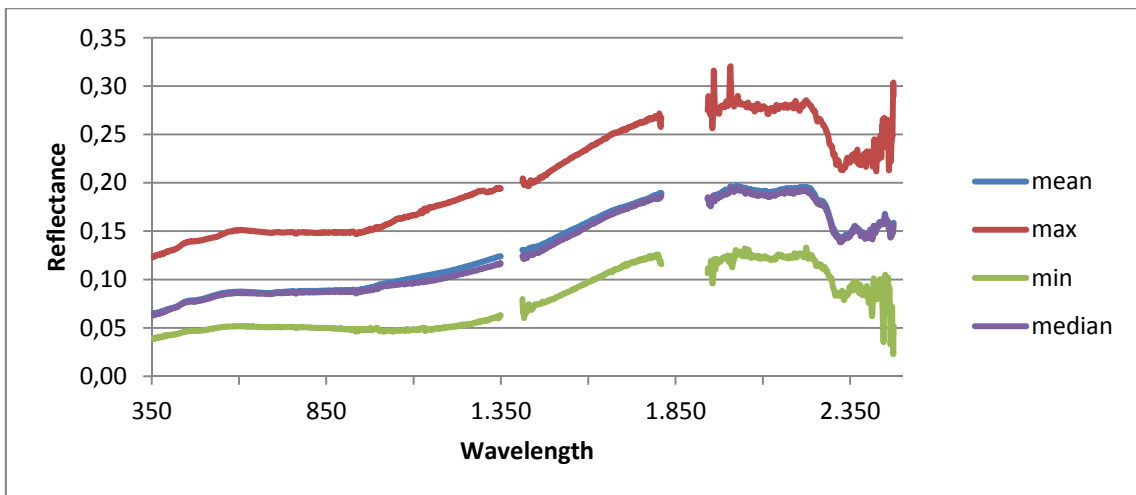


Figure 146. *Results of the measurement of the banded amphibolite at locality 7.*

Locality 8

Geology Light grey gneiss on the outside of the anticline.

GPS position N65.61664, W38.47402

Description of site 3 areas was measured. They were selected after the amount of lichen, so one area had little to no lichen while another had a lot. On top of the hill the exposures were relative flat and large so the areas measured were from 5 x 3 m to 10 x 2m. The elevation made sure we were measuring above the low clouds (fog).

Sample no. GGU 565508

Notes 3 measurement taken, 3 different exposures of the area to get different amounts of lichen and size of the measurement area tried.



Figure 147. *Locality 8. A) The surface with most lichen. B) Measurement of the surface with most lichen, in the background the fog over the fjord can be seen C) Reference measurement before measuring the area with little to no lichen. D) The surface with little to no lichen, remelting structures can be seen.*

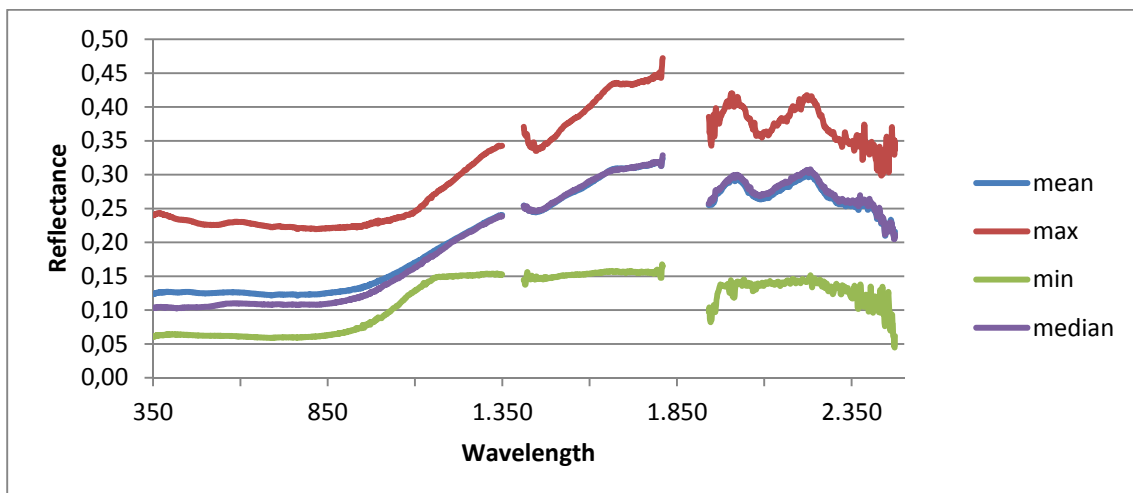


Figure 148. *Results of the first measurement at locality 8.*

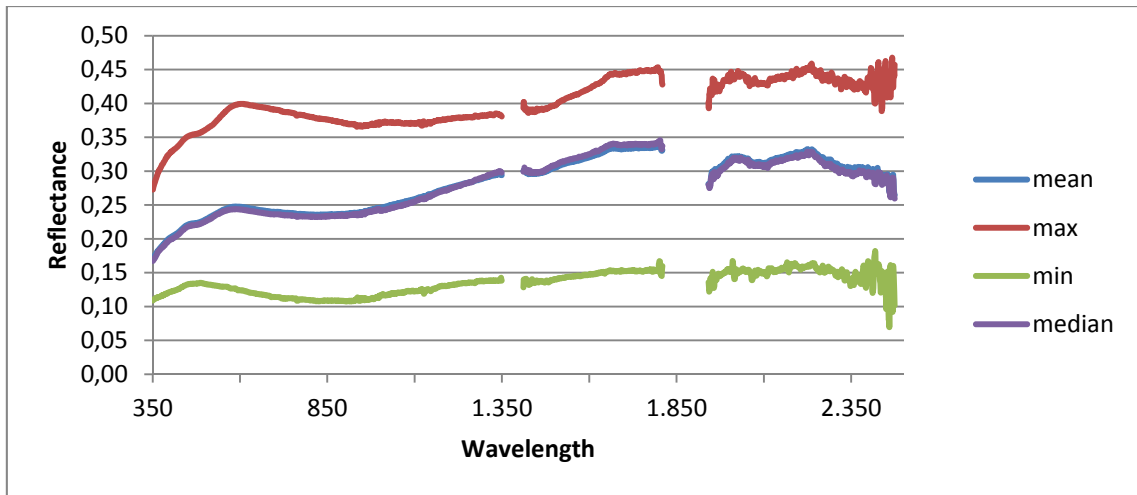


Figure 149. Results of the second measurement at locality 8, the site with lichen.

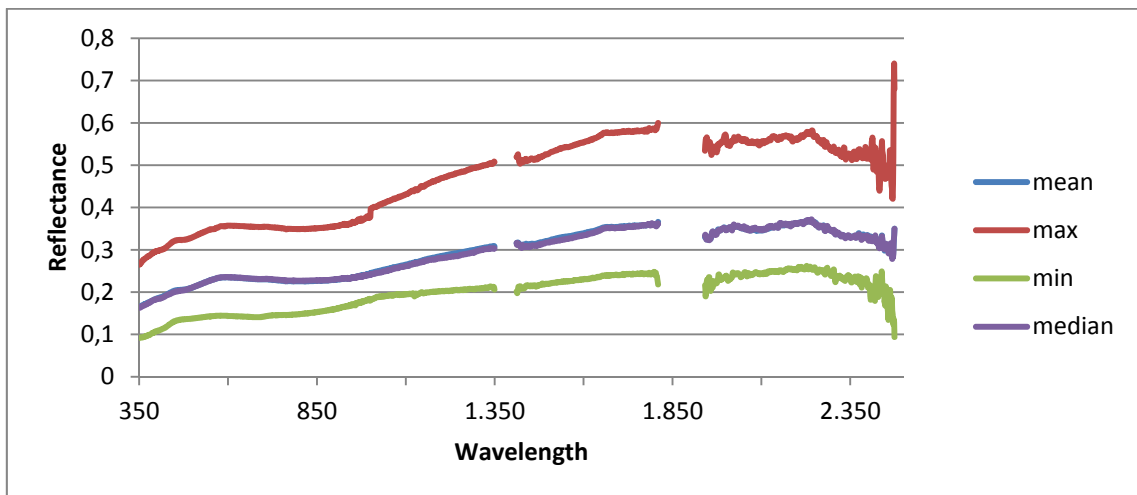


Figure 150. Results of the third measurement from locality 8, the area without lichen.

16/8-2014

Weather: High clouds, very pale blue sky, cleared up during the day.

Locality 9

Geology White rock with yellow weathering surface, rich in garnets. Consisting of quartz feldspar and garnet, the garnet content is not consistent. Thin dark veins and blobs can be found.

GPS position N65.76428, W38.10199

Description of site 4 measurements were taken; 1 with 240 spots and the remaining 3 with 120 spots.

Sample no. GGU 565509 & 565510

Notes Sample 565510 is from one of the dark veins as it was obvious that it was a different rock type than 565509.



Figure 151. Overview of the area at locality 9.

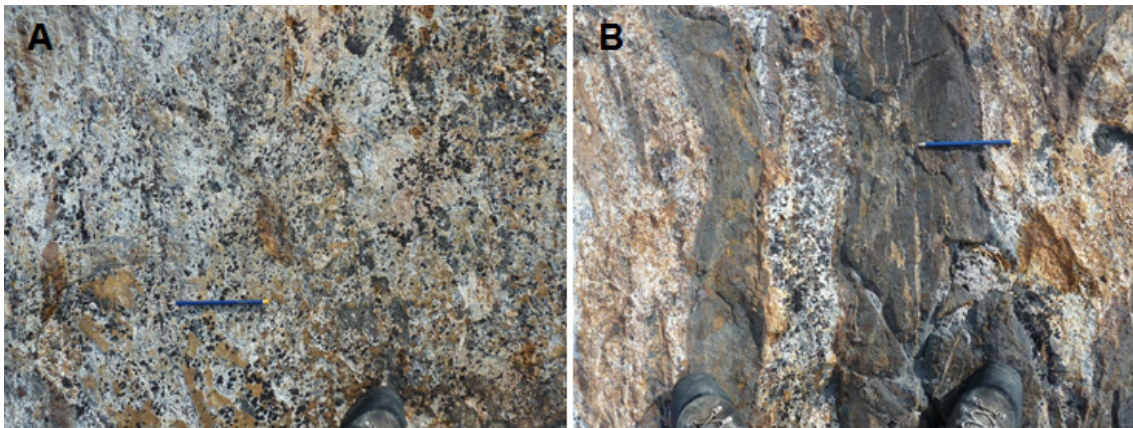


Figure 152. A) The main rock type that was measured at locality 9. The average amount of lichen can also be seen. B) Ultra-mafic blobs with the light rock.

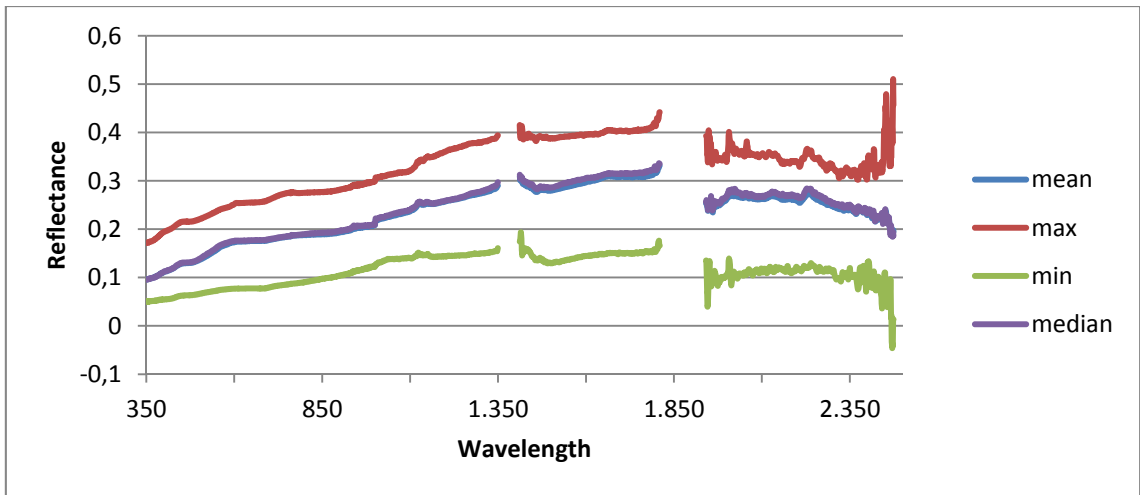


Figure 153. Results of the measurement from the main area at locality 9

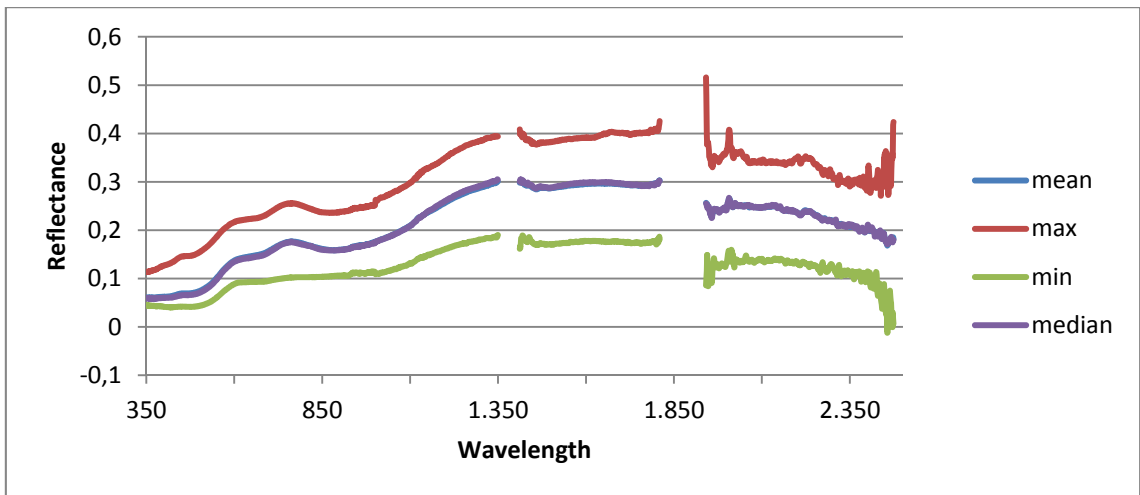


Figure 154. Results of the measurement from the iron stained part at locality 9.

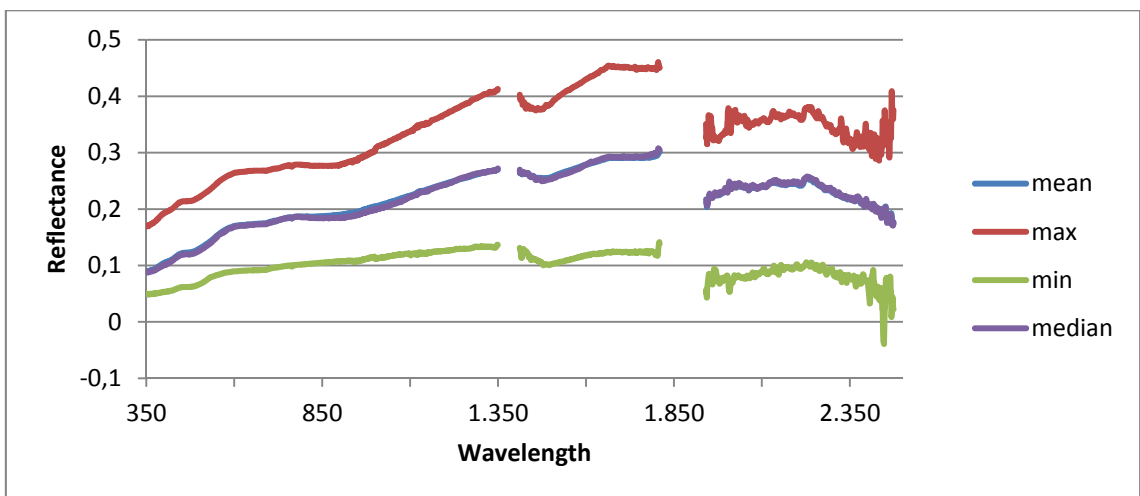


Figure 155. Result of the measurement from the part with dykes and tiny elongated blobs at locality 9.

Locality 10

Geology Mafic dyke, dark and iron stained

GPS position N65.77252, W38.10677

Description of site The largest area with best angle towards the sun was selected it was 3 x 1.5 m

Sample no. GGU 565511

Notes Significant amounts of lichen on the rock surface

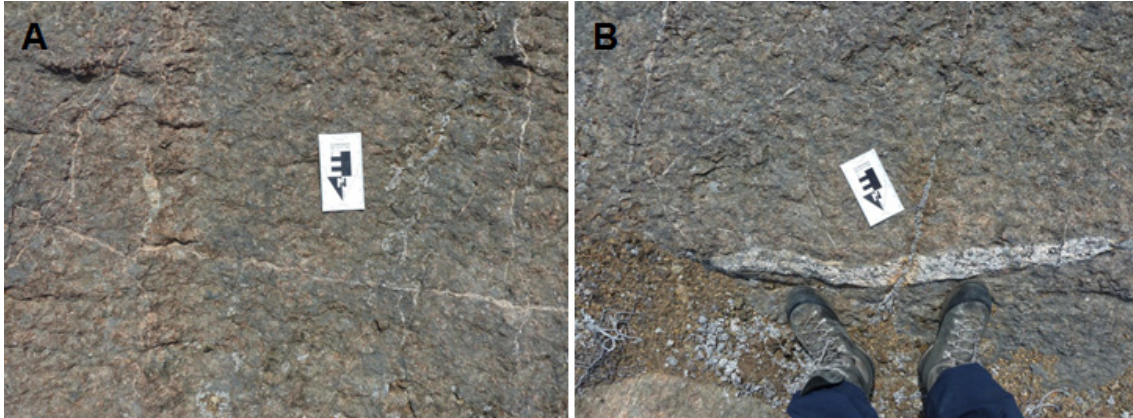


Figure 156. *Locality 10. A) Close up of the surface of the dyke, B) An inclusion in the dyke.*



Figure 157. *Measuring the spectra of the dyke at locality 10.*

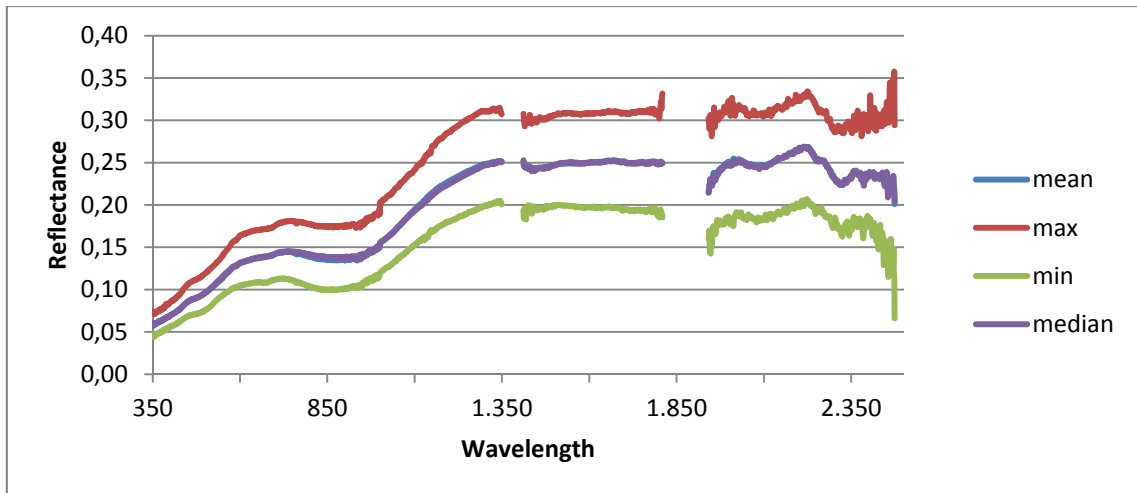


Figure 158. Result of the measurement of the dyke at locality 10.

Locality 11

Geology Very iron stained version of the white rock that was seen at locality 9. The iron staining can also be greisen alteration.

GPS position N65.77280, W38.10722

Description of site 20 x 40 cm

Sample no. GGU 565512

Notes The sample is very weathered and could be the same rock type as both locality 9 and locality 10.

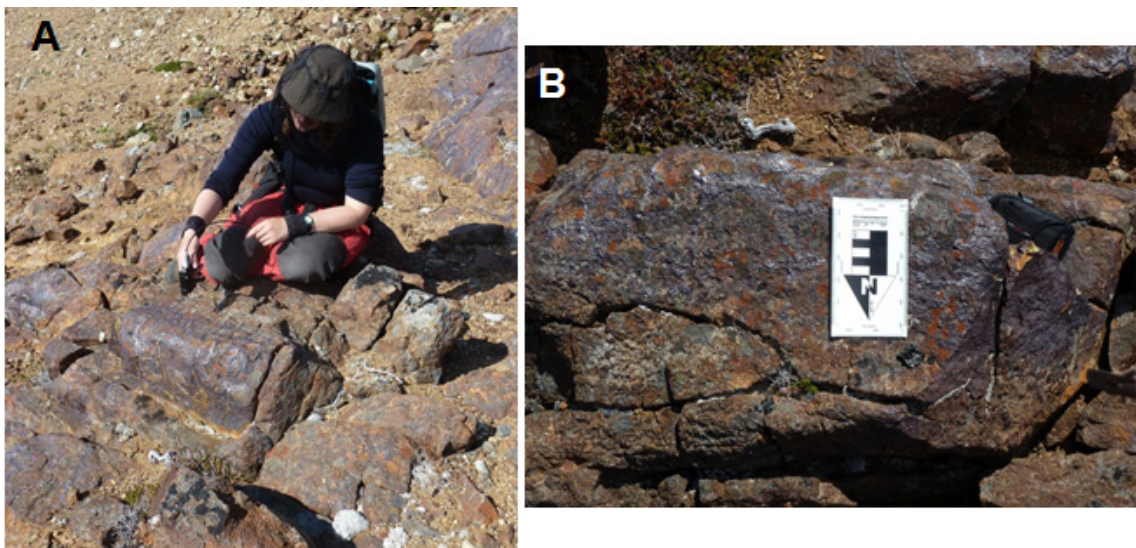


Figure 159. Locality 11. A) Measuring the greisen alteration, B) Close up of the measured rock.

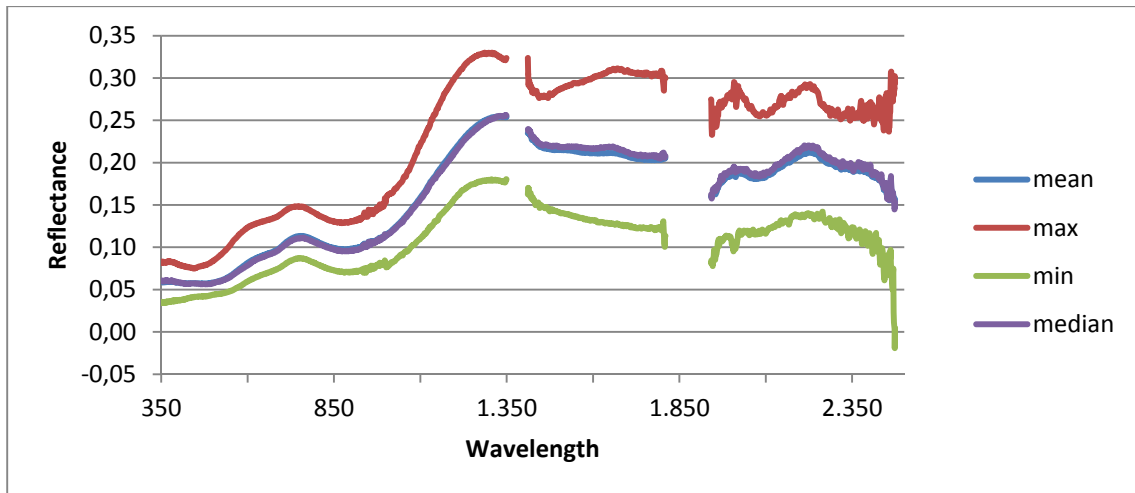


Figure 160. Results of the measurement at locality 11.

Locality 12

Geology White pale rock

GPS position N65.76900, W38.11805

Description of site 2 measurements, on areas with a lot of lichen.

Sample no. No sample taken but same geology as sample GGU 565509.

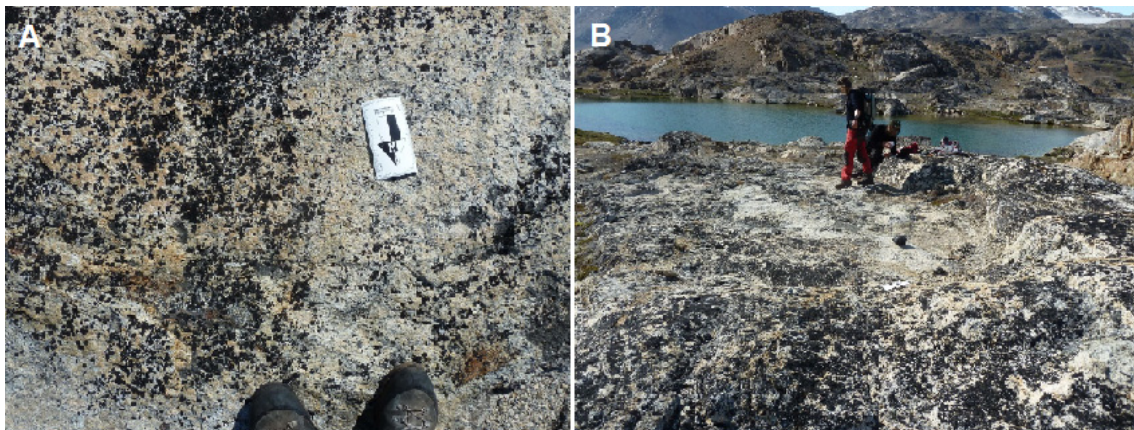


Figure 161. Locality 12. A) Here the amount of lichen is very apparent, B) Measurement while colleague is working with the computer.

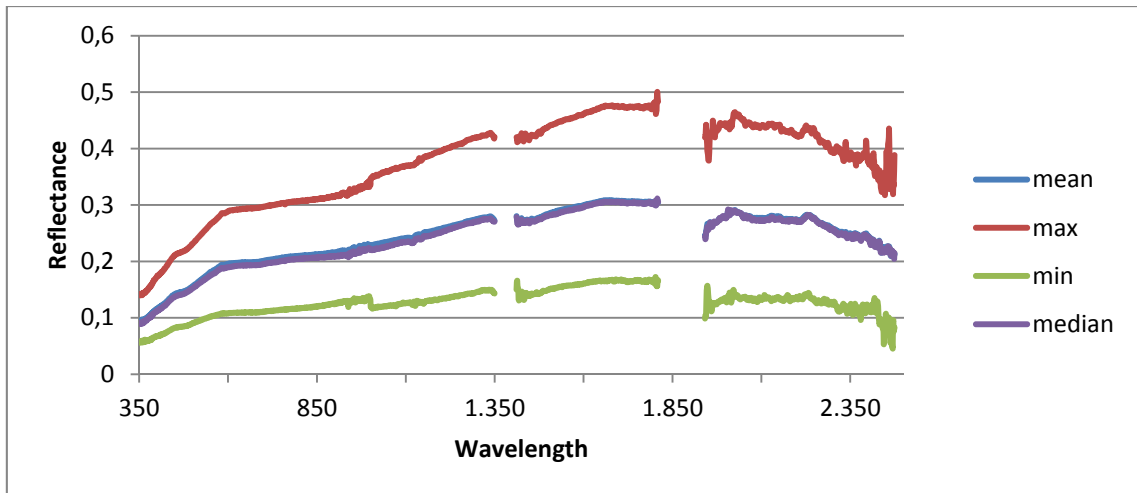


Figure 162. First measurement from locality 12.

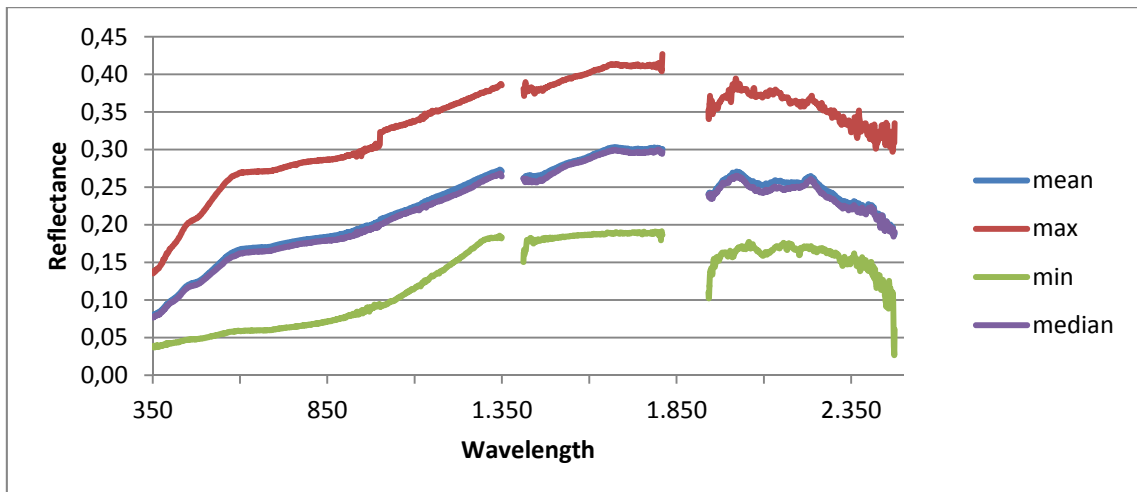


Figure 163. Second measurement from locality 12.

Locality 13

Geology Dark gneiss seen as a 20 m wide dyke cutting lighter coloured gneiss. The gneissic dyke has little to no lichen, contains two types of pegmatite, and fractures filled with a meta-conglomerate.

GPS position N65.78259, W38.04263

Description of site The main rock type was measured standing while the pegmatite and the meta-conglomerate were measured at a distance of 20–30 cm.

Sample no. GGU 565513, 565514, 565515, 565516, and 565517

Notes Sample 565513 and 565515 is from mafic dyke while 565514 is from a pegmatite with grains of up to 1.5 cm in diameter. Sample 565517 is from a coarser grained pegmatite with crystals of up to 5 cm in diameter, the pegmaties are no more than 10 cm wide. Sample 565516 is from a conglomerate that can be found as fracture filling but shows signs of having been metamorphosed.



Figure 164. *A big flat area that was measured at locality 13.*

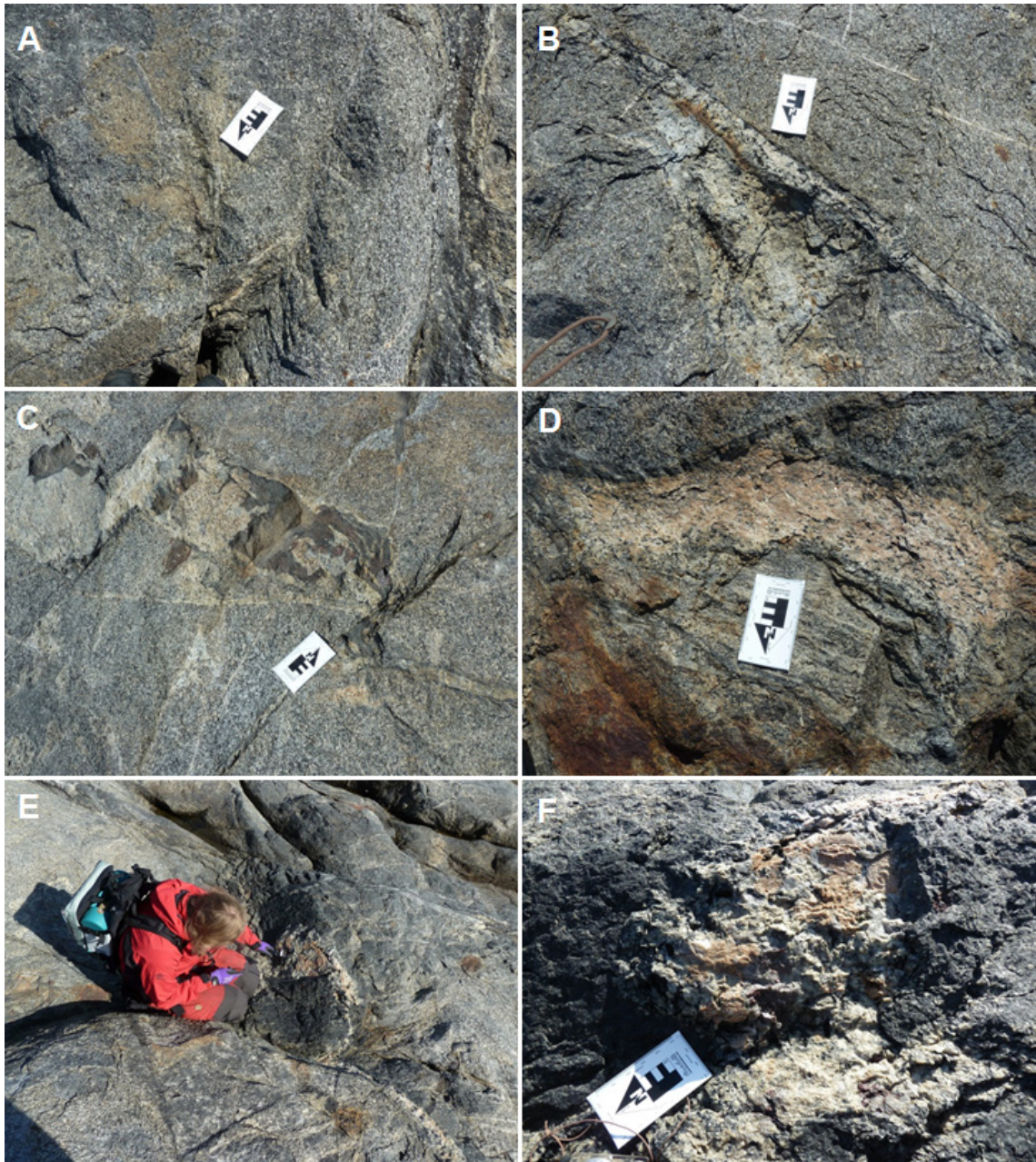


Figure 165. *Locality 13. A) Fracture conglomerate can be seen in the far right part of the picture, B) and C) Structures in the rock, D) The fine-grained pegmatite, E) Measurement of the coarse-grained pegmatite, F) Close-up of the coarse-grained pegmatite.*

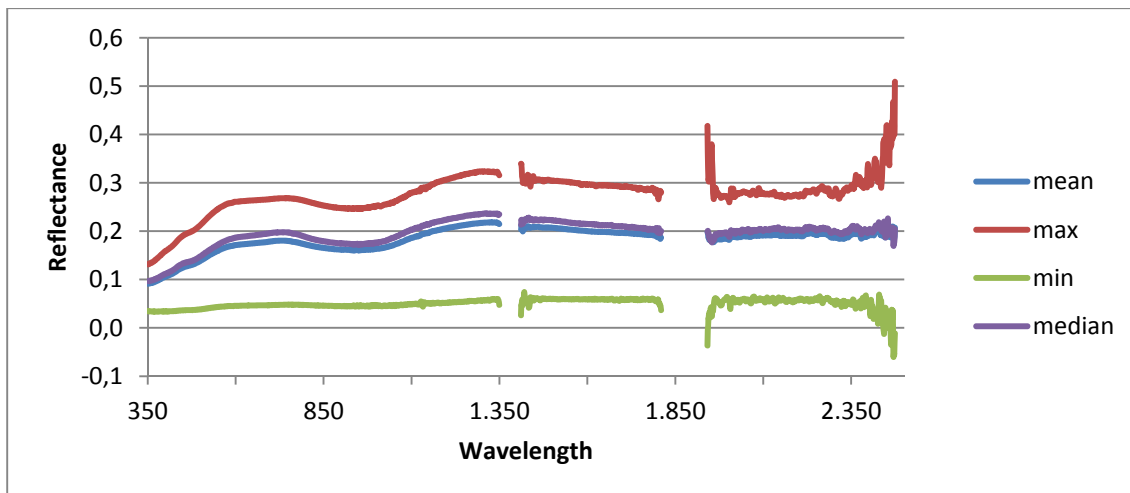


Figure 166. Results of the measurement at the big dyke at locality 13.

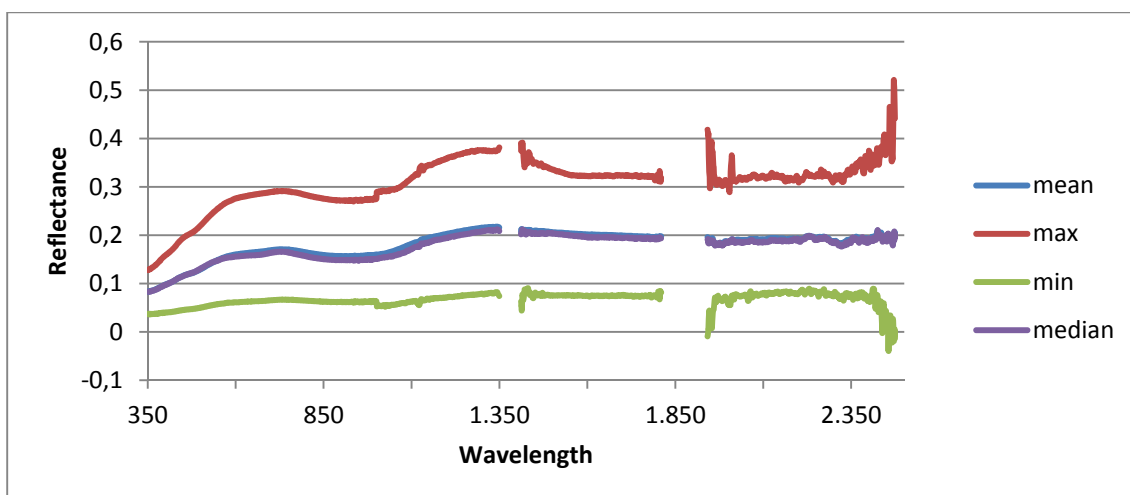


Figure 167. Results of the measurement of the area in Figure 164 at locality 13.

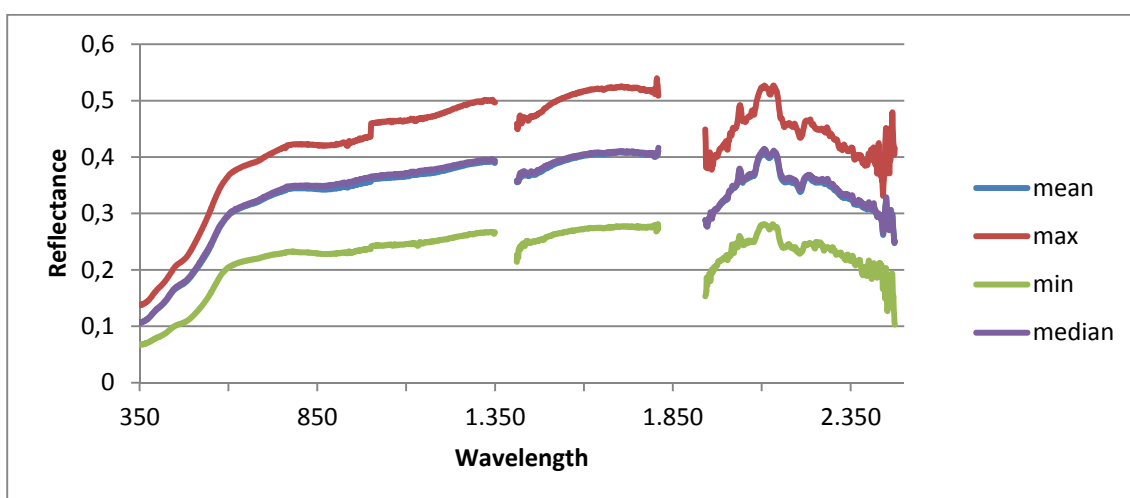


Figure 168. Results of the measurement of the medium-grained pegmatite at locality 13.

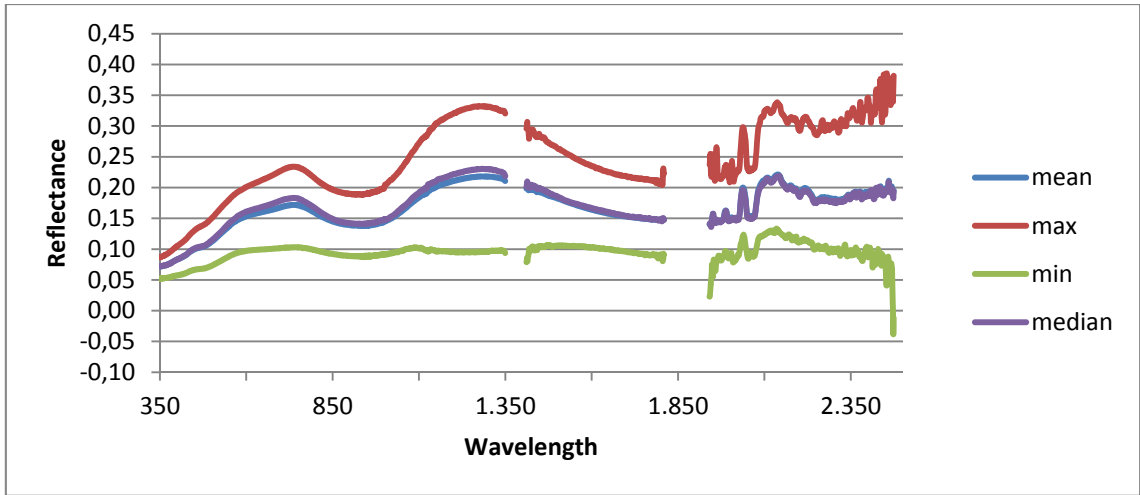


Figure 169. Results of the measurement of the dark inclusion in the dyke at locality 13.

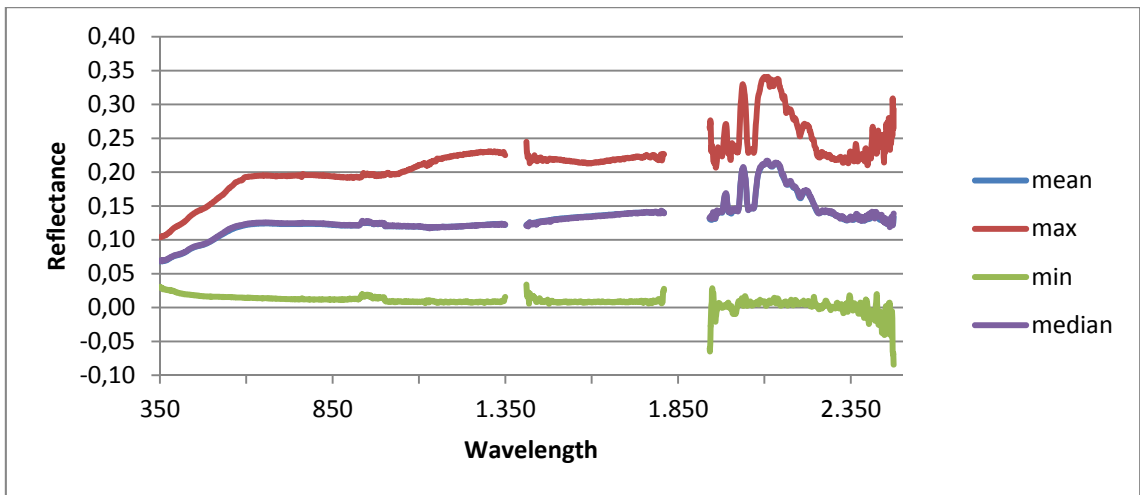


Figure 170. Results of the measurement of the meta conglomerate found as crack filling at locality 13.

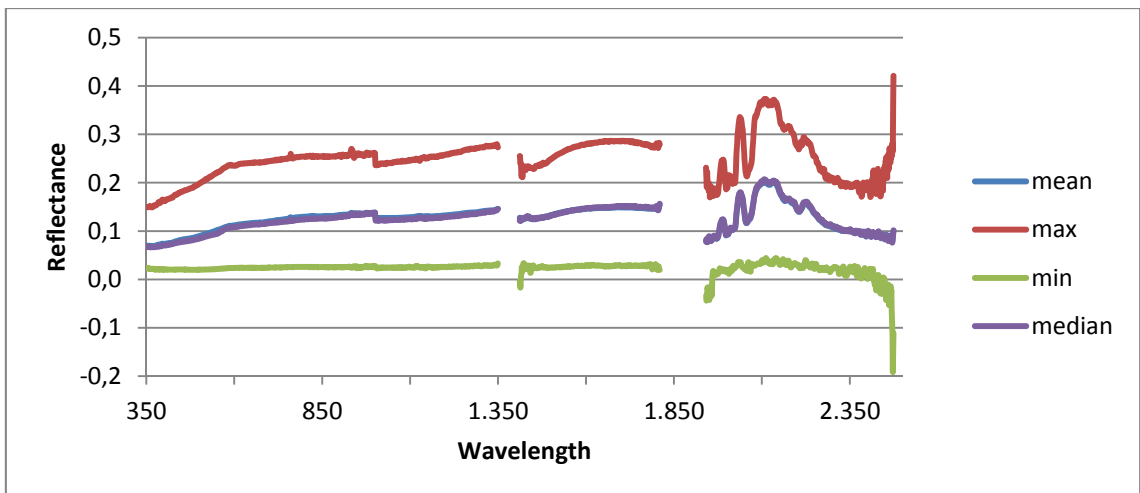


Figure 171. Results of the measurement of the coarse-grained pegmatite at locality 13.

Locality 14

Geology Banded gneiss with variation in the concentrations of dark minerals, the rock has schistosity. It is a light grey gneiss containing quartz, feldspar, garnet, and biotite.

GPS position N65.78231, W38.04346

Description of site Patches of rust were observed.

Sample no. GGU 565518



Figure 172. Overview of the area at locality 14.

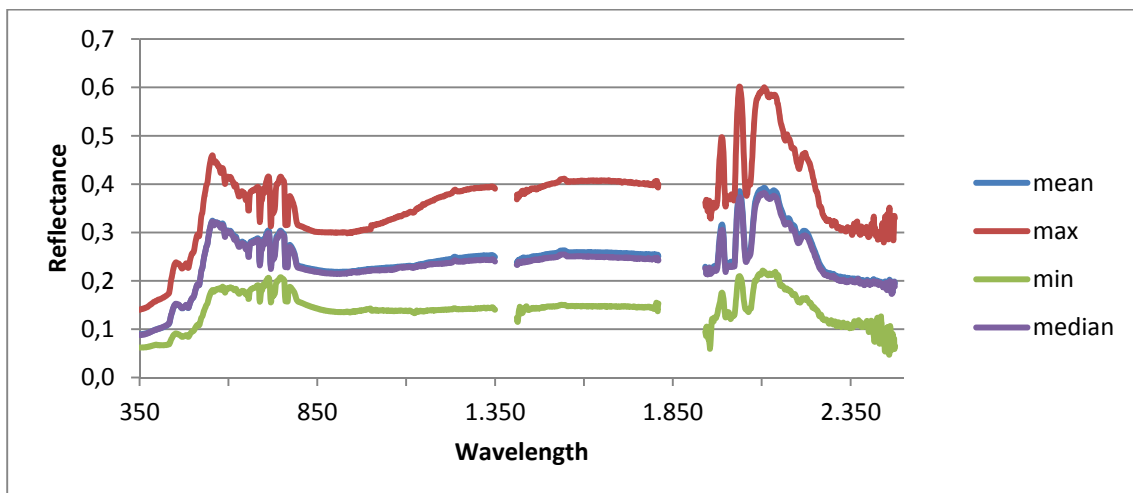


Figure 173. Results of the first measurement at locality 14.

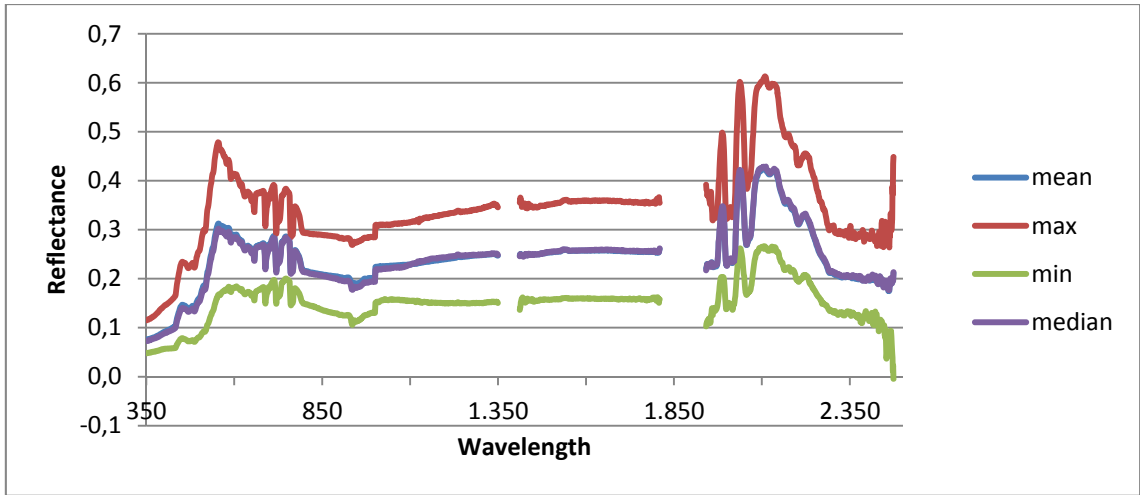


Figure 174. Results of the second measurement at locality 14.

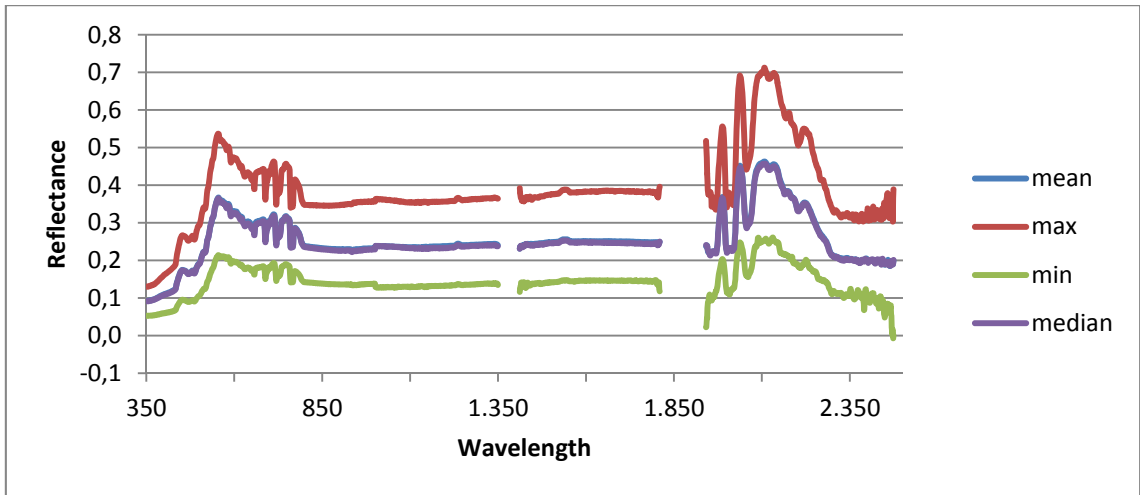


Figure 175. Results of the third measurement at locality 14.

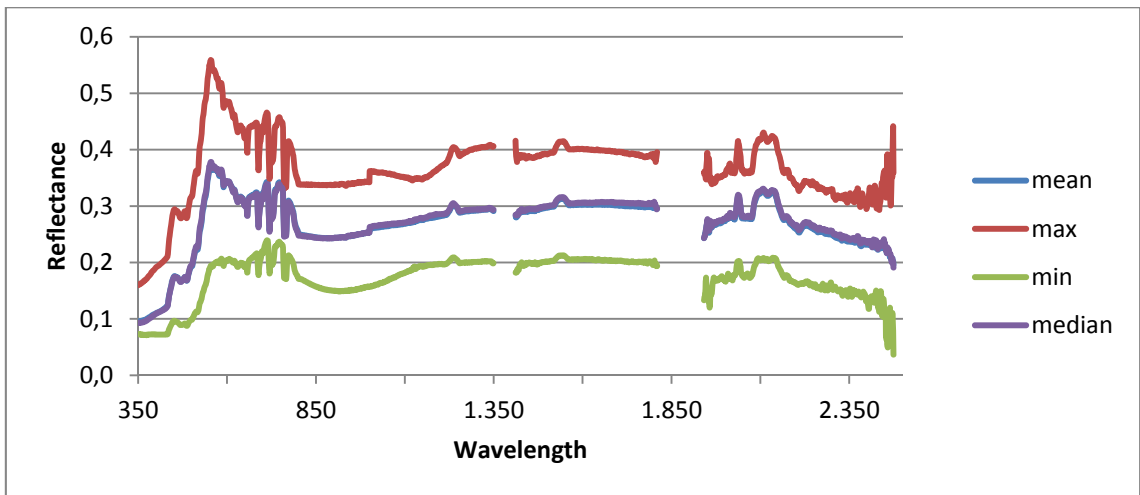


Figure 176. Results of the fourth measurements from locality 14.

Locality 15

Geology Banded gneiss, large bands of light rock intermingled with dark bands.

Description of site Many loose fragments on top of the ice polished rock.

GPS position N65.78454, W38.04467

Sample no. GGU 565519 and 565520

Notes 565519 represents a dark band while 565520 represents a light band.

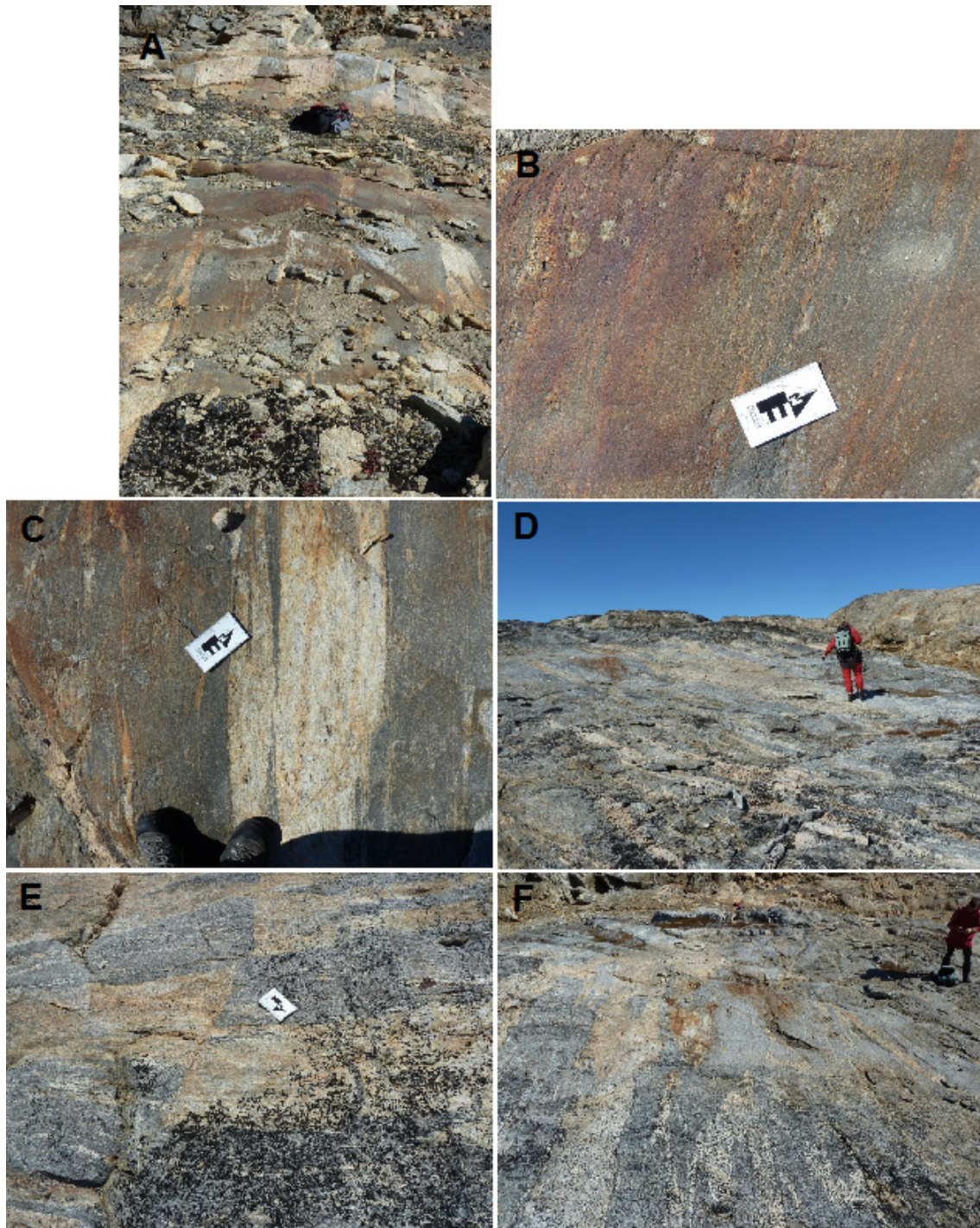


Figure 177. Locality 15. A) The wide bands are very apparent here, B) A rust covered area of a dark band, C) In some places the dark bands are more prominent than the light bands, D) measurement of the area with least lichen, E) A small fault in the gneiss, F) The bands are not uniform.

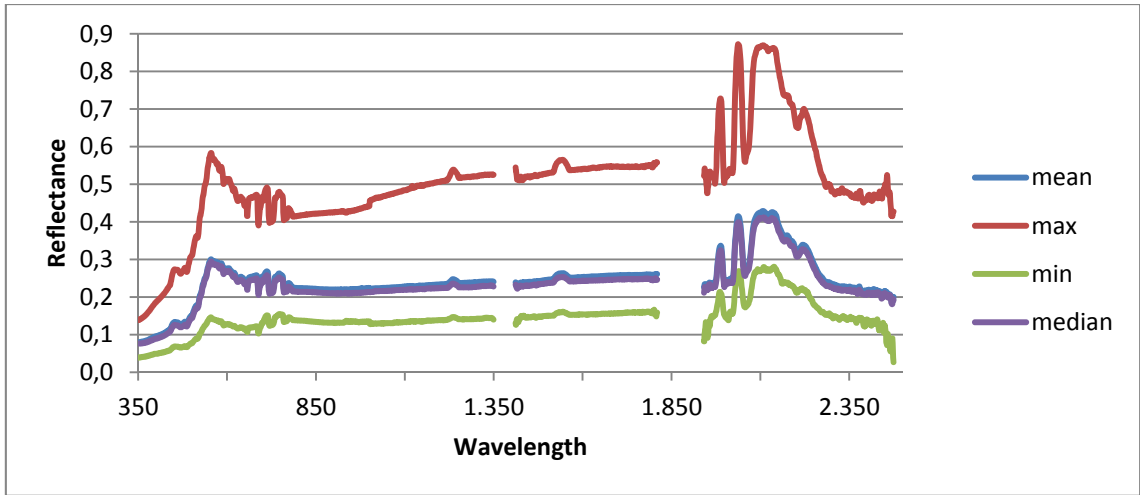


Figure 178. Results of the first measurement at locality 15.

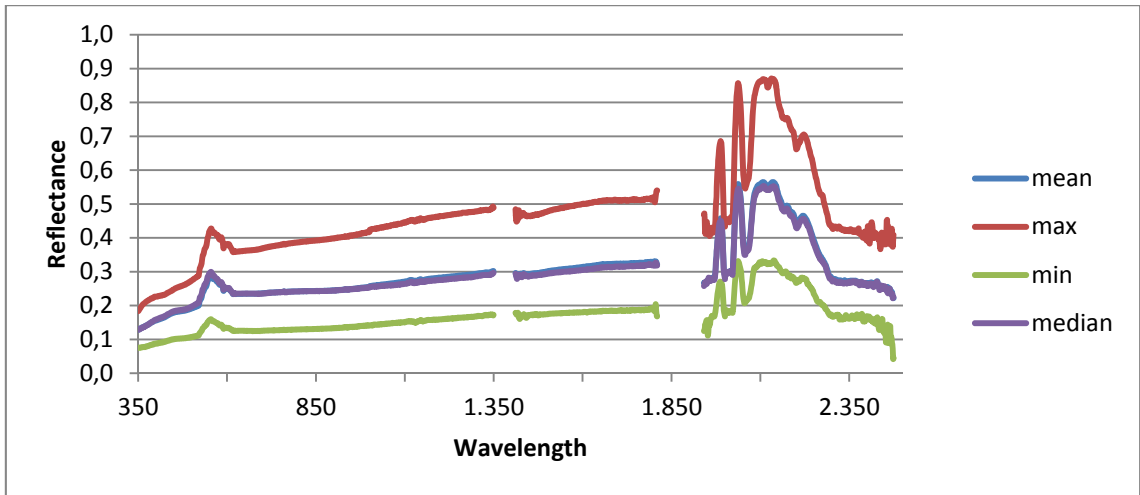


Figure 179. Results of the second measurement at locality 15.

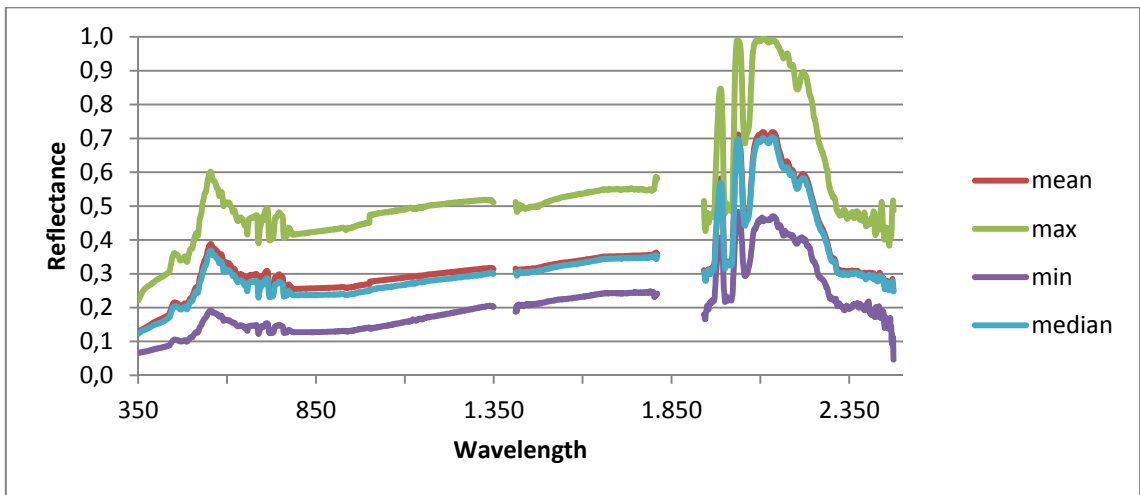


Figure 180. Results of the third measurements at locality 15.

Locality 16

Geology 30 m wide vertical sheet of granite, the dark minerals in the rock is aligned due to metamorphism. The granite appears as a white sheet cutting a more yellow rock that

GPS position N65.74651, W38.12523

Description of site Four areas were selected and measured at different distances. Area 1) 0.5 x 0.5 m with a distance of approx. 20 cm. Area 2) 1.5 x 3 m with lichen growing on it, measured from a standing position. Area 3) 30 x 40 cm with no lichen measured at a distance of 20 cm. Area 4) 3 x 3 m a small amount lichen is observed, measurement taken standing.

Sample no. GGU 565521



Figure 181. *This massive brittle sheet stands out in the landscape.*



Figure 182. *Locality 16. A) Getting ready for the measurement. B) Measuring small surface. C) Medium amount of lichen on this area. D) High amount of lichen growing on this area.*

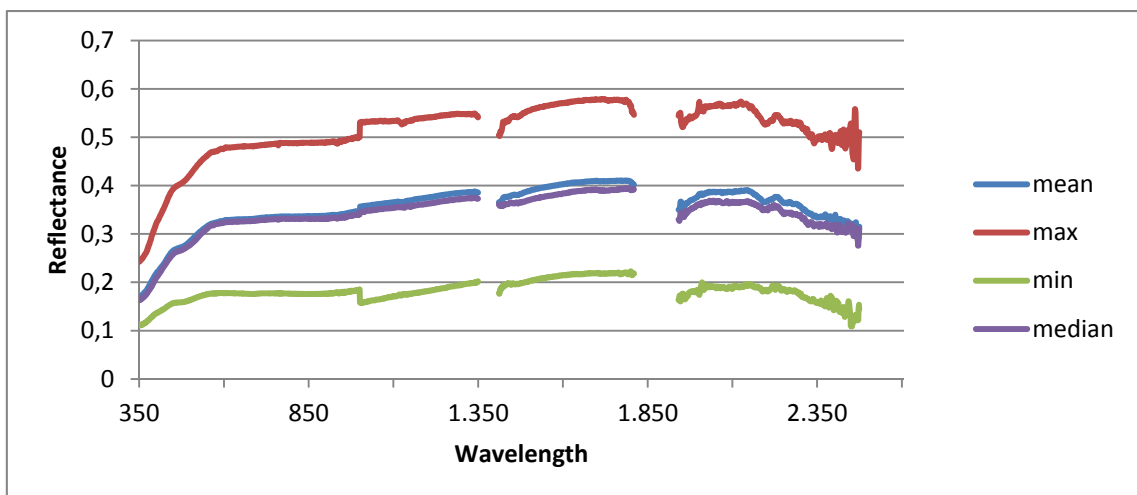


Figure 183. *Results from the first measurements at locality 16.*

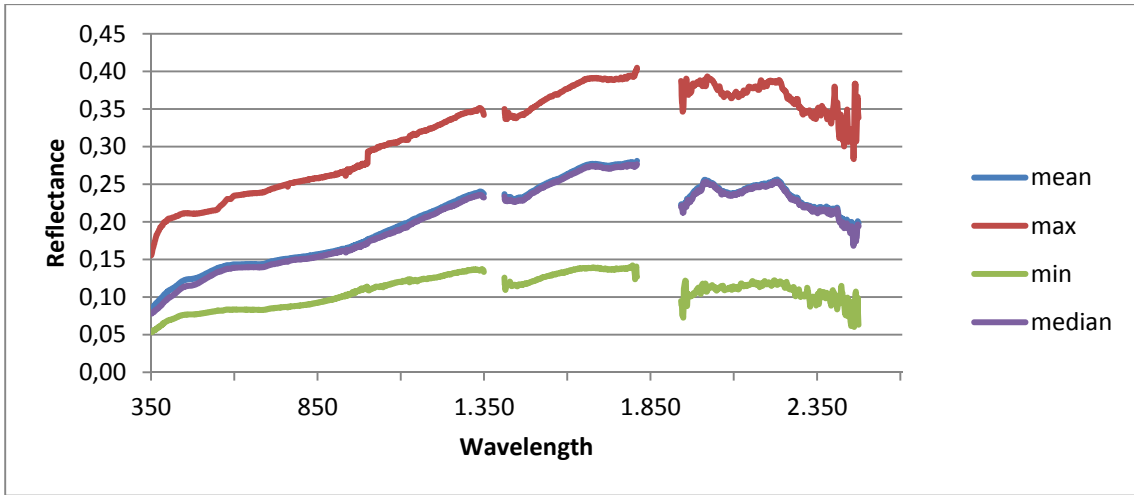


Figure 184. Results from the second measurement at locality 16.

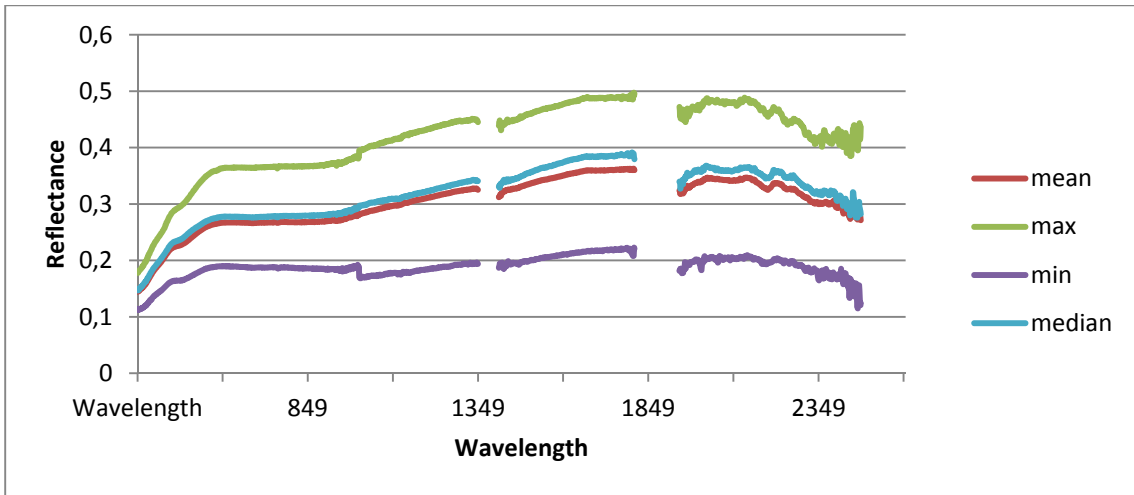


Figure 185. Results from the third measurement at locality 16.

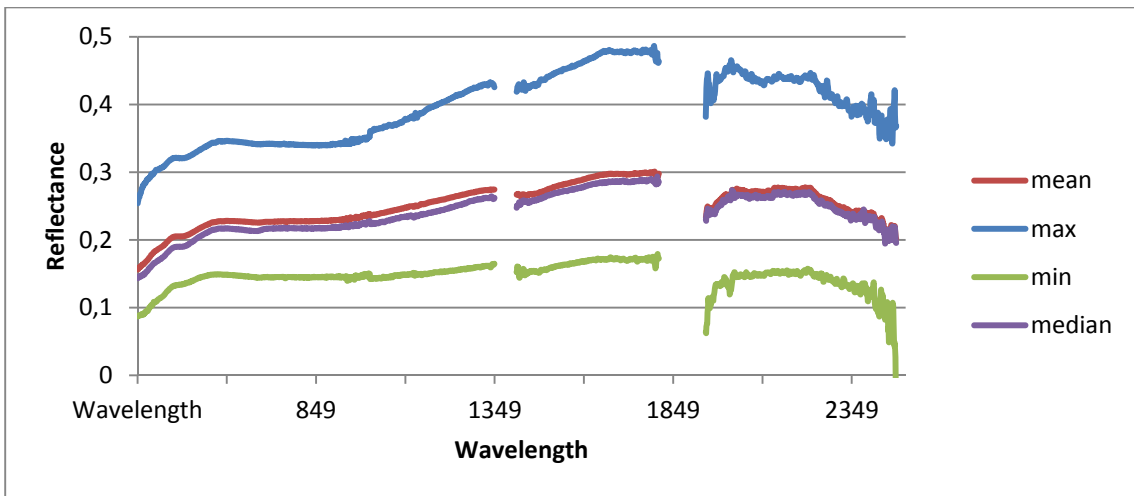


Figure 186. Results from the fourth measurement at locality 16.

Concluding remarks regarding the spectral measurements

The specters all look different depending on the different rocks measured; even the different gneisses show different signals. This might indicate that it is possible to differentiate between the different types of gneisses. The very rusty rock show a clearly different signal and this might be possible to use as a tracer for mineral deposits as many of the processes that moves iron also moves other metals.

References

- Bedini, E. (2011). Mineral mapping in the Kap Simpson complex, central East Greenland, using HyMap and ASTER remote sensing data. *Advances in Space Research*, 47, pp.60-73.
- Bedini, E. (2012). Mapping alteration minerals at Malmbjerg molybdenum deposit, central East Greenland, by Kohonen self-organizing maps and matched filter analysis of HyMap data, *International Journal of Remote Sensing*, 33:4, 939-961.
- Goetz, A.F.H. Making Accurate Field Spectral Reflectance Measurements, ASD Report, October 2012, 16 pp.
- Heincke, B. (2016). Regional geophysical data. In: Kolb, J., Stensgaard, B.M. & Kokfelt, T.F. (eds.). *Geology and mineral potential of South-East Greenland. Danmarks og Grønlands Geologiske Undersøgelse Rapport 2016/38*, 157 pp.
- Tukiainen, T. (2001). Projects MINEO and HyperGreen: airborne hyperspectral data acquisition in East Greenland for environmental monitoring and mineral exploration. *Geology of Greenland Survey Bulletin* 189, 122–126.
- Kolb, J., Stensgaard, B.M. & Kokfelt, T.F. (2016). *Geology and mineral potential of South-East Greenland. Danmarks og Grønlands Geologiske Undersøgelse Rapport 2016/38*, 157 pp.

Appendix A. Camp location

Location	Coordinates		Dates	Participants
Camp 1	N 65.6175	W 38.5506	8.-14.8.2014	AFJ, PRI, BHH
Camp 2	N 65.7642	W 38.1027	14.-20.8.2014	AFJ, PRI, BHH

Appendix B. List of localities visited

Locality ID	Description	Notes	Samples	Lat. (N)	Long. (W)	Elevation	Date
1	Base camp	Site where we tested the equipment		65.86632	37.00839	71	07-08-2014
2	Test site	Next to base-camp		65.86675	37.00833	102	07-08-2014
3	Camp 1	Southern camp		65.61752	38.55056	70	08-08-2014
4	080914 loc 1.1	Granit dal kl. 12.25	565501	65.57597	38.81036	53	09-08-2014
5	080914 loc 1.2	Granit dal		65.57585	38.81028	73	09-08-2014
6	080914 loc 1.3	Granit dal		65.57604	38.81032	49	09-08-2014
7	Muddy shore	Muddy	565502	65.66111	38.41373	48	10-08-2014
8	Gneiss by camp 1	Gneiss field-speck	565503	65.61704	38.54898	88	11-08-2014
9	081114 2.1	Dyke	565504	65.61774	38.54878	59	11-08-2014
10	Malachite	Malachite on surface of rock	565505	65.67626	38.55414	58	11-08-2014
11	0812 loc 1	Ultra mafic dyke	565506	65.61876	38.47968	84	12-08-2014
12	0811 loc 2	Dark gneiss	565507, 565522	65.61847	38.47655	126	12-08-2014
13	0811 loc 3	Light grey gneiss	565508	65.61664	38.47402	141	12-08-2014
14	Camp 2	Camp 2		65.76420	38.10269	65	14-08-2014
15	MT04	MT04		65.75938	38.16301	70	15-08-2014
16	0814 loc 1.1	Qz. garnet. amf. with dark dykes	565509, 565510	65.76428	38.10199	89	16-08-2014
17	0814 loc 2.1	Mafic intrusion	565511	65.77252	38.10677	62	16-08-2014
18	0816 loc 3	Very iron stained quartzite	565512	65.77280	38.10722	76	16-08-2014
19	0816 loc 4	Meta sandstone	565509, 565510	65.76900	38.11805	70	16-08-2014
20	0817 loc 1	Gneiss dyke	565513, 565514, 565515, 565516, 565517	65.78259	38.04263	50	17-08-2014
21	0817 loc 2	Light gneiss	565518	65.78231	38.04346	56	17-08-2014
22	0817 loc 3	Banded gneiss	565519, 565520	65.78454	38.04467	62	17-08-2014
23	0819 loc 1	Sheet intrusion	565521	65.74651	38.12523	84	19-08-2014